Development of Nanoparticles for Oral Delivery of Insulin

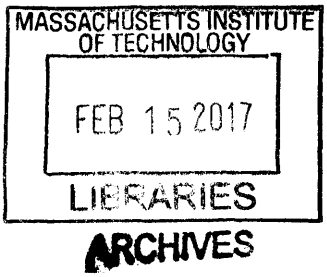

by

Sunandini Chopra

Bachelor of Mechanical Polymer Engineering, 2012
University of Akron

Submitted to the Department of Mechanical Engineering
in partial fulfillment of the requirements for the degree of

Doctor of Philosophy

at the

MASSACHUSETTS INSTITUTE OF TECHNOLOGY

February 2017

Author: Signature redacted

Sunandini Chopra
Department of Mechanical Engineering
Program of Polymer Science and Soft Matter
January 15, 2017

Certified by: Signature redacted

Rohit Karnik, Ph.D.
Department of Mechanical Engineering
Thesis Supervisor

Accepted by: Signature redacted

Rohan Abeyaratne, Ph.D.
Department of Mechanical Engineering
Chairman, Department Committee on Graduate Students

Development of Nanoparticles for Oral Delivery of Insulin

by

Sunandini Chopra

Submitted to the Department of Mechanical Engineering
on January 15, 2017, in partial fulfillment of the
requirements for the degree of
Doctor of Philosophy

Abstract

Parenteral administration remains the mainstay of drug administration for protein therapeutics. However, for diseases that require frequent drug dose over long periods of time, injections can result in patient incompliance and poor treatment outcomes. For such diseases, oral drug delivery is the most non-invasive and patient-compliant method of drug administration. Although oral delivery of many small molecule drugs is routine, oral delivery of protein drugs – e.g. insulin – presents several challenges including oral bioavailability of the protein therapeutic because of degradation in the stomach, inactivation and digestion of the therapeutics by the proteolytic enzymes in the luminal cavity, and poor permeability of drugs across the intestinal epithelium.

Polymeric nanoparticle (NP) carriers provide new opportunities for controlled delivery of drugs, and have the potential to address challenges associated with effective oral delivery of insulin. NPs can protect the protein therapeutic from degradation in the GI tract as well as allow targeted transport across the epithelial lining. An efficient NP based oral insulin delivery solution that can enable targeted transport of insulin across the GI tract must have (1) high insulin loading, (2) sub-100 nm size, (3) ability to release insulin before opsonization by macrophages and (4) the ability to be surface-functionalized with ligands that facilitate transport across the epithelium.

This work presents a detailed study on mechanistic understanding of polymeric insulin NP formation with a focus on the effect of synthesis parameters on insulin loading and NP size. We report how buffer conditions, ionic chelation, and NP preparation methods influence insulin loading in poly (lactic-co-glycolic acid)–b–

poly(ethylene glycol) (PLGA-PEG) NPs. We report a 10-fold increase in insulin loading with the use of chelating zinc ions and by the optimization of the pH during nanoprecipitation.

Next, we report the development of novel insulin Eudragit-PLGA-PEG blended NPs (Ins-Eud-NPs) with high insulin loading (13.1%) and sub-100 nm size. These NPs enable rapid release of insulin when triggered by a change in pH that occurs when the NPs cross the duodenal epithelium and go from acidic to neutral pH. The NPs are formed by successfully blending Eudragit S100, a commercially available polymer which dissolves at pH greater than 7 with a non-pH responsive polymer, PLGA-PEG. To enable effective transport of these NPs across the epithelial lining, NPs were designed to use the FcRn transport pathway that mediates IgG antibody transport across epithelial barriers. We report the successful chemical conjugation of the Fc fragment on the surface of Ins-Eud-NPs by overcoming the presence of non-ideal conjugation parameters owing to the pH restrictions of the system.

This dissertation provides mechanistic insights and helps to understand fundamental concepts about polymeric NP formation and protein encapsulation. The modular NP system developed in this work can be extended to other protein drug delivery systems that are subject to limited drug loading and restricted transport across epithelial barriers.

Thesis supervisor: Rohit Karnik, Ph.D.
Title: Associate Professor, MIT

This thesis has been examined by the following Thesis Committee:

Thesis Advisor

Rohit Karnik, Ph.D.
Associate Professor of Mechanical Engineering
Massachusetts Institute of Technology

Thesis Committee

Omid C. Farokhzad, M.D.
Associate Professor of Anesthesiology
Harvard Medical School

Roger Kamm, Ph.D.
Professor of Mechanical Engineering
Massachusetts Institute of Technology

Acknowledgements

I want to dedicate this thesis to my late mother, Dr. Bharti Chopra. She has had the most profound impact on my life, not just as a role model but also as my strongest pillar of strength and my loudest cheerleader. This thesis would not have been possible without her tireless efforts to personally tutor me as a child, the long hours she worked as a gynecologist after which she came back every day and worked even harder to take care of my brother and me, and the lessons of dedication, hard work, and perseverance that she taught me each day growing up. She was the reason I got interested in the sciences at a very young age. It was her belief in my abilities and her desire to provide me with the best resources and education that brought me to the United States. It was her selfless nature and modern thinking, way ahead of her times, that enabled me to pursue my dreams. My mother was a gifted person with the ability to think the unthinkable and to execute actions at a level that surpassed everyone. She was a woman of immense dignity, valor, and determination. She was blessed with a sense of eccentricity, which was exhibited in the passion with which she worked, loved, cared for and built relations. Going forward in life, I only hope to be blessed with a part of her eccentricity, to be able to work like her, to love like her and to value and build relations like she did. She has been my most valuable asset. Although she is not present today, I know that this work will make her proud and her applause would be the loudest. Thank you, Ma.

I also want to take this opportunity to express my sincere gratitude to my advisor, Professor Rohit Karnik, who has provided me unparalleled guidance and mentorship. I want to thank him for the optimism and positivity that he exudes, which also reflect in his conversations. His belief in me and his ability to probe the fundamental aspects of science were instrumental in helping me through the troughs. The insightful and pertinent questions that he asked were pivotal to this work. I am grateful to him for being so selflessly supportive and so incredibly gracious. I have not just learned how to do good science from him, but also kindness and compassion. The numerous times when I walked into his office, crestfallen and disappointed he was always successful in reversing that and ensuring that I was pumped with renewed excitement and enthusiasm to solve the problems I face. Professor Karnik's contributions were was paramount to the completion of this work.

I also want to thank my committee members, Professor Omid Farokhzad and Professor Roger Kamm. Professor Farokhzad has been a significant positive influence on my work and my life. He is a true visionary. His futuristic vision and

ability to think ahead of his time have helped me connect my work to the overarching goal and the big picture. I am thankful for his unconditional support, guidance, and understanding throughout this project.

Professor Kamm has been incredibly kind and generous with his time. He always asked the most pertinent questions, which made me think more about what I was doing and why. It helped me realign my efforts and thoughts to solve the right problems. His role in the completion of this work is invaluable.

I also want to express my profound appreciation for my family – my father, Lt. Col. Tilak Raj Chopra, my brother, Harsh Chopra, my uncle Dr. Vikas Praskash and my aunts Dr. Malini Dusey and Tulika Das. Each one of them has played a vital role in my upbringing and education. My father is my biggest well-wisher and my reality check button. He consistently makes me question and rethink my actions and agendas of life. He is an honest, frank and a doting father (who is more like my brother). My brother (who behaves like my father), is one of the most genuine people I know. I am thankful to him for always being there for me, supporting me unconditionally and setting an example of how to be an ideal human being. My uncle is the reason I came to the United States to pursue higher education. He was one of the reasons I wanted to pursue a doctoral degree. I want to express my heartfelt gratitude to him for recognizing my potential, and for bringing me to the United States against all the odds. My aunt, Malini Dusey has been instrumental in helping me develop into the person I am today. Her constant questioning of my actions, her honest opinions and her independent and joyful way of living life have several times made me question my motivation in life. I have had a roller coaster ride with her, but each day I am more in awe of her. Lastly, my aunt, Tulika Das, and I share a special relationship where we are more friends than anything else. I want to thank her for accepting me the way I am and for being my sounding board. Each one of these people mentioned was crucial to the completion of this thesis.

I also want to take this opportunity to thank all my teachers – from high school to undergrad to grad school. Each one of them has left an indelible mark on my life and helped me evolve my thinking. I want to particularly thank Professor Robert Langer, for his kind support, guidance, encouragement and access to laboratory equipment. Besides, I want to thank my friends and lab mates for their unwavering support. I want to thank Dr. Nicolas Bertrand, Dr. Suman Bose, Jaya Singh, Shruti Singh, Sidhant Jena, Kunal Poddar, Sneha Mandhan, Abel Cortinas, Akhilesh Bakshi, Vidhi Goel, Amy Wang and Trinh Nyguen for their help and support.

I am thankful to the wonderful people in my life who make me a better person each day. I hope you enjoy reading this thesis and I hope this helps to answer fundamental and pertinent questions that can have a positive impact in the area of drug delivery.

THIS PAGE INTENTIONALLY LEFT BLANK

CONTENTS

THIS PAGE INTENTIONALLY LEFT BLANK

List of Figures

injections, subcutaneous infusions, pulmonary delivery and oral delivery. Each of these methods have advantages and disadvantages. However, oral delivery is considered to be the most patient compliant and non-invasive way of administering insulin.

1.10. Some oral insulin delivery projects that are under development and clinical trial.

1.11. Physiology of the intestinal epithelium. Enterocytes, goblet cells, paneth cells and M-cells are some of the major cell types that make up the intestinal epithelium.

1.12. Barriers to effective delivery of insulin. Various chemical and physical barriers like changes in pH, high protease action and the presence of tight junctions make the problem of oral delivery very challenging.

1.13. Oral insulin delivery Nanoparticle Design criteria. The nanoparticles (NPs) must be able to protect insulin from the harsh chemical environment in the GI tract and from enzymatic degradation. The NPs must be sub-100 nm, have the ability to be functionalized and have the capability of delivering majority of insulin before the NPs can opsonized.

1.14. Choice of parameters for understanding the nanoprecipitation method better.

2.1. (a) Insulin standard curve in relation to the BSA standard curve for the BCA assay. (b) Relation between the insulin and BSA standard curves. (c) Effect of DMSO, zinc, and polymeric NPs on the insulin standard curve.

2.2. Ins-NPs and Ins-Zn NPs show the potential of long-term storage as they maintain (a) particle size and (b) zeta potential before and after undergoing the process of freeze-drying. (c) Ins-NPs and Ins-Zn-NPs are stable in water for up to 4 days from synthesis at RT. (d) Conformational stability of insulin in Ins-NPs and Ins-Zn-NPs was confirmed by comparing the circular dichroism spectra of standard insulin and insulin obtained from Ins-NPs and Ins-Zn-NPs before and after undergoing the process of freeze-drying.

2.3. *Insulin loaded PLGA-PEG nanoparticles (Ins-NP).* **(A)** Schematic of Ins-NP synthesis process by nanoprecipitation, where PLGA-PEG and insulin in dimethyl sulfoxide (DMSO) is added drop-wise to a stirred beaker containing water (or

buffer). TEM images of **(B)** Ins-NPs and **(C)** PLGA-PEG NPs without insulin. *Effect of buffer wash on Ins-NP characteristics.* **(D)** Schematic of the synthesis of Ins-NPs where NPs were either washed with PBS buffer (pH 7.4) or with water only. **(E)** Insulin loading and encapsulation efficiency show 25-fold higher insulin loading when NPs were washed with water only (8.95% ± 1.44) as compared to a PBS buffer wash (0.36% ± 0.19) (n = 3, p = 0.008). **(F)** NP size data show no significant difference in the size of the Ins-NPs when washed with water or buffer (n = 3, p = 0.074). Error bars represent ± s.d.

2.4. *Effect of adding insulin at different stages of nanoprecipitation on Ins-NP characteristics.* (A) Schematic showing the synthesis of Ins-NPs by including insulin mixed with PLGA-PEG in DMSO before nanoprecipitation (top), and by adding insulin in DMSO to empty PLGA-PEG NPs after their formation by nanoprecipitation (bottom). (B) Insulin loading and encapsulation efficiency show no significant dependence on the stage of adding insulin before (0.36%) or after (0.32%) nanoprecipitation (n = 3, p = 0.79), but (C) NP size shows a significant dependence (n = 3, p = 0.005). *Effect of mixing insulin in different phases on Ins-NP characteristics.* (D) Schematic showing the synthesis of Ins-NPs by adding DMSO with insulin and PLGA-PEG to water (top), and by adding DMSO with PLGA-PEG to water with insulin dissolved in it (bottom). (E) Insulin loading (and encapsulation efficiency) shows no significant dependence on including insulin in DMSO (0.36%) or in water (0.28%) (n = 3, p = 0.60), but (F) NP size shows a significant dependence (n = 3, p = 0.0006). Error bars represent ± s.d. Note: The NPs with the label 'Insulin added before' in Figure 2.4B and the NPs with the label 'Insulin in organic' in Figure 2.4E are the same nanoparticles.

2.5. Empty PLGA-PEG NPs (-25.44 mV) and Ins-NPs (-27.9 mV) was statistically insignificant. Zeta potential of the Ins-Zn-NPs (-22. 03 mV) is significantly lower than Ins-NPs and Empty PLGA-PEG NPs (** = $p < 0.05$).

2.6. *Effect of incorporating zinc ions in Ins-NPs.* (A) Schematic showing the formation of Ins-Zn hexamers (top) and of Ins-Zn-NPs (bottom). (B) Dark-field TEM/EDX image of unstained Ins-Zn-NPs. The lighter regions in the figure show the presence of NPs, and the red dots correspond to the presence of zinc. The presence of zinc in the same areas where Ins-Zn-NPs were detected confirms the presence of zinc in Ins-Zn-NPs. (C) Insulin loading and encapsulation efficiency show an increase in insulin loading with an increase in zinc ion concentration. Greater than 10-fold enhancement of insulin loading was obtained for insulin to zinc ratio of 1:9. (n = 3, p = 0.02). (D) The average diameter of empty PLGA-PEG NPs, Ins-NPs, and Ins-Zn-NPs. In case of Ins-Zn-NPs, the

average diameter did not change significantly when different amount of zinc ions are added. The average diameter of Ins-Zn-NPs was larger than that of empty PLGA-PEG NPs (n = 3, p = 0.0003) and Ins-Zn-NPs and Ins-NPs (n = 3, p = 0.0001). Error bars represent ± s.d.

2.7. *Effect of adding zinc ions at different stages of nanoprecipitation on Ins-Zn-NPs.* (A) Schematic showing the synthesis of Ins-Zn-NPs by adding Ins-Zn hexamers premixed with PLGA-PEG molecules in DMSO before nanoprecipitation (top). This forms NPs with high insulin loading (4.07%) and large NP diameter (127.6 nm). (B) Schematic showing the synthesis of Ins-Zn-NPs by adding Ins-Zn hexamers to empty PLGA-PEG NPs after nanoprecipitation (top). This forms NPs with high insulin loading (3.82%) and small NP diameter (78.7 nm). (C) Schematic showing the synthesis of Ins-Zn-NPs by adding zinc ions to preformed Ins-NPs after nanoprecipitation (top). This forms NPs with lower insulin loading (1.55%) and smaller NP diameter (57.9 nm). Dashed lines indicate sizes of empty PLGA-PEG and Ins-NPs for reference. Error bars represent ± s.d. For insulin loading n = 3 and p_{AB} = 0.74, p_{AC} = 0.034, p_{BC} = 0.016. For NP diameter n = 3 and p_{AB} = *0.0004,* p_{AC} = 0.0001, p_{BC} = 0.005.

2.8. *Effect of pH on Ins-Zn-NP and Ins-NPs.* (A) Schematic showing the synthesis of Ins-Zn-NPs in different buffers (pH 4.65, pH 6.1, and pH 6.5). (B) Insulin loading of Ins-Zn-NPs and Ins-NPs that were synthesized in buffers with different pH. Insulin loading increased with increasing pH. (C) Average diameter of empty PLGA-PEG NPs, Ins-NPs, and Ins-Zn-NPs synthesized in different buffers.

2.9. *Compilation of the effect of NP synthesis parameters on NP properties.* (A) Compilation of the NPs studied for the purpose of understanding the factors that affect insulin loading and NP size in Ins-NPs and Ins-Zn-NPs. The symbols in blue contain only PLGA-PEG and insulin while the orange symbols represent NPs that contain PLGA-PEG, insulin, and zinc. The size of empty PLGA-PEG NPs has been represented by a grey vertical bar, whose width represents the standard deviation. Ins-NPs (blue) have low loading and small size. Contrary to these NPs, Ins-Zn-NPs formed by including zinc during nanoprecipitation (orange circles) have higher insulin loading, but their diameter is larger. NPs synthesized by adding Zn ions to preformed Ins-NPs (light triangle) show smaller size and moderate loading. The optimal NPs are Ins-Zn-NPs (dark triangle) formed by adding Ins-Zn hexamers to pre-formed NPs combine high loading (3.82 %) and small size (78.7 nm diameter). (B) Qualitative summary of how different synthesis parameters affect insulin loading and size. *Insulin release.* (C) Release of insulin

from the optimal NPs (Ins-Zn-NPs with insulin loading 3.82%, NP size 78.7 nm) is comparable with the previously reported release of insulin from PLA-PEG NPs[1].

3.1. Schematic of the NP synthesis set-up. The Ins-Eud-NPs were synthesized using the nanoprecipitation method. The polymer and the drug was mixed in the organic solvent (DMSO) and the resulting solution was added drop-wise to a beaker with pH 5 buffer that was being constantly stirred at 2000 rpm. Following NP synthesis the NPs were washed multiple times with pH 5 buffer with 150 mM NaCl.

3.2. (a) Design of the dialysis set up to study the *in-vitro* release of insulin. (b) Absorbance from empty NPs when the dialysis devices were soaked for 4 h and 24 h. (c) *In-vitro* release of free insulin.

3.3. (A) Addition of Eudragit S100 in the NP formulation for Ins-Zn-NPs (12.8%) did not lead to an improvement in insulin loading when compared with the insulin loading of Ins-Eud-NPs (13.1%). However, presence of Eudragit leads to an improvement in insulin loading. **(B)** Ins-Zn-Eud-NPs failed to illicit the desired pH response. Insulin released at a faster rate at pH 6 as compared to pH 7.4. This can be attributed to both the pH vales being larger than the pH of the isolelectric point of insulin below which Ins-Zn hexamers are unstable.

3.4. (A) Schematic highlighting the failure of Eudragit S100 to self-assemble to form NPs without the application of an external stabilizer using the process of nanoprecipitation. **(B)** The volume size distribution of the Eudragit S100 aggregates which confirm the failure of Eudragit to self-assemble to form NPs using the nanoprecipitation method. **(C)** Schematic of our hypothesis that pH responsive polymer, Eudragit S100 when blended with non-pH responsive polymer can form pH responsive NPs.

3.5. Blending Eudragit S100 and PLGA-PEG in different ratios was successful in forming NPs. The inclusion limit of Eudragit in the system is 50% (w/w) Eudragit as it results in the formation of chunky aggregates. Moreover, increasing amount of Eudragit S100 blended in Emp-Eud-NPs did not affect the size of the NPs. However, on preparing Ins-Eud-NPs a size dependence on the amount of Eudragit was observed. The size of the NPs increased for the compositions that had 20% and 30% (w/w) Eudragit.

3.6. Eudragit does not have a significant effect on insulin loading up to 10% Eudragit in the NPs, but on increasing the Eudragit amount to 20% and 30% we achieve a higher loading.

3.7. NPs with larger diameter and poor insulin loading are formed at low pH buffers (pH 3 and pH 4) while NPs with high insulin loading and smaller size are formed in buffers with pH close to the isoelectric point of insulin *ie.* pH 5.6.

3.8. Increasing the amount of Eudragit in the NPs slowed doen the release of insulin after 2 h in pH 6 buffer. But no particular trend was observed in the release of insulin from Ins-Eud-NPs at pH 7.4. Moreover, NPs with 20% Eudragit and 80% PLGA-PEG show the maximum difference in the amount of insulin released in pH 6 and pH 7.4, thus suggesting that this NP composition produces the most pH responsiveness NPs.

3.9. A significant reduction in the rate at which insulin is released from the NPs at pH 6 is observed as compared to pH 7.4. The half-life of insulin in pH 7.4 is between 30-60 min, while the half-life of insulin in pH 6 is 240 min. However, the current measurement is limited by the resolution of the dialysis set-up (1h).

3.10. On normalizing the data with respect to the release of free insulin it can be seen that almost all of the insulin from the NPs gets released as soon as the NPs are exposed to pH 7.4, while there is a significant reduction in the release of insulin from the NPs in pH 6. The half-life od insulin at pH 6 was 90 min.

3.11. (A) Effect of reaction buffer on Fc conjugation on NP surface. Maximum Fc conjugation was obtained at pH 7.4, followed by pH 5 and pH 6 buffer. **(B)** Effect of reaction time on Fc conjugation. On incubating Ins-Eud-NPs with Fc-SH in pH 5 buffer for 2 h and 18 h, it was found that the Fc conjugation in 2 h (0.16%) was not much greater than the Fc conjugation in 18 h (0.23%). **(C)** On increasing the amount of Fc by 5 times Fc conjugation increased to 1.48%. **(D)** Higher Fc conjugation resulted in longer synthesis time, which resulted in a loss of insulin leading to a reduction in insulin loading in Ins-Eud-NPs-Fc NPs to 6.8%.

3.12. (A) Formation of NPs after 5 min stirring time and 1 mg/mL NP incubation concentration resulted in only 0.7% Fc conjugation. However, when all other synthesis conditions were kept the same and only the stirring time was changed to 15 min and the NP incubation concentration was increased to 10 mg/mL Fc conjugation increased to 1.48%. **(B)** Conjugation of Fc on the NP surface did not

effect the size of the NPs, size of Ins-Eud-NPs-Fc was 63.9 nm while the size of NPs without Fc was 68 nm.

3.13. Schematic of Ins-Eud-NP-Fc. The Ins-Eud-NP-Fc is prepared from biodegradable and biocompatible polymers like PLGA-PEG and Eudragit S100. Eudragit imparts the NPs an ability to respond release insulin on being stimulated by pH. The targeting ligand, Fc, has been conjugated to the surface of the NPs to enable them to cross the epithelial barrier by using the FcRn transcytosis pathway.

3.14 In vitro transepithelial transport data showed that Ins-Eud-NPs-Fc were transported 5 times more across the Caco-2 monolayer relative to non targeted Ins-Eud-NPs.

A1. Sample and separate and dialysis are the two most commonly used methods for measuring the *in vitro* drug release profile from polymeric nanoparticles.

A2. (A) Insulin release profile at pH 6 and pH 7.4 obtained by analyzing the data using the filtrate. **(B)** Insulin release profile at pH 6 and pH 7.4 obtained by analyzing the data using the supernatant. Both these curves are counterintuitive relative to the expected insulin release profile. The significant difference in the release curve at pH 6 and pH 7.4 is promising data.

A3. (A) Insulin release after 2 h in different incubation volumes shows that the amount of insulin released by the NPs stabilizes at higher NP incubation volumes suggesting that a non-equilibrium state reaches at high incubation volumes. **(B)** Insulin release profile at pH 6 and pH 7.4 obtained by analyzing the data using the supernatant and a large incubation volume of 15 mL. Although the insulin release can be quantified at initial time points, at later time points there is a decrease in the amount of insulin released which seems incorrect.

A4. Amount of insulin detected in the filtrate remained constant across the samples that were washed multiple times. However, the amount of insulin detected in the supernatant decreased as the NPs underwent multiple washes. Ins NP w/o any wash represents the case without any loss of insulin.

A5. On washing the NPs with pH 6 buffer, most of the insulin was retained in the supernatant as compared to the filtrate. This suggested that the analyzing the supernatant would give a more accurate estimation of the insulin content at each time point.

A6. (A) After spinning down a 50 µg/mL insulin solution halfway, the concentration of insulin obtained from the supernatant was 47 µg/mL, similar to the original solution while the concentration of insulin in the filtrate was much lower (28 µg/mL). **(B)** The sum of insulin detected in the filtrate and the supernatant do not add up to the total insulin that was centrifuged, confirming the loss of insulin in the centrifugation device.

A7. (A) On centrifuging down the entire volume of insulin, it was found that the concentration of insulin detected in the filtrate was less than the concentration of the original solution, suggesting that measurements done using the filtrate can be inaccurate. **(B)** The amount of insulin detected in the filtrate was only half of the total amount of insulin in the system. Moreover, the sum of insulin detected in the filtrate and supernatant do not add up to the total amount of insulin in the initial solution, suggesting a loss of insulin.

A8. Insulin left in Ins-Eud-NPs after insulin release at pH 3, pH 6, pH 7.4, and pH 9 initially decreased with time but at longer collection times the amount of insulin left in the NPs increased. However, a pH dependent release is seen from Ins-Eud-NPs as lesser amount of insulin is detected after insulin release in pH great than 7.

A9. (A) Inclusion of a magnetic stir bar in the dialysis device did not help in accurately measuring the insulin release profile. The released insulin failed to diffuse across the membrane fast enough thereby showing an almost constant amount of insulin left in the NPs. **(B)** Insulin release profile obtained by using the stirred dialysis device set-up could not be used to determine the drug release kinetics as there was inadequate release and variability in the data.

A10. Blue food dye also failed to diffuse out of the dialysis chambers in 60 min. Therefore, the current dialysis set-up cannot be used to measure rapid release of insulin from NPs.

A11. Insulin failed to diffuse out of the 10 nm, polycarbonate membrane dialysis chambers in 60 min.

A12. Schematic of the Float A Lyzer dialysis chamber.

A13. Food dye failed to rapidly diffuse out of the Float A lyzer dialysis chambers. Control in water is the food dye solution which was not dialyzed at all. Sample 1

is the food dye solution that was allowed to release food dye all night. It showed very little release of food dye. Lastly, Sample 2 is the sample that was allowed to release the food dye for 6 h with additional stirring inside the chamber.

A14. (A) Schematic of the dialysis set-up using Float A lyzers. To enable continuous stirring of the buffer outside the dialysis devices, the beaker was put on a magnetic stirring plate, which was further placed on an orbital shaker. **(B)** By increasing the convectional flow in the system and by choosing a suitable solvent, majority of the food dye solution managed to escape the dialysis device. Control in PBS is the blue food dye solution that was not exposed to the dialysis set up, while Sample 3 is the sample of blue food dye which was measured after dialysis for 2h 15 min.

A15. (A) Schematic of the Float A lyzer with a magnetic stirrer placed inside it. **(B)** Schematic of the Float A lyzer with an epoxy cylinder placed inside it.

A16. (A) Dialysis of yellow food dye. For both 50 kDa and 100 kDa MWCO dialysis membrane application of the epoxy cylinder is more effective relative to internal stirring. **(B)** Dialysis of blue food dye.100 kDa membrane is more effective than the 50 kDa membrane in allowing rapid diffusion of molecules across the membrane for both cases – stirring as well as moving epoxy cylinder. **(C)** Application of the epoxy cylinder did not seem to have a much greater advantage over using stirring to produce agitation and movement in the dialysis setup.

A17. On comparing the effectiveness of the application of the stir bar relative to the effectiveness of the epoxy cylinder, 50% of the insulin was diffused from the dialysis chambers with internal stirring and 60% of the insulin was released from chambers with the epoxy cylinder. The difference between the half-life of insulin using these two agitation methods was not drastically different.

A18. Release of free insulin solution from Float A lyzer devices (100 kDa MWCO) with internal stirring at 37°C. The half-life of insulin is less than one hour is which is good for measuring rapid release of insulin from polymeric carriers.

A19. Insulin release profile from Ins-Eud-NPs. Insulin releases rapidly at pH 7.4 and a slower release was observed at pH 6. The data has been plotted with the diffusion curve of free insulin solution, which superimposes with the insulin release curve at pH 7.4, indicating that insulin releases instantaneously from NPs at pH 7.4. However, the reduction in insulin release at longer time points continued to be puzzling.

A20. Changing the storage temperature of the NPs collected in between time points did not have a significant effect on the amount of insulin detected form that sample.

A21. On performing a dialysis experiment with only Emp-NPs, the absorbance values increased with time. Here, the absorbance values are plotted for equivalent amount of insulin to emphasize the effect of the data on the insulin release data.

A22. (A) A minor increase in the theoretical value of insulin is detected with an increase in incubation time in samples that were incubated in the Eppendorf tubes but a more prominent increase in the value of insulin was detected in NP samples that were incubated in the Float A lyzer dialysis chambers. **(B)** The value of absorbance obtained from the buffer solution increased with increasing time points. Here, we have plotted the theoretical amount of insulin calculated from the absorbance data.

A23. On incubating the dialysis chambers overnight in buffer and then using those devices to perform a dialysis experiment on Emp-NPs gives an almost constant value with increasing incubation times.

A24. Design of the dialysis set up to study the *in-vitro* release of insulin.

A25. *In vitro* release of Ins-Eud-NPs shows that there is a significant reduction in the rate at which insulin is released from the NPs at pH 6 as compared to pH 7.4. The half-life of insulin in pH 7.4 is between 30-60 min, while the half-life of insulin in pH 6 is 240 min. The release curve of free insulin superimposes on the release curve of insulin at pH 7.4.

A26. On normalized the insulin released in pH 6 and pH 7.4 with respect to the release rate of free insulin solution we can better visualize the difference in the release of insulin at pH 7.4 relative to pH 6.

List of Tables

Table 1. Properties of the semipermeable membrane on which the Caco-2 cells were grown.

CHAPTER 1

INTRODUCTION

1.1 Current trends in biotechnology

The advent of the biotechnology revolution has resulted in the discovery and commercialization of various new biopharmaceuticals[2]. Biopharmaceuticals include peptides, antibodies, and nucleic acids that are designed to have a therapeutic value. Due to improved efficacy, better technology and cutting edge innovation, biopharmaceuticals continue to lead the biotech sector. Figure 1.1 summaries the strengths, weakness, opportunities and threats of the application of biopharmaceuticals[3].

In 1982, after the discovery of the first biopharmaceutical Humulin (recombinant human insulin; Eli Lily, Indianapolis), only eight more biopharmaceuticals were launched in the market in the next decade. Following the approval of the first biopharmaceutical, since 1990s the biotech industry has matured due to a dramatic increase in the number of biologics that have been approved and been launched in the market[2]. Currently, more than 500 peptides are in preclinical development, 140 are in clinical trials, and around 60 have been approved by the FDA[3]. The rate at which these molecules have reached clinical stages has increased over the last decades as seen in Figure 1.2A (4.6 in the 1980s, 9.7 in the 1990s, 16.8 in 2000s, and 128 in 2012)[4-5]. Figure 1.2B shows that the approval rates of biopharmaceuticals in each five-year period since 1995 has been fairly constant, with approximately 54 approved biologics for 2010-2014. Moreover, since the 1990s till 2013, the biotech industry has reached an estimated total sales value of $140 billion as seen in Figure 1.3[2]. Humira (adalimumab) alone generated global sales of $11 billion in 2013 as seen in Figure 1.4. Figure 1.4 also lists the 20-top biopharmaceutical products of 2013.

This economic boom further accelerated and supported the development of several protein-therapeutics. Despite a variety in the kinds of biologics that have been approved since the 1990s, one aspect that remains constant is the way of administering these biologics. The majority of them are designed for parenteral delivery (intramuscular, subcutaneous, intravenous and intradermal, Figure 1.5A). Figure 1.5B shows that approximately 12 billion injections are administered annually with several unsatisfactory outcomes leading to 20 million infections and 100 million toxic reactions[2]. Due to these issues, nonparenteral

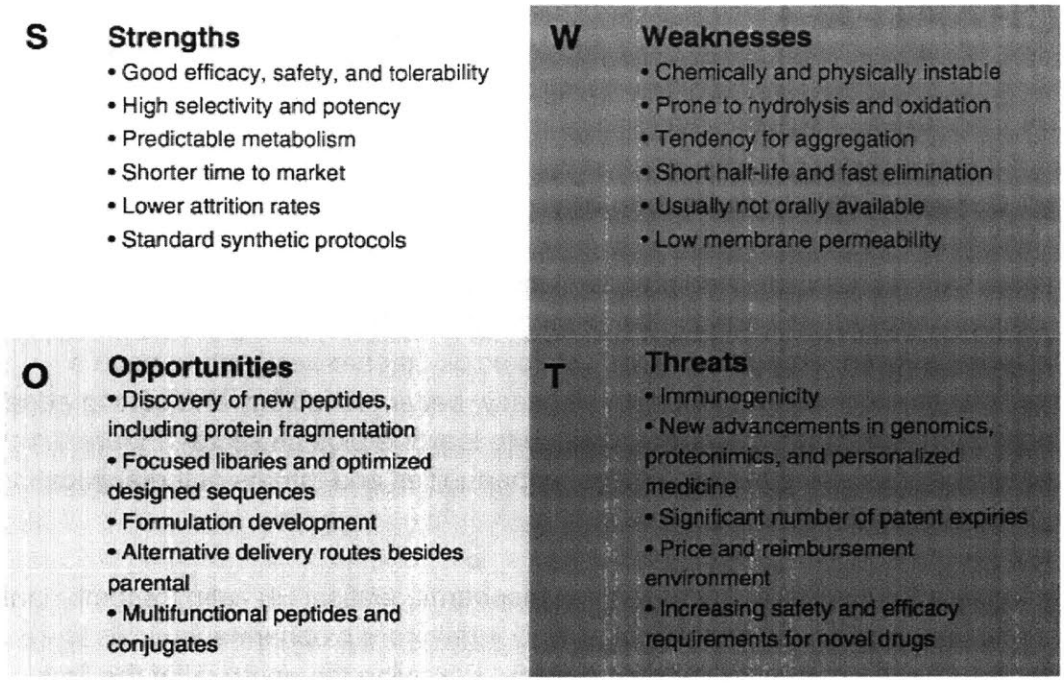

Figure 1.1. Strengths, weaknesses, opportunities and threats of the application and development of biopharmaceuticals.

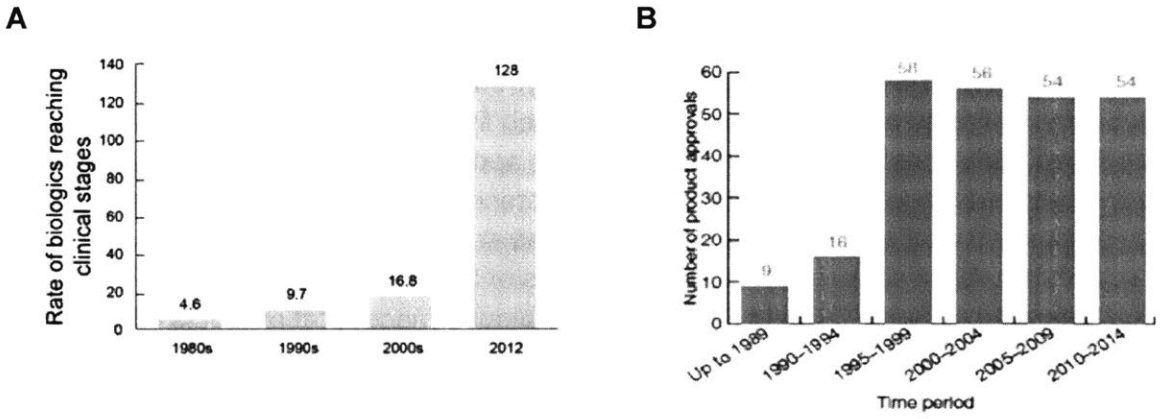

Figure 1.2. (A) The rate at which biopharmaceuticals have reached clinical stages has increased over the last decades with 4.6 in 1980s to 128 to 2012. **(B)** Approval numbers of biopharmaceuticals in each five-year period since 1995 has been fairly constant, with approximately 54 approved biologics for 2010-2014, but approval has significantly increased from early 1990s to now.

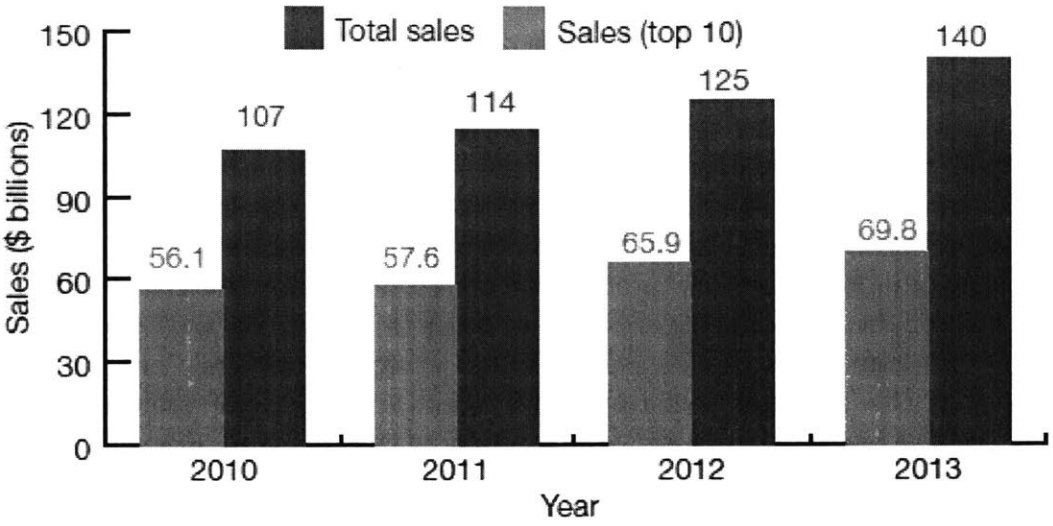

Figure 1.3. Annual biopharmaceutical sales value (cumulative product sales and sales for the ten top-selling products) for the period 2010 to 2013. This shows the increase in the economic value of protein therapeutics.

Ranking	Product	Sales ($ billions)[a]	Year first approved	Company	Patent expiry (EU)	Patent expiry (US)
1	Humira (adalimumab; anti-TNF)	11.00	2002	AbbVie & Eisai	2018	2016
2	Enbrel (etanercept; anti-TNF)	8.76	1998	Amgen, Pfizer, Takeda Pharmaceuticals	2015	2028
3	Remicade (infliximab; anti-TNF)	8.37	1998	J&J, Merck & Mitsubishi Tanabe Pharma	2015	2018
4	Lantus (insulin glargine)	7.95	2000	Sanofi	2014	2014
5	Rituxan/MabThera (rituximab; anti CD20)	7.91	1997	Biogen-IDEC, Roche	2013	2016
6	Avastin (bevacizumab; anti-VEGF)	6.97	2004	Roche/Genentech	2019	2017
7	Herceptin (anti-HER2)	6.91	1998	Roche/Genentech	2014	2019
8	Neulasta (pegfilgrastim)	4.39	2002	Amgen	2015	2014
9	Lucentis (ranibizumab; anti-VEGF)	4.27	2006	Roche/Genentech, Novartis	2016	2016
10	Epogen/Procrit/Eprex/ESPO (epoetin alfa)	3.35	1989	Amgen, J&J, KHK	Expired	2013
11	Novolog/Novorapid (insulin aspart)	3.13	1999	Novo	2015	2015
12	Avonex (IFN-β-1a)	3.00	1996	Biogen Idec	2015	2015
13	Humalog mix 50:50 (insulin lispro)	2.61	1996	Lilly	2015	2014
14	Rebif (IFN-β-1a)	2.59	1998	Merck Serono	2015	2013
15	Aranesp/Nesp (darbepoetin α)	2.42	2001	Amgen, KHK	2016	2024
16	Advate/Recombinate (Octocog α)	2.37	1992	Baxter		
17	Levemir (insulin detemir)	2.15	2004	Novo	[Levemir]	2014
18	Actrapid/Novolin (insulin)	2.02	1991	Novo	2017	
19	Erbitux (cetuximab; anti-EGF)	1.92	2004	Bristol-Myers Squibb, Merck Serono	2014	2016
20	Eylea (aflibercept; anti-VEGF)	1.88	2011	Regeneron, Bayer	2020	2021

[a]Financial data from LaMerie Business Intelligence. J&J, Johnson & Johnson

Figure 1.4. The 20 top-selling biopharmaceutical products in 2013. Humira leads the revenue production in 2013 followed by Enbrel and Remicade.

delivery routes like oral, nasal, pulmonary are preferred because they offer increased patient compliance resulting in improved treatment efficacy. However, some scientists believe that nonparenteral delivery routes will not drastically change the course of treatment and will merely result in better quality of life and treatment experience[2].

Although the mainstay of drug administration for biologics has been parenteral, some progress has been made on the front of nonparenteral drug delivery. One inhaled insulin product Afrezza (MannKind) had been approved in 2012 which is showing great promise[6]. This product was approved after a previous inhaled insulin product, Exubera (Pfizer), failed to deliver in the market and was taken off[7]. Other than this, some key players in insulin production have promising products in the pipeline. Novo Nordisk is currently developing an oral insulin candidate using Merrion (Dublin) technology that uses the GIPET® platform to deliver insulin along with a matrix consisting of medium-chain fatty acids that is designed to release insulin in the duodenum[8] whereas Oramed Pharmaceuticals (Jerusalem) is also working on an oral insulin formulation, which is based on components that protect insulin in the gastrointestinal tract in combination with absorption enhancers[9].

Intercontinental Marketing Statistics (IMS) Health projections suggest that the increasing trend in biologics approval will continue to rise and biologics will continue to increase in terms of overall market share of the pharmaceutical industry (18% in 2012 to 20% in 2017)[2]. Monoclonal antibodies and insulin therapies are expected to lead the spectrum. However, improved nonparenteral methods of delivery can open access to new frontiers and enable better treatment outcomes for several biologics.

1.2 Diabetes and Insulin

Scientists predict that the majority of innovations in alternative routes of drug delivery will be in monoclonal antibodies and insulin[2]. Insulin is a peptide that was discovered in 1921-1922 by Banting and Best, together with Macleod and Collip at the University of Toronto[10] . It is a natural hormone that is produced by the β-cells in the pancreas and controls the level of glucose in the blood by facilitating the uptake of glucose, especially in the liver, muscle and adipose tissue.

After food uptake, carbohydrates are converted into simple sugars, such as glucose. Glucose is absorbed by the intestines and carried to the liver where

much of it is stored as glycogen. The remainder is carried to the muscles and other tissues where it is either oxidized or stored as glycogen. In some cases the body fails to efficiently metabolize glucose and it circulates in increased quantities in the blood (hyperglycemia) and is excreted in the urine (glycosuria). This causes glucose to be unavailable to the body as a source of energy, which results in the conversion of glycogen to glucose so that the body can utilize it to fulfill its energy requirements. This results in a loss of protein in the body as it is converted to glucose. The body produces insulin to facilitate the uptake of glucose by the cells and thus reduce the level of glucose in the blood. In some cases there is insufficient production of insulin, which results in uncontrolled level of glucose in the blood. This condition is called Type 2 Diabetes. It is a metabolic disease in which carbohydrates are not sufficiently utilized by the body, thereby causing a derangement of the normal metabolism of proteins and fats as well as carbohydrates. This derangement of metabolism manifests in increased blood glucose levels, a voracious appetite, hyperglycemia (increase in the percentage of sugar in the blood) and glycosuria (sugar in the urine)[11].

Another type of diabetes, often confused with Type 2 Diabetes is Type 1 diabetes. Currently 5-10% of the people with diabetes have Type 1 diabetes[12]. Type 1 diabetes, also called Juvenile diabetes, mostly develops in children and teenagers, although it can appear at any age in the life cycle of a human. In Type 1 diabetes, the body's immune system attacks part of its own pancreas, for a reason that is not well understood. This results in complete destruction of the β-cells leading to absolute insulin deficiency[13].

Type 1 and Type 2 Diabetes have shown to have an adverse effect on multiple organs. Type 2 diabetes has shown to induce increased cardiovascular issues that can manifest as coronary artery disease, peripheral artery disease, and carotid artery disease[14]. A study has shown that many people with Type 2 diabetes have the same risk of a cardiovascular event as someone without diabetes who has already had their first heart attack[15]. In addition to the macrovasular complications of diabetes, several microvascular complications can also occur due to uncontrolled glucose levels in the blood. These are common in patients both with Type 1 and Type 2 diabetes and include eye damage (sometimes blindness), kidney damage (sometimes requiring dialysis or transplantation), and nerve damage (resulting in amputation, painful symptoms, erectile dysfunction, and other problems)[16-18].

Diabetes is the world's largest endocrine disease associated with increased morbidity and mortality rate[19]. The estimated worldwide prevalence of diabetes in

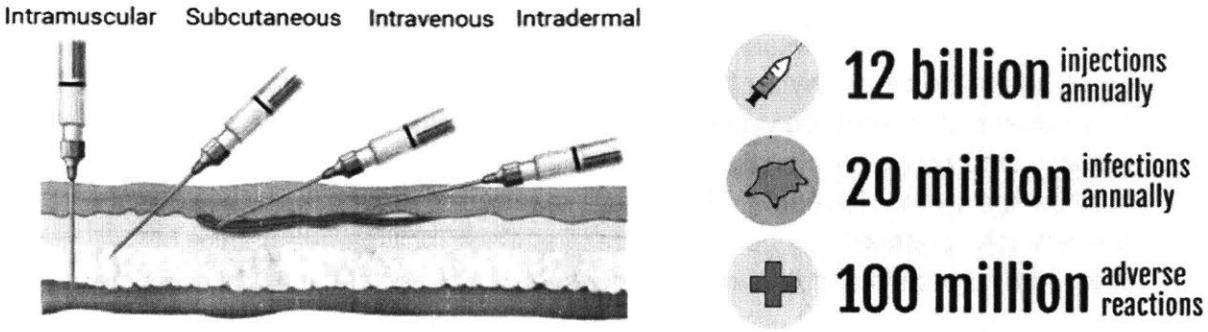

Figure 1.5. (A) The mainstay of drug administration for protein therapeutics via. intramuscular, subcutaneous, intravenous or intradermal injections. **(B)** Due to the popularity of biopharmaceuticals for various disease treatments in the last decade on an average 12 billion injections have been injected which have caused 20 million infections annually and 100 million adverse reactions.

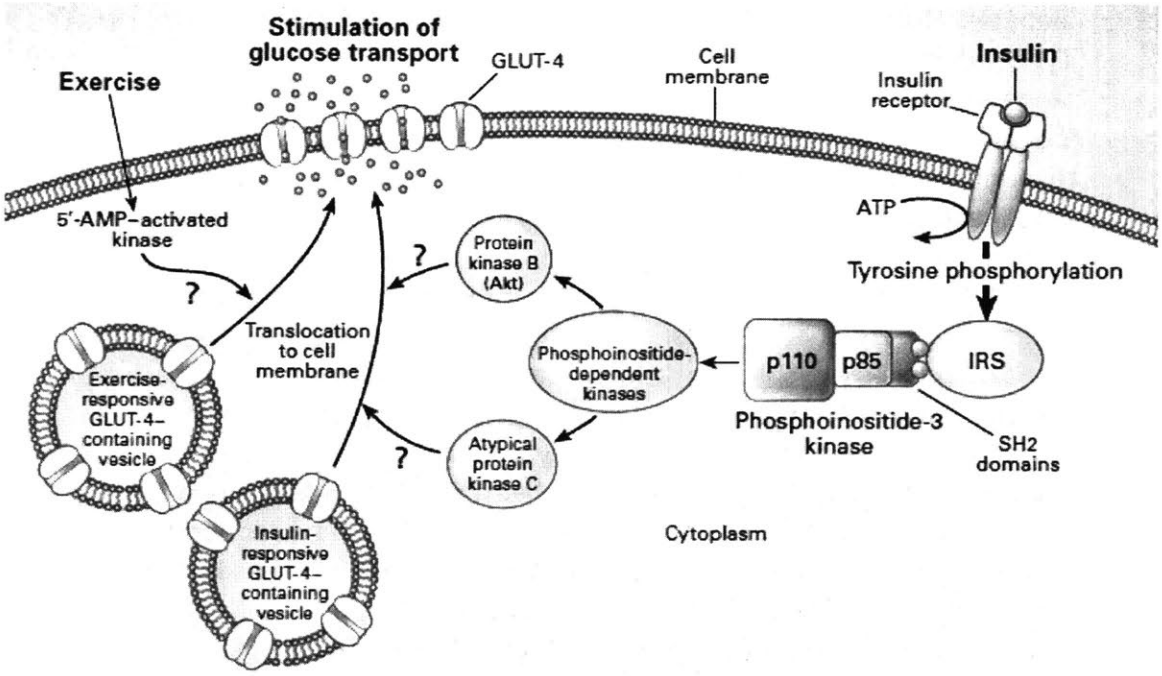

Figure 1.6. Mechanism of how insulin facilitates the uptake of glucose in muscle cells and adipocytes. Insulin binds to the GLUT-4 receptor in the plasma membrane, resulting in phosphorylation of the receptor. Activation of phosphoinositide-3 kinase is a major pathway in the mediation of insulin-stimulated glucose transport and metabolism.

adults (20 to 79 year of age) was 6.6% (285 million people) in 2010 and will increase to 7.8% (438 million people) by the year 2030[20]. More than 471 billions USD were spent on healthcare for diabetes in 2013[21]. Diabetes is generally controlled with the administration of oral medication (Type 2 diabetes) or by the use of insulin injections (Type 1 and more often Type 2 diabetes)[22]. Intake of exogenous insulin is considered as the essential treatment for Type 1 diabetes.

Insulin controls the homeostasis of glucose by binding to its receptors on target cells and facilitates the cells to use glucose as energy. On the advent of increased glucose concentration in the blood (hyperglycemia), the pancreas increase insulin production, because (1) insulin is key in facilitating the cells to intake glucose as use it as an energy source, and (2) insulin also encourages the storage of glucose as glycogen in the liver, muscle and fat cells. Insulin signaling pathways that regulate glucose metabolism in muscle cells and adipocytes make use of the glucose transporter GLUT-4. It is the main insulin responsive glucose transporter and is located primarily in muscle cells and adipocytes. The mechanism of how insulin facilitates the uptake of glucose in cells can be seen in Figure 1.6[23]. Figure 1.6 shows that the insulin-stimulated movement of GLUT-4 is initiated by the binding of insulin to the alpha subunits of the insulin receptor. This stimulates activation of tyrosine kinase phosphorylation at the beta subunits of the receptor, resulting in a cascade of catalytic activity of the receptor. The activated receptor then phosphorylates a number of intracellular proteins, which in turn alters their activity. Several intracellular proteins have been identified as phosphorylation substrates for the insulin receptor such as IRS-1. Binding of insulin to receptors on adipocytes and skeletal muscle cells leads rapidly to fusion of cell vesicles with the plasma membrane and insertion of the glucose transporter GLUT-4, thereby giving the cell an ability to efficiently take up glucose[24]. When blood levels of insulin decrease and insulin receptors are no longer occupied, the glucose transporters are recycled back into the cytoplasm. Unlike the adipocytes and the muscle cells, cells in the brain and liver do not require insulin to facilitate the uptake of glucose in the cells as they do not use GLUT-4 to transport glucose in the cell[23-24].

It has been reported that approximately 20 – 30% of all patients with diabetes take daily insulin injections to maintain their glucose levels in the appropriate range[25]. Depending on the severity of the disease, the treatment using insulin action may require three or more injections per day to meet the required glycemic levels. The need for insulin varies with the kind of diabetes that the patient has, patients with Type 1 fail to produce insulin due to permanent damage to the β-cells and thus require regular insulin to survive, while patients with Type 2

diabetes can possibly manage their condition with diet and exercise along with oral medication to control blood glucose levels. However, if diet and oral hyperglycemic agents fail to provide the needed glycemic control, patients with Type 2 diabetes have no choice but to start a treatment regime centered on the application of insulin.

The insulin molecule contains 51 amino acids. Although it is active as a monomer, during its biosynthesis and storage it assembles to dimers and in the presence of zinc, to hexamers. X-ray analysis has revealed the 3-dimensional structure of the insulin molecule in its hexameric, dimeric and monomeric states. Figure 1.7 shows that insulin, a polypeptide hormone is formed of two chains A (21 amino acids) and B (30 amino acids) that are connected by disulfide bridges. Insulin belongs to the group of peptides called IGF (insulin-like growth factors)[25].

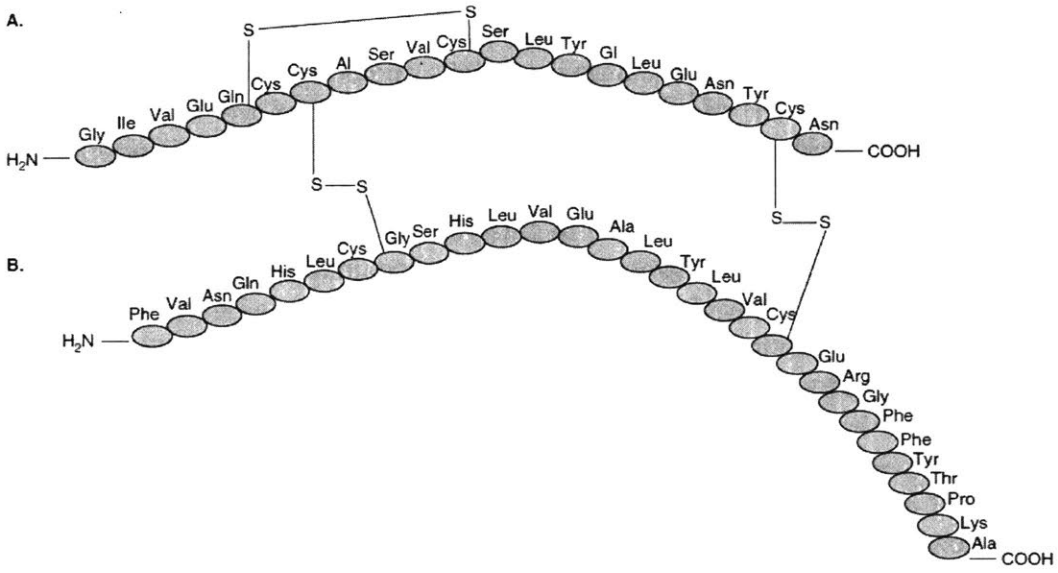

Figure 1.7. Structure of insulin. Insulin, a polypeptide hormone that is formed of two chains A (21 amino acids) and B (30 amino acids) that are connected by two disulfide bridges; an additional disulfide is formed within A chain.

1.3 Methods of insulin delivery

Various forms of insulin have been launched in the market such as short-acting, intermediate-acting and long-acting type insulin, which differ in their duration of action. However, as mentioned earlier all forms of exogenous insulin are

currently administered via injections. The frequency of injections for treatment of a metabolic disease like diabetes where frequent doses for long periods of time need to be taken result in extreme patient incompliance and poor treatment outcomes[26]. The most common route of insulin administration is subcutaneous insulin injections. The present practice is the use of one or more doses of insulin, injected subcutaneously. It can be considered that during a lifetime (75 years) a Type 1 diabetic patient receives nearly 80,000 injections[27]. Despite advances in devices for the injection of insulin (insulin pens and pumps), several approaches for alternative routes of insulin administration have been developed, such as pulmonary, colonic, nasal, buccal, transdermal and oral insulin delivery[28-29]. These have been summarized in Figures 1.8[30] and 1.9.

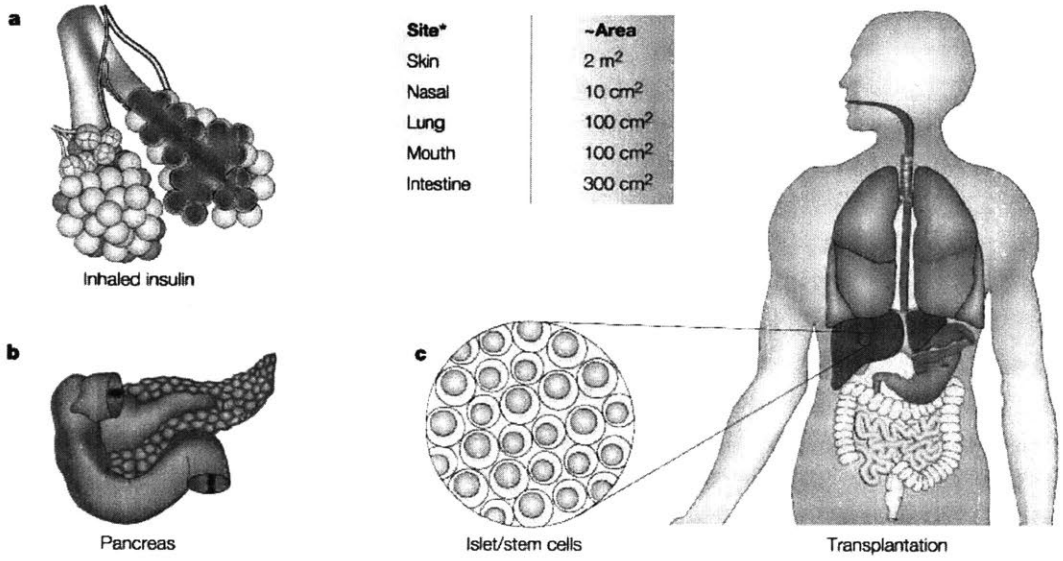

Figure 1.8. Alternative methods of insulin delivery. Various routes of delivery have been investigated for insulin delivery such as pulmonary, oral, transdermal, nasal, buccal and by islet transplantation.

Subcutaneous injections

The most common way of administering insulin is via subcutaneous insulin injections. Here the insulin is administered into the layer of skin, which is directly below the dermis and the epidermis. Usually, patients inject themselves in regions with abundant adipose tissue, to allow slow release into the blood and also to reduce pain. Various improvements have been made to insulin injections ranging from thinner and shorter needles to a more stable syringe body[31-32].

Of these modifications, one that stands out is the development of an injection port called i-port Advance®. It is a device that combines the injection port and the inserter in one device and eliminates the need for multiple punctures for multiple injections. The i-port Advance® can be worn on the patient body for up to 72 hours, and patients can inject themselves multiple times without puncturing themselves multiple times[32]. However, with syringe insulin the main challenges are the cumbersome preparation of inulin dose and the challenge of accurately dispensing what is needed. Since insulin in the vial or syringe form is cheaper, it is a good option for low-income patients.

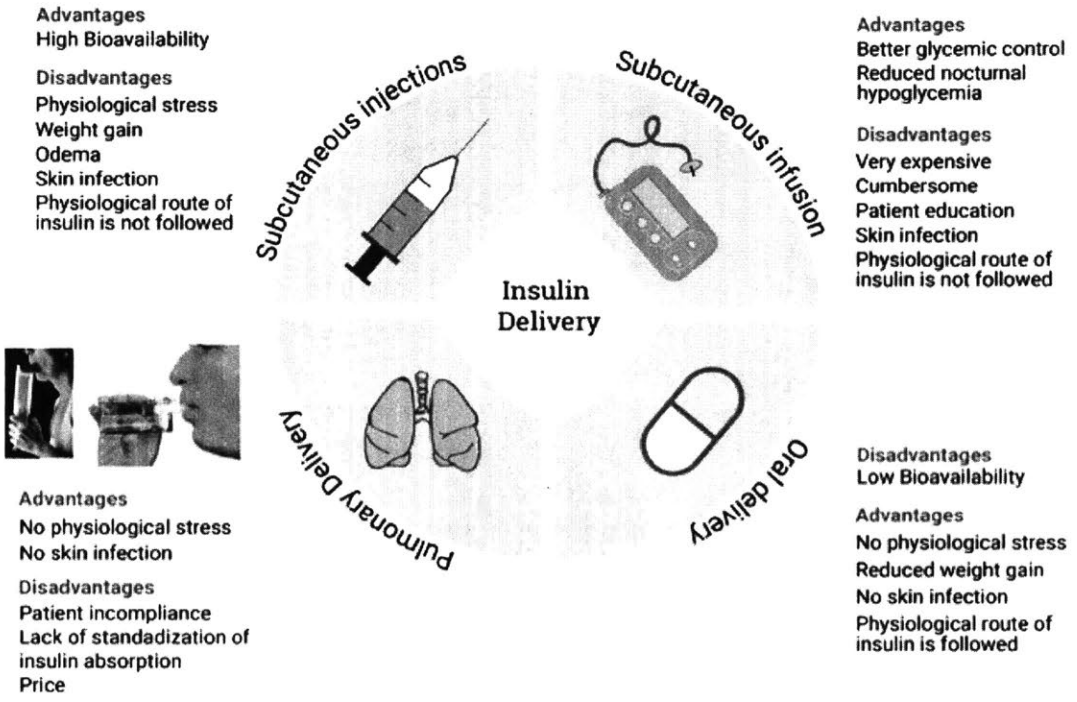

Figure 1.9. The most well examined methods of insulin delivery are subcutaneous injections, subcutaneous infusions, pulmonary delivery and oral delivery. Each of these methods have advantages and disadvantages. However, oral delivery is considered to be the most patient compliant and non-invasive way of administering insulin.

The most popular improvement in delivery of insulin via subcutaneous injections till date has been the insulin pen. The first commercially available insulin pen, NovoPen® (Novo Nordisk A/S Bagsvaerd, Denmark) was launched in the market in 1985[33-34]. Ever since then a series of NovoPens have been launched like NovoFine®, NovoFine Plus®, and NovoTwist® with improvements aimed to

making the process less painful and more accurate. Following the footsteps of NovoPen[34], multiple frugal versions of insulin pens have been launched in the market, which has resulted in improved accessibility and usage. The success of insulin pens resulted in several studies regarding improved needle design and injecting experience. Various needle diameters and needle tip shapes have been investigated and it has been reported that shorter and thinner needles have proven to cause less pain to patients[33]. These achievements in insulin pens have resulted in improved accuracy and a less painful experience for patients. However, despite these advancements patients still have to inject themselves with a needle each time causing psychological discomfort, especially to those who are needle phobic.

Continuous subcutaneous insulin infusion

In normal physiological conditions, large amounts of insulin is secreted by the pancreas in response to the increased glucose level after food uptake, while a small amount of insulin is secreted to control the hepatic glucose output[35]. The exogenous insulin taken by patients via subcutaneous means using insulin pens is unable to sense instantaneous insulin need and provides a predetermined insulin amount that can result in high glycemic variability. In an ideal case, a more physiologic delivery of insulin is desired. This can be achieved with the application of an insulin pump. The first commercially available insulin pump was launched in the market in 1979 in USA[36-37]. Since then major improvements and advancements have been made in the technology of insulin pumps. More portable, lighter, accurate and patient friendly pumps have been developed. Recently, insulin pumps that are capable of continuous glucose monitoring (CGM) have been launched that have open doors for diabetes treatment for Type 1 diabetes patients. Studies have shown that insulin pumps outperform multiple drug injections in achieving high efficacy, better glycemic control and fewer incidents of hypoglycemia[37-39]. However, insulin pumps fail to provide a needle-less solution to insulin delivery. Their application currently is limited by their high price, higher chances of subcutaneous infections, patient inconvenience, social stigma and a theoretical higher risk for diabetic ketoacidosis[40].

Pulmonary insulin delivery

The pulmonary route has an expansive surface area of over 140 m^2, with more than 95% absorptive surface area[29]. This promising physiology led to critical research interest in pulmonary delivery of insulin. Attempts to deliver insulin via the pulmonary route started as early as 1920s[41]. Pulmonary delivery research gained traction when some early studies reported that that delivery insulin via the

pulmonary route using a nebulizer was successful in producing a hypoglycemic response[42-43]. Despite the success achieved in insulin delivery via the pulmonary route, the mechanism of insulin absorption remains unclear. However, some studies have suggested that insulin transport could be dominated by transcytosis and paracellular mechanisms, but the debate around it still continues.

After decades of research US FDA approved the first inhaled insulin product in 2006. It was called Exubera®. Exubera® was a dry powder inhaler form of inhaled insulin. It used compressed air to disperse an insulin powder formulation into a spacer reservoir before inhalation. Powdered insulin (60%) was in a mixture of mannitol, glycine and sodium citrate. In a study where patients were given insulin via Exubera® before meals while the control group received subcutaneous injections 2-3 times a day, inhaled insulin intake showed similar HbA1c outcomes as subcutaneous insulin intake[44-45]. The estimated bioavailability of insulin was 5-6% relative to subcutaneous insulin[44, 46]. However, studies revealed increased hypoglycemia risk for smokers because more insulin absorption happened relative to non-smokers. All patients on Exubera® were also required to get biannual pulmonary function tests that added to healthcare costs[47]. Despite showing initial promise and providing a noninvasive route for insulin delivery, Exubera® was withdrawn from the market by Pfizer in 2007. Many speculate that this can be attributed to increased costs, need for subcutaneous injections while taking Exuber®, potential pulmonary damage, the bulky device and design and social stigma[44, 46, 48]

After the failure of Exubera®, on June 27, 2014, the US FDA approved another inhaled insulin product, Afrezza® (MannKind, Danbury, CT)[49]. It is a ultra-rapid acting inhaled insulin designed to improve postprandial glycemic control in patients with diabetes. This technology is based on drug delivery system developed by MannKind called Technosphere®[50]. This captures peptides by using a diketopiperazine derivative. It has been shown that this formulation self-assembles into a lattice array at low pH and dissolves when it is exposed to the neutral pH on the alveolar surface rapidly releasing insulin[49]. This drug is known to have a more rapid onset of action and a shorter duration of action compared to rapid insulin analogs (insulin aspart, insulin gluisine, and insulin lispro)[51-52]. Afrezza® has shown significant promise so far and can potentially be the breakthrough that was long awaited in the alternative insulin delivery space. However, some side effects that came to the forefront in some clinical trials of Afrezza® were hypoglycemia, cough, and throat pain and irritation[49]. Further studies need to be done on smokers and patients with asthma to see drug efficacy for those patients. However, long-term effect on pulmonary function and

the respiratory tract need to be investigated as well.

In addition to the above inhaled insulin products several products are under clinical trials such as AERx Insulin Diabetes Management System[53], Aerodose[54], ProMaxx[55] (Protein matrix microsphere) and Advanced Inhalation Research. Although the intrapulmonary route has shown a lot of promise, the low bioavailability continues to be a point of major concern. Other challenges associated with intrapulmonary delivery include the need for supplemental subcutaneous injections. Moreover, a long-acting intrapulmonary insulin formulation is expected to not be launched anytime soon. However, after the confirmation of long-term safety of intrapulmonary insulin, it can be called a successful alternate route of insulin administration.

Rectal delivery

Rectal delivery of insulin has gained interest because this route is a more physiological route for the application of insulin. Rectal delivery also allows avoidance of local enzymatic degradation with insulin entering the systemic circulation predominantly via the lymphatic system[56]. Another major advantage is the possibility of partial avoidance of the hepatic first-pass metabolism. However, absorption of insulin from the rectum is inconsistent and bioavailability in humans is very low (4–10%)[57-58]. Insulin absorption requires the application of enhancers or gels, which are another added element that can raise safety and financial concerns. Although some studies show promise this route of insulin administration seems far from realization[59-60].

Nasal delivery

The presence of large surface area for absorption (150 cm^2) makes nasal delivery an attractive route of insulin administration[61]. However, some challenges associated with nasal delivery are the presence of proteolytic enzymes, mucociliary clearance, and low pH of the nasal passage[62]. Various methods have been applied to increase insulin absorption across the nasal lining. Some of them include the application of absorption enhancers and protease inhibitors[63-64]. However, animal studies have revealed that the use of such absorption enhancers has an acute adverse effect on mucosal cells[61]. However, some studies report positive data about the faster absorption of insulin via the nasal route when compared to the subcutaneous route. But the bioavailability via the nasal route remains low (20%) relative to subcutaneous insulin[65]. A study showed that lyophilized nasal insulin in conjunction with sodium glycocholate achieved a glycemic control equivalent to twice daily isophane insulin in patients with Type 2 diabetes[66]. Another study reported that a gel formulation for nasal

insulin showed equivalent efficacy to subcutaneous injections and improved nasal tolerance in Type 1 diabetes patients[67].

Two technologies of nasal insulin that are under investigation are Nasulin™ (CPEX pharmaceuticals) and nasal insulin by Nastech Pharmaceutical Company Inc. Both insulin preparations have bioavailability of about 15-25% with the onset of action ~10-20 min[68-70]. Despite these few instances of promising studies using nasal insulin, nasal insulin is still restricted to laboratory research. Some side effects that have been reported in studies include nasal irritation and potential damage to the nasal mucosa[71-73]. Moreover, studies have not been done to study the effect of insulin in the presence of common nasal issues like the common cold. Current research has been promising but considerable research and work needs to be done in the area of nasal insulin delivery.

Buccal Delivery

Easy access to the oral cavity, large surface area for absorption, and low proteolytic activity of enzymes makes buccal delivery route another attractive insulin delivery route[74]. Studies have reported insulin absorption and bioavailability after the application of absorption enhancers and enzyme inhibitors[75-77]. Previously a study had reported reduction in blood glucose levels in Type 1 diabetes patients, however, this outcome was achieved after multiple applications of the human insulin spray designed for buccal delivery[78]. Due to the potential of insulin delivery via the buccal route, companies including Generex Biotechnology and Eli Lily are developing several products[79-80]. Products that are being developed by these companies are currently in clinical trial and show promise.

Transdermal delivery

Transdermal delivery of insulin is of interest to scientists primarily because of the large surface area of the skin and the absence of proteolytic enzymes, pH changes or degradation agents[81]. However, the main challenge associated with transdermal delivery is the impermeability of the skin to hydrophilic peptides likes insulin. This impermeability can be attributed primarily to the stratum corneum[82-83]. Therefore, much of the work in transdermal delivery has been around improving the permeability of the skin to allow efficient absorption of insulin. Some strategies to improve skin permeability that have been investigated are iontophoresis[84], a technique that uses small electric currents to temporarily makes the skin more permeable in a local area and microdermal abrasion by removing the stratus corneum, and electroporation[85]. Transfersulin is a kind of insulin that has been developed by a group, where they encapsulate insulin in

transferosomes, which squeeze by themselves to deliver insulin through skin pores[86]. Lastly, another group has developed a device, Insupatch that is used in addition to the insulin pump, and by the application of local thermal energy it enables increased absorption of insulin[87-88].

Despite the effort and innovation to enhance the transdermal delivery of insulin, success has been very limited. New approaches, possibly involving combinations of physical and chemical methods should be investigated[89].

Oral delivery

The practice of taking pills orally for majority of diseases has been the most intuitive and patient-compliant way of administering drugs. The frequency of insulin administration led to a need in the development of an oral formulation for insulin. In addition to convenience, patient compliance and improved treatment outcomes, another major reason why oral insulin is so sought after is that insulin action through oral delivery is very close to the natural physiological action of insulin. When taken orally, insulin that is absorbed by the intestinal epithelium reaches the liver through the portal vein and can directly inhibit hepatic glucose output[90].

Even though oral insulin is the preferred route of insulin administration, it is a very challenging problem. The absorption of insulin by the intestinal epithelium is very low due to the large size and hydrophilicity of the molecule. Also, proteolytic enzymes and changes in pH in the luminal cavity degrade insulin. Lastly, the selectively permeable nature of the epithelial lining due to the presence of tight junctions and specific transport mechanisms, doesn't allow small molecules to cross the epithelium with ease[91].

Multiple individual and combined strategies have been devised to enhance insulin absorption when administered orally. These include the co-administration and individual modification of insulin with antiproteases and/or permeation enhancers (such as cyclodextrins, bile salts, and surfactants), mucoadhesives, liposomes, polymeric drug delivery systems[92]. Despite these technological advancements in oral delivery techniques are challenged by reduced insulin bioavailability, poor absorption, and low glycemic control[93]. However, some products show promise and are being currently undergoing clinical trials and FDA approval. Figure 1.10 summarizes some of the technologies that are under development and clinical trials[94]. Other treatment options such as pancreas transplantation and islet-cell transplantation are being investigated. There is increased hope for the success of these strategies due to the advancements and

discoveries in newer immunosuppressant agents[30]. Significant amount of work as also been done in modifying insulin to impart it properties that will enable its delivery through the oral route. One such modified insulin formulation that is currently being evaluated in clinical trials is IN-105[89]. It was launched by Biocon, which is an Indian pharmaceutical company. This is a tablet form of insulin where a polyethylene glycol side chain at position B29 in the insulin structure improves the stability and increases the solubility of IN-105[89, 102]. This form of insulin has shown high absorption and improved solubility. Clinical trials have shown some promising data where the insulin dose has been found to be independent of body weight and significant improvement in postprandial glucose output[103]. Majority of this data was published in 2011, but ever since then the company has not released much information or outcomes of studies. However, in 2012 Biocon signed a contract with Bristol-Myers Squibb giving them the exclusive rights to further develop this technology and also to market it across the globe[93]

1.4 Physiology of the Gastrointestinal Tract

Agents that are orally ingested transit through the gastrointestinal (GI) tract. The GI tract consists of the oral cavity, oesophagus, stomach, small and large intestines. After ingestion, food is exposed to the saliva in the mouth after which it passes through the oesophagus, which is made of a stratified squamous epithelium and the submucosa. The oesophagus is characterized by the presence of a thin mucosal lining and the presence of both voluntary and involuntary muscles[95].

The oesophagus leads food to the stomach. The stomach is known to have a low pH of 1.2-3 due to the secretion of hydrochloric acid by the parietal cells. The cells in the stomach also secrete various digestive enzymes like pepsinogen and gastrin[96-97].

The stomach leads to the small intestine where majority of the chemical and mechanical digestion takes place. The upper small intestine is called the duodenum, which is followed by the jejunum and the ileum. The pH in the intestine ranges to pH 6 in the duodenum to pH 8 in the ileum[98-99]. Almost all the nutrients, electrolytes, and fluids are absorbed in the small intestine. This is possible because it is lined with absorptive cells (enterocytes), which allow selective absorption and also protects the host from unwanted pathogens. Figure 1.11 shows the structure of the intestinal epithelial lining[92].

Company	Name	Product	Action	Development phase	Clinical trials	References[#]
Access Pharmaceuticals, Inc	CobOral™ Insulin	Coated insulin-loaded nanoparticles	Short	Preclinical		accesspharma.com
Aphios Corporation	APH-0907	Nanoencapsulated insulin/biodegradable polymer nanospheres	Short	Preclinical		aphios.com
Biocon/Bristol-Myers Squibb	IN-105	Conjugated insulin	Short	II	NCT01035801 CTRI/2008/091/000276 CTRI/2009/091/000479 CTRI/2009/091/001008	biocon.com, clinicaltrials.gov, ctri.nic.in, Khedkar et al[7]
Diabetology Ltd	Capsulin™ OAD	Insulin with delivery system Axcess™	Short	II		diabetology.co.uk, Luzio et al[11]
Diasome Pharmaceuticals, Inc	HDV-Insulin	Hepatic-directed vesicle-insulin (nanocarrier)	Short	III	NCT00521378 NCT00814294	diasome.com, clinicaltrials.gov
Emisphere Technologies, Inc	Eligen® Insulin	Insulin with chemical delivery agents (Eligen®)	Short	I	NCT00982254	emisphere.com, clinicaltrials.gov, Kapitza et al[13]
Jordanian Pharmaceutical Manufacturing Co PLC	JPM Oral Insulin	Liquid delivery system with insulin chitosan nanoparticles		I		jpm.com.jo, Badwan et al[16]
Novo Nordisk A/S	NN1952	Insulin analog with oral delivery system GIPET®	Short		NCT01028404	novonordisk.com, novonordisk-trials.com, clinicaltrials.gov
	OI338GT (NN1953)	Insulin analog with oral delivery system GIPET®	Long	I	NCT01334034 NCT01931137 NCT01796366	
	OI362GT (NN1954)	Insulin analog with oral delivery system GIPET®	Long	I	NCT01597713	
	OI287GT (NN1956)	Insulin analog with oral delivery system GIPET®	Long	I	NCT01809184	
Oramed, Inc	ORMD-0801	Insulin with protein oral delivery system POD™	Short	II	CTRI/2009/091/000371 NCT00867594 NCT01889667	oramed.com, clinicaltrials.gov, ctri.nic.in, Eldor et al,[17] Eldor et al[19]
Oshadi Drug Administration Ltd	Oshadi Icp	Insulin, proinsulin, and C-peptide in Oshadi carrier	Short	II	NCT01120912 NCT01973920 NCT01772251	clinicaltrials.gov
NOD Pharmaceuticals, Inc/ Shanghai Biolaxy, Inc	Nodlin	Insulin with bioadhesive nanoencapsulation (NOD Tech)	Intermediate	II	ChiCTR-TRC-12001872	chictr.org, Li et al[20]

Figure 1.10. Some oral insulin delivery projects that are under development and clinical trial[94].

The most abundant cells in the small intestine are the enterocytes. They are marked by a dense brush border and are specialized for transporting nutrients across the epithelial lining[92, 100]. Following enterocytes, goblet cells are the next most abundant cells in the intestinal epithelium. The abundance of goblet cells increases from the duodenum to the ileum. Their main function is mucus secretion[101]. The immune action in the small intestine is initiated by the secretion of the paneth cells, which are located in the base of the crypts of Lieberkuhn[102-103]. Another important cell type in the small intestine is the M cells. These are specialized epithelial cells, which are found in the Peyer's patch. M cells have been a cell-type of interest for groups that have designed technologies to allow

passage of insulin carriers across the epithelial lining. They are characterized by a flattened apical surface, fewer cytoplasmic lysosomes, and the absence of mucus covering their surfaces[104]. Studies have shown that M cells can take up foreign objects (antigens, microorganisms) and then deliver it to the underlying region. Due to this ability scientists have readily studied M cells as a passage across the epithelial lining[105].

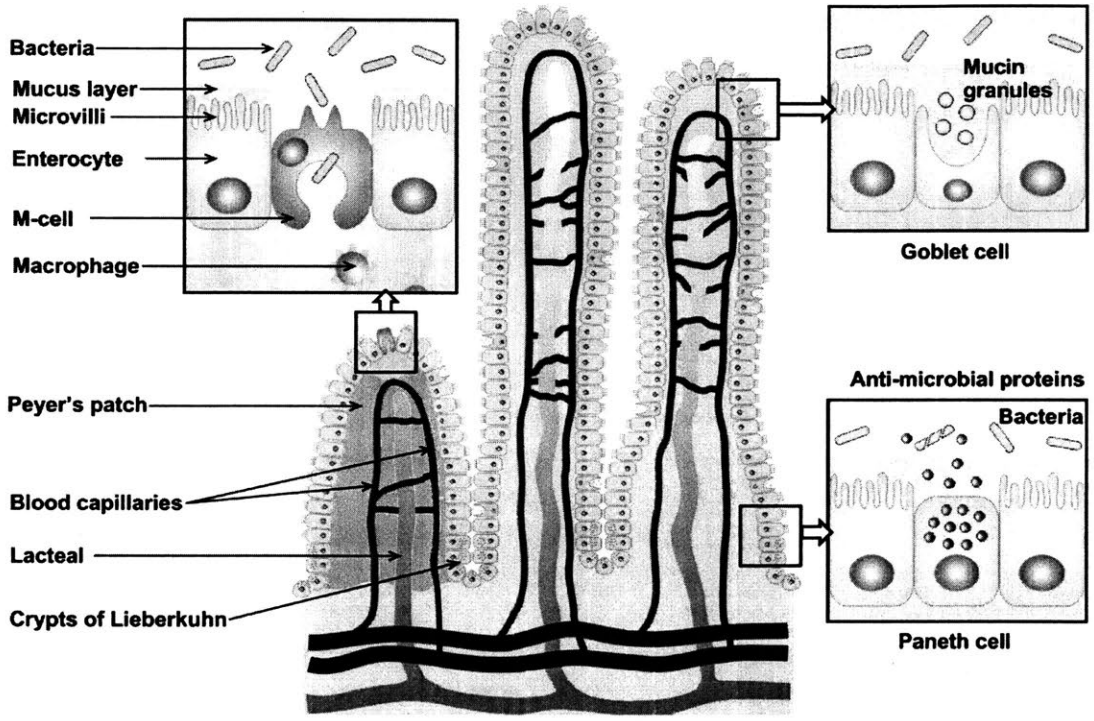

Figure 1.11. Physiology of the intestinal epithelium. Enetrocytes, goblet cells, paneth cells and M-cells are some of the major cell types that make up the intestinal epithelium.

Other than these unique and specialized cell types present in the small intestine, another feature that makes its physiology interesting is the physical integrity of the intestinal epithelium that can be attributed to the presence of tight junctions between consecutive epithelial cells. In addition to the highly selective cells these tight junctions aid in imparting the selectively impermeable character to the epithelial lining[106]. Tight junctions are comprised of a combination of complex transmembrane proteins such as claudins, occludins, and junctional adhesion molecules[107-108]. Due to this unique composition, the intestinal epithelial lining has succeeded in being an efficient barrier preventing pathogens from entering

the body yet allowing efficient absorption of nutrients.

Following the small intestine, digestive products enter the large intestine. By the time they reach the large intestine, the majority of the nutrition and useful products have already been removed. The large intestine carries out the removal of water from the digestive products and passes them in the form of semi solid feces to the rectum[109].

This elaborate gastrointestinal tract efficiently extracts all the nutrients required by the body and also provides a strong barrier to allow passage of unwanted pathogens.

1.5 Barriers to effective Oral Delivery

As mentioned in earlier section, oral insulin is the most desired way of administering insulin not just due to high patient compliance and improved treatment outcomes but also because oral delivery of insulin can mimic the physiological fate of insulin and potentially provide better glucose homeostasis[98]. However, although oral insulin is an extremely desirable solution, it is a highly challenging task. The challenges of oral delivery are primarily due to the innate structure and physiology of the GI tract in addition to the large size and hydrophilic nature of insulin. The orally administered protein drugs such as insulin are normally degraded by the chemical and enzymatic action in the GI tract. The intestinal transport of such drugs is also limited due to the absorption barriers present in the intestinal epithelium[110]. Insulin faces three main barriers, which make oral insulin delivery challenging – chemical barrier, enzymatic barrier and absorption barrier. These barriers have been summarized in Figure 1.12. Thus, understanding the characteristics and function of these barriers is essential in designing an effective carrier for oral administration of insulin.

The complex chemical environment in the GI tract makes insulin stability a big issue. Insulin is a peptide, which makes it susceptible to degradation by the harsh chemical environment. Throughout its transit along the GI tract it is exposed to a large variation in pH ranging from acidic in the stomach (pH 1.2-3) to basic in the small intestine (pH 6-8)[111]. The drastic change in the pH in the GI tract can potentially cause pH-induced oxidation, deamidation or hydrolysis of protein drugs resulting in a loss of their biological activity[110].

The proteolytic enzymes in the GI tract digest majority of orally administered proteins and break them down into smaller fragments that can be absorbed by

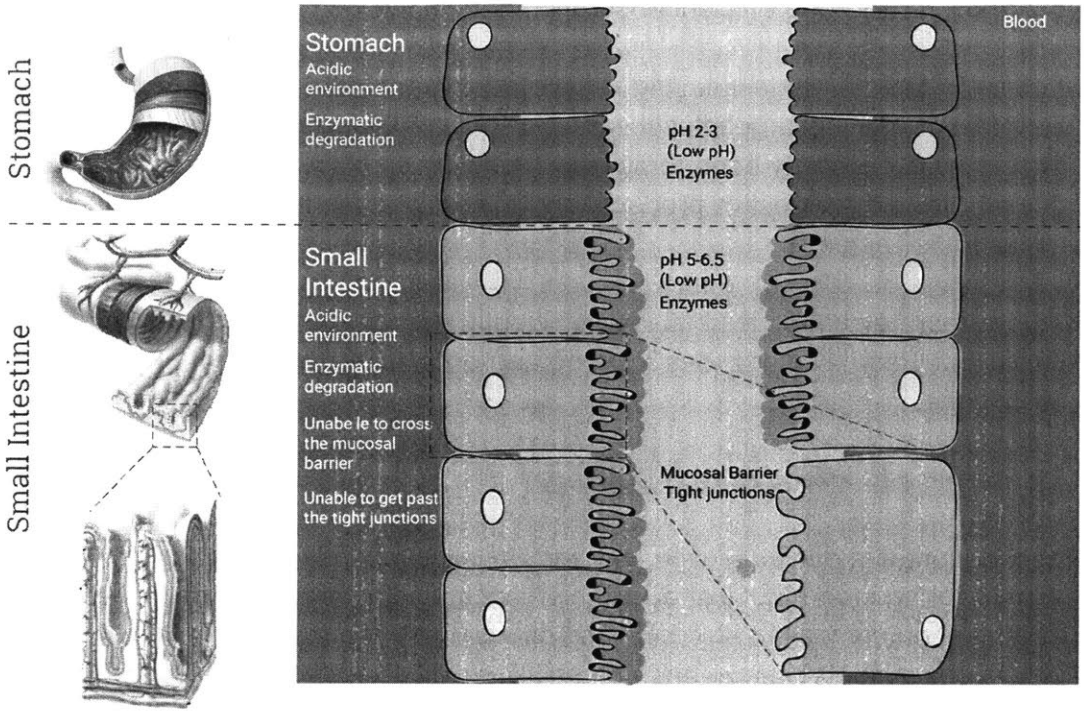

Figure 1.12. Barriers to effective delivery of insulin. Various chemical and physical barriers like changes in pH, high protease action and the presence of tight junctions make the problem of oral delivery very challenging.

enterocytes[112]. Insulin being a protein drug is also susceptible to this enzymatic degradation. Enzymatic degradation of orally administered protein drugs begins in the stomach where pepsin is secreted, and then, in the small intestine the degradation continues due to the presence of pancreatic enzymes such as trypsin, chymotrypsin elastase and carboxypeptidases[113]. Among the various proteases mentioned above, insulin is mainly degraded by trypsin, chymotrypsin and carboxypeptidases in the intestinal lumen as well as in the mucus layer[114]. Additionally, insulin can be degraded by specific enzymes in the cytosol such as the insulin degrading enzyme. Lastly, the extensive first-pass metabolism by liver microsomes further reduces the dose fraction of insulin that would have potentially entered systemic circulation[115-116].

Other than the pH changes and the enzymatic degradation, another major challenge is presence of multiple physical barriers, which significantly reduces insulin absorption. The first barrier encountered by such drugs is the mucus layer, which functions as a diffusional and enzymatic barrier and replenishes itself every 4-5 h[117-118]. The mucus lining prevents the passage of external

pathogens across the epithelial lining[117, 119]. The mucus lining poses another challenge due to its net negative charge. Drugs that are positively changed get stuck in the mucus lining due to electrostatic attraction and drugs that are negatively charged get repelled. Insulin is net negatively charged at physiological pH and is expected to face electrostatic repulsion[117]. If a drug is able to bypass the mucus barrier, the next line of barrier is the intestinal epithelium. It has been reported that drug permeation may occur across the epithelium, either through the transcellular or paracellular routes[120]. For oral drugs, especially those that are liphophilic below molecular weight of 700 Da, transcellular passive diffusion is more common[121]. Most protein drugs are hydrophilic with a MW exceeding 3000 Da, making it difficult for them to traverse through the cell membranes[110, 122]. Transport across the intestinal epithelium via the paracellular route is minimal, due to the presence of tight junctions[106]. Only small hydrophilic drugs, with a MW of less than 200 Da, can transport through the paracellular pathway. In the absence of permeation enhancers, protein drugs are generally excluded from this route[107-108]. Consequently, despite the availability of different transport pathways, most protein drugs possess an inadequate absorption following oral administration.

Together both the chemical and the physical barriers to oral insulin delivery make this an extremely challenging problem. An ideal oral insulin solution should be designed to circumvent or bypass these barriers. Hence it will have to use multiple strategies and techniques to successfully deliver insulin across the intestinal lining with high bioavailability.

1.6 Strategies for Oral Delivery

The chemical, enzymatic and absorption barriers presented by the GI tract pose major challenges to oral delivery of protein drugs. Several strategies such as the use of permeation enhancers, mucoadhesives, protease inhibitors and polymeric drug delivery carries have been studied to improve oral delivery of protein therapeutics. This section deals with each of the strategies and highlights the advantages and disadvantages associated with each.

1.6.1 Permeation enhancers

Permeation enhancers, as the name suggests help make the epithelial lining more permeable to allow easy passage of drugs by enhanced paracellular and transcellular transport. Permeation enhancers such as bile salts, fatty acids, surfactants, salicylates, chelators and zonula occludens toxin are some common enhancers that have been studied extensively[123]. They enable increased

transport of drugs across the epithelial lining by either increasing membrane fluidity, decreasing mucous viscosity or by temporarily opening up the tight junctions. Bile salts and fatty acids are most commonly used to increase permeability of the lipid bilayer cell membrane of the intestinal epithelium[124]. A study where insulin was dispersed in a fatty acid matrix emulsified with sodium glycocholate showed the desired hypoglycemic effect on rabbits when delivered orally[125]. Insulin associated with micelles in conjunction with bile salts has shown to increase the permeation of insulin by accessing a paracellular pathway[124]. In addition, a significant decrease in plasma glucose levels has been observed in a study where insulin was encapsulated in an enteric coating along with permeation enhancers like sodium salicylate[126]. The use of bile salts and fatty acids is non-specific and causes uncontrolled permeations in the epithelial lining. To overcome this challenge a permeation enhancer, zonula occludens toxin (ZOT) has been studied, which works by increasing the permeability of the tight junctions. It acts without compromising the overall intestinal lining; its action is reversible and effective[127]. An *in vivo* study using ZOT has shown a 10-fold increase in insulin absortion in rabbit ileum and jejunum but had no effect on insulin absorption in the colon[127].

A permeation enhancer based product that has reached clinical trials is Capsulin It is an enteric-coated capsule that is filled with human insulin in addition to absorption and solubility enhancers[128]. The outer coating is designed to protect insulin from proteolytic enzymes as well as low pH and the absorption and solubility enhancers are utilized to improve insulin absorption.Capsulin is another insulin formulation, which is being developed by Diabetology using their patented Axcess delivery system. The application of Capsulin in patients in clinical trials has failed to produce a clear dose dependent plasma insulin response[128]. Moreover, in a study with 16 patients with Type 2 Diabetes who consumed Capsulin twice daily before meals failed to show the desired glycemic response[129]. Despite some shortcomings, Capsulin technology continues to improve and further get developed[128-129]. In July 2012, Diabetology announced an exclusive license agreement with USV Limited, an Indian pharmaceutical company, to develop and commercialize oral insulin in India[94]
ORMD-0801 is another technology based on the application of permeation enhancers that has reached advanced clinical studies. ORMD-0801 is an oral insulin formulation developed by a company, Oramed based on their patented technology called Protein Oral Delivery (POD)[94]. This includes the design of an enteric-coated capsule that protects insulin from enzymatic degradation and pH changes during its journey through the stomach and the gastrointestinal tract and releases the insulin in the small intestine[130]. The technology also uses additional

absorption enhancers that consist of known pharmacopeia additives with a well-studied safety record[8] in conjunction with the enteric coating. ORMD-0801 has undergone extensive clinical testing in multiple Phase 1 and 2 clinical trials. In some patients ORMD-0801 worked well and produced the desired glycemic control while in others it showed no effect (for example in a study ORMD-0801 showed no effect in 3 out of 8 patients)[131]. Therefore, the lack of reproducibility and consistency in insulin action in a wide span of patients is the biggest shortfall of ORMD-0801[132].

Despite these improvements and the development of promising technologies the use of absorption enhancers continues to be limited by the fact that once cell membranes are permeabilized or tight junctions are opened, transport is enhanced not only for peptide and protein drugs but also for undesirable toxic molecules present in the GI tract[122].

1.6.2 Protease inhibitors

Since insulin is a peptide drug it is highly susceptible to degradation by trypsin, α-chymotrypsin, and elastase, and to a lesser extent, by brush-border membrane-bound enzymes[133]. For the successful delivery of insulin it is imperative to ensure its protection from digestive enzymes. Various strategies have been put in place to prevent enzymatic degradation of insulin such as the use of enteric coatings, polymeric carriers and hydrogels[133].

Another well studied and broadly applied strategy is the use of enzyme inhibitors. Enzyme inhibitors are administered along with insulin and their action inhibits the enzymes from degrading insulin. A study done by Yamamoto et al. evaluated the effects of five different enzyme inhibitors— sodium glycocholate, camostat mesilate, bacitracin, soybean trypsin inhibitor, and aprotinin— on the intestinal metabolism of insulin in rats[134]. The results of the study indicated that sodium glycocholate, camostat mesilate, and bacitracin were effective in improving the physiological availability and bioactivity of insulin in the large intestine. However, none of these enzyme inhibitors was effective in the small intestine[134]. Other studies have also investigated the use of enzyme inhibitors and their action in different regions of the GI tract[135-139]. A particular area of interest has been the co-administration of enzyme inhibitors with mucoadhesive or regular polymer matrix or drug carrier. Studies with their co-administration have shown successful protection of insulin against trypsin, α -chymotrypsin, and elastase[140].

However, the use of enzyme inhibitors has been intensely debated primarily due

to the lack of specificity of enzyme inhibitor action. Since they deactivate multiple nonspecific enzymes they do not degrade regular proteins that need to be degraded. This can result in toxic effects and can potentially alter the normal physiology of the GI tract due to insufficient break down of food proteins.

1.6.3 Mucoadhesives

The role of mucoadhesives is to increase the adhesion between polymeric carriers and the intestinal mucosa, thereby increasing the residence time at the site of drug absorption to increase the drug concentration gradient[141]. The residence time of the polymer has to be well tuned with the half-life of the payload. If the payload gets released after the replenishment of the mucus, the payload along with the mucoadhesive carrier gets scarified along with the mucosal cells[142]. Mucoadhesives are usually co-administered with protease inhibitors to provide an additional mechanism of protection for insulin degradation[143-144].

Several polymers are known to show promise in the application of oral delivery because they exhibit a dual property of mucoadhesiveness as well as the ability to protect from proteolytic enzymes. Examples of some mucoadhesive polymers are poly(lactic acid), poly(sebacic acid), poly(lactic-co-glycolic acid) and poly(methacrylic acid)- poly(ethylene glycol)[145-149]. These interact with the mucus via hydrogen bond formation, polymeric entanglement with mucins or/and hydrophobic interactions. A well-studied way of using mucoadhesive materials for oral insulin delivery has been the development of pH responsive polymeric carriers. One such study used poly(methacrylic acid)- poly(ethylene glycol) as a pH-responsive carrier to form microparticles which was successful in producing a greater glycemic response without damaging the mucus[149-151]. Another successful strategy of using mucoadhesive polymers like poly(methacrylic acid)-poly(ethylene glycol) has been the formation of multifunctional pH-dependent hydrogels which showed a high (~10%) pharmacological availability of insulin[152-153].

Despite these advancements in the application of mucoadhesives, more work is needed to tune the materials to deliver the payload with more control and precision before the end of the material residence time.

1.6.4 Polymeric drug carriers

Polymeric drug carriers have gained added interest in the last few decades as a potential solution of oral formulation. Multifunctional microparticles and nanoparticles have shown to have the capability of providing solutions to multiple issues that pose a challenge to oral delivery of insulin. By using the appropriate material NPs can protect insulin from the harsh pH environment and enzymatic degradation in the GI tract, the surface of NPs can be functionalized with targeting ligands that can enable the transport of insulin drugs across the epithelial lining, control the release rate, and target drug delivery to specific intestinal sites[154]. The small size increases the specific surface area, allowing increased contact area with the epithelial surface and a greater potential for non-specific uptake by cells through transcytosis endocytotic pathways.
It has been shown that pathogens and microparticles smaller than 10 μm enter the gut-associated lymphoid tissues (GALT) while the submicron particles enter the intestine via M cells and enterocytes, and by paracellular routes[155].
Traditionally, M cells have been targeted for oral delivery because they have less protease activity, a relatively sparse glycocalyx surface and are known to transport molecules across the epithelial barrier through a transcytosis pathway[156-157]. However, some issues associated with transport across the epithelial lining using M cells is that they are fewer in number as compared to enterocytes and after transport the payload gets delivered to the underlying dendritic cells and lymphocytes which can harm the payload by an immune response. Therefore, targeting M cells may be a promising approach for developing oral vaccines but it is not ideal[155].

Various polymeric materials have been used to design microparticle and nanoparticle drug carriers such as dextran[158-159], chitosan[160-162], poly(lactic acid) (PLA)[163], poly(glycolic acid) (PGA), poly(lactic-co-glycolic acid and poly(methacrylic acid)[164-165]. in particular, a class of well-studied polymeric drug carriers is the liposome. Liposomes have shown promising results in being carriers for oral delivery of insulin. In a study, double liposomes containing insulin were examined in combination with aprotinin[166]. In a similar approach, Zelihagül et al. investigated the penetration properties of various liposome formulations containing insulin through a Caco-2 cell monolayer. They found that the oral co-administration of insulin and sodium taurocholate incorporated liposomes significantly decreased blood glucose levels[167]. Liposomes are promising carriers for oral delivery of insulin. However, some issues associated with their application are that it is challenging to synthesize sub-100 nm liposomes, which would be ideal for transport of insulin across the intestinal epithelium.

Microparticles are another well-investigated polymeric carrier. Various methods like, double and single emulsion[168], solvent displacement (nanoprecipitation) methods[168], and layer-by-layer self-assembly[169] technique are used to synthesize microparticles. A study showed the development of alginate – chitosan microcapsules that provided a simple method for controlling the loading and release of protein molecules within polysaccharide microcapsules[170]. Chitosan has been used extensively to develop microparticles and nanoparticles because of its excellent properties that make it mucoadhesive and help to enhance permeation of the epithelial lining[171]. However, the future of chitosan based particle based drug carriers is dependent on the advancements made in the ability to control the carrier size and improve size distribution of chitosan particles. Issues related to poor bioavailability and repeatable release behavior also limit the use of chitosan particle based systems[172]. Due to the complex chemical environment of the GI tract, pH responsive polymeric particles have been area of interest for scientists. For this purpose Eudragit S100 microspheres have been developed which show potential to act as an oral carrier for peptide drugs like insulin[173]. Since size of microparticles exceeds the minimum size required for ligand based transcytosis pathways, microparticles have not been designed for the application of transport pathways. However, one microparticle based technology has reached advanced clinical stages. This non-acylated amino acids microparticle carrier for insulin was developed by Emisphere Technologies [30]. Here, insulin is designed to diffuse through the lipid bilayers before non-covalent complex dissociated after crossing the epithelial-cell membrane[174]. Data from the clinical trials reports faster absorption of insulin relative to subcutaneous insulin but also faster clearance of insulin (within 2 h). In 2010 Emisphere announced an exclusive license and development agreement with Novo Nordisk to develop oral formulations of Novo's insulins using Emisphere's delivery technology (Eligen)[94].

However, it is essential to be able to achieve precise and targeted delivery of insulin. For targeted delivery solutions polymeric nanoparticles have been studied because their size can be modulated to meet the size requirements of multiple transport pathways. NOD Pharmaceuticals, a Chinese subsidiary has developed a patented nanoparticle (NP) based oral insulin formulation called Nodlin. In this technology insulin in encapsulated in NPs that are embedded in an enteric coating capsule[175]. This oral form of insulin is designed to supplement basal insulin. Therefore various clinical studies have been done where the efficacy of Nodlin has been compared with the efficacy of injected Humulin[175]. Although the overall response to both forms of insulin was similar, a major

difference in the metabolic effect was observed[94]. Studies continue and strategies of improving the existing Nodlin technology are underway.

To ensure efficient delivery, other NP studies have resulted in the development of NP solutions that are designed to exploit a particular transport pathway. One such pathway that has been investigated is the folic acid pathway, which is mediated by the folate receptor. This receptor has been used in targeted drug delivery in cancer treatment formulations[176], protein delivery[176] and gene delivery[177]. Jain et al. reported the successful development of folate – decorated PLGA nanoparticles designed for oral delivery of insulin. These NPs exhibited a two-fold increase in the oral bioavailability as compared to subcutaneously administered insulin solution. Their study concluded that these NPs would be sufficient to control blood glucose for 24 h after one time administration. However, a challenge associated with their widespread utilization is the low expression of the folate receptor in healthy enterocytes[178].

Another pathway, the Vitamin B_{12} transport pathway is one of the most extensively studied transport pathway for oral delivery of peptides. Vitamin B_{12} is also called the Cobalamin (Cbl). It is a large molecule that must be bound to specialized transport proteins to gain entry to the cells. In oral administration systems it is known to bind to intrinsic factor (IF), a protein released from the parietal cells in the stomach and proximal cells in the duodenum. The Cbl-IF complex then binds to the IF-receptor located on the surface of the ileum and is internalized by the cells[179]. It has been shown that in humans, uptake of cobalamin is approximately 1 nmol per intestinal passage. Vitamin B_{12} pathway has been used for the transport of luteinizing hormone releasing factor[180], erythropoietin[181], alpha-interferon[182] and insulin[183]. Chalasani et al. reported a 29.4% pharmacological availability of insulin delivered via Vitamin B_{12} coated dextran NPs relative to subcutaneous insulin. These NPs resulted in a reduction of glycemia by 70 – 75% within 5 h, with basal levels being attained in 8 – 10 h in STZ diabetic rats[159].

Another targeted transport pathway is the transferrin pathway. Transferrin plays a role in the uptake of iron by the cells and tissues. Transferrin receptors (TfRs) have been widely explored for receptor-mediated delivery of anticancer agents[184-185], in enhancing the transport of drugs across the blood brain barrier[186-187], and also transport across the epithelial cells of the intestine[188]. Transferrin can be chemically conjugated to the drug/payload. This complex then binds with the TfR on the cell surface. This binding is sensed by the cells and results in an uptake of the Tf–TfR complex. The association between transferrin

and the TfR is a pH sensitive association. Due to a reduced pH in the endosomes, on reaching the endosomes the association between transferrin and TfR breaks and transferrin is recycled to the cell surface[28]. It has been shown that in polarized cells such as the epithelial and endothelial cells, transferrin can be transcytosed from the apical to the basolateral membrane[189]. The presence of transferrin receptors in high densities in human GI epithelium[190], and the ability of transferrin to resist tryptic and chymotryptic degradation makes it a very promising receptor[191]. In 1996 Shah et al. successfully conjugated transferrin to insulin via disulfide linkages and demonstrated that the conjugation resulted in 5–15-fold increase in insulin transport across Caco-2 cell monolayer[192].

Another pathway, the FcRn pathway has shown promising results in the development of targeted polymeric NP based drug delivery platforms[1, 193]. The neonatal Fc receptor (FcRn) is responsible for mediating IgG transport across epithelial barriers. Recently, Eric et al. reported that with the successful conjugation of the Fc ligand on the surface of PLA-NPs, a substantial glucose reduction and control was demonstrated in in vivo studies. The bioavailability of insulin was reported to be 10%[193]. Due to the abundance of the Fc receptor in the human GI tract and the promise shown by this pathway, we discuss it in greater detail in the next section.

Since transport pathways like the ones mentioned above do not cause the tight junctions to open even momentarily, this approach is most desirable in terms of toxicity and damage to the epithelium.

1.7 FcRn Transcytosis pathway

The intestinal epithelium forms a selective barrier that prevents foreign bodies from crossing the epithelial lining and reaching the underlying tissue. As mentioned in the previous section various strategies have been devised to circumvent this barrier and successfully transport drugs across the intestinal lining. However, the multiple pathways mentioned in Section 1.6.4 tested for oral insulin delivery have their share of advantages and disadvantages. Some are limited by the low abundance of their respective receptor while the others are limited by the challenge of conjugating the ligand to the payload. One particular pathway that has shown potential as an efficient pathway for transporting NPs across the intestinal lining is the FcRn pathway[1, 193].

The neonatal Fc receptor (FcRn) is primarily responsible for mediating serum IgG transport across epithelial barriers. It plays a significant role in early life in the

transport of IgG from mother to fetus and neonate for passive immunity and later in the development of adaptive immunity[194]. The FcRn is able to fulfill these roles due to the efficient bidirectional transport of IgG across epithelial barriers. In addition to this, FcRn is the homeostatic receptor responsible for extending the serum half-life of albumin in adults[195].

Other than the intestines[194, 196], FcRn is also expressed in many other tissues in the adult animal, such as the vascular endothelium[197], lungs[198-199], the blood–brain barrier[200], and the glomerular filter in the kidneys[201-202]. However, FcRn is not highly expressed in the intestine of adult rodents, which imposes a challenge for *in vivo* tests[203-204]. In epithelial tissues, FcRn is known to facilitate the bi-directional transport of molecules from the apical-to-basolateral as well as basolateral-to-apical by a pH sensitive mechanism as shown by Dickinson et al.[194]. Fc binds with FcRn at pH less than 6.5, and interaction between Fc and FcRn weakens at pH greater than 7-7.4 and causes the FcRn to release the Fc. The FcRn gets recycled and is able to transport multiple Fc molecules cross the epithelial lining[205].

Structurally, FcRn is composed of a α-chain homologous to Major Histocompatibility Complex (MHC) class-I like molecules and a soluble light chain, β-2 microglobulin[206]. Under slightly acidic conditions (pH 6-6.5), FcRn binds with the CH_2 and the CH_3 domains of heavy chains in the Fc region of the IgG and releases the IgG at neutral-to-basic pH (pH 7–7.4)[207]. The pH dependence is induced by the protonation of histidine residues located at the interface of CH_2 and CH_3 domains of the Fc region of IgG, at acidic pH that aides in the formation of salt bridges with acidic residues on FcRn surface. Formation of these salt bridges is instrumental in stabilizing the hydrophobic interactions between Fc and FcRn at acidic pH[208].

The FcRn pathway has been used to increase the half-life of protein drugs and also to transport drugs across epithelial barriers such as the intestinal epithelium and the pulmonary mucosa. Various proteins, such as erythropoietin[209], follicle-stimulating hormone[209-210], interferon-alpha and -beta, have been conjugated to the Fc region of human IgG to facilitate such drug delivery upon inhalation through the upper airway where FcRn resides in humans and non-human primates[211]. Recently, Pridgen et al. showed the successful transport of Fc conjugated insulin-loaded PLA-PEG NPs across the intestinal barrier, resulting in efficient transport and delivery into the systemic circulation. The study showed a pharmacological bioavailability of insulin of 10%[1].

Therefore, the FcRn pathway shows immense promise owing to its abundance across multiple epithelial tissues across the body; particularly the intestines and the easy conjugation and repeatability associated with this pathway make it an attractive pathway for investigation and optimization.

1.8 Desired characteristics in a NP based oral drug delivery solution

Designing NPs for oral delivery of insulin using pathways like the FcRn pathway require the development of small NPs; both *in vitro* studies using Caco-2 cells (human adenocarcinoma cell line) and *in vivo* studies in rats have shown that the uptake of smaller NPs (~100 nm) is significantly more efficient than that of larger NPs (500 nm, 1 μm, 5 μm)[193]. However, it has been challenging to achieve high loading of hydrophilic protein drugs, including insulin, in PLGA-PEG or PLA-PEG NPs while maintaining small NP size, because the hydrophobic core (*i.e.*, PLGA and PLA) resists interactions with the hydrophilic protein drugs[212]. For example, the insulin loading in the NPs used in the FcRn study was low (~0.5 wt %)[1]; assuming 10% bioavailability and typical insulin dose of ~3 mg per dosage[213], a 0.5 wt % loading translates to an impractically high oral intake of ~6 g NP/dosage. On the other hand, although some studies have shown high insulin loading in particles[214-216], the particle size (17.4 μm – 120 nm) is too large to permit use of transcytosis pathways to cross the epithelial barrier of the intestine.

Moreover, once the NP surface is decorated with a transport ligand, it becomes an even more attractive target for macrophages. Therefore, it is important to design a NP system, which can protect insulin from the harsh chemical environment in the GI tract and from the action of degradation enzymes as well as to release majority of the insulin before the NPs are opsonized by the macrophages.

Hence, the main challenges associated with making NPs that can efficiently deliver large protein molecules across the intestinal epithelium are: (1) to ensure that the NP diameter is small (less than 100 nm), (2) to ensure that the NP has a high protein loading, (3) to make the drug and the NP survive the changes in pH in the complex environment of the gastrointestinal tract, and (4) to trigger quick release of majority of the drug before the NP is excreted from the body. These requirements give rise to goals of this thesis and have been summarized in Figure 1.13.

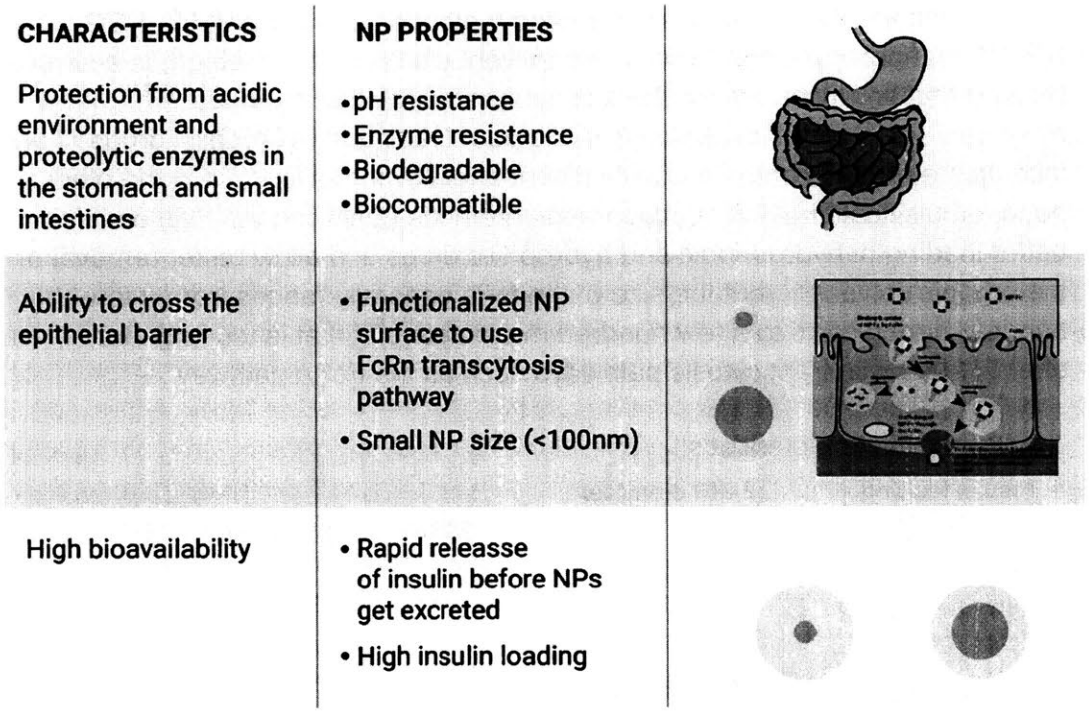

Figure 1.13. Oral insulin delivery Nanoparticle Design criteria. The nanoparticles (NPs) must be able to protect insulin from the harsh chemical environment in the GI tract and from enzymatic degradation. The NPs must be sub-100 nm, have the ability to be functionalized and have the capability of delivering majority of insulin before the NPs can opsonized.

1.8 Thesis goals

The overall goal of this thesis is to *develop sub-100 nm nanoparticles with high insulin loading, capable of delivering bioactive insulin before the nanoparticles get cleared.* The overall goal has been divided into four specific thesis aims.

Aim 1: Understand the effect of synthesis parameters on NP size and insulin loading.

A challenge associated with the development of PLGA-PEG NPs for drug delivery is obtaining small NPs with high insulin loading. Usually, an increase in insulin loading results in an increase in NP size.

Currently, nanoprecipitation, oil-in-water (O/W) emulsification-solvent evaporation, and water-in-oil-in-water (W/O/W) emulsification-solvent

evaporation are the most commonly used methods for making PLGA-PEG NPs[217]. Nanoprecipitation (also called solvent displacement method) is a simple method that produces smaller NPs as compared to other methods[218,219]. However, some of its drawbacks include poor loading of hydrophilic drugs[220] and incomplete removal of the organic solvent after NP formation[221]. On the other hand, emulsification-solvent evaporation methods (O/W and W/O/W) enable better loading of hydrophobic and hydrophilic drugs and allow better removal of the organic solvent[221], but the size of the NPs generally ranges from a few hundred nanometers to a few hundred micrometers[222] that is too large for effective use with transcytosis pathways such as the FcRn pathway[1, 193].

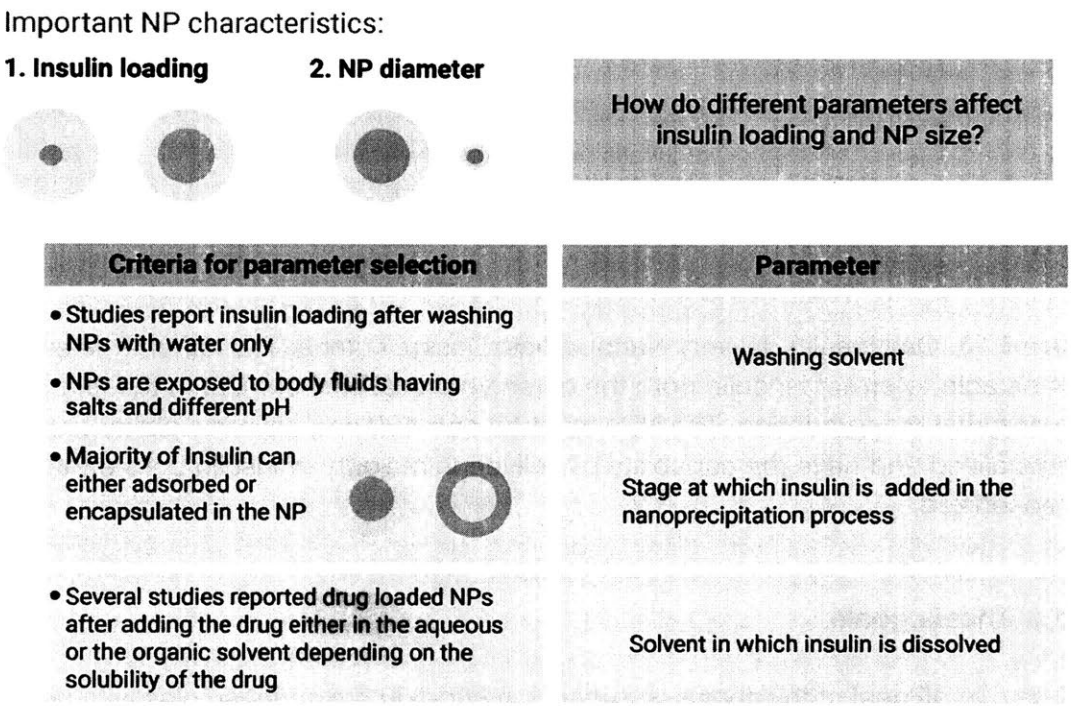

Figure 1.14. Choice of parameters for understanding the nanoprecipitation method better.

In this thesis we use nanoprecipitation for NP synthesis and leverage the fact that it can enable production of smaller NPs as compared to the commonly used synthesis methods like double and single emulsion, while investigating ways of overcoming its drawback of poor insulin loading.

Here we use PLGA-PEG, a block copolymer, to form NPs. PLGA-PEG has been extensively studied as a protein delivery carrier because of its biodegradability and biocompatibility, well-established safety in clinical trials, tunable surface

properties for targeted delivery, and their capability to protect the protein drug from pH and proteolytic enzymes[223-225]. Previous studies have also shown gastric stability of PLGA-PEG, which makes it an ideal material for oral delivery platforms[226-227 214].

In this thesis we provide a systematic multi-step approach to control NP characteristics. To gain a better understanding of the effect of NP synthesis parameters on insulin loading and NP size we perform experiments to study the effect of the washing buffer, stage of adding insulin and the solvent for insulin on NP characteristics. This has been outlined in Figure 1.14.

Aim 2: Improve insulin loading and ensure sub-100 nm diameter of NPs.

To improve insulin loading while retaining a small NP size, we take inspiration from previous studies that have shown an improvement in insulin adsorption on flat surfaces and particle systems (including PLGA-PEG micro and nanoparticles) by incorporating chelating ions like zinc into their systems[214-216, 228-229]. This increase in adsorption has been attributed to the formation of stable insulin-zinc (Ins-Zn) hexamers[216, 230]. In fact, it has been shown in previous studies that the presence of zinc enhances insulin stability and is widely used for the design of long acting insulin[231]. Ins-Zn hexamer formation first involves the formation of insulin dimers, followed by the assembly of two dimers with two zinc ions to give a tetramer $(Zn^{2+})_2 (In)_4$, which then combines with another dimeric unit to give an insulin hexamer $(Zn^{2+})_2 (In)_6$. We demonstrate a 10-fold increase in insulin loading with the help of zinc chelation. We also show ways of optimizing the size of NPs using the insights that we gained from Aim 1.

Aim 3: Enable rapid release of insulin from NPs and ensure high insulin loading and sub-100 nm size.

To enable rapid release of insulin from NPs we develop an environment-responsive drug delivery platform comprised of hybrid polymeric NPs which can efficiently encapsulate insulin, and yet maintain small NP size. These NPs elicit a secondary response when the pH of their surrounding environment changes from acidic to neutral/or basic, which occurs when the NPs cross over from the acidic gastrointestinal environment to the blood stream.

These NPs are synthesized by blending a pH responsive polymer, Eudragit S100 with a non-pH responsive polymer, PLGA-PEG. We report a study that helped finalize the final formulation of the pH responsive NP Finally, we demonstrate

rapid release of insulin from these NPs at pH 7.4 and a significant reduction in the release of insulin in pH 6.

Aim 4: Conjugate targeting ligand on rapid insulin releasing NPs and demonstrate effective transport in an *in vitro* transepithelial model.

The pH responsive NPs are designed to exploit the FcRn transcytosis pathway to efficiently delivery insulin to blood. A recent study has reported the conjugation of Fc fragment of the IgG in PLA-PEG NP surface at physiological pH using the maleimide-thiol chemistry[1]. We show the successful conjugation of the Fc fragment on the surface of the NPs using thiol-maleimide chemistry at pH 5 by overcoming various synthsis challenges. Lastly, we demonstrate a 5 times higher transport of Fc targeted NPs relative to NPs without the Fc fragment, in an in vitro Caco-2 transepithelial model.

CHAPTER 2

Design of Insulin-Loaded Nanoparticles Enabled by Multi-Step Control of Nanoprecipitation and Zinc Chelation

2.1 Abstract

Nanoparticle (NP) carriers provide new opportunities for controlled delivery of drugs, and have potential to address challenges such as effective oral delivery of insulin. However, due to the difficulty of efficiently loading insulin and other proteins inside polymeric NPs, their use has been mostly restricted to the encapsulation of small molecules. To better understand the processes involved in encapsulation of proteins in NPs, we study how buffer conditions, ionic chelation, and preparation methods influence insulin loading in poly (lactic-co-glycolic acid)–b–poly(ethylene glycol) (PLGA-PEG) NPs. We report that, although insulin is weakly bound and easily released from the NPs in the presence of buffer ions, insulin loading can be increased by over 10-fold with the use of chelating zinc ions and by the optimization of the pH during nanoprecipitation. We further provide ways of changing synthesis parameters to control NP size while maintaining high protein loading. These results provide a simple method to enhance insulin loading of PLGA-PEG NPs, and provide insights that may extend to other protein drug delivery systems that are subject to limited loading.

2.2. Introduction

Recent years have seen the development of many protein-based therapeutics that, due to their biological nature, are expected to be less toxic and more successful in clinical trials than their chemically synthesized counterparts[232]. These therapeutic proteins include monoclonal antibodies, cytokines, tissue growth factors, vaccines, and gene transfer products[233] that are used for prevention and treatment of diseases, *e.g.* biologic disease-modifying anti-rheumatic drugs for rheumatoid arthritis[234], monoclonal antibodies for cancer[235], and insulin for diabetes[236]. However, therapeutic proteins tend to have poor chemical and physical stability against external factors like pH, temperature, and surface interactions. The high molecular weight of proteins, their ionizable nature, their susceptibility to gastrointestinal enzymes, and their inability to permeate the

mucosal tissue and the epithelial barrier in the intestine, all limit their oral bioavailability[1].Most biological agents are therefore limited to the parenteral administration, which is more invasive and poorly accepted by patients.

Among these therapeutics, oral delivery of insulin – a hydrophilic protein that plays a key role in regulating glucose metabolism – is particularly important due to the increased incidence of diabetes in the population[237]. To improve the compliance of patients and decrease the number of subcutaneous injections required to control diabetes, oral, nasal, pulmonary and ocular routes of administration have been proposed for insulin. [238-239]. In fact, an inhaled formulation of insulin was approved by the FDA in 2006, but was discontinued in 2007 due to increased costs and device design complications[238]. Regardless, oral delivery is regarded as the most patient-compliant route of administering insulin.

Recently, polymeric nanoparticle (NP) carriers have shown promise for drug delivery for treatment of a variety of diseases[218, 240-247], including oral delivery of proteins and of insulin for type II diabetes[1, 223, 248-251]. Relevant to oral delivery, NPs can be easily prepared from a variety of materials, targeting ligands on NPs can facilitate therapeutics to cross the epithelial barrier[250], and NPs can protect encapsulated and adsorbed therapeutics from pH changes and enzymatic degradation in the gastrointestinal tract[193, 250, 252]. Some proteins that have been incorporated in polymeric NP-based drug delivery systems include tetanus toxoid[253], insulin[254], and interleukin 2 (IL-2)[255].

NPs prepared from a variety of materials such as chitosan, gelatin, poly-alkyl-cyano-acrylates, dextran and polycaprolactone have been explored for oral insulin delivery[227, 248-249, 256]. However, PLGA-PEG NPs and poly (lactic acid)–*b*–poly (ethylene glycol) (PLA-PEG) NPs are preferred and have been extensively studied as protein delivery carriers because of their biodegradability and biocompatibility, well-established safety in clinical trials, tunable surface properties for targeted delivery, and their capability to protect the protein drug from pH and proteolytic enzymes[223-225]. Previous studies have also shown gastric stability of PLGA-PEG, which makes it an ideal material for oral delivery platforms[226-227 214]. In particular, PLA-PEG NPs designed to exploit the FcRn transcytosis pathway to cross the gastroepithelial barrier and enter into the bloodstream have shown remarkable promise for oral delivery of insulin[1] The FcRn transport pathway involves targeting insulin-loaded NPs to the neonatal Fc receptor (FcRn) that mediates active transport of IgG antibodies across the epithelial barrier in the GI tract, resulting in efficient transport across the intestinal

epithelium into the systemic circulation for insulin delivery. However, utilizing the FcRn pathway requires small NP size; both *in vitro* studies using Caco-2 cells (human adenocarcinoma cell line) and *in vivo* studies in rats have shown that the uptake of smaller NPs (~100 nm) is significantly more efficient than that of larger NPs (500 nm, 1 μm, 5 μm)[193]. However, it has been challenging to achieve high loading of hydrophilic protein drugs, including insulin, in PLGA-PEG or PLA-PEG NPs while maintaining small NP size, because the hydrophobic core (*i.e.*, PLGA and PLA) resists interactions with the hydrophilic protein drugs[212]. For example, the insulin loading in the NPs used in the FcRn study was low (~0.5 wt %)[1]; assuming 10% bioavailability and typical insulin dose of ~3 mg per dosage[213], a 0.5 wt % loading translates to an impractically high oral intake of ~6 g NP/dosage. On the other hand, although some studies have shown high insulin loading in particles[214-216], the particle size (17.4 μm – 120 nm) is too large to permit use of transcytosis pathways to cross the epithelial barrier of the intestine. Hence, better understanding of the factors and mechanisms that determine insulin loading, with the goal of designing NPs with higher insulin loading while retaining a small NP size, is essential.

In this work, we study the influence of key steps and process conditions in the synthesis of insulin-loaded PLGA-PEG NPs (Ins-NPs) formed by nanoprecipitation and tailor the process to realize enhanced insulin loading while maintaining sub-100 nm NP size[257]. Specifically, we demonstrate the synthesis of insulin-zinc-PLGA-PEG NPs (Ins-Zn-NPs) that uses chelating zinc ions to achieve a greater than 10-fold increase in insulin loading while maintaining small size (<100 nm) required for FcRn-mediated transcytosis[1]. We also show that these NPs are stable for long-term storage and that insulin maintains it conformational structure after being loaded in the NPs. This study provides insights into the mechanisms of formation of Ins-NPs and illustrates simple methods for improving insulin loading in PLGA-PEG NPs while controlling NP size. These findings can be extended to similar polymeric and protein systems and can lead to significant advancements in the area of NPs based protein delivery by proving a systematic way of overcoming the two main challenges *ie.* improving protein loading and controlling NP size.

2.3. Experimental Section

2.3.1. Materials

Human recombinant insulin, dimethyl sulfoxide (DMSO), and zinc chloride were purchased from Sigma-Aldrich. $PLGA_{10k}$-PEG_{5k} was purchased from Akina Inc. (West Lafayette, IN, USA). Micro bicinchoninic acid (BCA) protein assay kit was

purchased from Lamda Biotech, Inc. (St. Louis, MO, USA). Phosphate Buffer Saline (PBS) was purchased from Life Technologies (Green Island, NY, USA). Deionized (DI) water was used for all the experiments.

2.3.2. Methods

2.3.2.1. Synthesis of Ins-NPs and Ins-Zn-NPs

For the preparation of Ins-NPs by the nanoprecipitation method (Figure 2.3A), we premixed 120 µL of insulin (10 mg/mL) solution in DMSO with 400 µL of $PLGA_{10k}$ -PEG_{5k} (10 mg/mL) solution in DMSO. The resulting solution was added drop wise to 4 mL DI water or buffer solution. The solution was stirred for at least two hours at 2000 rpm. The resulting NP solution was purified by ultrafiltration using Amicon Ultracel 100 kDa membrane filters to remove free insulin and organic solvent. The NPs were washed twice with PBS and twice with DI water at 3000 g centrifugation for 15 min each or 4 times with DI water only. The NPs were resuspended in PBS to a final concentration of 10 mg/mL. As controls, NPs were prepared with PLGA-PEG solution alone using the same procedure without the addition of insulin. In all experiments, the ratio of the organic to the aqueous phase remained constant at 13:100.

Ins-Zn-NPs were prepared by first mixing insulin (10 mg/mL) and zinc chloride (5 mg/mL) in DMSO in 1:3, 1:6, and 1:9 molar ratios of insulin:zinc. To 120 µL of this solution, 400 µL of $PLGA_{10k}$ -PEG_{5k} (10 mg/mL) was added. The resulting solution was added drop wise to 4 mL DI water or buffer solution for 2 h under magnetic stirring at 2000 rpm. The NPs were purified by the aforementioned process.

2.3.2.2. Characterization of Ins-NPs and Ins-Zn-NPs

The amount of insulin loaded in Ins-NPs and Ins-Zn-NPs was quantified by using a low protein BCA assay kit. After the purification process, Ins-NPs and Ins-Zn-NPs were resuspended in PBS to a final concentration of 1 mg/mL and heated at 60°C for 1 h to release insulin. Then, 125 µL of NP solution was added to each well in a 96 well-plate followed by the addition of 125 µL of bicinchoninic acid (BCA) assay working solution. After incubating the NPs at 60°C for 30 min, the amount of insulin was analyzed using a TECAN UV spectrophotometer (Mannedorf, Switzerland) according to the manufacturer's instructions. As a control, NPs without insulin were also measured by the same procedure. The weight percent of insulin in the NPs was measured as the insulin loading and the

fraction of insulin in the NPs was measured as encapsulation efficiency. Three separate experiments were performed for each data point.

For measuring the hydrodynamic radius and zeta potential, the NPs were washed and reconstituted in 1 mL of DI water at a NP concentration of 0.5 mg/mL. The solution was loaded in disposable low-volume cuvettes to measure the hydrodynamic radius and NP size distribution and in folded capillary cells to measure the zeta potential using the Zetasizer NanoZS instrument (Malvern Instruments Ltd., U.K.).

2.3.2.3. Measurement of insulin loading

Insulin loading in Ins-NPs and Ins-Zn-NPs was quantified using a low protein BCA assay kit (Lamda Biotech). NPs were synthesized, purified, and resuspended in PBS to a final concentration of 1 mg/mL. They were then incubated at 60°C for 2 h to allow for release of insulin from the NPs. 125 µL of the NP solution was added to each well in a 96 well-plate followed by the addition of 125 µL of BCA working solution (prepared according to the manufacturer's instructions. After adding the working solution the well-plate was covered with aluminum foil to ensure uniform heating of the NP samples at 60°C for 30 min. The amount of insulin was analyzed using a TECAN UV spectrophotometer (Mannedorf, Switzerland), which measured the absorbance of 562 nm wavelength by NP samples. Empty PLGA-PEG NPs and blank buffer (pH 7.4) were included in the analysis as controls. For each set of measurement, insulin and/or bovine serum albumin (BSA) standard curve was also measured. The absorbance values of the standard curve were plotted against their respective concentration values to obtain a linear equation to calibrate absorbance to concentration.

$y = Ax + B$; y = Absorbance, x = Concentration of insulin (µg/mL)

$$\text{Concentration} = \frac{\text{Absorbance-B}}{\text{A}}$$

The concentration of insulin in each sample was measured using the equation obtained from the standard curve. The data in this paper has been reported with reference to the insulin standard curve. For data points where only the BSA standard curve was used as reference, the calibration equation was adjusted using the relation between the insulin and the BSA standard curves as seen in Figure 2.1 (a) *i.e.* each concentration value was divided by a factor of 1.3 (Figure 2.1 (b)). After NP synthesis, the total volume of each NP sample was recorded. The total amount of insulin in the sample was calculated by taking the product of the concentration of insulin and the volume of each sample.

$$\text{Amount of insulin } (\mu g) = \text{Concentration } \left(\frac{\mu g}{mL}\right) \times \text{Sample volume (mL)}$$

The total amount of insulin added to each batch of the NPs and the weight of the NPs in each batch were known, from which the insulin loading and encapsulation efficiency were calculated using the following equations:

$$\text{Insulin loading (\%)} = \frac{\text{Total amount of insulin detected}}{\text{Weight of the NPs}} \times 100\%$$

$$\text{Encapsulation Efficiency (\%)} = \frac{\text{Total amount of insulin detected}}{\text{Total amount of insulin added}} \times 100\%$$

The value of insulin loading in the Ins-NPs and Ins-Zn-NPs was measured after subtracting the absorbance of the empty NPs from the absorbance of the insulin loaded NPs.

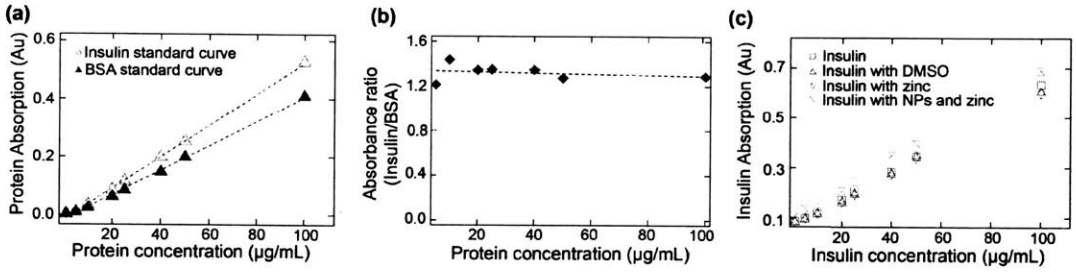

Figure 2.1. (a) Insulin standard curve in relation to the BSA standard curve for the BCA assay. (b) Relation between the insulin and BSA standard curves. (c) Effect of DMSO, zinc, and polymeric NPs on the insulin standard curve.

The effect of zinc, DMSO and empty PLGA-PEG NPs on the BCA assay was also studied. Similar concentrations (as in the Ins-NPs) of DMSO, zinc and empty NPs were added to the insulin standard curves. We saw that zinc and DMSO did not affect the BCA assay standard curve as seen in Figure 2.1 (c). This verified that the 11-fold increase in insulin loading seen in the Ins-Zn-NPs was due to the presence of more insulin and not due to the interaction of zinc with the reagents of the BCA assay. However, the presence of empty PLGA-PEG NPs resulted in a slight deviation of the standard curve, which was more prominent at higher concentrations. We therefore subtracted the absorbance of empty NPs from Ins-NPs and Ins-Zn-NPs to get an accurate measurement of insulin loading.

2.3.2.4. In vitro insulin of release

The *in vitro* release of insulin was studied by dividing a batch of Ins-Zn-NPs equally into 100 kDa Float A Lyzer (Spectrum Labs) units and incubating them at 37°C in PBS (pH 7.4). At each predetermined time interval, an aliquot of the NPs

was taken and measured for insulin loading using the BCA assay, which included heating at 60°C for 1 h as previously described. In order to increase the accuracy of the dialysis setup, a 3 mm magnetic stirrer was inserted in each Float A Lyzer unit, to allow continuous mixing of the Ins-Zn-NP solution inside the dialysis chambers. Furthermore, the beaker with the dialysis chambers was kept on an orbital shaker, to ensure mixing of the buffer solution outside the dialysis chambers. Three experiments were performed for each data point The

2.3.2.5. Transmission Electron Microscopy

Ins-NPs and PLGA-PEG NPs without insulin were imaged using a FEI Tecnai TEM at an acceleration voltage of 80 kV. The TEM sample was prepared by depositing 10 µL of the NP suspension (1.0 mg/mL) onto a 200-mesh formvar-carbon-coated copper grid. After 20 min of incubation, excess sample on the grid was blotted away with filter paper. The grids were negatively stained for another 20 min at room temperature with sterile-filtered 2% (w/v) uranyl acetate aqueous solution. The grids were then washed once with DI water and air-dried prior to imaging. The TEM images of Ins-NPs and PLGA-PEG NPs without insulin are shown in Figure 2.3B and 2.3C.

TEM-based energy-dispersive X-ray spectroscopy (EDX) was performed using a JEOL-2100 Field Emission Electron Microscope at 200 kV with an Oxford X-Max 80 mm^2 high angle annular dark field (HAA DF) detector. The NP samples were prepared on a 200-mesh carbon coated TEM grid. 7 µL of the sample was deposited on each grid and was allowed to completely dry out. The grids were then washed once with DI water and air-dried prior to the EDX analysis.

2.3.2.6. Zeta potential measurement

NP zeta potential was studied by diluting the NP solution to 0.1 mg/mL with water. The NP solution was loaded in folded capillary cells to measure the zeta potential using the Zetasizer NanoZS trument (Malvern Instruments Ltd., U.K.). From Figure 2.5 it can be seen that the zeta potential of Empty PLGA-PEG NPs (-25.44 mV) and Ins-NPs (-27.9 mV) is statistically insignificant (n = 3, p = 0.3144). However, the zeta potential of the Ins-Zn-NPs (-22. 03 mV) is significantly (n =3, p = 0.03928) lower than that of Ins-NPs and Empty PLGA-PEG NPs. This difference can be attributed to the presence of positively charged zinc ions on the surface of the NP that could have resulted in the reduction of the zeta potential of the Ins-Zn-NPs.

2.3.2.7. Stability of nanoparticles during storage

The stability of NPs was accessed by measuring the size and zeta potential of the NPs before and after freeze-drying them. An insignificant change in particle size and zeta potential was observed when insulin loaded NPs were freeze-dried and stored in 4°C as seen in Figure 2.2 (a) and (b). 5mL of 0.1mg/mL NP solution was filtered using a 0.4µm PTFE filter and then freeze-dried in a of 10% (w/v) sucrose solution. The freeze-dried NPs were stored in 4°C and then reconstituted in water to make a 0.1 mg/mL solution. The NPs size and zeta potential were measured both before and after the freeze-drying process.

The stability of the NPs in solution was also studied by measuring their size for up to a week when the NPs were stored in water at RT. Figure 2.2 (c) shows that particle size is stable up to 4 days in water after which an increase in particle size is observed potentially due to aggregation.

2.3.2.8. Conformational stability of insulin

The conformational integrity of insulin encapsulated in Ins-NPs and Ins-Zn-NPs was detected using far UV circular dichroism (CD) spectroscopy (J-1500, JASCO, Tokyo, Japan). Standard insulin solution and insulin released from the NPs were analyzed in the far UV region of 260-190 nm. Data speed and scanning pitch were 0.5 nm and 50 nm/min respectively. The data obtained was converted to molecular ellipticity using the following equation.

$$[\theta]_{mrv} = \frac{\theta \times M_{mrw}}{10 \times c \times l}$$

θ is ellipticity (mdeg), M_{mrw} is mean residence molecular weight (g/mol), c is concentration (mg/mL) and is the path length (cm) of the cuvette.
Figure 2.2 (d) shows the overlay of the CD spectrum of standard insulin solution and the insulin solution released from different NP formulations. It is evident from Figure 2.2 that the CD spectra of insulin released from the NPs superimposed with the CD spectrum of standard insulin solution, confirming the conformational integrity of insulin after being encapsulated in the NPs. This figure also shows the overlay of the CD spectrum of insulin solution released from NPs that were freeze-dried and then later reconstituted in water. The figure confirms that insulin loaded in the NPs is successful in maintaining conformational stability after being loaded in the NPs.

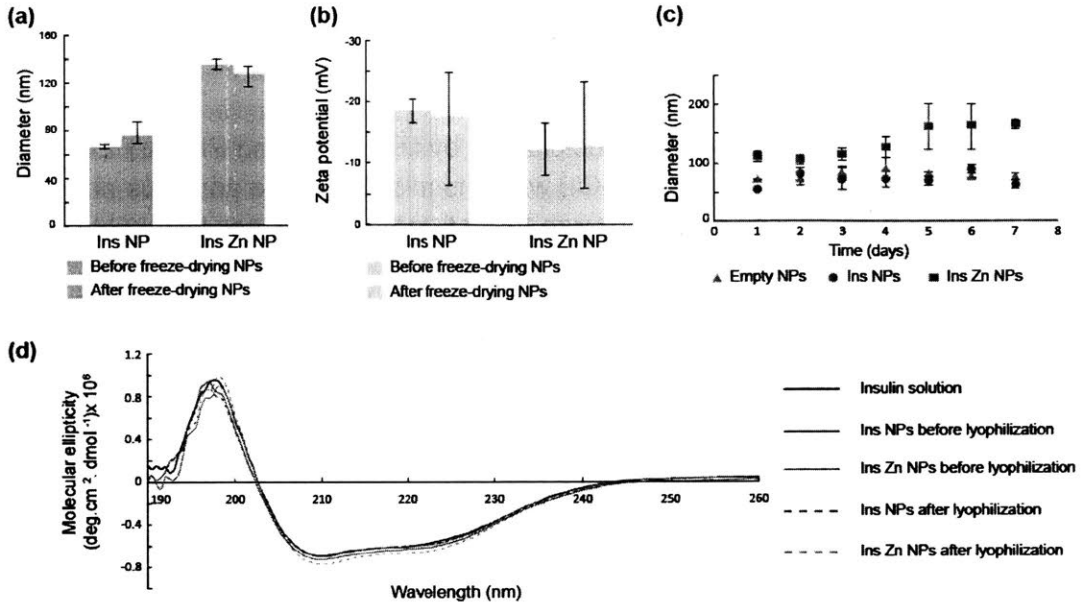

Figure 2.2. Ins-NPs and Ins-Zn NPs show the potential of long-term storage as they maintain (a) particle size and (b) zeta potential before and after undergoing the process of freeze-drying. (c) Ins-NPs and Ins-Zn-NPs are stable in water for up to 4 days from synthesis at RT. (d) Conformational stability of insulin in Ins-NPs and Ins-Zn-NPs was confirmed by comparing the circular dichroism spectra of standard insulin and insulin obtained from Ins-NPs and Ins-Zn-NPs before and after undergoing the process of freeze-drying.

2.4. Results and Discussion

Nanoprecipitation, oil-in-water (O/W) emulsification-solvent evaporation, and water-in-oil-in-water (W/O/W) emulsification-solvent evaporation are the most commonly used methods for making PLGA-PEG NPs. Nanoprecipitation (also called solvent displacement method) is a simple method that produces smaller NPs as compared to other methods[218,219]. However, some of its drawbacks include poor loading of hydrophilic drugs[220] and incomplete removal of the organic solvent after NP formation[221]. On the other hand, emulsification-solvent evaporation methods (O/W and W/O/W) enable better loading of hydrophobic and hydrophilic drugs and allow better removal of the organic solvent[221], but the size of the NPs generally ranges from a few hundred nanometers to a few hundred micrometers[222] that is too large for effective use with transcytosis pathways such as the FcRn pathway[1, 193]. We therefore focused on nanoprecipitation and leveraged the fact that it can enable production of smaller

NPs as compared to the commonly used synthesis methods like double and single emulsion, while investigating ways of overcoming its drawback of poor insulin loading.

Ins-NPs were prepared by nanoprecipitation by first dissolving PLGA-PEG and insulin in an organic solvent (DMSO), which is miscible in the aqueous phase[258], and then adding the solution drop-wise to a stirred aqueous solution (water or buffer solution) to form NPs (Figure 2.3A). Here DMSO is the solvent and water is the anti-solvent. Once in contact with water, PLGA-PEG and insulin self-assemble to form spherical NPs. TEM images in Figure 2.3B and 2.3C show that Ins-NPs and empty PLGA-PEG NPs are spherical and fairly monodisperse with diameters less than 100 nm.

The long-term stability of NPs was accessed by measuring the size and zeta potential of the NPs before and after freeze-drying them; an insignificant change in particle size and zeta potential was observed (Figure 2.2a and 2.2b). The stability of the NPs in solution was also studied and it revealed that particle size was stable up to 4 days in water after which an increase in particle size was observed potentially due to aggregation (Figure 2.2c).
The conformational integrity of insulin after encapsulation in freshly synthesized NPs as well as NPs that were stored after freeze-drying was confirmed using circular dichroism spectroscopy (Figure 2.2d).

2.4.1. Effect of washing buffer on insulin loading

Several studies have reported insulin loading in polymeric NPs after washing the NPs with water only[259-261]. However, since water wash alone is not representative of the environment that the NPs are exposed to *in vivo*, it is important to understand whether insulin loading is affected by the presence of ions in the buffer. We therefore investigated the effect of buffer wash on insulin loading and NP size by preparing Ins-NPs and washing them either with DI water or with PBS buffer (pH 7.4 with 155 mM NaCl) (Figure 2.3D). Ins-NPs washed only with DI water showed insulin loading of 8.95 % (Figure 2.3E). By contrast, washing the NPs with PBS decreased the insulin loading by more than an order of magnitude to 0.36 % (Figure 2.3E). The NP diameter also decreased slightly after PBS wash (from 65.2 nm to 62.8 nm), but the change was not significant (n = 3, p = 0.074) (Figure 2.3F). To understand whether the pH of the buffer had a stronger role in removing the weakly-bound insulin or the presence of 155 mM NaCl in the buffer, we washed the NPs with an unbuffered 155 mM NaCl solution and the

NPs showed a loading of 2.4% while washing the NPs with a pH 7.4 buffer without the155 mM NaCl resulted in a loading of 0.85% (Figure S3).

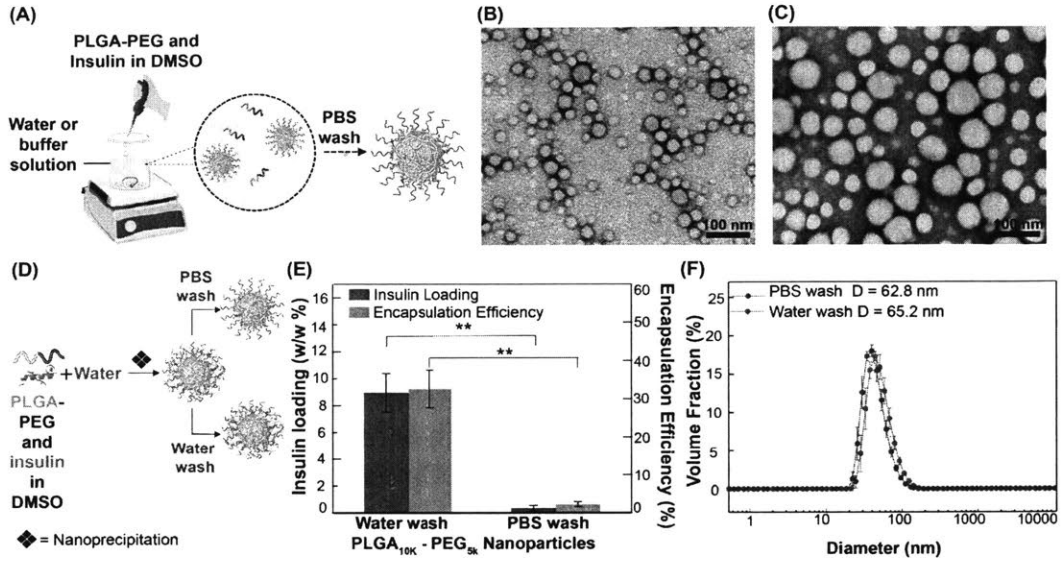

Figure 2.3. *Insulin loaded PLGA-PEG nanoparticles (Ins-NP).* **(A)** Schematic of Ins-NP synthesis process by nanoprecipitation, where PLGA-PEG and insulin in dimethyl sulfoxide (DMSO) is added drop-wise to a stirred beaker containing water (or buffer). TEM images of **(B)** Ins-NPs and **(C)** PLGA-PEG NPs without insulin. *Effect of buffer wash on Ins-NP characteristics.* **(D)** Schematic of the synthesis of Ins-NPs where NPs were either washed with PBS buffer (pH 7.4) or with water only. **(E)** Insulin loading and encapsulation efficiency show 25-fold higher insulin loading when NPs were washed with water only (8.95% ± 1.44) as compared to a PBS buffer wash (0.36% ± 0.19) (n = 3, p = 0.008). **(F)** NP size data show no significant difference in the size of the Ins-NPs when washed with water or buffer (n = 3, p = 0.074). Error bars represent ± s.d.

The 25-fold decrease in insulin loading with minimal change in NP diameter upon buffer wash suggests that insulin in the case of NPs washed with DI water is primarily associated with the corona of the NPs *via* electrostatic and hydrophobic interactions where entropic factors could also be operative[215, 262]. During a PBS wash, the NPs are exposed to pH 7.4 (at which insulin is more soluble than unbuffered water), thereby facilitating release of insulin. Although NaCl does not play as large a role as pH, it potentially facilitates removal of insulin by shielding electrostatic interactions. The results also suggest that some regions of insulin bind *via* its local positively and negatively charged patches to the corona of the NPs through electrostatic interactions, as seen in other negatively charged

proteins like α-lactalbumin[263]. Here, the partial negative charges most likely facilitate the interactions. Similar removal of loosely bound insulin from silica and chromium surfaces on rinsing with buffer has also been observed[228-229]. These results illustrate that washing of NPs using an appropriate solution is extremely important because it can dramatically alter the measured insulin loading. In the case of a DI water wash, the insulin loading of NPs is high, but it does not account for the effect of exposure to pH and salts. On the contrary, PBS wash gives a low loading of insulin but is more representative of *in vivo* environments. Therefore, we used the more conservative PBS wash in the rest of the study to assess the effect of various factors on insulin loading in NPs.

2.4.2. Mechanism of NP formation

The above results raise the question whether insulin simply adsorbs to the NP surface and plays little role in the process of nanoprecipitation. Such adsorption of small molecules on the surface of PLGA-PEG nanoparticles due to hydrophobic interactions has been reported recently[264-265]. If this hypothesis is true, we can expect the insulin loading to be similar regardless of whether insulin is added to the precursors during nanoprecipitation, or if it is added to the NPs after nanoprecipitation.

We therefore investigated the effect of the stage at which insulin is added during NP formation; specifically, we compared insulin loading of NPs formed by adding insulin along with PLGA-PEG before nanoprecipitation (Figure 2.4A (top), as described in section2.3.2.1), with NPs formed by adding insulin to empty PLGA-PEG NPs after they were already formed by nanoprecipitation (Figure 2.4A (bottom)). Interestingly, similar insulin loading was obtained regardless of whether insulin was added before or after nanoprecipitation (Figure 2.4B). However, smaller NPs (62.8 nm) were produced when insulin was mixed with PLGA-PEG before nanoprecipitation (Figure 2.4C). By contrast, larger NPs (80.5 nm) were formed when insulin was added to already-formed PLGA-PEG NPs; furthermore, their size was similar to that of empty PLGA-PEG NPs (84 nm). On studying the zeta potential of these NPs, we found that the zeta potential of Empty PLGA-PEG NPs and Ins-NPs was not significantly different (Figure 2.5).

The results only partially support the hypothesis that NP formation is independent of insulin – on one hand, we obtain similar insulin loading by simply adding insulin to already formed PLGA-PEG NPs, and on the other hand, the NPs are clearly smaller in size than PLGA-PEG NPs when insulin is added to DMSO along with PLGA-PEG before nanoprecipitation. This effect offers a potentially

useful method to make smaller NPs; however, it also raises the question as to

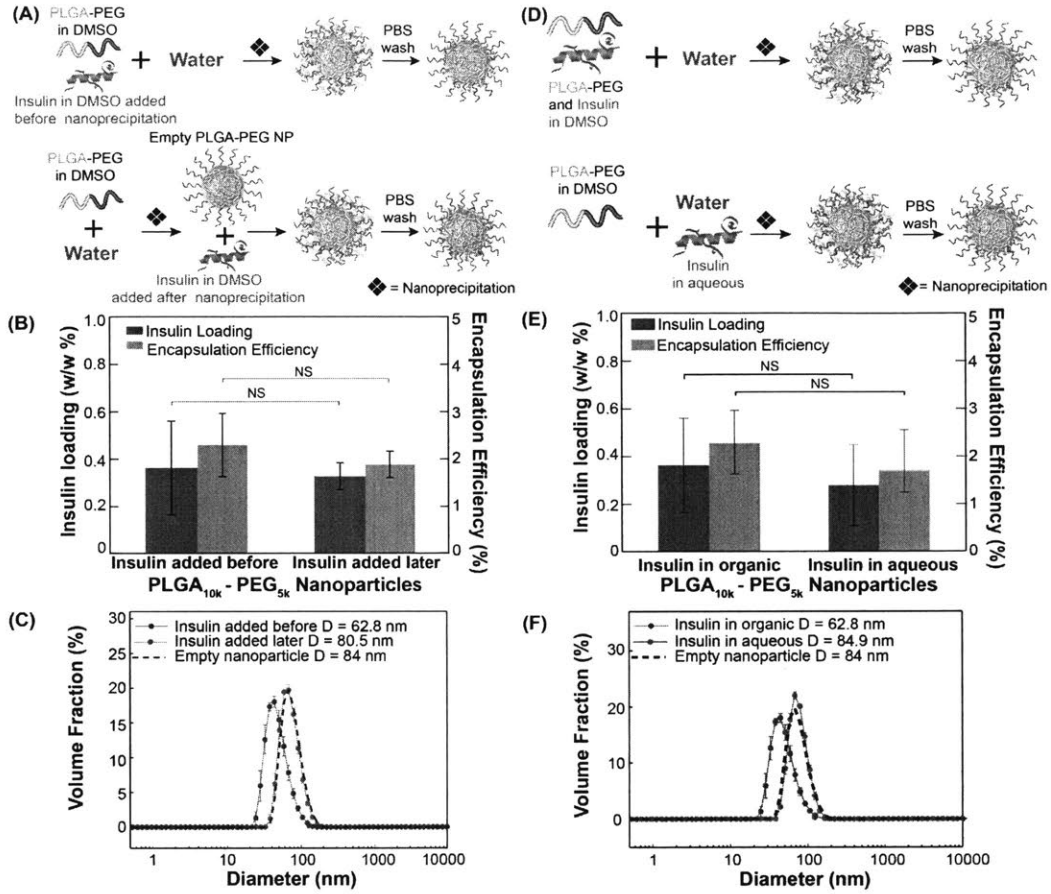

Figure 2.4. *Effect of adding insulin at different stages of nanoprecipitation on Ins-NP characteristics.* (A) Schematic showing the synthesis of Ins-NPs by including insulin mixed with PLGA-PEG in DMSO before nanoprecipitation (top), and by adding insulin in DMSO to empty PLGA-PEG NPs after their formation by nanoprecipitation (bottom). (B) Insulin loading and encapsulation efficiency show no significant dependence on the stage of adding insulin before (0.36%) or after (0.32%) nanoprecipitation (n = 3, p = 0.79), but (C) NP size shows a significant dependence (n = 3, p = 0.005). *Effect of mixing insulin in different phases on Ins-NP characteristics.* (D) Schematic showing the synthesis of Ins-NPs by adding DMSO with insulin and PLGA-PEG to water (top), and by adding DMSO with PLGA-PEG to water with insulin dissolved in it (bottom). (E) Insulin loading (and encapsulation efficiency) shows no significant dependence on including insulin in DMSO (0.36%) or in water (0.28%) (n = 3, p = 0.60), but (F) NP size shows a significant dependence (n = 3, p = 0.0006). Error bars represent ± s.d. Note: The NPs with the label 'Insulin added before' in Figure 2.4B and the NPs with the label 'Insulin in organic' in Figure 2.4E are the same nanoparticles.

whether a similar reduction in NP size occurs if insulin is included in the aqueous phase instead of DMSO during nanoprecipitation (Figure 2.4D). We find that insulin loading is similar regardless of whether insulin was dissolved in water or in DMSO (Figure 2.4E), or added later to pre-formed NPs. However, dissolving insulin in the organic phase along with PLGA-PEG produced smaller sized NPs (62.8 nm) as compared to the NPs that were formed by including insulin in water (84.9 nm) (Figure 2.4F). Interestingly, the size of NPs formed by nanoprecipitation with insulin in the aqueous phase is similar to that of empty PLGA-PEG NPs without insulin, and to that of Ins-NPs formed by adding insulin to already formed PLGA-PEG NPs. The results show that insulin affects NP size only when it is dissolved in the organic phase (DMSO) along with PLGA-PEG, and in all other cases it does not change NP size compared to PLGA-PEG NPs without insulin.

The fact that nearly all of insulin is washed off by PBS, and that the insulin loading of NPs formed with insulin dissolved in water during nanoprecipitation is indistinguishable from insulin loading of NPs formed by adding insulin to PLGA-PEG NPs, indicates that insulin is loosely associated with the NP corona rather than encapsulated within the hydrophobic core. The fact that NPs can be loaded with insulin by simply adding insulin to NPs implies that NPs can be pre-formed to desired characteristics and subsequently loaded with insulin, thereby decoupling NP formation from insulin loading. It suggests that when insulin is included in the aqueous phase during nanoprecipitation or added after nanoprecipitation, its role in NP formation is passive – it simply adsorbs to the corona of the NPs and does not otherwise alter the NPs. However, when insulin is dissolved in the organic phase along with PLGA-PEG, it does influence the NP size, which presents a way to prepare smaller NPs compared to the corresponding PLGA-PEG NPs without insulin. This reduction in size of NPs when insulin is present during nanoprecipitation may be attributed to the hydrophilic nature of insulin that could act as a surfactant, potentially by associating with PLGA-PEG to stabilize smaller NPs and preventing their aggregation. These insights allow us to optimize the NP size and insulin loading, as illustrated below.

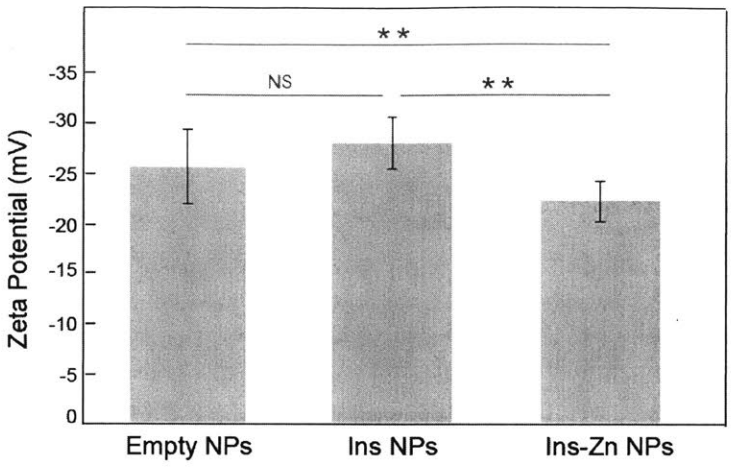

Figure 2.5. Empty PLGA-PEG NPs (-25.44 mV) and Ins-NPs (-27.9 mV) was statistically insignificant. Zeta potential of the Ins-Zn-NPs (-22. 03 mV) is significantly lower than Ins-NPs and Empty PLGA-PEG NPs (** = $p < 0.05$).

2.4.3 Enhancing insulin loading by zinc chelation

To improve insulin loading while retaining a small NP size, we took inspiration from previous studies that have shown an improvement in insulin adsorption on flat surfaces and particle systems (including PLGA-PEG micro and nanoparticles) by incorporating chelating ions like zinc into their systems[214-216, 228-229]. This increase in adsorption is attributed to the formation of stable insulin-zinc (Ins-Zn) hexamers[216, 230]. In fact, it has been shown in previous studies that the presence of zinc enhances insulin stability and is widely used for the design of long acting insulin[231]. Ins-Zn hexamer formation first involves the formation of insulin dimers, followed by the assembly of two dimers with two zinc ions to give a tetramer $(Zn^{2+})_2 (In)_4$, which then combines with another dimeric unit to give an insulin hexamer $(Zn^{2+})_2 (In)_6$ (Figure 2.6A (top))[266]. The tendency for protein adsorption is generally expected to increase with molecular weight and hydrophobicity of the protein[266]. Moreover, the strength of a polyvalent interaction (like Ins-Zn hexamer with the NP surface) can be much stronger than that which can be achieved by a fewer number of interactions (like Ins monomer with NP corona)[267,268-269]. Given the larger size of the Ins-Zn hexamer and its lower solubility in water[270], we expect that incorporation of zinc ions in the Ins-NP system will improve insulin loading. Previous studies have also suggested that the presence of zinc ions ensures the integrity of the functional secondary structure of insulin, thereby maintaining its bioactivity[215-216]. Similar results have also been shown for other proteins like human growth hormone and human nerve growth factor[215].

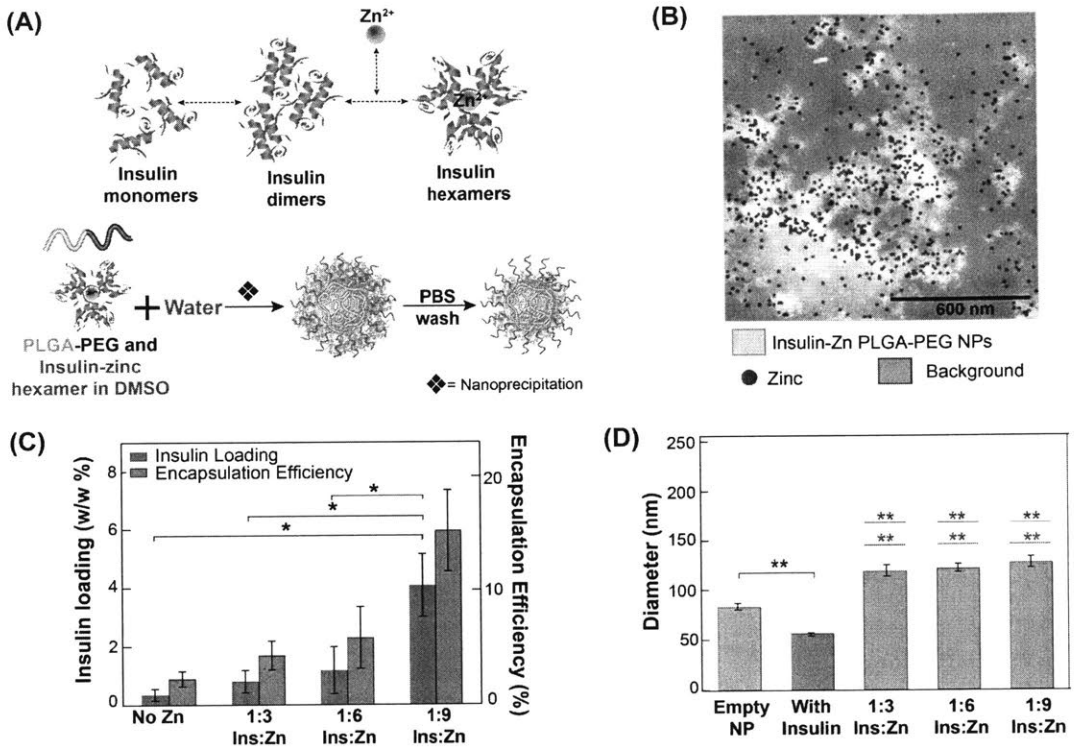

Figure 2.6. *Effect of incorporating zinc ions in Ins-NPs.* (A) Schematic showing the formation of Ins-Zn hexamers (top) and of Ins-Zn-NPs (bottom). (B) Dark-field TEM/EDX image of unstained Ins-Zn-NPs. The lighter regions in the figure show the presence of NPs, and the red dots correspond to the presence of zinc. The presence of zinc in the same areas where Ins-Zn-NPs were detected confirms the presence of zinc in Ins-Zn-NPs. (C) Insulin loading and encapsulation efficiency show an increase in insulin loading with an increase in zinc ion concentration. Greater than 10-fold enhancement of insulin loading was obtained for insulin to zinc ratio of 1:9. (n = 3, p = 0.02). (D) The average diameter of empty PLGA-PEG NPs, Ins-NPs, and Ins-Zn-NPs. In case of Ins-Zn-NPs, the average diameter did not change significantly when different amount of zinc ions are added. The average diameter of Ins-Zn-NPs was larger than that of empty PLGA-PEG NPs (n = 3, p = 0.0003) and Ins-Zn-NPs and Ins-NPs (n = 3, p = 0.0001). Error bars represent ± s.d.

We therefore investigated the effect of including zinc ions in the organic phase along with insulin at different molar ratios (1:3, 1:6, 1:9 of Ins:Zn) to form Ins-Zn-NPs, where the stoichiometry for a hexamer is 1:3 (Figure 2.6A). TEM EDX analysis confirmed the presence of zinc ions in the resulting NPs (Figure 2.6B), where the zinc signal was co-localized with that from the PLGA-PEG NPs. We

observed a monotonic increase in insulin loading as the amount of zinc ions was increased in the NPs while maintaining the same insulin and PLGA-PEG concentrations (Figure 2.6C). At an Ins:Zn molar ratio of 1:9, the NPs showed more than 10-fold higher insulin loading (4.07%) as compared to Ins-NPs without zinc (0.36%). On measuring the hydrodynamic diameter of Ins-Zn-NPs, we observed that the size of Ins-Zn-NPs (127.6 nm) was significantly greater than the size of Ins-NPs (62.8 nm) and also the size of empty PLGA-PEG NPs (84 nm) (Figure 2.6D). The zeta potential of Ins-Zn NPs (-22.03 mV) was also significantly lower as compared to the zeta potential of empty NPs (-25.44 mV) and Ins-NPs (-27.9mV) (Figure 2.5). However, the size of these NPs was independent of the amount of zinc ions added to the system. This increase in size of the NPs is expected since the hexameric form of insulin is less soluble in the aqueous phase as compared to its monomeric form, which could promote NP aggregation and lead to larger NPs. Moreover, the presence of zinc ions in the NPs did not affect the conformational integrity of insulin that was confirmed by circular dichroism spectroscopy (Figure 2.2d)[215].

2.4.4. Optimizing the size of Ins-Zn-NPs

Based upon our earlier understanding of the Ins-NPs (Section 2.4.2), we hypothesized that it would be possible to generate sub-100 nm NPs with high insulin loading by adding zinc or Ins-Zn to already-formed PLGA-PEG NPs. NP characteristics of Ins-Zn-NPs, synthesized by adding Ins-Zn hexamers mixed in DMSO along with PLGA-PEG and added before nanoprecipitation (Figure 2.7A), were compared with Ins-Zn-NPs formed by adding Ins-Zn hexamers to pre-formed PLGA-PEG NPs (Figure 2.7B) and Ins-Zn-NPs formed by adding zinc ions to preformed Ins-NPs (Figure 2.7C).

Ins-Zn-NPs formed by adding zinc ions to already synthesized Ins-NPs (Figure 2.7C), showed a reduction in NP size from 127.6 nm to 57.9 nm (similar to size of Ins-NPs), but the insulin loading decreased from 4.07% to 1.55% (Figure 2.7A and 2.7C). When Ins-Zn hexamers were added after assembling empty PLGA-PEG NPs by nanoprecipitation, the resulting Ins-Zn-NPs were 78.7 nm in diameter (similar to the size of empty PLGA-PEG NPs) while maintaining more than 10-fold higher insulin loading (3.82 %) compared to Ins-NPs. Here, we again observe that addition of Ins-Zn hexamers (or zinc ions) to pre-formed empty PLGA-PEG NPs (or pre-formed Ins-NPs) does not change the hydrodynamic diameter of those NPs. However, the size of the Ins-Zn-NPs (~120 nm) formed by including Ins-Zn in the organic phase (DMSO) is much larger than that of PLGA-PEG NPs (~80 nm), analogous to, but opposite to the effect of including

insulin in DMSO during formation of Ins-NPs. These results point to a general principle, where addition of insulin to pre-formed NPs enables insulin loading without affecting NP size, but including insulin in the same solution as the polymeric precursor can influence NP size.

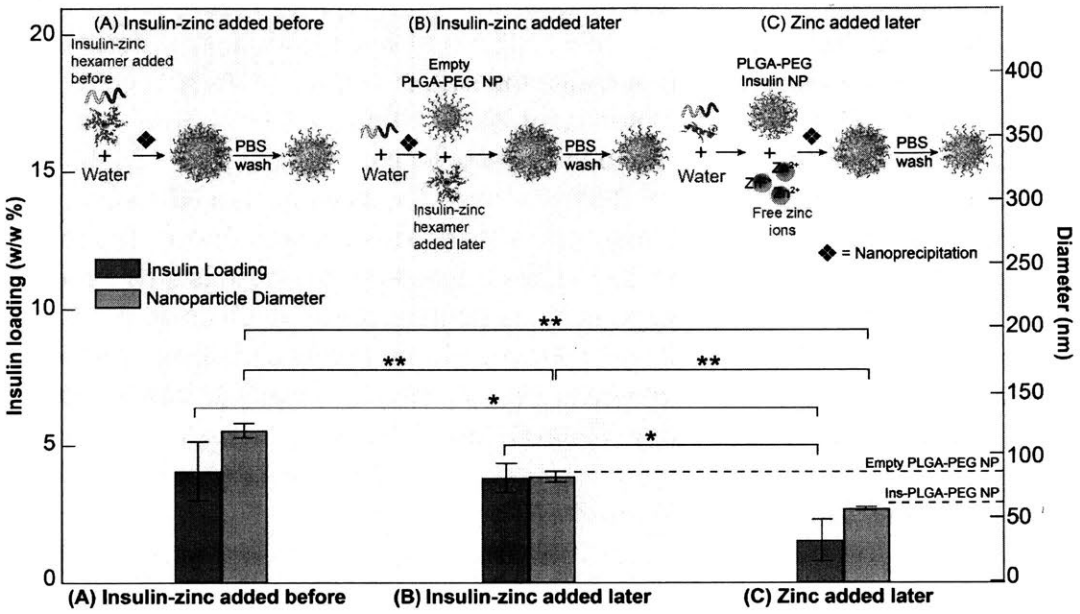

Figure 2.7. *Effect of adding zinc ions at different stages of nanoprecipitation on Ins-Zn-NPs.* (A) Schematic showing the synthesis of Ins-Zn-NPs by adding Ins-Zn hexamers premixed with PLGA-PEG molecules in DMSO before nanoprecipitation (top). This forms NPs with high insulin loading (4.07%) and large NP diameter (127.6 nm). (B) Schematic showing the synthesis of Ins-Zn-NPs by adding Ins-Zn hexamers to empty PLGA-PEG NPs after nanoprecipitation (top). This forms NPs with high insulin loading (3.82%) and small NP diameter (78.7 nm). (C) Schematic showing the synthesis of Ins-Zn-NPs by adding zinc ions to preformed Ins-NPs after nanoprecipitation (top). This forms NPs with lower insulin loading (1.55%) and smaller NP diameter (57.9 nm). Dashed lines indicate sizes of empty PLGA-PEG and Ins-NPs for reference. Error bars represent ± s.d. For insulin loading $n = 3$ and $p_{AB} = 0.74$, $p_{AC} = 0.034$, $p_{BC} = 0.016$. For NP diameter $n = 3$ and $p_{AB} = 0.0004$, $p_{AC} = 0.0001$, $p_{BC} = 0.005$.

2.4.5. Effect of pH on formation of Ins-Zn-NPs

Insulin exhibits pH-dependent behavior with an isoelectric point of 5.6[271], which imparts insulin a net negative charge at pH greater than pH 5.6 and a net positive charge at pH less than 5.6. Since our findings suggest that the synthesis of Ins-NPs by nanoprecipitation could be affected partially by electrostatic interactions,

we expect to be able to control the insulin loading by changing the net charge on insulin by altering the pH of the system.

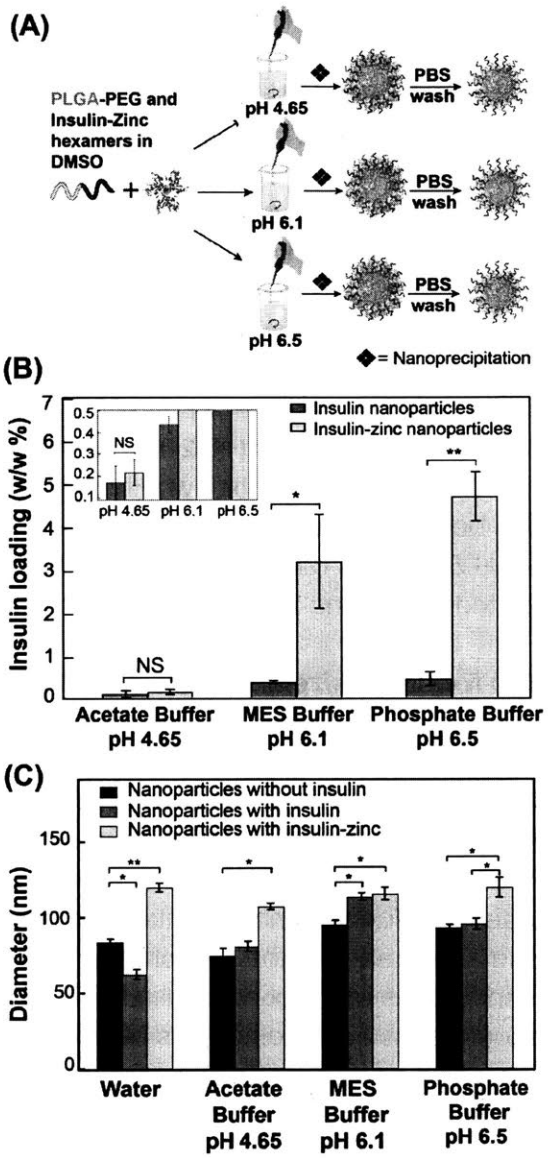

Figure 2.8. *Effect of pH on Ins-Zn-NP and Ins-NPs.* (A) Schematic showing the synthesis of Ins-Zn-NPs in different buffers (pH 4.65, pH 6.1, and pH 6.5). (B) Insulin loading of Ins-Zn-NPs and Ins-NPs that were synthesized in buffers with different pH. Insulin loading increased with increasing pH. (C) Average diameter of empty PLGA-PEG NPs, Ins-NPs, and Ins-Zn-NPs synthesized in different buffers.

To better understand the role of pH, we synthesized Ins-Zn-NPs in three different buffers: acetate buffer (20 mM, pH 4.65), MES buffer (20 mM, pH 6.1) and phosphate buffer (20 mM, pH 6.5) (Figure 2.8A). In the case of Ins-Zn-NPs, insulin loading increases with increasing pH (Figure 2.8B), which can be attributed to the larger net negative charge on insulin at pH greater than 5.6, which enables stronger interactions with insulin and zinc ions[215]. Ins-Zn-NPs prepared at pH 6.5 showed higher insulin loading (4.7%) than the Ins-Zn-NPs prepared in DI water (4.07 %). Therefore, by optimizing the pH of the system, insulin loading can further be improved in PLGA-PEG NPs. A similar trend was observed in the case of Ins-NP without zinc, where insulin loading slightly increased with increasing pH (Figure 2.8B). It is noteworthy that at pH 4.65, zinc ions did not have any effect on insulin loading in PLGA-PEG NPs, and the insulin loading both with and without zinc was similar (~0.2 %). This observation can be attributed to the net positive charge on insulin below pH 5.6 that leads to a reduction in the interactions between insulin and zinc and makes the Ins-Zn hexamers unstable below pH 5.6[215]. By contrast to insulin loading, pH does not have a significant effect on the size of Ins-Zn-NPs (Figure 2.8C).

2.4.6. *Optimization of NPs for small size and high insulin loading*

The key factors that affect NP characteristics and how they can be altered to control two important NP characteristics – insulin loading and NP size – are summarized in Figure 2.9A and 2.9B. It is evident from the representation in these figures that Ins-NPs are smaller in size but show poor insulin loading, while the inclusion of zinc in these NPs during nanoprecipitation helps to increase the insulin loading but results in an increase in the size of the NPs. We also see that addition of insulin at different stages and mixing insulin in different phases affects NP size but does not change the insulin loading. This behavior was exploited in optimizing the insulin loading and size of Ins-Zn-NPs. On addition of zinc ions to pre-formed Ins-NPs, insulin loading increased 4-fold (1.55% from 0.36%) without resulting in an increase in the size of Ins-NP (57.9 nm). Furthermore, the strategic inclusion of insulin-zinc hexamers to pre-formed empty PLGA-PEG NPs results in a greater than 10-fold high insulin loading (3.82%) and small NP size (78.7 nm), thus making them promising NPs for oral delivery of insulin using a transcytosis pathway like the FcRn pathway.

Figure 2.9C shows the rate at which insulin is released from the Ins-Zn-NPs (where Ins-Zn is added later; Insulin loading 3.82%, NP size 78.7 nm). The half-

life of insulin in these NPs is around 60 min. The release curve of Ins-Zn-NPs is similar to the insulin loaded PLA-PEG NPs release curve which was reported in an earlier study where the insulin loading in PLA-PEG NPs was about 0.5%[1].

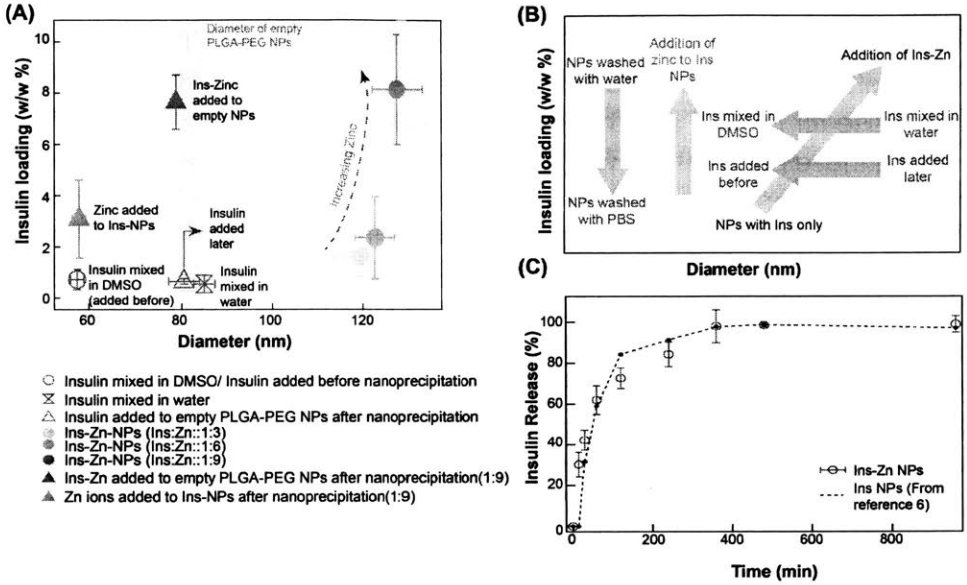

Figure 2.9. *Compilation of the effect of NP synthesis parameters on NP properties.* (A) Compilation of the NPs studied for the purpose of understanding the factors that affect insulin loading and NP size in Ins-NPs and Ins-Zn-NPs. The symbols in blue contain only PLGA-PEG and insulin while the orange symbols represent NPs that contain PLGA-PEG, insulin, and zinc. The size of empty PLGA-PEG NPs has been represented by a grey vertical bar, whose width represents the standard deviation. Ins-NPs (blue) have low loading and small size. Contrary to these NPs, Ins-Zn-NPs formed by including zinc during nanoprecipitation (orange circles) have higher insulin loading, but their diameter is larger. NPs synthesized by adding Zn ions to preformed Ins-NPs (light triangle) show smaller size and moderate loading. The optimal NPs are Ins-Zn-NPs (dark triangle) formed by adding Ins-Zn hexamers to pre-formed NPs combine high loading (3.82 %) and small size (78.7 nm diameter). (B) Qualitative summary of how different synthesis parameters affect insulin loading and size. *Insulin release.* (C) Release of insulin from the optimal NPs (Ins-Zn-NPs with insulin loading 3.82%, NP size 78.7 nm) is comparable with the previously reported release of insulin from PLA-PEG NPs[1].

2.5. Conclusions

Realizing the full potential of polymeric NP based protein therapeutics will require more efficient loading of proteins in these NPs. To understand the factors that control protein loading in NPs, we systematically investigated the effect of individual steps of the nanoprecipitation process including the washing step, the mixing phase for insulin, and the stages of adding insulin to the system. First, by controlling these parameters, we have shown that the type of wash can dramatically influence the measured insulin loading in Ins-NPs, where buffer wash removes majority of the insulin compared to water wash. Second, we also demonstrate that smaller Ins-NPs can be formed by dissolving insulin along with the PLGA-PEG molecules in organic phase (DMSO) before nanoprecipitation. In the case of Ins-Zn-NP system, more than 10-fold increase in insulin loading compared to Ins-NPs was obtained by using Ins-Zn hexamers. We also applied the insights obtained from the Ins-NP system to Ins-Zn-NP system to achieve small NP diameter while maintaining high insulin loading. In particular, we find that insulin and/or zinc may be added to pre-formed NPs to load insulin without affecting the NP size. Third, in addition, insulin loading in Ins-Zn-NP system could be optimized by tuning the pH of the system. This study illustrates how simple modifications of the nanoprecipitation process can provide insights that enable realization of NPs with desired properties. This approach can potentially extend to other protein-encapsulating NP systems to understand the mechanisms of protein loading and to devise processes to enhance protein loading in NPs formed by nanoprecipitation.

CHAPTER 3

Design of pH-Responsive Nanoparticles

3.1 Abstract

Parenteral administration remains the mainstay of drug administration for protein therapeutics. However, for diseases that require frequent drug dose over long periods of time, injections can result in patient incompliance and poor treatment outcomes. For such diseases, oral drug delivery is the most non-invasive and patient-compliant method of drug administration. Although oral delivery of many small molecule drugs is routine, oral delivery of protein drugs – e.g. insulin – presents several challenges including oral bioavailability of the protein therapeutic because of degradation in the stomach, inactivation and digestion of the therapeutics by the proteolytic enzymes in the luminal cavity, and poor permeability of drugs across the intestinal epithelium. To circumvent these challenges we have designed a pH-responsive nanoparticle (NP) drug delivery platform. We show that Eudragit S100 and poly (lactic-co-glycolic) acid (PLGA-PEG) can be blended to form NPs with high insulin loading (13.1%), small NP size (83 nm), and with the ability to rapidly release insulin when exposed to basic pH. We designed the NPs for the neonatal Fc receptor targeted transcytosis pathway. We demonstrate a 5-fold greater transport across a Caco-2 monolayer in an in vitro epithelial model, in NPs functionalized with Fc (NPs-Fc) relative to NPs without the targeting ligand. This pH-responsive targeted drug delivery platform provides a nontoxic way to safely transport insulin across the intestinal lining to blood.

3.2 Introduction

Currently, biologics and nanoparticle (NP)-based therapies are administered primarily via intravenous or subcutaneous injections[2, 272]. For diseases that require frequent doses over prolonged periods of time, such methods of drug administration result in patient incompliance and inconvenience[28, 30, 273-274]. Among the alternate routes of administration such as oral, pulmonary, colonic, nasal, buccal, and transdermal, oral delivery is considered to be the most desirable because of the improved patient compliance, convenience, and cost effectiveness as a direct result of flexible schedule, less demands on medical staff, and less frequent hospital or clinic visits[90, 238, 275-278]. Therapeutic biologics are large protein molecules such as insulin, calcitonin etc[233-236] that face many chemical and physical barriers along the gastrointestinal tract that may limit their

absorption or result in their denaturation and degradation[110]. Such barriers include the extreme pH environments, enzymatic degradation, and poor permeability across the intestinal epithelium [279]. The large size of the protein therapeutics, and their sensitivity to the complex gastrointestinal environment comprised of a wide range of pH[111] and enzyme activity, makes it challenging to deliver these biologics orally[280].

Various strategies have been adopted in the past to address the challenges of efficient oral delivery of protein therapeutics including inhibition of enzymatic action[133-135, 137-138], application of permeation enhancers[123-126] and mucoadhesives[141-143], there are illustrated in detail in Chapter 1, Section 1.2.. However, major issues have been identified with each of the strategies such as uncontrolled permeation of the intestinal lining, access to unwanted toxic pathogens, incomplete food digestion, and clearing of the payload along with the mucosal lining[135, 142, 144, 280]. Other strategies of overcoming the barriers of oral delivery of biologics include the application of pH sensitive hydrogels[281], which are composed of polymeric material that can be engineered to exhibit mucoadhesive properties[282]. However, these particles have shown to interact with the tight junctions present in the intestinal lining, opening them reversibly thereby causing similar concerns as the non-specific permeation enhancers[283].

A more specific transportation of therapeutic proteins across the intestinal epithelial barrier can be achieved by targeting them to receptors that traffic proteins across the intestinal lining using a transcytosis pathway. This can be achieved by conjugating protein biologics to ligands capable of targeting the receptors that are associated with transcytosis pathways[185, 284]. Several receptors have been investigated for receptor mediated drug delivery to transport therapeutic agents conjugated with targeting ligands. One such well-studied receptor is the transferrin receptor[184-185, 285], which has been used for transport of therapeutic agents across the blood-brain barrier[186-187] as well as the intestinal epithelium[188]. Vitamin B_{12} pathway is also a well-studied pathway that has been used to transport luteinizing hormone releasing factor[180], erythropoietin[181], alpha-interferon[182] and insulin[183]. Another receptor mediated transport pathway that has been used transport insulin is the folic acid pathway[286]. The receptor mediated transcytosis technology addresses the safety issues associated with the previous strategies; however, its impact is limited by poor efficiency originating from 1:1 ratio of drug molecules and targeting ligands.

Recently, polymeric nanoparticle (NP) carriers have shown promise in drug delivery for treatment of a variety of diseases[218, 240-247], including oral delivery of

proteins such as insulin[1, 223, 248-251]. Advantageous to oral delivery, NPs can be easily prepared from a variety of materials, targeting ligands can be conjugated on NP surfaces that can facilitate therapeutics to cross the epithelial barrier[250], and NPs can protect encapsulated and adsorbed therapeutics from pH changes and enzymatic degradation in the gastrointestinal tract[193, 250, 252]. The application of NPs enables design of customized and specific carriers which can be obtained by modulating physiochemical parameters such as size, surface charge, hydrophobicity, which result in controlled drug release properties[287]. Moreover, the small size of the NPs can be leveraged to obtain increased contact area with the epithelial surface and non-specific uptake by cells through transcytosis pathways.
NPs encapsulate several molecules of the therapeutic agent thereby enabling the transport of multiple molecules per receptor, which is conjugated on the NP surface.

A recent study demonstrated the successful transport of poly(lactic acid)-poly(ethylene glycol) PLA-PEG NPs across the intestinal epithelium using the FcRn transcytosis pathway. The study demonstrated that the NPs crossed the gastroepithelial barrier and entered systemic circulation showing remarkable promise for oral delivery of insulin[1]. Moreover, the FcRn pathway has been used to increase the half-life of protein drugs and also to transport drugs across epithelial barriers such as the intestinal epithelium and the pulmonary mucosa. Various proteins, such as erythropoietin[209], follicle-stimulating hormone[209-210], interferon-alpha and interferon-beta, have been conjugated to the Fc region of human IgG to facilitate such drug delivery upon inhalation through the upper airway where FcRn resides in humans and non-human primates[211].

In humans, the neonatal Fc receptor (FcRn) is present on the apical membrane of the absorptive epithelial cells predominantly in the upper small intestine (duodenum). The FcRn is responsible for the active transport of IgG antibodies across the polarized epithelial barrier through the processes of transcytosis. Under slightly acidic conditions (pH 6-6.5), FcRn binds with the CH_2 and the CH_3 domains of heavy chains in the Fc region of the IgG and releases the IgG at neutral-to-basic pH (pH 7–7.4)[207]. The pH dependence is induced by the protonation of histidine residues located at the interface of CH_2 and CH_3 domains of the Fc region of IgG, at acidic pH that aides in the formation of salt bridges with acidic residues on FcRn surface. Formation of these salt bridges is instrumental in stabilizing the hydrophobic interactions between Fc and FcRn at acidic pH[208].

The Fc portion of IgG enables the target payload-NPs to be actively transported across the intestinal epithelium by targeting the FcRn receptor. In the duodenum the pH is low (pH 5-6.5) and thus enables the IgG to bind to the FcRn on the apical membrane of absorptive epithelial cells. During intracellular trafficking across the cell, NP-Fc continues to bind to the FcRn with high affinity as the complex passes through endosomal compartments that have acidic pH. Once on the basolateral side, exocytosis results in exposure to an environment with physiological pH (pH 7.4), causing dissociation of Fc from the FcRn and release of NP-Fc into the extracellular environment of the lamina propria. The NP-Fc is then free to diffuse through the lamina propria and enter the lymphatic and systemic circulation[1, 193].

Application of the FcRn pathway has many advantages over other strategies used for oral delivery. First, the FcRn pathway uses does not compromise the integrity of the epithelial barrier preventing toxic reactions. Second, this approach does not require any modification of the therapeutic protein. Third, the FcRn receptor is abundantly present on absorptive epithelial cells that form a significant percentage of the absorptive area of the intestine[194, 196]. Fourth, multiple therapeutic agents get transcytosed per FcRn thereby improving the efficiency of the receptor mediated transcytosis technology.

However, one challenge associated with this strategy is that once the NP-Fc reach the systemic circulation they become highly susceptible to clearance by the mononuclear phagocyte system as the presence of Fc fragments enhance clearance of the NPs. Once the NPs cross the intestinal epithelium, they are susceptible to clearance by the mononuclear phagocyte system. This problem is exacerbated in the case of FcRn-targeted NPs that are decorated with Fc fragments that enhance clearance of the NPs. Rapid release of the payload after transcytosis of NPs into the blood stream is one way of addressing this issue, i.e. the drug is released rapidly before the NPs are cleared.
Moreover, it has been shown that transport pathways like the FcRn pathway work most efficiently for small NPs[1, 193]. *In vitro* studies using Caco-2 cells (human adenocarcinoma cell line) and *in vivo* studies in rats have shown that the uptake of smaller NPs (~100 nm) is significantly more efficient than that of larger NPs (500 nm, 1 μm, 5 μm)[193]. It has also been shown using nanogold labeled IgG Fc and electron tomography analysis that the vesicles containing FcRn are 60-120 nm or smaller[288]. Therefore, preparing particles with sizes less than 100 nm is necessary for uptake by intestinal epithelial cells.

Therefore, the main challenges associated with making NPs which can efficiently deliver large protein molecules across the intestinal epithelium are: (1) to ensure that the NP diameter is small (less than 100 nm), (2) to ensure that the NP has a high protein loading, (3) to make the drug and the NP survive the changes in pH in the complex environment of the gastrointestinal tract, and (4) to trigger quick release of majority of the drug before the NP is excreted from the body.

To overcome these challenges, in this study we have designed an environment-responsive drug delivery platform comprised of hybrid polymeric NPs, which can efficiently encapsulate therapeutic proteins, and yet maintain small NP size. These NPs are designed to elicit a secondary response when the pH of their surrounding environment changes from acidic to neutral/or basic, which occurs when the NPs cross over from the acidic gastrointestinal environment to the blood stream.

These NPs are made by blending one pH responsive polymer with a non-pH responsive polymer that can typically form NPs by itself without mixing with the pH-responsive polymer. The non-pH-responsive polymer aids in the formation of NPs, whereas the pH-responsive polymer imparts pH-responsiveness to the NP. The NPs are formed by nanoprecipitation method at a pH in which the pH-responsive polymer is insoluble. This aids in the self-assembly of the NP. As the results show, the pH during NP formation can be optimized to increase the drug loading and possibly also the degree of pH-responsiveness. The ratio of the two polymer components can be changed to optimize loading and NP size. When the NPs thus formed are exposed to a pH at which the pH-responsive polymer dissolves, it triggers a change in the NP where the drug payload is rapidly released.

To demonstrate the above technology, we used an acrylate and methacrylate based pH responsive polymer, Eudragit S100 as the pH responsive polymer, and blended it with poly(lactic-co-glycolic acid)-poly(ethylene glycol) (PLGA-PEG) to make NPs with insulin as the payload for oral delivery. These NPs were decorated with the Fc fragments so that they can be used in the FcRn transcytosis pathway[1]. Ins-Eud-NPs were designed to release insulin when triggered by a change in pH from acidic to neutral. This property of the NPs can be utilized to enable oral delivery of insulin using the FcRn pathway, where the NPs remain intact in the stomach (pH 2-3), upper small intestine (pH 5-6) and in the cellular endosomes (pH 5) where the pH is acidic but on coming in contact with blood (pH 7.4), Eudragit S100 begins to dissolve and the NP loses its integrity, resulting in rapid release of insulin.

The application of this platform can be extended from oral delivery to any system, which desires a secondary response due to a change in the pH of the environment (acidic to neutral/basic). Further, this pH responsive characteristic of the NPs can be extended to other large protein molecule systems and other kinds of payloads (such as small molecule drugs) and other transport pathways including intracellular pathways that involve change of pH.

3.3 Experimental Section

3.3.1 Materials

Human recombinant insulin, dimethyl sulfoxide (DMSO), zinc chloride, sodium acetate, sodium phosphate, MES hydrate, and Traut's reagent were purchased from Sigma-Aldrich. $PLGA_{10k}$-PEG_{5k}, $PLGA_{10k}$ -PEG_{5k}-Maleimide and $PLGA_{50k}$–FKR 648 were purchased from Akina Inc. (West Lafayette, IN, USA). Eudragit was donated by Evonik (Essen, Germany). Micro bicinchoninic acid (BCA) protein assay kit was purchased from Lamda Biotech, Inc. (St. Louis, MO, USA). Phosphate Buffer Saline (PBS) was purchased from Life Technologies (Green Island, NY, USA). Human Fc fragment was purchased from Bethyl Laboratories (Montgomery, TX, USA). Deionized (DI) water was used for all the experiments.

3.3.2 Methods

3.3.2.1 Synthesis of Eud-NPs and Eud-Ins-NPs

For the preparation of Ins-Eud-NPs by the nanoprecipitation method (Figure 3.1), we premixed 30% (w/w) of insulin (10 mg/mL) solution in DMSO with 20% (w/w) Eudragit S100 (10 mg/mL) solution and 80% (w/w) $PLGA_{10k}$ -PEG_{5k} (10 mg/mL) solution in DMSO. The resulting solution was added drop wise to 4 mL Acetate buffer solution (pH 5, 10 mM). The solution was stirred for at least two hours at 2000 rpm. The resulting NP solution was purified using ultrafiltration using Amicon Ultracel 100 kDa membrane filters to remove free insulin and organic solvent. The NPs were washed with 15 mL of Acetate buffer (pH 5, 10 mM, 150 mM NaCl) at 3000 g by centrifugation. The NPs were resuspended in Acetate buffer (pH 5, 10 mM, 150 mM NaCl) to a final concentration of 10 mg/mL. As a control, NPs were prepared with PLGA-PEG solution alone using the same procedure without the addition of insulin and without the addition of Eudragit S100. In all experiments, the ratio of the organic to the aqueous phase remained constant at 13:100.

Ins-Zn-Eud-NPs were prepared by first mixing insulin (10 mg/mL) and zinc chloride (5 mg/mL) in DMSO in 1:9 molar ratios of insulin : zinc such that insulin is 30% (w/w) of the polymer. To this solution, 20% (w/w) Eudragit S100 (10 mg/mL) solution and 80% (w/w) $PLGA_{10k}$ -PEG_{5k} (10 mg/mL) was added. The resulting solution was added drop wise to 4 mL Acetate buffer solution (pH 5, 10 mM) and mixed for at least two hours at 2000 rpm. Then, the NPs were purified by the aforementioned process.

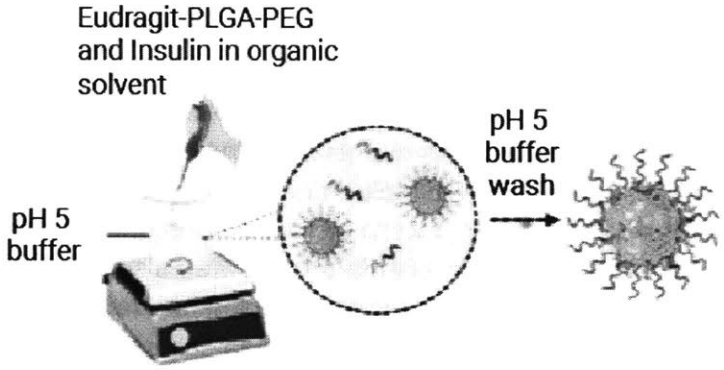

Figure 3.1. Schematic of the NP synthesis set-up. The Ins-Eud-NPs were synthesized using the nanoprecipitation method. The polymer and the drug was mixed in the organic solvent (DMSO) and the resulting solution was added drop-wise to a beaker with pH 5 buffer that was being constantly stirred at 2000 rpm. Following NP synthesis the NPs were washed multiple times with pH 5 buffer with 150 mM NaCl.

3.3.2.2 Characterization of Eud-NPs and Ins-Eud-NPs

The amount of insulin loaded in Ins-Eud-NPs was quantified by using a low protein BCA assay kit. After the purification process, Ins-Eud-NPs were resuspended in Acetate buffer (pH 5, 10 mM, 150 mM NaCl) to a final concentration of 1 mg/mL and heated at 60°C for 1 h to release insulin. Then, 125 µL of NP solution was added to each well in a 96 well-plate followed by the addition of 125 µL of bicinchoninic acid (BCA) assay working solution. After incubating the NPs at 60°C for 30 min, the amount of insulin was analyzed using a TECAN UV spectrophotometer (Mannedorf, Switzerland) according to the manufacturer's instructions. As a control, NPs without insulin were also measured by the same procedure. The weight percent of insulin in the NPs was

measured as the insulin loading and the fraction of insulin in the NPs was measured as encapsulation efficiency. Three separate experiments were performed for each data point.

For measuring the hydrodynamic radius, the NPs were washed and reconstituted in 1 mL of Acetate buffer (pH 5, 10 mM) at a NP concentration of 0.5 mg/mL. The solution was loaded in disposable low-volume cuvettes to measure the hydrodynamic radius and NP size distribution using the Zetasizer NanoZS instrument (Malvern Instruments Ltd., U.K.).

3.3.2.3 Measurement of insulin loading

Insulin loading in Ins-Eud-NPs was quantified using a low protein BCA assay kit (Lamda Biotech). Empty PLGA-PEG-Eudragit NPs and blank buffer (10 mM pH 5 Acetate buffer with 150 mM NaCl) were included in the analysis as controls. For each set of measurement, insulin standard curve was also measured. The absorbance values of the standard curve were plotted against their respective concentration values to obtain a linear equation to calibrate absorbance to concentration.

$y = Ax + B$; y = Absorbance, x = Concentration of insulin (µg/mL)

$$\text{Concentration} = \frac{\text{Absorbance} - B}{A}$$

The concentration of insulin in each sample was quantified using the calibration obtained from the standard curve. After NP synthesis, the total volume of each NP sample was recorded. The total amount of insulin in the sample was calculated by taking the product of the concentration of insulin and the volume of each sample.

$$\text{Amount of insulin (µg)} = \text{Concentration } \left(\frac{\mu g}{mL}\right) \times \text{Sample volume (mL)}$$

The total amount of insulin added to each batch of the NPs and the weight of the NPs in each batch were known, from which the insulin loading and encapsulation efficiency were calculated using the following equations:

$$\text{Insulin loading (\%)} = \frac{\text{Total amount of insulin detected}}{\text{Weight of the NPs}} \times 100\%$$

$$\text{Encapsulation Efficiency (\%)} = \frac{\text{Total amount of insulin detected}}{\text{Total amount of insulin added}} \times 100\%$$

The value of insulin loading in the Ins-Eud-NPs was measured after subtracting the absorbance of the empty NPs from the absorbance of the insulin loaded NPs.

3.3.2.4 In vitro insulin release

The *in vitro* release of insulin was studied in 20 mM Phosphate buffer (pH 7.4, 150 mM NaCl), which simulated the pH of blood and in 20 mM MES buffer (pH 6, 150 mM NaCl), which simulated the pH of the duodenum. This was done by dividing a batch of Ins-Eud-NPs equally into 100 kDa Float A Lyzer (Spectrum Labs) units and incubating them at 37°C in 20 mM Phosphate buffer (pH 7.4, 150 mM NaCl). At each predetermined time interval, an aliquot of the NPs was taken and measured for insulin loading using the BCA assay, which included heating at 60°C for 1 h as previously described. In order to increase the accuracy of the dialysis setup, a 3 mm magnetic stirrer was inserted in each Float A Lyzer unit, to allow continuous mixing of the NP solution inside the dialysis chambers. Furthermore, the beaker with the dialysis chambers was kept on an orbital shaker, to ensure mixing of the buffer solution outside the dialysis chambers. Three experiments were performed for each data point.

The *in vitro* release of insulin was studied by dividing a batch of Ins-Eud-NPs equally into aliquots and placing them in 100 kDa, Float-A-lyzer (Spectrum Labs) dialysis devices and incubating them at 37°C in 20 mM Phosphate buffer (pH 7.4, 150 mM NaCl). The detailed study of designing the *in vitro* release experiment protocol and set-up is elucidated in the Appendix. *The* dialysis devices were prepared according to the manufacturer's guidelines. The Float-A-Lyzer devices were pre-wetted, by soaking in 15% ethanol solution in a vacuum chamber for 20 minutes, in order to get rid of glycerin and achieve maximum membrane permeability. In addition, a vacuum chamber was used to allow maximum wetting of the dialysis membrane. This was followed by thoroughly washing the membranes twice with DI water. In each wash, the solution inside the devices was aspirated out, replaced with and soaked in DI water for 30 minutes. In order to ensure the presence of a concentration gradient to allow movement of insulin, the NP samples in the devices and the surrounding buffer had to be continuously stirred with a 3 mm magnetic stirrer was inserted into each device. 1.25 mL of the 1 mg/mL NP solution was added to each device, which were placed in a large beaker with pH 7.4 or pH 6 buffer at 37°C. Typically, 9-10 dialysis devices were placed in a beaker with 800-900 mL of pH 7.4 or pH 6 buffer. In order to ensure the movement of the magnetic stirrers the base of the devices had to be close to the bottom of the beaker, which made it difficult to add an additional stirrer in the beaker to stir the dialysis buffer. Therefore, for continuous stirring of the buffer outside the dialysis devices, the beaker was put on a magnetic stirring plate, which was further placed on an orbital shaker. This set up is illustrated in Figure 3.2 (a). At each predetermined time interval, an aliquot of the NPs was taken and

measured for insulin loading using the BCA assay. Three experiments were performed for each data point.

As a control experiment we measured the absorbance values of empty NPs with time using the BCA assay after soaking the devices for 4 h. In the ideal case, this value should be a constant independent of time and should be subtracted from the absorbance values obtained from Ins-Eud-NPs to get the correct loading value. However, we saw that the absorbance of empty NPs increased with time. This observation can be attributed to the presence of chemicals that can leach out of the dialysis device and interfere with the BCA assay. Therefore, to completely get rid of any interfering agents, after inserting stirrers in the devices, we filled them with pH 7.4 or pH 6 buffer and stirred them for 24 h in a beaker containing pH 7.4 or pH 6 buffer. On repeating the control experiment with devices that were soaked and stirred in buffer, we were able to achieve a constant absorbance value for empty NPs detected by the BCA assay (Figure 3.2 (b)). Therefore, all dialysis devices were pre-soaked overnight before release experiments to ensure a steady baseline signal for the empty NPs.
Another control experiment where the rate at which free insulin diffuses out of the dialysis devices was performed to measure the temporal resolution of the experimental set up. The half-life of free insulin was found to be 1 h as seen in Figure 3.2 (c). This experimental set up can therefore be used to study the release profile of drugs, which have a half-life of more than 1 h.

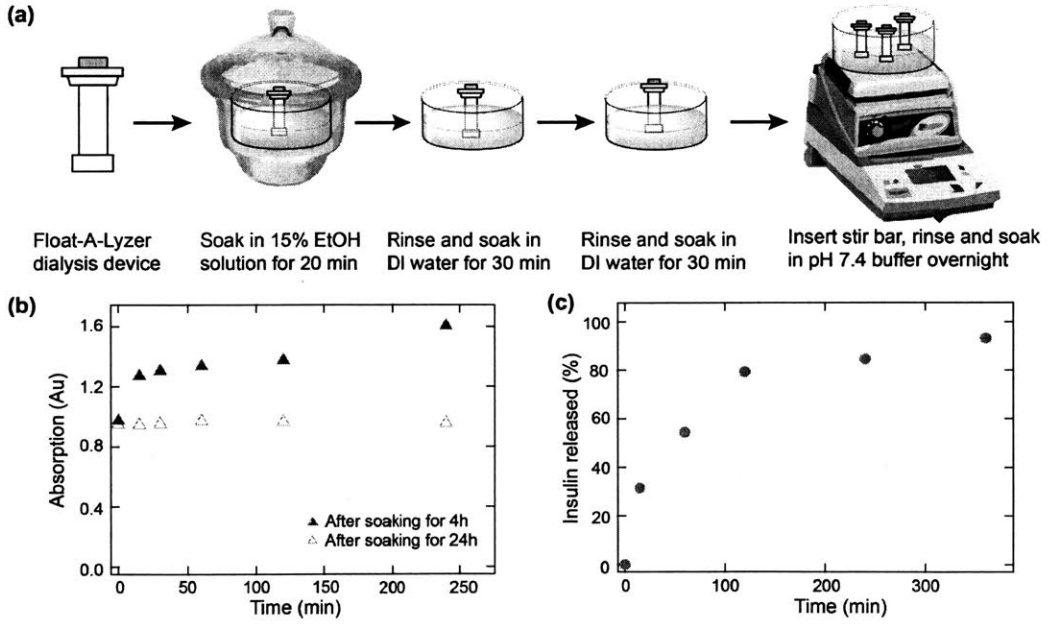

Figure 3.2. (a) Design of the dialysis set up to study the *in-vitro* release of

insulin. (b) Absorbance from empty NPs when the dialysis devices were soaked for 4 h and 24 h. (c) *In-vitro* release of free insulin.

3.3.2.5 Synthesis of Eud-NP-Fc

To prepare Ins-Eud-NPs we premixed 30% (w/w) of insulin (10 mg/mL) solution in DMSO with 20% (w/w) Eudragit S100 (10 mg/mL) solution, 70% (w/w) $PLGA_{10k}$ -PEG_{5k} (10 mg/mL) and 10% (w/w) $PLGA_{10k}$ -PEG_{5k} -Maleimide (10 mg/mL) solution in DMSO. The resulting solution was added drop wise to 4 mL Acetate buffer solution (10 mM pH 5). The solution was stirred for 15 min at 2000 rpm. The resulting NP solution was purified using ultrafiltration using Amicon Ultracel 100 kDa membrane filters to remove free insulin and organic solvent. The NPs were washed with 15 mL of Acetate buffer (10 mM, pH 5, with 150 mM NaCl, 5 mM EDTA) at 3000 g by centrifugation. The NPs were resuspended in Acetate buffer (10 mM, pH 5, with 150 mM NaCl) to a final concentration of 10 mg/mL.

While the NPs were being washed, 5 mg/mL Fc solution was reacted with 5 mg/mL 2-imminothiolane solution in the molar ratio of 10:1 (Traut's reagent to IgG Fc). 100 uL of this thiolated Fc was added to 400 uL of 10 mg/mL NPs in Acetate buffer (10 mM, pH 5, with 150 mM NaCl). Thiolated Fc and the NPs were incubated for 2 h after which the NPs were washed with three times the volume of Acetate buffer (10 mM, pH 5, with 150 mM NaCl) in 1.5 mL Amicon Ultracel 100 kDa membrane filters at 10 000 g. NPs were resuspened in Acetate buffer (10 mM, pH 5, with 150 mM NaCl) at a concentration of 1 mg/mL.

As control experiment, NPs were prepared with PLGA-PEG solution alone using the same procedure without the addition of insulin and without the addition of Eudragit S100. In all experiments, the ratio of the organic to the aqueous phase remained constant at 13:100.

To prepare fluorescently labeled Ins-Eud-NP-Fc 10% (w/w) of $PLGA_{50k}$ – FKR 648 was added to the organic solution in addition to 30% (w/w) insulin, 20% (w/w) Eudragit, 70% (w/w) $PLGA_{10k}$ -PEG_{5k} and 10% (w/w) $PLGA_{10k}$ -PEG_{5k} (10 mg/mL). The resulting solution was added drop wise to 4 mL Acetate buffer solution (10 mM, pH 5) and the NPs were synthesized and purified in the aforementioned method.

3.3.2.6 Characterization of Eud-NP-Fc

The amount of Fc conjugated to the Ins-Eud-NPs was quantified by using a low protein BCA assay kit. After the purification process, Ins-Eud-NP-Fc and Eud-NP-Fc were resuspended in acetate buffer (10 mM, pH 5, with 150 mM NaCl) to a final concentration of 1 mg/mL and heated at 60°C for 1 h to release insulin. Then, 125 µL of NP solution was added to each well in a 96 well-plate followed by the addition of 125 µL of bicinchoninic acid (BCA) assay working solution. After incubating the NPs at 60°C for 30 min, the amount of insulin was analyzed using a TECAN UV spectrophotometer (Mannedorf, Switzerland) according to the manufacturer's instructions. As a control, NPs without insulin and Fc, NPs without Fc and NPs without insulin were also measured by the same procedure. The weight percent of insulin in the NPs was measured as the insulin loading and the fraction of insulin in the NPs was measured as encapsulation efficiency. To estimate the Fc conjugation the absorbance signal from Ins-Eud-NP was subtracted from the absorbance signal of Ins-Eud-NP-Fc. Three separate experiments were performed for each data point.

For measuring the hydrodynamic radius, the NPs were washed and reconstituted in 1 mL of Acetate buffer (10 mM, pH 5) at a NP concentration of 0.5 mg/mL. The solution was loaded in disposable low-volume cuvettes to measure the hydrodynamic radius and NP size distribution using the Zetasizer NanoZS instrument (Malvern Instruments Ltd., U.K.).

3.3.2.7 *In vitro* Transcytosis

Cyprotex (Cambridge, MA) is an external company that performed the transepithelial transport study. The study was done using 96-well plate Transwell plates (Corning) with a Caco-2 cell in media (ATCC formulated Eagle's Minimum Essential Medium with aqueous penicillin (100 units/mL), streptomycin (100 units/mL), and fetal bovine serum (FBS, 20%)). 24 hours before the transport experiment, fresh media was added in the apical and basolateral chambers in the Transwell plates. On the day of the experiment the media was changed to HBSS pH 6 in the apical chamber and HBSS pH 7.4 in the basolateral chamber and allowed to equilibrate for 1 h at 37°C and 5% CO_2.

Caco-2 cells were grown in tissue culture flasks that were trypsinized, suspended in medium, and the suspensions were applied to wells of a Millipore 96 well transwell plate. The cells were allowed to grow and differentiate for three weeks, feeding at 2 day intervals. The properties of the semipermeable membrane can

be found in Table 1. 75 µL of 5 mg/mL fluorescently labeled NPs were added to the apical side and the amount of permeation was determined on the basolateral side. Caco-2 cells were incubated with the NPs for 2 h before the NP solution was sampled from the apical as well as the basolateral chamber. At the end of the experiment the sampled apical and basolateral solutions were lyophilized and dissolved in DMSO and their fluorescence signal was measured using a TECAN Safire plate reader (Mannedorf, Switzerland).

3.4 Results and Discussion

3.4.1 Effect incorporating Eudragit in Ins-Zn-NPs

Ins-Zn-NPs with high insulin loading (3.82%) and small NP diameter (78.7 nm) were previously synthesized. However, for an ideal NP solution for oral delivery of insulin it is important for majority of the insulin to be released as soon as the NP reaches blood in systemic circulation otherwise due to the presence of ligands on the NP surface, there is a high probability that the NPs would be opsonized by macrophages. However, pH responsive NPs that would protect insulin and remain intact at pH less than 7.4 and instantly release insulin at pH 7.4 would be an ideal solution. To achieve this we hypothesized that blending a pH responsive polymer with our existing Ins-Zn-NP technology would produce pH responsive NPs. To test the hypothesis, we blended Eudragit S100, a copolymer of methacrylic acid and methyl methacrylate, with PLGA-PEG to form Eud-Ins-Zn-NPs by the process mentioned in Section 3.3.2.1. The insulin loading obtained from these Eud-Ins-Zn-NPs was compared with that of Eud-Ins-NPs without zinc.

It was observed that the insulin loading in the case of Eud-Ins-Zn-NPs (12.2%) was similar to the loading of Eud-Ins-NPs (13.1%) as seen in Figure 3.3A. This indicates that the presence of zinc did not provide an added advantage by increasing insulin loading. However, the addition of Eudragit significantly improved insulin loading in Eud-Ins-NPs (13.1%) when compared with the loading in Ins-Zn-NPs (3.82%).

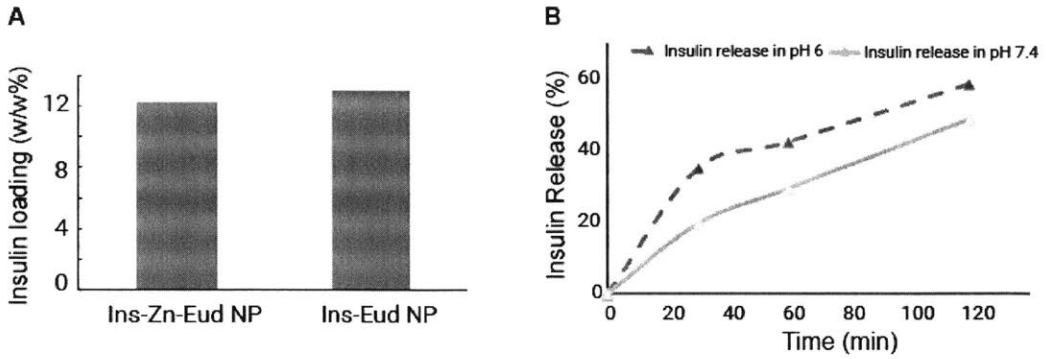

Figure 3.3. (A) Addition of Eudragit S100 in the NP formulation for Ins-Zn-NPs (12.8%) did not lead to an improvement in insulin loading when compared with the insulin loading of Ins-Eud-NPs (13.1%). However, presence of Eudragit leads to an improvement in insulin loading. **(B)** Ins-Zn-Eud-NPs failed to illicit the desired pH response. Insulin released at a faster rate at pH 6 as compared to pH 7.4. This can be attributed to both the pH vales being larger than the pH of the isolelectric point of insulin below which Ins-Zn hexamers are unstable.

Further, we performed a 2-hour test release experiment to investigate if the presence of zinc ions helped release insulin faster in pH 7.4 as compared to pH 6. Figure 3.3B shows that Eud-Ins-Zn-NPs did exhibit the desired pH responsive behavior, in fact, the response was opposite of what was expected. Eud-Ins-Zn-NPs released insulin much faster at pH 6 as compared to that at pH 7.4.

Both the insignificant change in insulin loading and the opposite response to pH can be attributed to the breakdown of Ins-Zn hexamers at pH below the isoelectric point of insulin (pH 5.6)[215]. Since the pH of the synthesis buffer (pH 5) was very close to the isoelectric point of insulin the Ins-Zn hexamers could be unstable at that pH and hence did not show an improvement in insulin loading as compared to Eud-Ins-NPs without zinc. Similarly, in the test release experiment the desired effect was not observed in the Eud-Ins-Zn-NPs because both pH 6 and pH 7.4 are above the isoelectric point of insulin that potentially causes the Ins-Zn hexamers to get compromised and thus fail to illicit the desired pH response.

These results suggest that although the addition of zinc ions to the NPs system did not provide the additional benefits of improved loading or the desired pH response, the application of Eudragit S100 in the NP system showed promise.

3.4.2 Formation of Eud-NPs

The application of Eudragit showed promise in improving insulin loading as well as in producing a pH dependent response as mentioned in Section 3.4.1. Moreover, Eudragit is one of the most widely used pH dependent polymers[289]. Eudragit has been used to form enteric coatings[290], microspheres[291] and nanoparticles[292-293]. Majority of the nanoparticles and microparticles have been produced in conjunction with a stabilizer like polyvinyl alcohol (PVA)[291, 294] or dispersants like poloxamer[292, 295] and polysorbates[291] using techniques like supercritical antisolvent[293], quasi emulsion solvent diffusion[292, 294-295] or salting out[296]. However, not many studies have focused on the formation of Eudragit S100 NPs using the solvent displacement method.

To synthesize Eud-NPs using the solvent displacement method we used a synthesis buffer with a pH less than 7 to ensure that the pH of the NP set up was less than the dissolution pH of the polymer (pH 7). The NPs were synthesized with only Eudragit S100 as mentioned in Section 3.2.2.1. However, NPs were not formed by this method as seen in Figure 3.4A and 3.4B. Figure 3.4B shows the presence of aggregates in the solution and not NPs. This can be attributed to the absence of a stabilizer, dispersant or an amphiphilic polymer, which can readily form NPs.

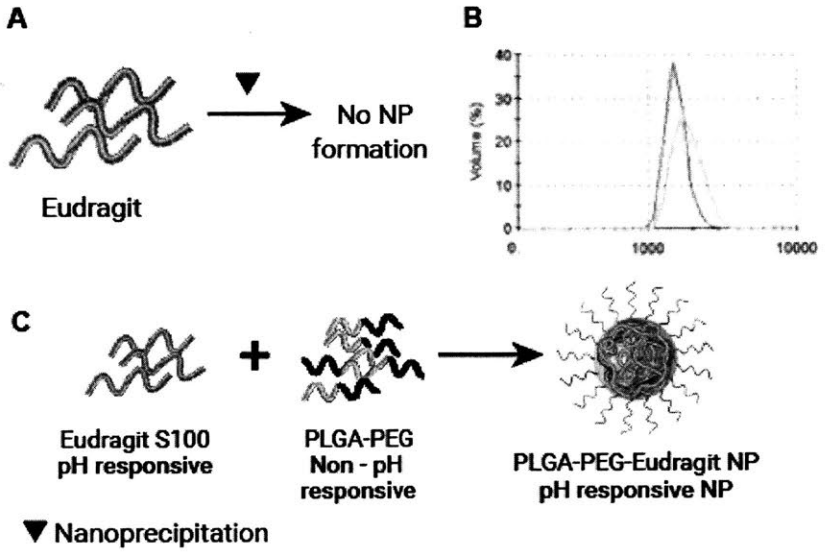

Figure 3.4. (A) Schematic highlighting the failure of Eudragit S100 to self-assemble to form NPs without the application of an external stabilizer using the process of nanoprecipitation. **(B)** The volume size distribution of the Eudragit S100 aggregates which confirm the failure of Eudragit to self-assemble to form

NPs using the nanoprecipitation method. **(C)** Schematic of our hypothesis that pH responsive polymer, Eudragit S100 when blended with non-pH responsive polymer can form pH responsive NPs.

Since Eudragit S100 failed to form NPs stand-alone, we hypothesized that by adding Eudragit, a pH responsive polymer, to PLGA-PEG, a well-studied polymer for NP formation, we can form NPs which would illicit a response to changes in pH as illustrated in Figure 3.4C. To test the hypothesis it was imperative to estimate the optimum amount of Eudragit in the system that can lead to NP formation.

3.4.3 Effect of Eudragit on NP size

Previous studies show that microspheres can be formed by blending Eudragit S100 with PLGA-PEG using the double emulsion process using polysorbate as a dispersant and poly vinyl alcohol as the stabilizer[291]. However, little work has been done on exploring the formation of sub-100 nm particles using Eudragit S100 and PLGA-PEG using the solvent displacement method (nanoprecipitation). We hypothesized that the addition of sufficient amount of an amphiphilic polymer capable of readily forming NPs can aid in Eudragit S100 NP formation using nanoprecipitation as seen in Figure 3.4C.

To find the optimum ratio of PLGA-PEG to Eudragit S100 that results in NP formation we blended increasing amounts of Eudragit with PLGA-PEG and formed NPs at a pH 5, which is less than the dissolution pH of Eudragit according to the method mentioned in Section 3.2.2.1. For this purpose we blended the polymers (Eudragit : PLGA-PEG) in the ratio 0.5:9.5, 1:9, 1:4, 3:7 and 1:1 by weight.

As seen in Figure 3.5A blending up to 30% (w/w) Eudragit S100 with PLGA-PEG forms sub-100 nm monodisperse NPs and at 50% (w/w) Eudragit S100 the system reaches the limiting point of blending Eudragit with PLGA-PEG to form NPs. This is suggested by the large aggregates obtained along with a poor size distribution indicative of the inability to form NPs. In the formation of Empty Eud-NPs increasing amounts of Eudragit in the system did not affect the NPs size, up to 30% Eudragit as seen in Figure 3.5.

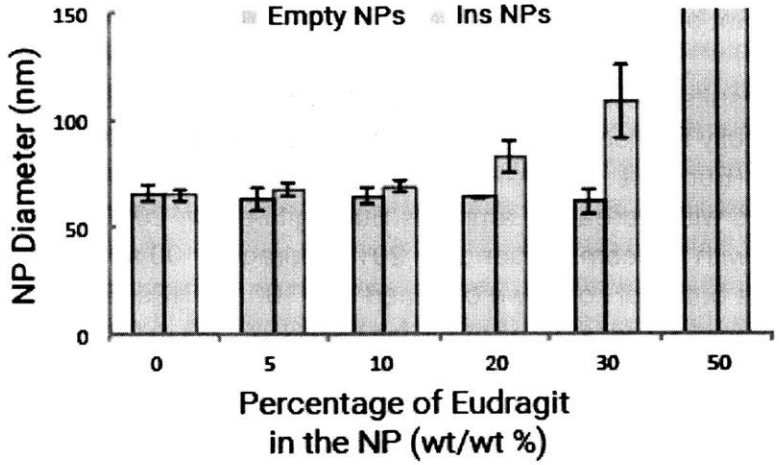

Figure 3.5. Blending Eudragit S100 and PLGA-PEG in different ratios was successful in forming NPs. The inclusion limit of Eudragit in the system is 50% (w/w) Eudragit as it results in the formation of chunky aggregates. Moreover, increasing amount of Eudragit S100 blended in Emp-Eud-NPs did not affect the size of the NPs. However, on preparing Ins-Eud-NPs a size dependence on the amount of Eudragit was observed. The size of the NPs increased for the compositions that had 20% and 30% (w/w) Eudragit.

After confirming the formation of NPs by blending varying compositions of Eudragit and PLGA-PEG we investigated whether the inclusion of insulin in the NPs will affect the NP properties. To test the effect of addition of insulin in the NPs we synthesized NPs according to the process mentioned in Section 3.2.2.1 by adding 30% (w/w) insulin and blending the polymers (Eudragit : PLGA-PEG) in the ratio 0.5:9.5, 1:9, 1:4, 3:7 and 1:1 by weight. As seen with the Empty Eud-NPs 50% (w/w) of Eudragit S100 in the system resulted in no particle formation. However, Figure 3.5 shows that Ins-Eud-NPs can be formed successfully by mixing insulin with different compositions of the polymers. Unlike the trend in Empty Eud-NPs where increasing amounts of Eudragit in the system did not affect NP size, an increase in the NP size was observed in Ins-Eud-NPs on adding 20% (w/w) and 30% (w/w) of Eudragit in the NPs as compared to 5% (w/w) and 10% (w/w) Eudragit. However, on increasing the Eudragit amount to 20% the NP size remains sub-100 nm (83 nm), which meets our design criteria. This increasing NP size can be attributed to possible interactions between the anionic polymer, Eudragit S100, and the positively charged amino acids of insulin. Moreover, at pH 5, which is below the isoelectric point of insulin, insulin

has a net positive charge and hence potentially interacts strongly with the anionic Eudragit S100 forming a polymer and insulin complex which increases in size as the amount of Eudragit increases.

These results show that Empty Eud-NPs as well as Ins-Eud-NPs can be successfully formed by blending Eudragit S100 and PLGA-PEG in a ratio less than 1:1 (Eudragit : PLGA-PEG). Although by the addition of insulin the NP size increased with increasing amounts Eudragit beyond 20% (w/w) Eudragit in the system, with NP composition with 20% Eudragit S100 and 80% PLGA-PEG and synthesis buffer pH of 5, we obtained sub-100 nm NPs (83 nm).

3.4.4 Effect of Eudragit on Insulin loading

The increase in the size of Ins-Eud-NPs observed on increasing the amount of Eudragit in the system beyond 20% (w/w) suggested possible interactions between insulin and Eudragit. This increased interaction between Eudragit and insulin, could also improve insulin encapsulation. In order to test this hypothesis we synthesized NPs with increasing amounts of Eudragit and measured the amount of insulin loading. In Figure 3.6 we observe that Eudragit does not have a significant effect on insulin loading up to 10% Eudragit in the NPs, however, on increasing the Eudragit amount to 20% we achieve a higher loading (13%), while the NP size remains small (83 nm). At amounts of Eudragit greater than 20%, insulin loading increases but NP size increases to more than 100 nm, and at 50% Eudragit composition, we obtain NPs with a poor size distribution indicative of the inability to form NPs.

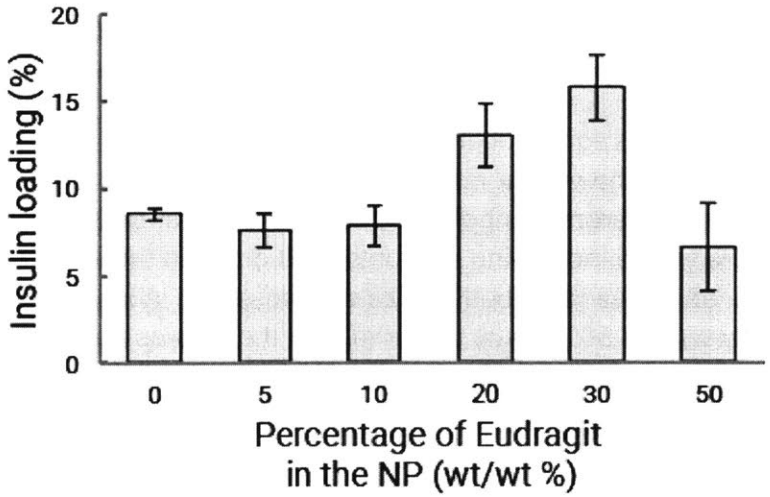

Figure 3.6. Eudragit does not have a significant effect on insulin loading up to 10% Eudragit in the NPs, but on increasing the Eudragit amount to 20% and 30% we achieve a higher loading.

The increase in NP size and insulin loading with increasing amounts of Eudragit beyond 20% (w/w) can be attributed to the enhanced interactions between the anionic Eudragit S100 and the net positively charged insulin at pH 5. Since the pH of the synthesis buffer is close to the isoelectric point of insulin (pH 5.6[271]), insulin exhibits reduced solubility and possibly precipitates during NP formation resulting in increased insulin encapsulation.

3.4.5 Effect of synthesis buffer on NP size and insulin loading

Properties of both Eudragit S100 and insulin are sensitive to changes in pH. Eudragit S100 has a pH-dependent solubility, as it dissolves above pH 7. Insulin has an isoelectric point of 5.6 that means it is net positively charged at pH less than 5.6 and is net negatively charged at pH greater than 5.6. Insulin is observed to be more soluble in aqueous medium in its charged state *i.e.* in pH less than 4 and pH greater than 7. It has been shown in a previous study that the solubility behavior of a drug is particularly important, since it influences the partitioning behavior of the drug between an organic phase and an aqueous phase, which determines the loading efficiency[297]. In order to investigate the effect of pH of the synthesis buffer in which Ins-Eud-NPs we synthesized, on insulin loading and NP size.

Since from the studies in Section 3.4.1- 3.4.5 we observed that the most optimum NPs in terms of size and insulin loading formed when 20% (w/w) Eudragit was blended with 80% (w/w) PLGA-PEG. We synthesized Ins-Eud (20%)-PLGA-PEG (80%) NPs in pH 3, 4, 5 and 6. In Figure 3.7 we see that large diameter NPs with low insulin loading were formed at pH 3 and pH 4. As we increase the pH of the synthesizing buffer to pH 5 and 6, we obtain NPs with better loading and smaller size.

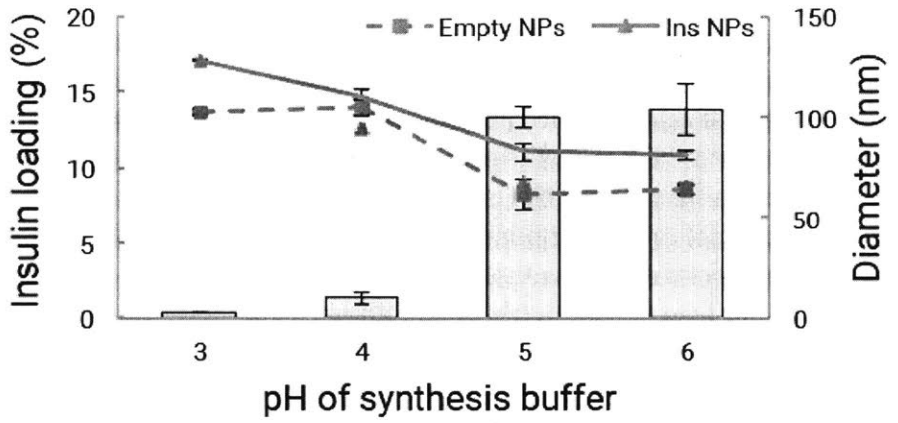

Figure 3.7. NPs with larger diameter and poor insulin loading are formed at low pH buffers (pH 3 and pH 4) while NPs with high insulin loading and smaller size are formed in buffers with pH close to the isoelectric point of insulin *ie.* pH 5.6.

Since pH 6 is closer to the dissolution pH of Eudragit S100, we chose pH 5 as the pH of the synthesis buffer. Therefore, for our purpose the optimum composition for the formation of the Ins-Eud-PLGA-PEG NPs is 20% Eudragit S100 and 80% PLGA-PEG and the optimum pH for synthesis is pH 5. Under these conditions the NPs have a 13% insulin loading and 83 nm diameter.

3.4.6 Effect of Eudragit on pH triggered Insulin release

Having optimized NP formulation for optimum insulin loading and NP size in sections 3.4.1-3.4.6, we explored the effect of the presence of increasing amounts of Eudragit on the pH responsiveness of Ins-Eud-NPs. Maximum pH responsiveness is a desired property for an ideal NP solution for oral drug delivery because it will enable the rapid release of insulin from the NPs before the NPs get opsonized by macrophages. For this purpose the NPs should remain stable and intact at pH less than 7.4 as is found in the duodenum (pH 6-6.5) as well as in the endosomes (pH 5) and once the NPs reach blood (pH 7.4) they should instantly release majority of the insulin.

To test this, we synthesized NPs with increasing amounts of Eudragit and measured the amount of insulin they released in pH 6 and pH 7.4 after 2 hours. Figure 3.8 shows the effect of the amount of Eudragit on the pH responsiveness of the NPs. It can be seen that decreasing amounts of insulin is released in 2 h in

pH 6, as the amount of Eudragit increases in the NP. But there is no noticeable trend in the release of insulin in 2h in pH 7.4. However, on comparing the release of insulin in pH 6 and pH 7.4 for each composition of the NP, it can be seen that the pH responsiveness of the NPs increases as the amount of Eudragit increases in the NPs up to 20%.

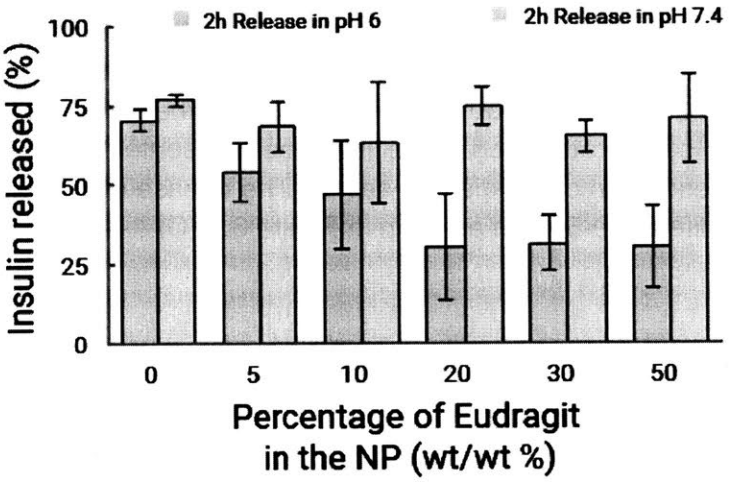

Figure 3.8. Increasing the amount of Eudragit in the NPs slowed doen the release of insulin after 2 h in pH 6 buffer. But no particular trend was observed in the release of insulin from Ins-Eud-NPs at pH 7.4. Moreover, NPs with 20% Eudragit and 80% PLGA-PEG show the maximum difference in the amount of insulin released in pH 6 and pH 7.4, thus suggesting that this NP composition produces the most pH responsiveness NPs.

Therefore, from these experiments we can conclude that 20% Eudragit and 80% PLGA-PEG is the optimum composition of the NPs as it enables maximum loading and pH responsiveness, with a size less than 100 nm. The NPs in these experiments were made in pH 5.

3.4.7 pH sensitive *in vitro* release of insulin from Ins-Eud-NPs

24 hour *in vitro* release of Ins-Eud-NPs was measured according to the method mentioned in Section 3.3.2.4. Figure 3.9 shows the *in vitro* release of 20% Eudragit NPs which were synthesized in pH 5. It shows that there is a significant reduction in the rate at which insulin is released from the NPs at pH 6 as compared to pH 7.4. The detected half-life of insulin in pH 7.4 is between 30-60 min, while the half-life of insulin in pH 6 is 240 min. Although the measured half-life of insulin at pH 7.4 was 30-60 min, we predict that the actual half-life would be shorter. This can be attributed to the limitations presented by the measurement resolution of the dialysis set-up. The release of free insulin solution also had a half-life of 30-60 min as seen in Figure 3.2 (C).

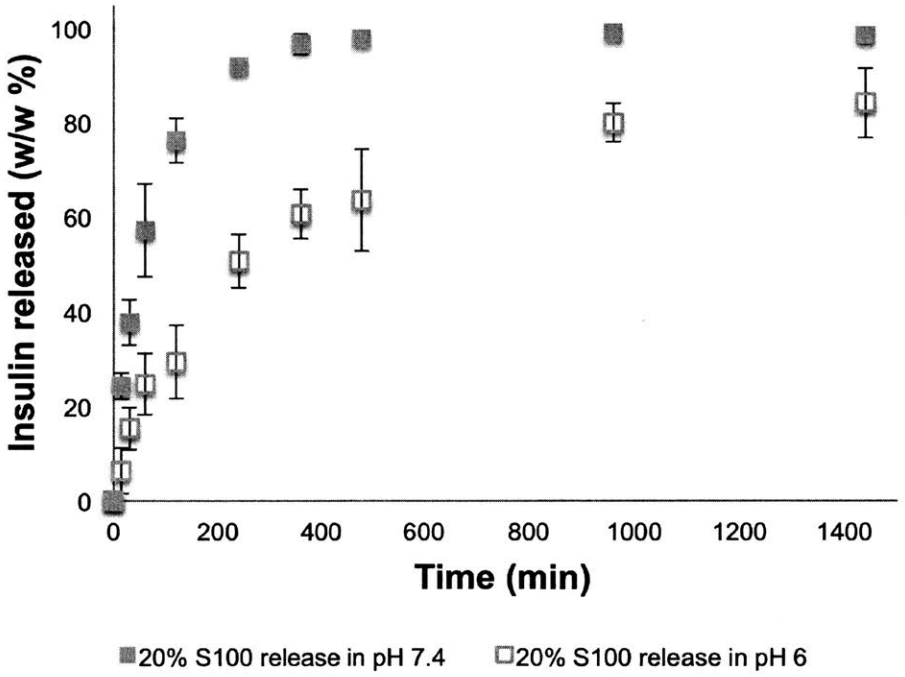

Figure 3.9. A significant reduction in the rate at which insulin is released from the NPs at pH 6 is observed as compared to pH 7.4. The half-life of insulin in pH 7.4 is between 30-60 min, while the half-life of insulin in pH 6 is 240 min. However, the current measurement is limited by the resolution of the dialysis set-up (1h).

To better visualize this data and to account for the maximum measurement resolution of the experimental setup, we normalized the insulin released in pH 6 and pH 7.4 with respect to the release rate of free insulin solution using the mass flux relation given in Equation 1. In this relation, $\dot{m}$ is the mass flux, k is diffusive

permeability, C_1 is the concentration of the solution in the dialysis chamber, and C_2 is the concentration of the solution in the dialysis buffer. Similarly, V_1 is the volume of the solution in the dialysis chamber and V_2 is the volume of the dialysis buffer. A is the area of the membrane in contact with the dialysis solution. Figure 3.10 shows that almost all of the insulin from the NPs gets released as soon as the NPs are exposed to pH 7.4, while there is a significant reduction in the release of insulin from the NPs in pH 6.

$$\dot{m} = k(c_1 - c_2)A = -V_1 \frac{dc_1}{dt} = V_2 \frac{dc_2}{dt} \qquad \text{Eq. 1}$$

Therefore, these NPs would remain intact and prevent the loss and degradation of insulin in the stomach (pH 1-3), and in the upper intestine (pH 5-6) and trigger quick release of insulin once the NPs reach the blood (pH 7.4). The crossover of the NPs from the upper intestinal area, through the intestinal lining will be achieved via the FcRn pathway.

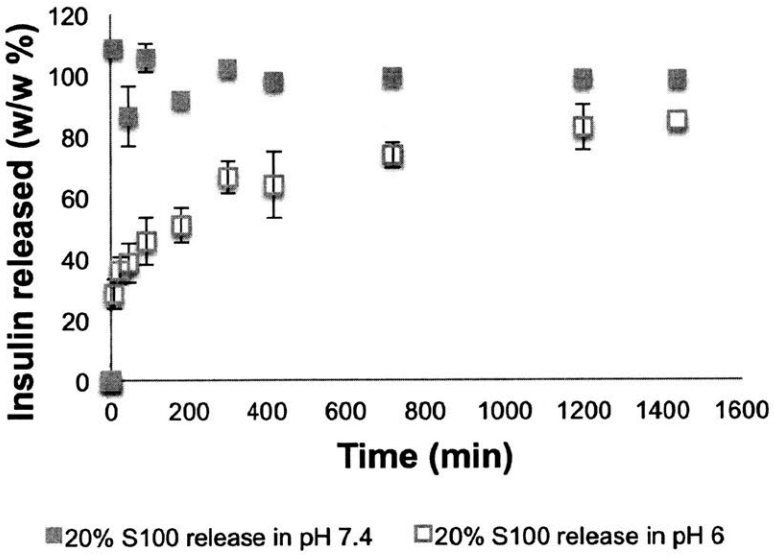

Figure 3.10. On normalizing the data with respect to the release of free insulin it can be seen that almost all of the insulin from the NPs gets released as soon as the NPs are exposed to pH 7.4, while there is a significant reduction in the release of insulin from the NPs in pH 6. The half-life od insulin at pH 6 was 90 min.

3.4.8 Fc conjugation approach and challenges

Various transport pathways have been used to target NPs for oral delivery of insulin such as the FcRn, transferrin and folic acid pathway. However, due to the abundance of the FcRn in the human intestines and due to the recent success of the application of the FcRn pathway, we designed the Ins-Eud-NPs with the Fc fragment on the NP surface. A previous study has reported the successful conjugation of the Fc fragment of the IgG on the surface of the PLA-PEG NPs by using maleimide-thiol chemistry[1]. [298]The challenge in using the same chemistry for the Ins-Eud-NPs was that the maleimide-thiol chemistry is most efficient at physiological pH (pH 7.4). However, due to the pH restrains in the Ins-Eud-NP system, we had to optimize the conjugation protocol parameters such as conjugation buffer, reaction time, concentration of the NPs, and amount of Fc used.

In order to conjugate the Fc fragment on the NP surface we synthesized the NPs in the aforementioned process, however, we included 10% $PLGA_{10k}$-PEG_{5k} with a maleimide terminal group (PLGA-PEG-mal). IgG-Fc was modified using 2-iminothiolane (Traut's reagent), which is a water-soluble reagent that reacts with primary amines to introduce thiol groups. The thiol-modified Fc (Fc-SH) was then be incubated with the NPs to allow for the thiol-maleimide conjugation reaction to occur. Once the reaction was complete, the NPs-Fc were washed to remove any unconjugated Fc. The Fc conjugated to the surface of the NPs was then quantified using a BCA protein assay.

Various challenges were overcome to optimize the above reaction. The thiol-maleimide reaction occurs rapidly at pH 7.4. However, since the Ins-Eud-NP system is sensitive to pH, it was important to explore the conjugation efficiency at different reaction buffers. For this purpose we incubated Ins-NPs with Fc-SH in three different buffers (pH 5, pH 6 and pH 7.4) for 2 h. As expected, maximum Fc conjugation occurred when the reaction buffer pH was 7.4 as seen in Figure 3.11A. For reasons that are unclear, we observed more conjugation at pH 5 than at pH 6.

Since the Fc conjugation at pH 6 was less than that at pH 5, next we investigated the effect of reaction time on Fc conjugation in pH 5 buffer. We incubated the NPs with Fc-SH for 2 h and 18 h. Although great amount of Fc was conjugated when the NPs and Fc-SH were incubated for 18 h, this value was not much greater than the Fc conjugation obtained after incubating for 2 h. A major disadvantage of longer incubation times is that they tend to increase the amount

of insulin lost in the NPs. For this reason we performed the rest of the experiments by incubating the NPs for 2 h.

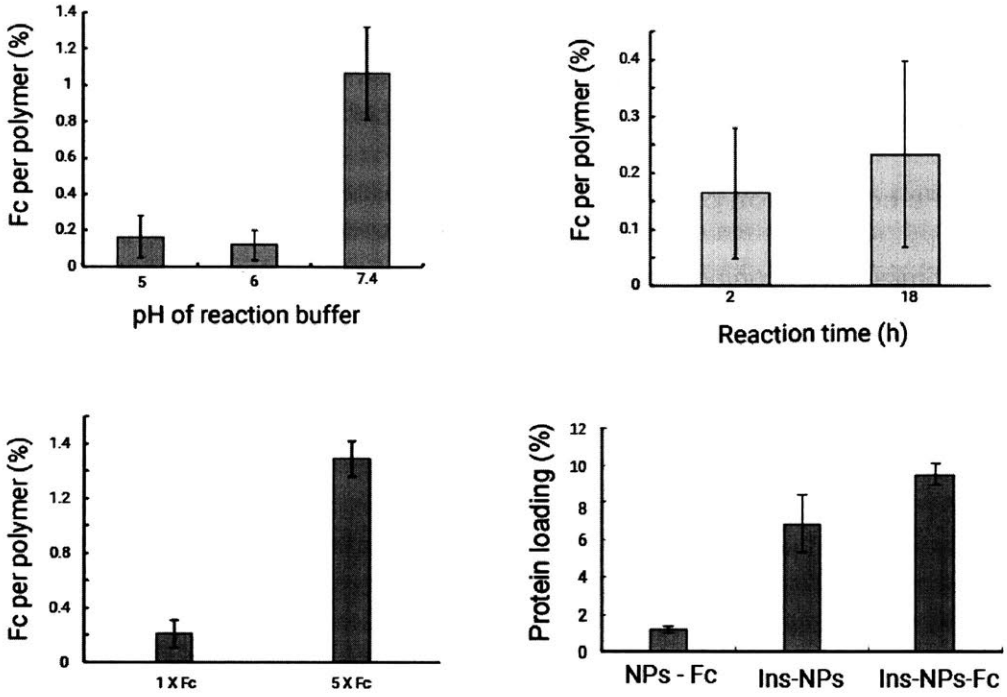

Figure 3.11. (A) Effect of reaction buffer on Fc conjugation on NP surface. Maximum Fc conjugation was obtained at pH 7.4, followed by pH 5 and pH 6 buffer. **(B)** Effect of reaction time on Fc conjugation. On incubating Ins-Eud-NPs with Fc-SH in pH 5 buffer for 2 h and 18 h, it was found that the Fc conjugation in 2 h (0.16%) was not much greater than the Fc conjugation in 18 h (0.23%). **(C)** On increasing the amount of Fc by 5 times Fc conjugation increased to 1.48%. **(D)** Higher Fc conjugation resulted in longer synthesis time, which resulted in a loss of insulin leading to a reduction in insulin loading in Ins-Eud-NPs-Fc NPs to 6.8%.

To improve Fc conjugation another approach is to increase the amount of Fc that is incubated with the NPs. Larger amount of Fc will also possibly prevent NP aggregation since there will be sufficient free Fc to bind to reactive groups on the NPs. However, if the amount of Fc is significantly less than the amount of NPs, it can potentially lead to NP crosslinking as a single Fc molecule can react with the available reactive groups in more than one NP. So far we were adding 20.48 µL of 5 mg/mL Fc to 4 mL of 1 mg/mL NPs. To test the effect of increasing the amount of Fc in the conjugation stem, we increased the amount of Fc added to 5

times. Figure 3.11C shows that the addition of 5 times more Fc significantly improved the Fc conjugating on the NP surface.

Although we succeeded in improving the Fc conjugation from 0.2% to 1.48%, the amount of insulin loading in the NPs dropped from 13.1% to 6.8%. This loss in the insulin loading occurred to due to the increase in reaction time as well synthesis time.

3.4.9 Fc conjugation optimization

By optimizing the conjugation parameters we were successful in developing Ins-Eud-NPs-Fc with 1.48% Fc conjugation. However, the long synthesis time led to loss of insulin from the NPs resulting in the net insulin loading in Ins-Eud-NPs-Fc to drop from 13.1% to 6.8%.

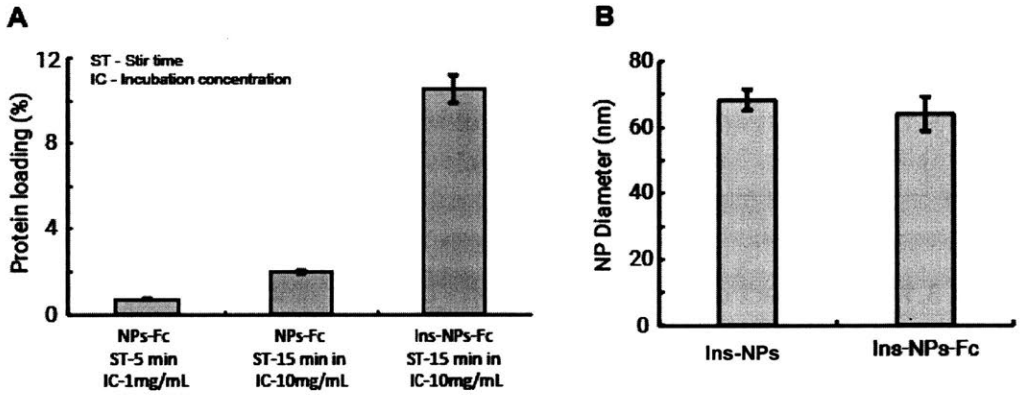

Figure 3.12. (A) Formation of NPs after 5 min stirring time and 1 mg/mL NP incubation concentration resulted in only 0.7% Fc conjugation. However, when all other synthesis conditions were kept the same and only the stirring time was changed to 15 min and the NP incubation concentration was increased to 10 mg/mL Fc conjugation increased to 1.48%. **(B)** Conjugation of Fc on the NP surface did not effect the size of the NPs, size of Ins-Eud-NPs-Fc was 63.9 nm while the size of NPs without Fc was 68 nm.

In order to improve these NPs we have to further improvise the NP synthesis and the Fc conjugation prcoess. Two steps that consume majority of the time in the process are the 2 h stirring time that enables stable NP formation and the 2 h Ins-NPs and Fc-SH incubation time. The NPs get washed after each of these time periods to either get rid of the excess drug, organic solvent, polymer or to get rid of the unreacted Fc. In addition to that the released insulin also gets

washed away. Another potential way of controlling the loss of the insulin by the NPs is by reducing the concentration of NPs that is being incubated with Fc-SH. The increase in concentration will prevent the formation of a strong concentration gradient, preventing insulin to readily get released by the NPs.

To test this, we prepared NPs after adding drop wise the organic polymer and insulin solution to a beaker with acetate buffer (pH 5, 10 mM) that was constantly being stirred at 2000 rpm. The NPs were allowed to equilibrate for 5 min (as opposed to 2 h in other experiments) after which they were washed multiple times to get rid of excess insulin and the organic solvent. Following that the NPs were resuspended in acetate buffer (pH 5, 10 mM) to form a 1 mg/mL NP solution. Fc-SH and the Ins-Eud-NPs were then incubated for 2 h, followed by washing them and then quantifying the Fc conjugation using the BCA assay. Figure 3.12A shows that this enables us to get only 0.7% Fc conjugation as opposed to 1.48% that we had obtained earlier.

This observation suggested that controlling the concentration of the NPs when they are incubated with Fc-SH could help improve the Fc conjugation efficiency as a higher concentration of NPs will result in greater interaction and reaction points for the thiolated Fc. We repeated the aforementioned experiment after making two changes. First, instead of stirring the organic solutions with the aqueous phase for 5 min, we did that for 15 min to enable the NPs to stabilize and to allow more organic solvent to evaporate. Second, instead of incubating the Ins-Eud-NPs at a 1 mg/mL concentration with the thiolated Fc, we incubated Ins-Eud-NPs at 10 mg/mL concentration. Figure 3.12A shows that the insulin loading in the NPs increased from 6.8% to 8.5% and the Fc conjugation also increased to 1.9%.

On characterizing the size of the Ins-Eud-NPs-Fc, we see (Figure 3.12B) that the size of Ins-Eud-NPs-Fc was 63.9 nm while the size of NPs without Fc was 68 nm. Therefore, the conjugation of Fc did not affect the size of the NPs considerably.

By optimizing the synthesis and conjugation parameters we were able to develop Ins-Eud-NPs-Fc with 1.9% Fc conjugation, 8.5% insulin loading, 63.9 nm hydrodynamic radius and high pH responsiveness. A schematic of the NP can be seen in Figure 3.13.

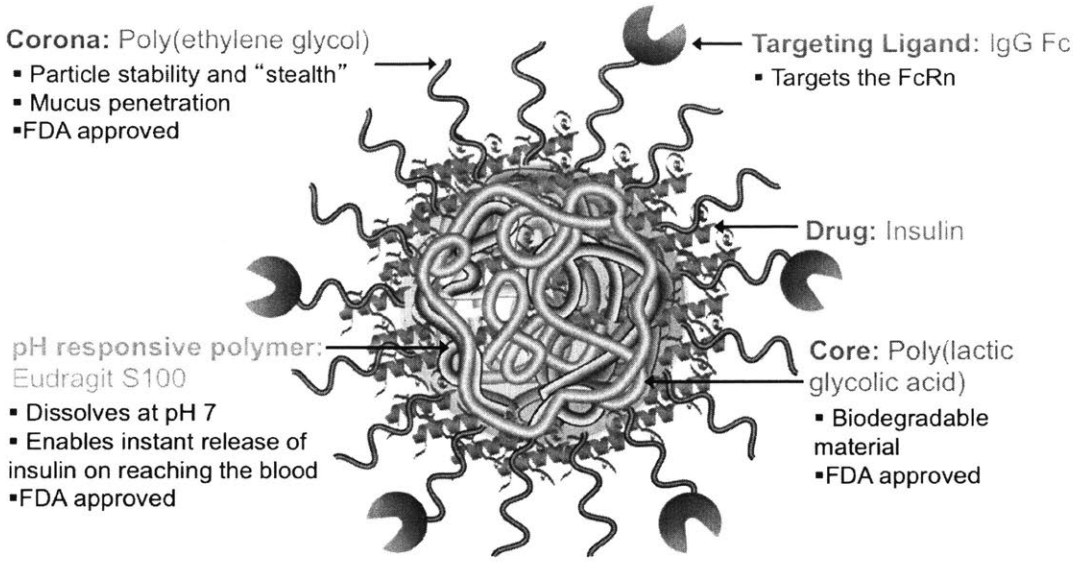

Figure 3.13. Schematic of Ins-Eud-NP-Fc. The Ins-Eud-NP-Fc is prepared from biodegradable and biocompatible polymers like PLGA-PEG and Eudragit S100. Eudragit imparts the NPs an ability to respond release insulin on being stimulated by pH. The targeting ligand, Fc, has been conjugated to the surface of the NPs to enable them to cross the epithelial barrier by using the FcRn transcytosis pathway.

3.5.10 NP in vitro transcytosis

Transport of drugs and NPs across the epithelial lining has been investigated using a standard transcytosis assays[299]. Studies have shown the successful transport of small molecules across a Caco-2 cell monolayer on porous membranes on transwell plates[1, 194], that is typically used a model of the intestine for drug permeability. Caco-2 cells have been reported to express human FcRn that has been used for IgG transport studies. One particular study showed the successful transport of Fc targeted insulin loaded PLA-PEG NPs across a caco-2 cell monolayer[194]. Targeting the NPs to the FcRn resulted doubling the NPs that crossed the Caco-2 monolayer, as compared to the NPs that were not targeted with the Fc fragment[1].

As mentioned in Section 3.3.2.7. the transepithelial NP transport experiments were done by Cyprotex. To study the NP transepithelial transport of Ins-Eud-NPs-Fc we used an *in vitro* epithelial monolayer model with Caco-2 cells as decribed in Section 3.3.2.7. We used fluorescently labeled NPs to measure transport across the Caco-2 monolayer. The transport set-up was designed to mimic the chemical conditions presents in the intestine, where the apical side of

the transport chamber, which was representing the duodenum was filled with HBSS at pH 6 and the basolateral chamber which was representing blood was filled with HBSS at pH 7.4. 75 µL of 5 mg/mL NPs were added to the apical side and the transport set up was placed on an orbital shaker to incubate for 2 h to allow for transport. After NP transport, the solution from the apical side as well as the basolateral side was collected and lyophilized. Later, the solution was dissolved in DMSO and their fluorescence signal was measured using a TECAN Safire plate reader. As a control, NPs without Fc targeting were also used to compare the transport with NPs conjugated with the Fc fragment.

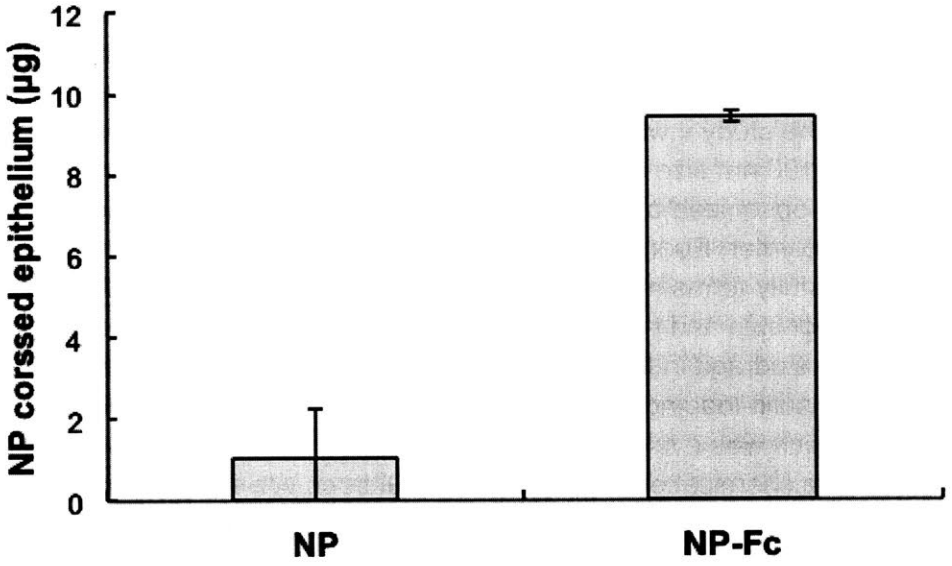

Figure 3.14 In vitro transepithelial transport data showed that Ins-Eud-NPs-Fc were transported 5 times more across the Caco-2 monolayer relative to non targeted Ins-Eud-NPs.

Membrane diameter	4.26 mm
Membrane thickness	10 µm
Cell growth area	0.14 cm^2
Initial NP concentration	5 mg/mL

Table 1. Properties of the semipermeable membrane on which the Caco-2 cells were grown.

In Figure 3.14 *in vitro* transepithelial transport data shows that there was 5 times greater transport of Ins-Eud-NPs-Fc across the Caco-2 monolayer relative to non-targeted Ins-Eud-NPs. 375 µg of Ins-Eud-NPs were added to the apical

chamber and 9.4 µg of Ins-Eud-NPs targeted with Fc were successful in crossing the epithelial barrier, while only 1.02 µg of non-targeted Ins-Eud-Fc-NPs were successful in crossing the Caco-2 monolayer. This 5 times increase in the transport rate confirms that targeting NPs with Fc ligand enables a larger uptake of NPs.

3.5.11 Conclusion

Targeted drug delivery using polymeric carriers has been an area of interest for decades. Several strategies have been explored to by using different materials, synthesis process and targeted transport pathways. However, the key to an ideal NP solution is to use multiple strategies in a way that they complement each other. In this study we show how some of these strategies can be put together to develop an efficient NP based drug delivery system for oral delivery of insulin. At the onset of the study it was critical to design the system to have high insulin loading, sub-100 nm size and the ability to release the majority of insulin before the NPs gets opsonized by macrophages. We showed that blending a pH responsive polymer, Eudragit S100 with a non-pH responsive polymer, PLGA-PEG successfully forms monodispersed NPs. We optimized key NP properties – insulin loading, size and pH responsiveness – by investigating the effect of incorporating Eudragit in the system. This enables us to develop Ins-Eud-NPs with 13.1% insulin loading and 83 nm size. These NPs exhibited the desired pH response, which was evaluated using *in vitro* insulin release data at conditions that mimic the chemical environment in the GI tract. We showed that the majority of insulin was released rapidly on exposing the NPs to pH 7.4 buffer while the half-life of insulin in pH 6 was 90 min. To enable the Ins-Eud-NPs to cross the intestinal epithelial barrier we used the FcRn pathway because NPs targeted with the Fc ligand have been shown to successfully cross the intestinal epithelium and because of the abundance of FcRn in the human intestinal lumen. We used a well-studied conjugation chemistry, maleimide – thiol chemistry to conjugate Fc on the surface of the NPs. By methodically studying the impact of various processing parameters – reaction time, reaction buffer, NP concentration, and concentration of Fc – on insulin loading and Fc conjugation, we were able to circumvent the challenges associated with maleimide – thiol chemistry at a pH much lower (pH 5) than the optimum pH (pH 7.4) for this conjugation chemistry. We were able to produce Ins-Eud-NPs-Fc with 8.5% insulin loading, 63 nm size and 1.9% Fc conjugation. Lastly, we showed that the NPs were able to cross the epithelial lining as tested using a Caco-2 cell model. In this work we developed and exhibited the application of a pH responsive system that will protect insulin from the hard chemical environment in the stomach (pH 2-3) and in the

duodenum (pH 6-6.5) and will be readily transcytosed using the FcRn pathway. The NPs will protect the insulin in the endosomes (pH 5) and will get released in the basal side into blood (pH 7.4). Here the basic pH of blood will trigger the NP to release the majority of insulin in the blood. This modular NP formulation has potential to provide a way to efficiently transport various drugs across the intestines. In fact, FcRn is found in other organs in the body like the brain, kidneys, livery and lungs and this formulation can potentially be used to transport drugs across the epithelial lining at numerous sites.

CHAPTER 4

Conclusion and Outlook

Parenteral delivery has been the mainstay for administering insulin to patients with diabetes. Even after decades of research done by groups across the world, state of the art for insulin delivery continues to be subcutaneous injections. Physicians and patients over the years have unanimously agreed that innovation in the field of alternative insulin delivery is necessary due to increasing level of patient incompliance and poor treatment outcomes owing to the frequent need of insulin injections for prolonged periods of time. As a result, several strategies of alternative insulin delivery like oral, pulmonary, buccal, rectal, nasal and transdermal have been investigated. Significant advancements have been made in these drug delivery methods particularly in insulin delivery via the oral and the pulmonary route. Although a couple of pulmonary delivery formulations have reached advanced stages of FDA approval and commercialization, no oral formulation of insulin has been launched in the market with success.

Due to the ease of administration and the possibility of action of insulin in a physiological manner through the liver makes oral delivery of insulin very desirable. Although oral insulin is the more preferred way of administering insulin, it is a very complex and challenging problem. These challenges are attributed to the harsh chemical environment in the GI tract due to the presence of varying pH, the presence of protease inhibitors and the strongly regulated intestinal epithelial barrier, which prevents efficient absorption of insulin. The application of nanoparticles (NPs) to overcome these challenges has been extensively explored. By choosing an appropriate material, NPs can be designed to protect insulin from the harsh chemical environment in the GI tract, from enzymatic degradation and can allow targeted transport across the gastrointestinal lining by enabling surface functionalization with a targeting ligand.

Various NP formulations and transport pathways have been studied such as neonatal Fc Receptor, Vitamin B12, folic acid and transferrin pathway. Due to the recent success in transporting PLA-PEG NPs across intestinal linings, an abundance of FcRn in the intestinal lumen and due to the efficient transport of IgG across the epithelial lining via FcRn, the FcRn pathway was of particular interest to the work presented in this thesis.

To design an effective oral insulin delivery system, various key design criteria have been identified such as (1) NPs must be sub-100 nm to allow the application of a pathway like the FcRn, (2) NPs must have high insulin loading to ensure high bioavailability and less consumption of polymer per insulin dose, (3) NPs must have the ability to be functionalized by a ligand of a transport pathway, and (4) the majority of insulin must get released from the NPs before the NPs get opsonized by macrophages to ensure higher bioavailability.

Keeping the above design criteria at the forefront, this thesis provides detailed work and insights into achieving each of these requirements. To understand the factors that control protein loading in NPs, we systematically investigated the effect of individual steps of the nanoprecipitation process including the washing step, the mixing phase for insulin, and the stages of adding insulin to the system. We demonstrated that smaller Ins-NPs could be formed by dissolving insulin along with the PLGA-PEG molecules in organic phase (DMSO) before nanoprecipitation. We provided a simple way to increase the insulin loading in PLGA-PEG NPs by zinc chelation. Ins-Zn-NP exhibited more than 10-fold increase in insulin loading compared to Ins-NPs. We also demonstrated ways of achieving small NP diameter while maintaining high insulin loading. In particular, we found that insulin and/or zinc may be added to pre-formed NPs to load insulin without affecting the NP size. Also, insulin loading in Ins-Zn-NP system could be optimized by tuning the pH of the system. This part of the thesis illustrates how simple modifications of the nanoprecipitation process can provide insights that enable the realization of NPs with desired properties. This approach can potentially extend to other protein-encapsulating NP systems to understand the mechanisms of protein loading and to devise processes to enhance protein loading in NPs formed by nanoprecipitation.

After demonstrating ways of improving NP size and insulin loading, we focused on developing a pH responsive NP system that will rapidly release insulin when exposed to neutral pH. We showed how the application of Ins-Zn hexamers along with PLGA-PEG and a pH-responsive polymer, Eudragit failed to produce NPs with improved insulin loading or the desired pH response. However, we demonstrated that blending a pH responsive polymer, Eudragit S100 with a non-pH sensitive polymer, PLGA-PEG successfully formed monodispersed NPs.

We optimized key NP properties – insulin loading, size and pH responsiveness – by investigating the effect of incorporating Eudragit in the system. This study enabled us to develop Ins-Eud-NPs with 13.1% insulin loading and 83 nm size. These NPs exhibited the desired pH response, i.e., slow release at pH 6 that is

experienced in the GI tract before transcytosis and rapid release at physiological pH encountered after transcytosis, which was evaluated using *in vitro* insulin release data at conditions that mimic the chemical environment in the GI tract. We showed that the majority of insulin was released rapidly on exposing the NPs to pH 7.4 buffer while the half-life of insulin in pH 6 was 90 min.

To enable the Ins-Eud-NPs to cross the intestinal epithelial barrier using the FcRn pathway, we functionalized the NPs with Fc. We used the well-studied maleimide–thiol chemistry to conjugate Fc on the surface of the NPs. By methodically studying the impact of various processing parameters – reaction time, reaction buffer, NP concentration, and concentration of Fc – on insulin loading and Fc conjugation, we were able to circumvent the challenges associated with use of the maleimide – thiol chemistry at a pH much lower (pH 5) than the optimum pH (pH 7.4) for this conjugation chemistry. We realized Ins-Eud-NPs-Fc with 8.5% insulin loading, 63 nm size and 1.9% Fc conjugation.

Lastly, we showed that the NPs were able to cross the epithelial lining as tested using a Caco-2 cell model. In this work, we developed and exhibited the application of a pH-responsive system that will protect insulin from the harsh chemical environment in the stomach (pH 2-3) and in the duodenum (pH 6-6.5) and will be readily transcytosed using the FcRn pathway. It is expected that the NPs will protect the insulin in the endosomes (pH 5) and will get released on the basal side into blood (pH 7.4). Next, the basic pH of blood will trigger the NP to release the majority of insulin in the blood. This modular NP formulation has potential to provide a way to transport various drugs across the intestines efficiently.

To conclude, this thesis has made contributions in gaining insights on improving NP characteristics and in developing a modular pH-responsive NP system that has potential applications beyond just oral delivery of insulin.

In the drug-delivery industry, several NP systems have been designed for oral insulin delivery. However, the long-term efficacy and success of these formulations will be determined by their ability to provide glycemic control in larger animals and humans. Reliably quantifying the dose required to control glucose levels will be another challenging frontier as high doses of insulin may induce mitogenic changes in the GI epithelium, as insulin is also a growth factor. Therefore, given the complexity of the problem, a multilayered NP system with multiple facets will be needed to be a complete solution for oral delivery of insulin.

Future outlook

Ins-Eud-NPs-Fc, as well as the Ins-Zn-NPs, exhibit improved NP characteristics as well improved *in vitro* efficacy. However, there are multiple aspects that need more investigation, modifications, and improvements.

As reported in this work, Ins-Zn-NPs demonstrated promise as an insulin carrier with high insulin loading and well-controlled NP size. Zinc chelation is an easy to execute and controllable way of improving protein loading in polymeric carriers. This mechanistically sound approach can be extended to other protein delivery systems, which struggle with the challenge of inadequate protein loading. The roadmap provided in Chapter 2 about optimizing NP properties can be applied directly to other systems to gain better insights and to improve protein loading and control NP size.

Ins-Eud-NPs-Fc demonstrated improved efficacy in *in vitro* studies, however, a detailed investigation of the transport of Ins-Eud-NPs-Fc is needed. Effect of various parameters like temperature, Fc saturation, and Fc blocking agents need to be studied to gain a mechanistic understanding of the underlying functioning of the NP system *in vitro*.

In addition to more *in vitro* tests, this formulation needs to be tested *in vivo* to understand the pharmacokinetics of the NPs accurately. *In vivo* experiments designed to understand the time scale of the action of the NPs, elimination of the NPs, release of insulin in the GI tract and studies determining the dose-dependent glycemic response, need to be performed.

A challenge associated with the Ins-Eud-NPs-Fc is the presence of the Fc on the surface of the NPs that makes these NPs a very attractive target for opsonization by macrophages. The Ins-Eud-NPs-Fc pH-responsive system is designed to ensure maximum release of insulin before the NP gets degraded or excreted. However, a possibility of an even more efficient system is the possible conjugation of Fc on the NP surface using pH-sensitive chemical linkers. These linkers can be designed to dissolve at pH 7.4 resulting in shedding of the Fc. This strategy will enable a longer circulating NP and can open doors to long-acting oral insulin formulations.

Lastly, it has been reported that Fc is not just found in human intestines, but also in the epithelial lining of other organs like the brain, liver, lungs, and kidneys.

Most of these epithelial linings have a similar chemical composition regarding the pH of the solutions on either side of the membrane. Therefore, Eud-NPs-Fc can be modified to suit the transportation of protein therapeutics across the epithelial lining of these organs.

THIS PAGE INTENTIONALLY LEFT BLANK

Appendix

Optimization of *in vitro* release study protocol for insulin release from Ins-NPs

Nanoparticles (NPs) formed from biodegradable polymers such as poly(lactic acid) (PLA) and poly(lactic-co-glycolic acid) (PLGA) have been extensively used as drug delivery carriers for protein therapeutics[300-303]. NPs are a particularly good solution for oral delivery of protein drugs because they enhance stability of protein therapeutics, provide continuous and controlled drug release, enable reduced dosage, decrease systemic side effects, protect the protein from the harsh chemical environment in the gastrointestinal tract, and allow surface functionalization which can open a whole avenue of targeted delivery possibilities[300, 304-306].

A key feature of polymeric NPs is the ability to release drugs in a controlled way. Successful estimation of drug release from NPs requires well-characterized *in vitro* or *in vivo* studies. In the initial screening of potential NPs, *in vitro* drug release is very common as it enables the assessment of the drug release profile in a fairly cost effective, accurate and quick way. This is why before testing the pharmacokinetics of the formulation *in vivo*, it is first tested *in vitro*.

Currently, the most common methods used to study drug release from microspheres are the sample and separate[214, 307-308]and the dialysis[212, 261, 309]methods[310]. These methods have been illustrated in Figure A1. The more conventional method is the sample and separate method in which drug-loaded NPs are incubated in an EppendorfEppendorf tube and at predetermined time points, the solution is centrifuged using an Amicon filter to separate the free released drug from the NPs. Advantages of the sample and separate method are accurate measurement of the initial burst of drug from microspheres and the ease of the setup. However, some of the disadvantages include the possibility of the system reaching equilibrium before all the drug has been released and the loss of drug in the filter of the centrifugation device. To overcome these challenges partially, the both the supernatant and the filtrate is sometime analyzed for the drug content.

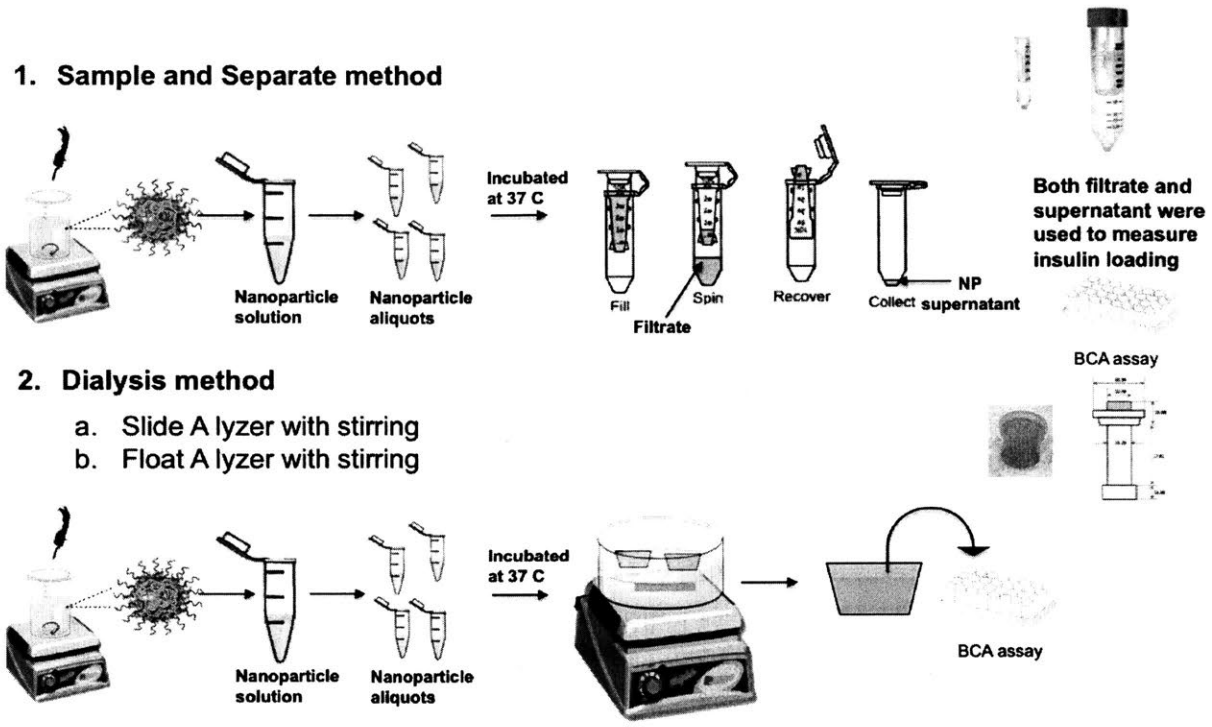

Figure A1. Sample and separate and dialysis are the two most commonly used methods for measuring the *in vitro* drug release profile from polymeric nanoparticles.

The second popular method for estimating the in vitro release of drugs from nanoparticles and microparticles is dialysis. Here, instead of incubating the samples in Eppendorf tubes, the drug loaded NP samples are incubated in dialysis chambers that are suspended in a dialysis buffer. A dialysis membrane of an appropriate molecular weight cut off separates the NP solution from the dialysis buffer. As the NPs release the drug, it diffuses through the dialysis membrane into the dialysis buffer. One way of estimating the released drug is to sample the dialysis buffer or to samples the NPs at predetermined time points. One challenge associated with sampling the dialysis buffer is that usually the volume of the dialysis buffer is 10-20 times the volume of the dialyzing solution, therefore after the drug releases into the buffer solution the concentration of the resulting solution is very low and often it is hard to analyze it due to limited resolution of protein detection assays and techniques. One advantage of this system is the ease of sampling. However, depending on the preparation of the dialysis chambers the initial setup can be very cumbersome and similar to the sample and separate method, the sample can reach equilibrium in the dialysis

set up as well.

In order to measure the initial burst release from NPs, the sample and separate method is considered to be more effective because the slow equilibration limits an accurate analysis of initial drug levels in formulations using the dialysis method[310].

Insulin *in vitro* release profile using the sample and separate method

For this study we used the sample and separate method to study the *in vitro* release of insulin from Ins-Eud-NPs. We prepared Eud (10%) PLGA-PEG (90%) Insulin (30%) NPs using the nanoprecipitation method. We made a final NP concentration of 1 mg/mL. Next, we made 200 µL volume aliquots of the NPs and at predetermined time points centrifuged each aliquot using a Millipore Amicon filter (MWCO 100kDa) for 10 min at 10,000 g. We collected and analyzed samples from both the supernatant as well as the filtrate. Figure A1A shows that when the filtrate, which contains released insulin is analyzed the data shows an almost flat line denoting that there is not much change in the amount of insulin released by the NPs with time. When the data is analyzed using the supernatant from the same NPs as seen in Figure A1B, the data initially shows that insulin is getting released from the NPs but at longer time intervals less insulin is released which is counterintuitive. In both Figures A1A and A1B the amount of insulin released is expected to increase with time till all the insulin is released from the NPs. Although we were unable the ascertain the release profile of insulin using the sample and separate method, a promising observation that we made was that there is a distinct difference in the amount of insulin released in in pH 6 (MES buffer, 20 mM, 150 mM NaCl) as compared to pH 7.4 (Phosphate buffer, 20 mM, 150 mM NaCl).

From the almost flat line in Figure A2A it appears that insulin released from the NPs and the insulin adsorbed on the NP surface are in equilibrium with the each other. This observation can be attributed to the free insulin possibly re-adsorbing to the NP surface with time with no increase in the amount of insulin released with time, possibly due to changes such as rearrangements of the polymer chains in the NP that alter the position of insulin equilibrium. We also cannot rule out the possibility of the filtration step interfering with the assay, since there is clearly loss in the amount (data in Figures A2A and A2B does not always add up to 100%). This could also explain why the amount of insulin released decreases with increase in time as seen in Figure A2B.

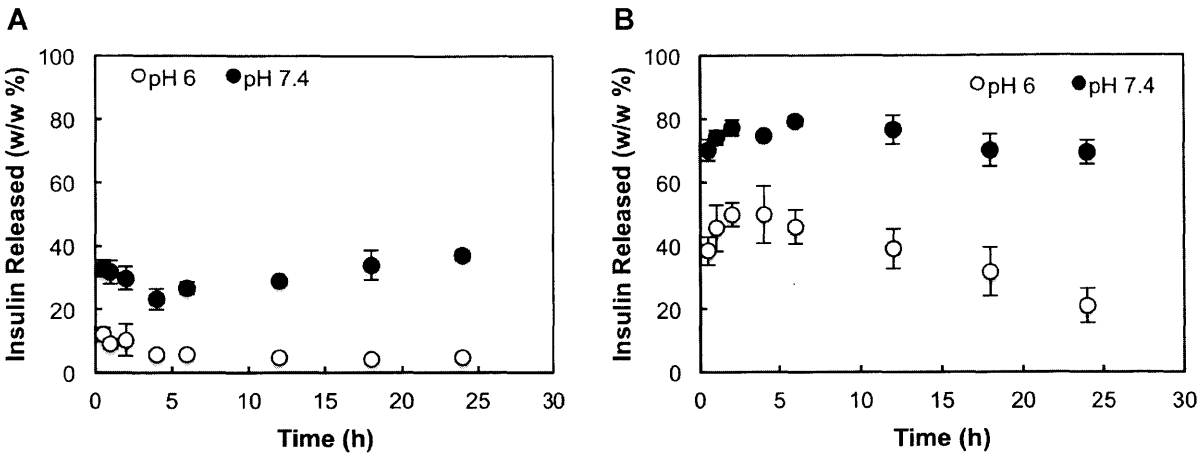

Figure A2. (A) Insulin release profile at pH 6 and pH 7.4 obtained by analyzing the data using the filtrate. **(B)** Insulin release profile at pH 6 and pH 7.4 obtained by analyzing the data using the supernatant. Both these curves are counterintuitive relative to the expected insulin release profile. The significant difference in the release curve at pH 6 and pH 7.4 is promising data.

Although our study faced the potential challenge of the NP system reaching equilibrium, this has not been reported or discussed in previous studies.

The sample and separate release method where we sampled 200 µL of solution at each time point failed to estimate the release kinetics of insulin from Ins-Eud-NPs. As mentioned previously, the NP system potentially reached equilibrium as time proceeded and that enabled released insulin to again adsorb on the NP surface. One way of disrupting the equilibrium is to significantly reduce the concentration of the NP solution.

Effect of incubation volume on insulin in vitro release profile measurement

We performed an experiment to understand the impact of incubation volume on the amount of detected released insulin. We measured the insulin loading after incubating the NPs in different incubation volumes (400 µL, 2 mL, 5 mL, 10 mL and 14 mL) for a 2-h time period. Figure A3A shows that the amount of insulin released stabilizes at higher NP incubation volumes. This suggests that at larger incubation volumes the equilibrium is disrupted and potentially generate more accurate data.

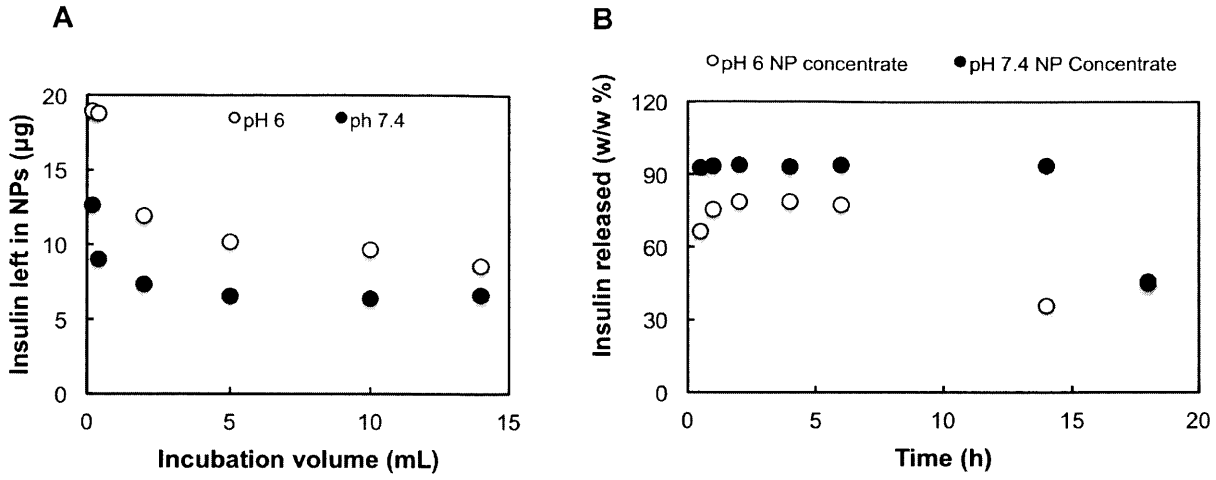

Figure A3. (A) Insulin release after 2 h in different incubation volumes shows that the amount of insulin released by the NPs stabilizes at higher NP incubation volumes suggesting that a non-equilibrium state reaches at high incubation volumes. **(B)** Insulin release profile at pH 6 and pH 7.4 obtained by analyzing the data using the supernatant and a large incubation volume of 15 mL. Although the insulin release can be quantified at initial time points, at later time points there is a decrease in the amount of insulin released which seems incorrect.

Having observed that large incubation volumes possibly provide more accurate data, we performed an experiment where after synthesizing Ins-Eud-NPs we incubated the same volume in 15 mL of buffer instead of 200 µL. Figure A3B shows that released insulin can be quantified at initial time points but at later time points there is a decrease in the amount of insulin released which is counter intuitive. From these results we can conclude that the sample and separate method fails to accurately estimate the amount of insulin released at larger time points. Since these challenges have not been reported in literature, it was important to further investigate the system to gain a better understanding.

Loss of insulin in the centrifugation device during multiple washing steps

Previous studies have reported successful application of the sample and separate method to study the *in vitro* release of drugs from NPs. However, as mentioned earlier we were unable to ascertain the insulin release profile from the data we obtained using the sample and separate method.

We were unable to successfully estimate the insulin release profile because potentially some insulin was getting trapped in the washing device due to adsorption on the cellulose filter instead of being in solution in the supernatant or the filtrate. Moreover, we had very different results of insulin release on analyzing the data using the filtrate and the supernatant from the same NPs. To test our hypothesis and to understand whether the filtrate or the supernatant was a more reliable source to analyze the data, we studied the effect of replacing the Amicon filter after every washing step. This would explain if there was any loss of insulin due to the protein affinity of the filter material. Since insulin has a better solubility in pH 7.4 buffer it is expected to get washed away more readily with using this as the washing buffer. In order to have the maximum detection of insulin even after some loss we selected pH 7.4 buffer as the washing buffer for the initial experiments. This was not an *in vitro* release study, instead, it was an experiment to better understand the role of the filter in multiple washing cycles and to select whether we should use the filtrate or the supernatant to analyze the release data.

We synthesized Ins-Eud-NPs and divided them into 4 aliquots each with a volume of 200 µL. We did not wash one aliquot at all, washed the second aliquot only once with 200 µL pH 7.4 buffer, washed the third aliquot twice, each time using 200 µL pH 7.4 buffer and a fresh Amicon filter and lastly we washed the fourth aliquot of NPs thrice, each time using 200 µL pH 7.4 buffer and a fresh Amicon filter. We measured the amount of insulin present in the filtrate and the supernatant in each case. Ideally the amount of insulin detected in the filtrate and concentrate in each case should add up to the amount of insulin present in the sample where the NPs were not washed at all. Any sum of insulin less than that can be regarded at lost.

Figure A4 shows that the amount of insulin detected in the filtrate remained constant across the multiple washed samples. However, the amount of insulin detected in the supernatant decreased as the NPs underwent multiple washes. This decrease in the amount of insulin detected can be attributed to the loss of NPs as they get trapped in the filter membrane and insulin as it gets adsorbed to the filter material.

From these observations it can be seen that there is loss of insulin from the NPs due to protein adsorption in the filter membrane. To minimize this loss of insulin only one filter must be used to wash a batch of NPs without replacing filters between washing cycles. These results also indicate that if an extremely small amount of insulin is present in the NP solution, it might get lost in the filter and would be hard to detect it in the filtrate as well as the concentrate.

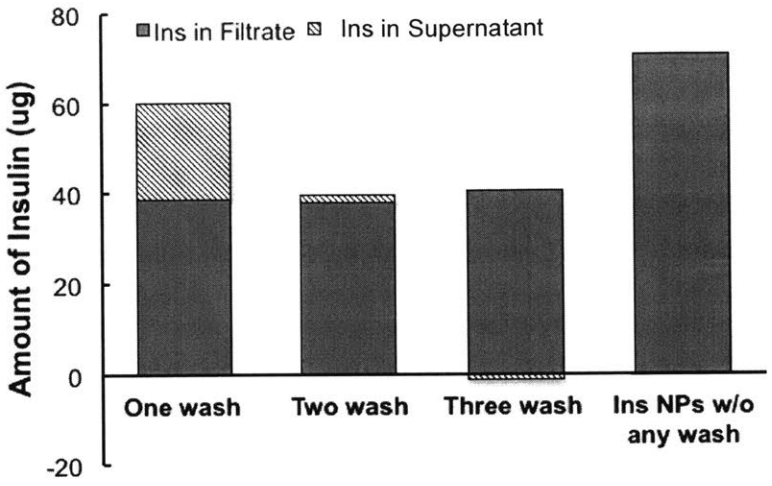

Figure A4. Amount of insulin detected in the filtrate remained constant across the samples that were washed multiple times. However, the amount of insulin detected in the supernatant decreased as the NPs underwent multiple washes. Ins NP w/o any wash represents the case without any loss of insulin.

To further confirm whether free insulin is being lost in the filter during the washing step we synthesized Ins-Eud-NPs and divided the NP solution in two equal volumes of 200 µL each. We did not wash one half of the NPs, but washed the other half with pH 6 buffer (MES buffer, 20 mM, 150 mM NaCl). It was expected that by washing the NPs with pH 6 buffer (MES buffer, 20 mM, 150 mM NaCl), less insulin would get released. As expected most of the insulin was retained in the supernatant as compared to the filtrate (Figure A5). However, on calculating the insulin release profile using the filtrate data and the concentrate data, we found a mismatch.

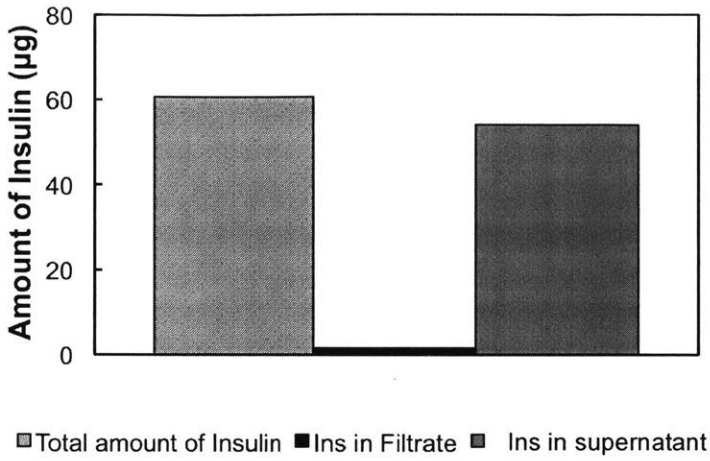

Figure A5. On washing the NPs with pH 6 buffer, most of the insulin was retained in the supernatant as compared to the filtrate. This suggested that the analyzing the supernatant would give a more accurate estimation of the insulin content at each time point.

To further understand the system better, as a control experiment we took a solution with a known concentration of insulin (50 µg/mL) and centrifuged it such that we had half of the insulin solution left both in the supernatant and as well as in the filtrate. If insulin does not get lost in the Amicon filter then the concentration of insulin both in the filtrate as well as in the supernatant should be the same. However, Figure A6A shows that the concentration of insulin obtained from the supernatant (47 µg/mL) was similar to the original concentration of insulin (50 µg/mL) used for the experiment while the concentration of insulin in the filtrate was much lower (28 µg/mL). Moreover, Figure A6B shows that the sum of insulin detected in the filtrate and the supernatant do not add up to the total insulin that was centrifuged. This indicates that some of the insulin gets trapped/lost in the filter of the centrifugation device and does not reach the filtrate. Therefore, using the filtrate data to study the *in vitro* release of insulin from NPs would not be accurate, as it would fail to account for the amount of insulin lost in the filter.

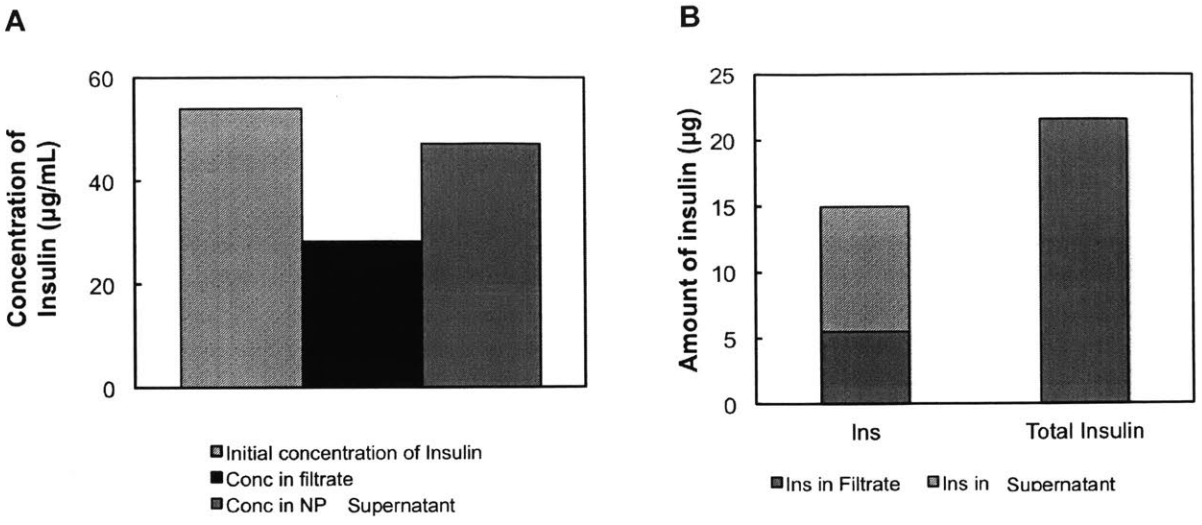

Figure A6. (A) After spinning down a 50 µg/mL insulin solution halfway, the concentration of insulin obtained from the supernatant was 47 µg/mL, similar to the original solution while the concentration of insulin in the filtrate was much lower (28 µg/mL). **(B)** The sum of insulin detected in the filtrate and the supernatant do not add up to the total insulin that was centrifuged, confirming the loss of insulin in the centrifugation device.

Lastly, we performed another control experiment where we took a known solution of insulin (70 µg/mL) and centrifuged such that the entire volume of the insulin solution (other than the dead volume) passed through the filter. If there was no loss of insulin during the washing step, the concentration and the amount of insulin detected in the filtrate should be almost equal to that of initial insulin solution. But Figure A7A shows that the concentration of insulin detected in the filtrate was less than the concentration of the original solution. Figure A7B shows that only half of the amount of insulin is detected in the filtrate. Moreover, the amount of insulin detected in the filtrate and supernatant do not add up to the total amount of insulin in the initial solution. This validated that some insulin is getting lost in the centrifugation device, potentially by getting adsorbed to the filter material. This further confirms that e amount of insulin released from the filtrate data gives a lower and inaccurate value.

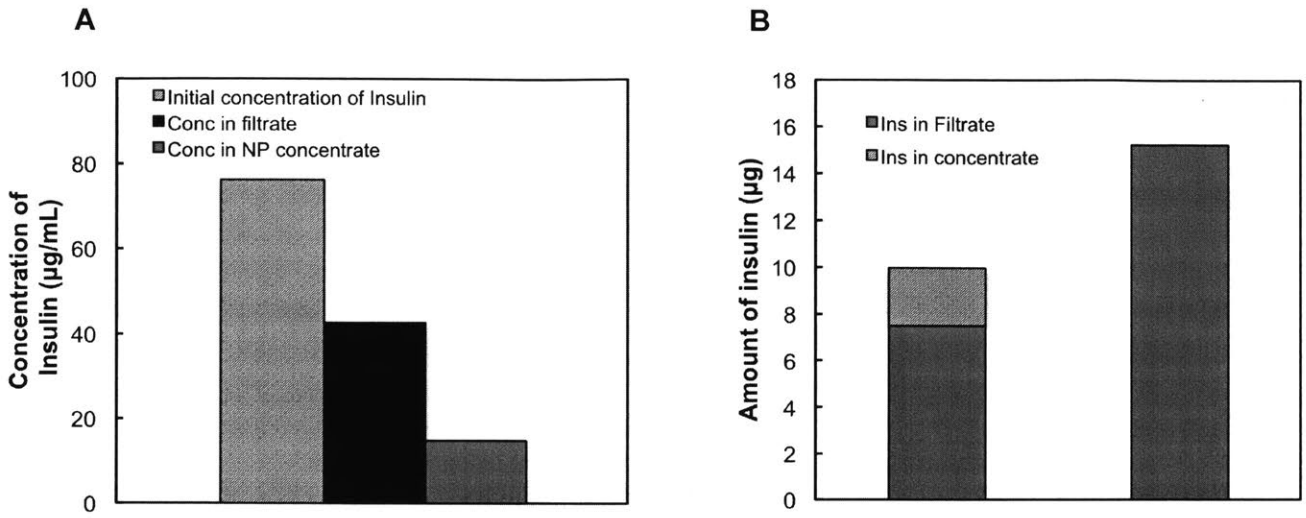

Figure A7. (A) On centrifuging down the entire volume of insulin, it was found that the concentration of insulin detected in the filtrate was less than the concentration of the original solution, suggesting that measurements done using the filtrate can be inaccurate. **(B)** The amount of insulin detected in the filtrate was only half of the total amount of insulin in the system. Moreover, the sum of insulin detected in the filtrate and supernatant do not add up to the total amount of insulin in the initial solution, suggesting a loss of insulin.

The above results suggest that both the filtrate and the supernatant are not ideal for measuring the *in vitro* release of insulin from Ins-Eud-NPs. Hence, we performed the rest of the studies using the second most common *in vitro* release method *i.e.* dialysis method.

***In vitro* release of insulin using the dialysis method – Slide A Lyzer**

We used the dialysis method to study the *in vitro* release of insulin from Ins-Eud-NPs. We prepared Eud (10%) PLGA-PEG (90%) Insulin (30%) NPs using the nanoprecipitation method and made a final NP concentration of 1mg/mL. We divided the NP solution into 1 mL volume aliquots and added them to 8 Slide A lyzer units (Maximum volume: 2 mL, MWCO 20 kDa) and collected the NP solution from the dialysis units at predetermined time points. The dialysis chambers were placed in a large buffer bath, in which the respective buffer was constantly being stirred using a magnetic stir bar. We performed the experiment with 4 different pH buffer solutions to better understand the role of pH in the *in*

vitro release of insulin. We used citrate buffer (pH 3, 20 mM, 150 mM NaCl), MES buffer (pH 6, 20 mM, 150 mM NaCl), phosphate buffer (pH 7.4, 20 mM, 150 mM NaCl) and Carbonic buffer (pH 9, 20 mM, 150 mM NaCl). Figure A8 shows that amount of insulin left in the NPs initially decreased with time as expected, but then at longer collection times, the amount of insulin left in the NPs increased. Ideally, the amount of insulin left in the NPs should have consistently decreased with time. Even though we did not see a release curve that enabled understanding of the release kinetics of insulin from these NPs, we saw a pH dependence in the insulin released. Larger amounts of insulin was being released in buffers with pH greater than 7. The lesser amount of insulin released at large time points was also observed in the previous release experiments that we had performed using the sample and separate method. As in that case, here also it could be that that the released insulin possibly gets adsorbed on the surface of the NPs stimulated by a state of equilibrium reached by the system at longer incubation times.

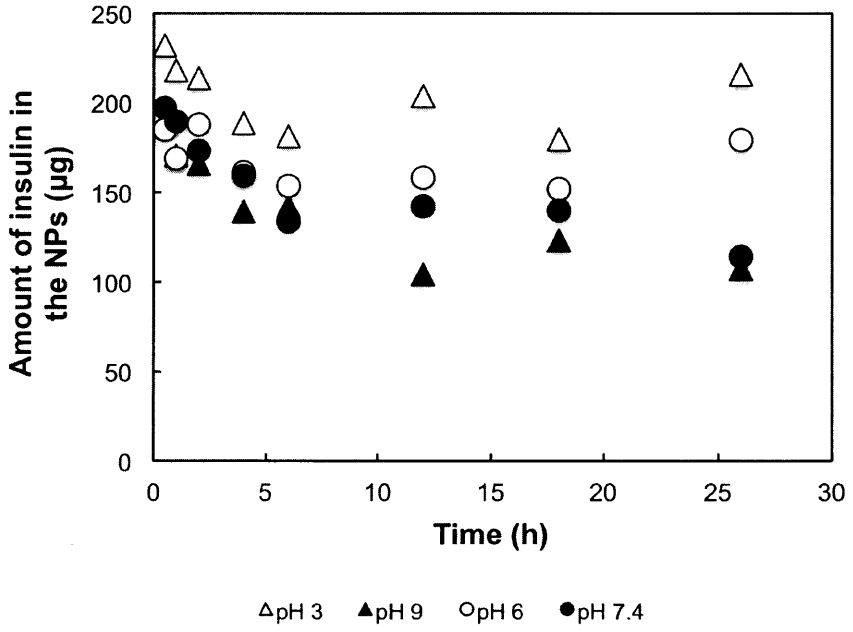

Figure A8. Insulin left in Ins-Eud-NPs after insulin release at pH 3, pH 6, pH 7.4, and pH 9 initially decreased with time but at longer collection times the amount of insulin left in the NPs increased. However, a pH dependent release is seen from Ins-Eud-NPs as lesser amount of insulin is detected after insulin release in pH great than 7.

Effect of stirring the NP sample in the dialysis chamber

On using a 20 kDa Slide A lyzer unit to study the release profile of insulin from Ins-Eud-NPs we found that at longer time intervals the released insulin fails to escape the dialysis device and instead adsorbs on the NP surface. This manifests in less insulin released at longer time points as compared to shorter time points. To enable faster escape of insulin from the dialysis chamber we performed an experiment where we added a magnetic stirrer in each dialysis chamber and measured the insulin release from Ins-Eud-NPs using the stirred dialysis devices in pH 3, pH 6, pH 7.4 and pH 9 over a period of 1 h. The updated experimental set up had stirring both inside the dialysis chamber as well as in the buffer outside the chamber. The hypothesis was that this increased convectional flow in the system would enable faster escape of insulin from the dialysis chamber and hence prevent adsorption of insulin on the NP surface by ensuring a non-equilibrium system. Figure A9A shows that free released insulin failed to diffuse across the membrane fast enough. In fact, in the first 1 h, insulin hardly diffused from the NP solution into the dialysis buffer. Insulin release profile obtained in Figure A9B using the stirred dialysis device set-up could not be used to determine the drug release kinetics, as there was inadequate release and variability in the data.

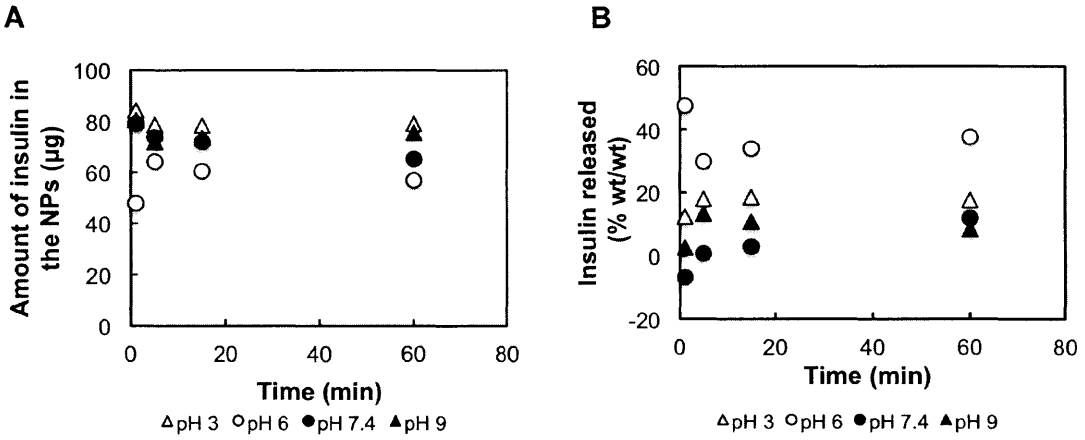

Figure A9. (A) Inclusion of a magnetic stir bar in the dialysis device did not help in accurately measuring the insulin release profile. The released insulin failed to diffuse across the membrane fast enough thereby showing an almost constant amount of insulin left in the NPs. **(B)** Insulin release profile obtained by using the

stirred dialysis device set-up could not be used to determine the drug release kinetics as there was inadequate release and variability in the data.

The very slow diffusion of insulin could be because the large size of insulin (56 kDa) as compared to the MWCO of the dialysis membrane (20 kDa) and also its hydrophilic nature at philological pH. Ideally, it is recommended that the pores in the dialysis membrane be 10 times larger than the size of the cargo being diffused. However, we were restricted by manufacturing capability because 20 kDa is the largest MWCO that is available in the Slide A lyzer. However, to test the effect of size we performed the same experiment using the blue food dye in PBS. Figure A10 shows that the diffusion of blue food dye across the 20 kDa membrane was also very slow. This could possibly be the case because of the absence of enough convection in the system to allow unhindered movement of free solution and due to the affinity of the test solutions with the material of the Slide A Lyzer membranes.

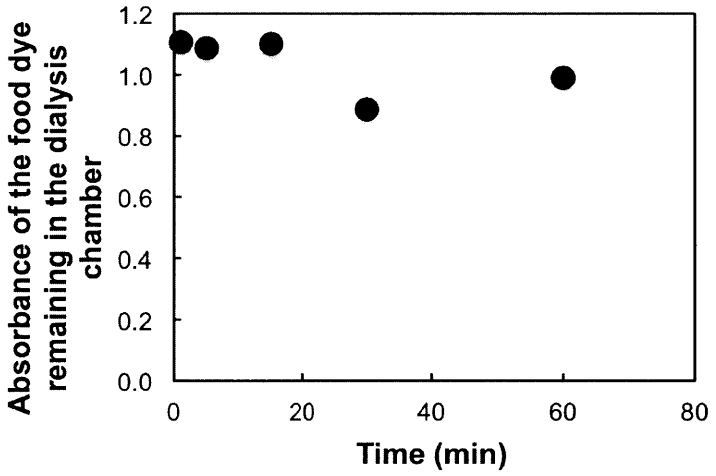

Figure A10. Blue food dye also failed to diffuse out of the dialysis chambers in 60 min. Therefore, the current dialysis set-up cannot be used to measure rapid release of insulin from NPs.

Effect of using a large pore size polycarbonate membrane in the Slide A Lyzer

The dialysis experiment using 20 kDa Slide A Lyzer device with additional convection showed very slow diffusion of both insulin and food dye out of the dialysis chamber. This could be attributed to lack of sufficient convectional movement, small pore size of membrane or the high protein affinity of the dialysis

membrane. To study if the pore size of the dialysis membrane and the material of the membrane could be responsible for poor diffusion of insulin across the dialysis chamber, we performed the same dialysis experiment with a 10 nm pore size polycarbonate membrane. Since the size of insulin is around 5500 Da 10 nm membrane would have large enough pores to provide unhindered movement of insulin molecules. To prepare dialysis units with 10 nm polycarbonate membranes, we cut out the 20 kDa membranes from the Slide A Lyzer devices and used epoxy to carefully adhere 10 nm polycarbonate membranes and trimmed off the excess membrane around the edges.

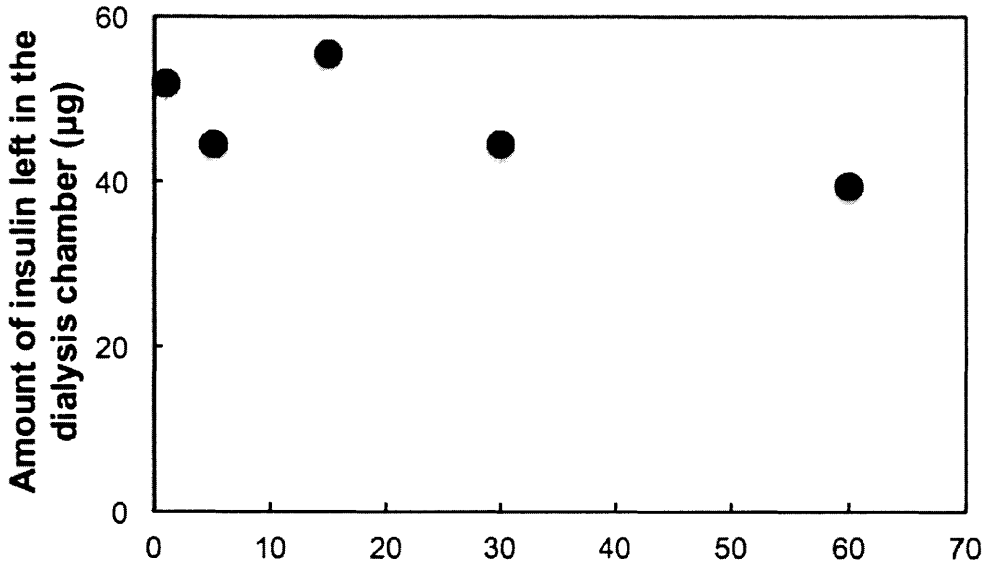

Figure A11. Insulin failed to diffuse out of the 10 nm, polycarbonate membrane dialysis chambers in 60 min.

We performed an experiment using the 10 nm polycarbonate dialysis devices where we added a magnetic stirrer in each dialysis chamber and measured the insulin released from Ins-Eud-NPs in pH 3, pH 6, pH 7.4 and pH 9 over a period of 1 h. The hypothesis was that the larger pore size (10 nm) of the membrane as well as the different material (polycarbonate) would provide unhindered movement of insulin molecules across the membrane. However, Figure A11 shows that insulin failed to diffuse fast enough from the dialysis chambers. These data suggest that the poor diffusion of released insulin across the chamber could be because of the structure of the dialysis unit in conjunction with lack of enough convection in the system. The shape of the Slide A lyzer is in the form of an open cylinder with the dialysis membrane in the base of the cylinder. This allows

insulin to diffuse only through the surface area of the membrane in contact with the solution, which is only at the base of the device.

The above results suggest that mixing of the liquid in the dialysis device as well as the area of the membrane in contact with the NP solution play a major role in accurately estimating the *in vitro* release of insulin from Ins-Eud-NPs.

In vitro release of insulin using the dialysis method – Float A lyzer

Stirring inside the dialysis chamber as well as in the buffer outside the chamber is important to allow unhindered movement of insulin to accurately estimate the rapid release of insulin from Ins-Eud-NPs. In addition to stirring, previous experiments suggest that the role of surface area of the membrane in contact with the NP solution also plays a significant role in accurately estimating the amount of insulin released. To validate this hypothesis, we performed a dialysis experiment using a different dialysis chamber, Float A lyzer. As seen in Figure A12, the Float A lyzer has a cylindrical chamber which holds the NP solution made of the dialysis membrane, providing increased surface area which is in contact with the NP solution. We used a MWCO (100 kDa) that is 18 times the molecular weight of insulin (5.6 kDa) to ensure unhindered movement of insulin across the membrane.

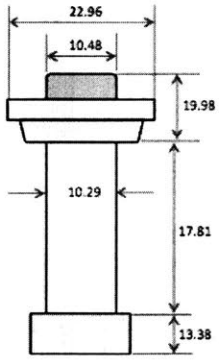

Figure A12. Schematic of the Float A Lyzer dialysis chamber.

Diffusion of food dye in water using Float A lyzer

To test the efficacy of the device we tested the diffusion of food dye in a water bath. The dialysis devices were prepared according to the manufacturer's

guidelines. They were pre-wetted, by soaking in 15% ethanol solution in a vacuum chamber for 20 minutes, in order to get rid of glycerin and achieve maximum membrane permeability. In addition, a vacuum chamber was used to allow maximum wetting of the dialysis membrane. This was followed by thoroughly washing the membranes twice with DI water. In each wash, the solution inside the devices was aspirated out, replaced with and soaked in DI water for 30 minutes.

The Float A lyzer chambers were filled with 1.25 mL of food dye solution in water and were submerged in a water bath which was stirred using a magnetic stir bar. Figure A13 shows that very little amount of food dye diffused out of the chamber. This low diffusion can be attributed to the lack of enough movement/ agitation in the sample. Another possible reason can be the application of water as the solvent for the dye as well as the different solvent. Food dye is more readily soluble and forms a more stable solution in PBS as compared to water.

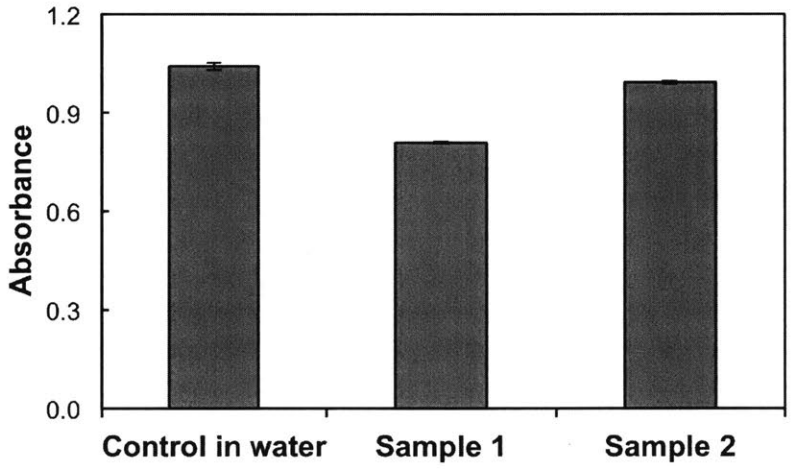

Figure A13. Food dye failed to rapidly diffuse out of the Float A lyzer dialysis chambers. Control in water is the food dye solution which was not dialyzed at all. Sample 1 is the food dye solution that was allowed to release food dye all night. It showed very little release of food dye. Lastly, Sample 2 is the sample that was allowed to release the food dye for 6 h with additional stirring inside the chamber.

Diffusion of food dye in PBS using Float A lyzer and additional stirring

Poor movement of insulin and the choice of an inadequate solvent for the food dye potentially caused poor diffusion of the food dye as seen in Figure A13. PBS is an ideal solvent to dissolve food dye as presence of additional salt in the buffer helps to stabilize the food dye solution. Moreover, to ensure the presence of a

concentration gradient to allow movement of food dye in the devices, the surrounding buffer had to be continuously stirred with a 3 mm magnetic stirrer that was inserted into each device. 1.25 mL of the food dye solution was added to each device, which was placed in a large beaker with pH 7.4. In order to ensure the movement of the magnetic stirrers the base of the devices had to be close to the bottom of the beaker, which made it difficult to add an additional stirrer in the beaker to stir the dialysis buffer. Therefore, for continuous stirring of the buffer outside the dialysis devices, the beaker was put on a magnetic stirring plate, which was further placed on an orbital shaker. This set up is illustrated in Figure A14A .

At each predetermined time interval, the food dye solution was sampled and the absorbance was measured using a TECAN plate reader. The absorbance from each of the collected time points was compared with the absorbance of the initial solution of food dye. Figure A14B shows that the majority of food dye had diffused out of the dialysis chambers in 2h 15 min. This data validated our initial hypothesis that the presence of adequate movement and the choice of the right buffer for dialysis can significantly improve the rate of diffusion from the Float A lyzer devices.

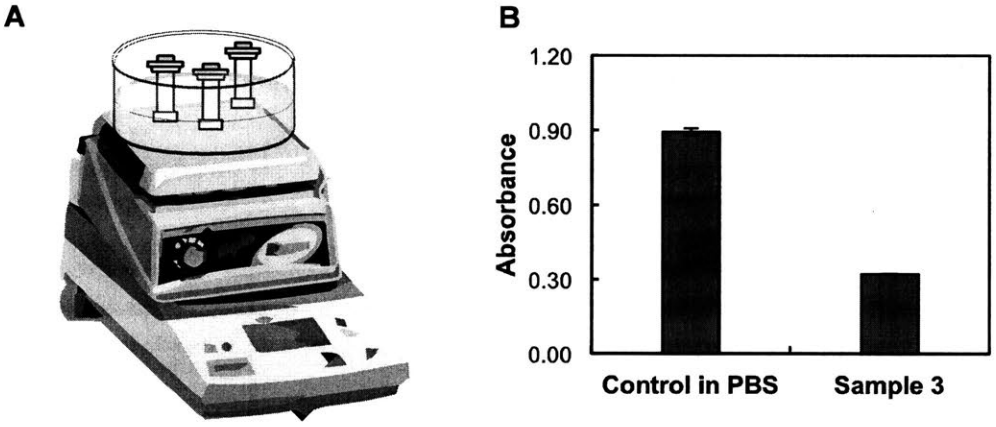

Figure A14. (A) Schematic of the dialysis set-up using Float A lyzers. To enable continuous stirring of the buffer outside the dialysis devices, the beaker was put on a magnetic stirring plate, which was further placed on an orbital shaker. **(B)** By increasing the convectional flow in the system and by choosing a suitable solvent, majority of the food dye solution managed to escape the dialysis device. Control in PBS is the blue food dye solution that was not exposed to the dialysis set up, while Sample 3 is the sample of blue food dye which was measured after dialysis for 2h 15 min.

Effect of different agitation mechanisms and different MWCO dialysis membranes

Generation of adequate agitation was crucial to the successful and unhindered diffusion of molecules across the dialysis membranes in Float A lyzer dialysis devices. Our previous observations validate how adding additional stirring in the dialysis set up enabled faster diffusion of blue food dye. Stirring helps in rapidly renewing the layer of the food dye solution, which is in contact with the dialysis membrane enabling a continuous concentration gradient and faster movement of molecules across the membrane. Possibly reducing the thickness of the layer of food dye solution would enable faster contact of food dye molecules with the dialysis membrane when compared to regular stirring using a magnetic stirrer.

To design a set up that would create a thin layer of the solution around the membrane we customized the Float A lyzer units. We prepared epoxy cylinders with 17 mm height and 8 mm diameter and inserted them in the Float A lyzer devices. A schematic of the Float A lyzer with the stir bar and the epoxy cylinder can be seen in Figure A15. To enable rotation of the epoxy cylinder within the devices to allow rapid renewing of the layer of food dye in contact with the dialysis membrane the beaker with the dialysis devices with epoxy cylinders was placed on an orbital shaker. This not only helped agitate the dialysis buffer but also enabled continuous movement of the epoxy cylinder in the dialysis devices.

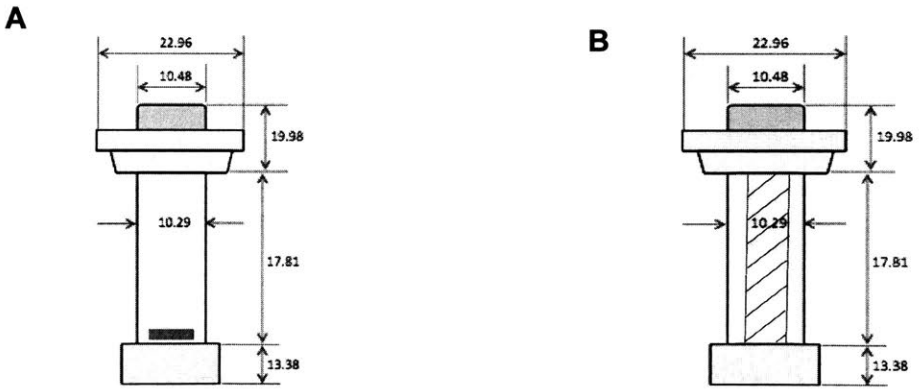

Figure A15. (A) Schematic of the Float A lyzer with a magnetic stirrer placed inside it. **(B)** Schematic of the Float A lyzer with an epoxy cylinder placed inside it .

We performed a dialysis experiment using 2 different dyes (yellow and blue), 2 different MWCO dialysis membranes (50 kDa and 100 kDa) and 2 different agitation mechanisms (stirring and moving epoxy cylinder). We added 1.25 mL of food dye solution in PBS to each of the dialysis devices and sampled at predetermined time points. The sampled volumes were analyzed using a TECAN plate reader. Figure A16A shows that using the100 kDa MWCO dialysis membrane yellow food dye has a shorter half-life when the food dye solution is stirred inside the dialysis chambers. The 100 kDa membrane did not show much more improvement when the samples were collected from the devices which had an epoxy cylinder in them. However, in both cases 50 kDa as well as 100 kDa membranes the application of the epoxy cylinder in the devices proved to be better at enabling the measurement of rapid diffusion of molecules across the dialysis membrane as opposed to just stirring.

In the experiments with blue food dye, Figure A16B shows that the 100 kDa membrane was significantly better than the 50 kDa membrane in allowing rapid diffusion of molecules across the membrane for both cases – stirring as well as moving epoxy cylinder. However, the results of another experiment (Figure A16C) show that the use of the epoxy cylinder did not seem to have a much greater advantage over using stirring to produce agitation and movement in the dialysis setup.

From the above observations, it was evident that the dialysis membrane with 100 kDa MWCO is more suited for studying rapid diffusion of molecules. Also, even though the application of the epoxy cylinder was more efficient, the sampling process in the presence of the epoxy cylinder was more cumbersome. Each time before sampling the dialysis membrane had to be cut open using a razor and then the pipette had to be inserted in the cut to extract the sample from the device. Since it was not a precise technique of sampling, each time a different amount of sample was lost in the process, leading to unwanted errors.

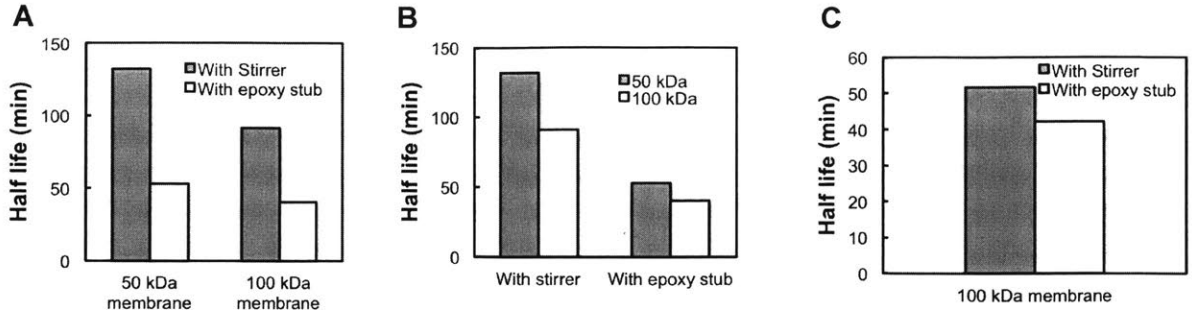

Figure A16. (A) Dialysis of yellow food dye. For both 50 kDa and 100 kDa MWCO dialysis membrane application of the epoxy cylinder is more effective relative to internal stirring. **(B)** Dialysis of blue food dye.100 kDa membrane is more effective than the 50 kDa membrane in allowing rapid diffusion of molecules across the membrane for both cases – stirring as well as moving epoxy cylinder. **(C)** Application of the epoxy cylinder did not seem to have a much greater advantage over using stirring to produce agitation and movement in the dialysis setup.

Diffusion of insulin from 100 kDa dialysis devices using different agitation methods

Previous experiments with food dye suggested the 100 kDa MWCO dialysis membranes are more suited for our study. Although the application of the epoxy cylinder as the agitation mechanism was more efficient, retrieving the sample was a cumbersome and inconsistent process. The 100 kDa was a straightforward selection, but to select the appropriate agitation mechanism we did some more experiments.

We studied the diffusion of free insulin solution in PBS using the two methods of producing agitation, by stirring the sample and by including the epoxy cylinder in the device. To allow continuous agitation of the beaker with the dialysis devices with both the stir bars and the epoxy cylinders was placed on an orbital shaker. We allowed the insulin to diffuse out of the chambers for 2 hours after which we sampled the solutions. The dialysis experiment was performed at 25°C. Figure A17 shows that the 50% of the insulin was diffused from the dialysis chambers with internal stirring and 60% of the insulin was released from chambers with the epoxy cylinder.

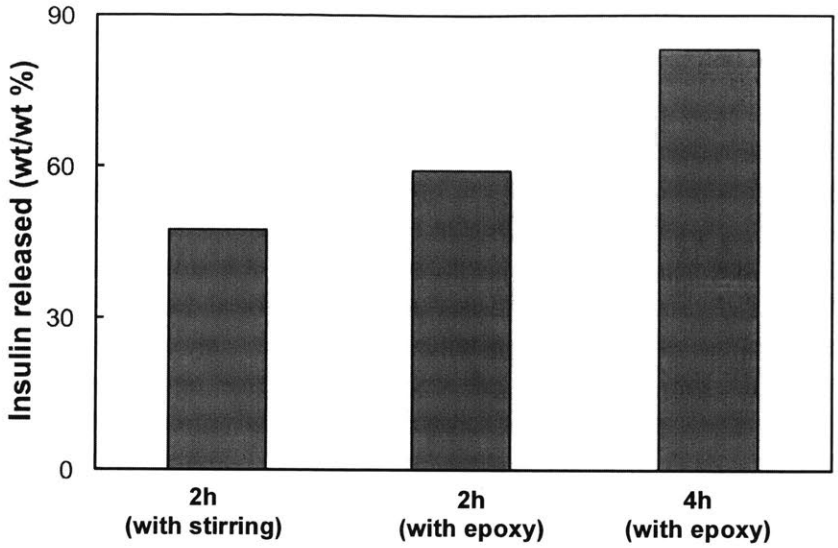

Figure A17. On comparing the effectiveness of the application of the stir bar relative to the effectiveness of the epoxy cylinder, 50% of the insulin was diffused from the dialysis chambers with internal stirring and 60% of the insulin was released from chambers with the epoxy cylinder. The difference between the half-life of insulin using these two agitation methods was not drastically different.

These results suggest that the application of the epoxy cylinder is slightly better than internal stirring in the dialysis devices. However, when we consider the inconsistency in the collection volume of the sampled solution as in the case with the epoxy cylinder, use of the stir bar seemed more repeatable and efficient. However, for the estimation of insulin release from Ins-Eud-NPs, a resolution of 2 h as half-life of insulin is not ideal. With the current resolution of the dialysis set up it will be hard to estimate the amount of insulin released in the first few hours.

Diffusion of insulin from 100 kDa dialysis devices with stirring at 37°C

The application of 100 kDa dialysis membrane accompanied by internal stirring to maintain the concentration gradient and allow movement of the sample so far allowed diffusion of insulin with a half-life of 2 h. The above experiments were performed at 25°C. However, at temperatures closer to the physiological temperature (37°C) diffusion is expected to be faster due to an increase in the kinetic energy of the system due to increased temperature. To test that hypothesis we performed the insulin diffusion experiment at 37°C. We studied the diffusion of free insulin solution in pH 6 MES buffer (20 mM, 150 mM NaCl) and in pH 7.4 PBS buffer (20mM, 150 mM NaCl) using 100 kDa MWCO

membrane Float A lyzer dialysis devices with additional internal stirring. To allow continuous agitation of the beaker with the dialysis devices was placed on an orbital shaker. This not only helped agitate the dialysis buffer but also enabled continuous movement of the magnetic stir bar. We sampled the insulin solution in the dialysis chambers at predetermined time points (0, 15, 60, 120, 240 and 360 min). Figure A18 shows that by performing the experiment at increased temperature (37°C), insulin diffuses out faster from the dialysis chambers. Insulin solution has a half –life of less than 1 h. Moreover, the insulin diffusion curve at pH 6 superimposes with the insulin diffusion curve at pH 7.4 which indicates that the solubility of insulin in the two buffers does not affect the diffusion of insulin from the dialysis chambers.

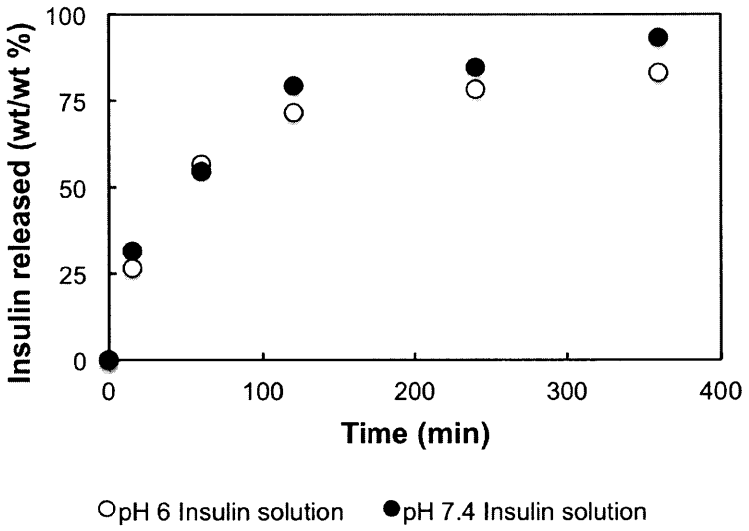

Figure A18. Release of free insulin solution from Float A lyzer devices (100 kDa MWCO) with internal stirring at 37°C. The half-life of insulin is less than one hour is which is good for measuring rapid release of insulin from polymeric carriers.

Initial test release of insulin from Ins-Eud-NPs

The *in vitro* release of insulin was studied by dividing a batch of Ins-Eud-NPs equally into aliquots and placing them in 100 kDa, Float-A-lyzer dialysis devices and incubating them at 37°C in 20 mM Phosphate buffer (pH 7.4, 150 mM NaCl). The dialysis devices were prepared according to the manufacturer's guidelines. In order to ensure the presence of a concentration gradient to allow movement of insulin, the NP samples in the devices and the surrounding buffer had to be continuously stirred with a 3 mm magnetic stirrer was inserted into each device.

1.25 mL of the 1 mg/mL NP solution was added to each device, which were placed in a large beaker with pH 7.4 or pH 6 buffer at 37°C. Typically, 9-10 dialysis devices were placed in a beaker with 800-900 mL of pH 7.4 or pH 6 buffer. In order to ensure the movement of the magnetic stirrers the base of the devices had to be close to the bottom of the beaker, which made it difficult to add an additional stirrer in the beaker to stir the dialysis buffer. Therefore, for continuous stirring of the buffer outside the dialysis devices, the beaker was put on a magnetic stirring plate, which was further placed on an orbital shaker. At each predetermined time interval, an aliquot of the NPs was taken and measured for insulin loading using the BCA assay. Figure A19 shows that insulin gets released at a faster rate at pH 7.4 as compared to pH 6. The half-life of insulin released in pH 7.4 was a little less than 1h while the half-life of insulin released in pH 6 was 2h. However, at longer time points we see a decrease in the amount of insulin released both in pH 7.4 as well as pH 6.

Figure A19 also shows that on superimposing the data of a control experiment as mentioned in the previous section where the rate of free insulin diffusion was characterized. We find that the rate of diffusion of free insulin is almost identical to the rate at which insulin is released in pH 7.4. This suggests that the rate of release of insulin at pH 7.4 is indistinguishable from the rate of release of free insulin solution, thereby indicating that at pH 7.4 the Ins-Eud-NPs behave like an insulin solution i.e. rapid release of insulin from the NPs. Here the measured release rate of insulin in pH 7.4 is limited by the resolution of the dialysis set up.

Although the above results helped us better understand the release kinetics of insulin in pH 7.4 and pH 6, we continued to see aberrant measurements at later time points.

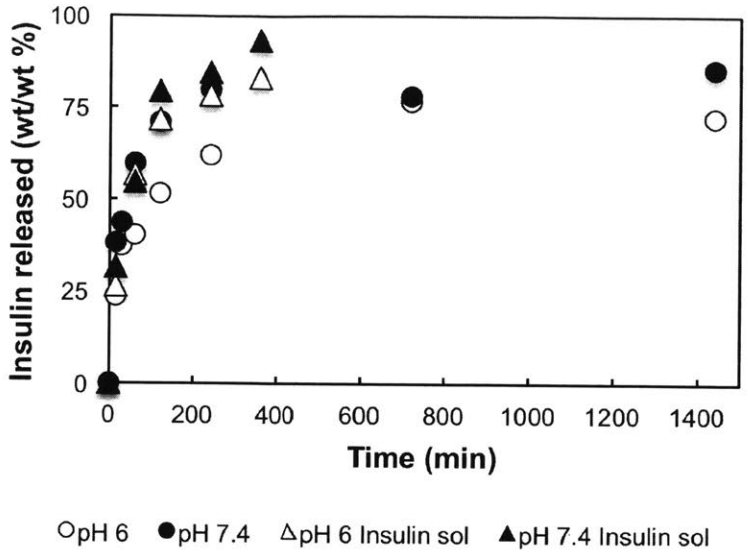

Figure A19. Insulin release profile from Ins-Eud-NPs. Insulin releases rapidly at pH 7.4 and a slower release was observed at pH 6. The data has been plotted with the diffusion curve of free insulin solution, which superimposes with the insulin release curve at pH 7.4, indicating that insulin releases instantaneously from NPs at pH 7.4. However, the reduction in insulin release at longer time points continued to be puzzling.

Effect of storage temperature of the NP sample in between release time points

After the changes mentioned in the above section we were successful in obtaining a release curve for Ins-Eud-NPs. However, the reduction in the insulin released at later time points indicated that possibly the storage conditions of the samples in between collection points could be a source of interference. For the previous release experiments we collected samples at predetermined time points and stored them at room temperature (25°C) in Eppendorf tubes. At the end of 24 hours, all the samples were analyzed together using the BCA assay. Our hypothesis was that the storage temperature and conditions could be causing changes within the samples that could explain these outliers at longer time points.

To test this hypothesis we performed a dialysis experiment using Ins-Eud-NPs and collected the NP at predetermined time points. After collection we stored one half of the sample at room temperature (25°C) and the other half at 4°C. Figure

A20 shows that storing the NP samples at different temperatures in between collection time points did not have a significant impact on the amount of insulin detected.

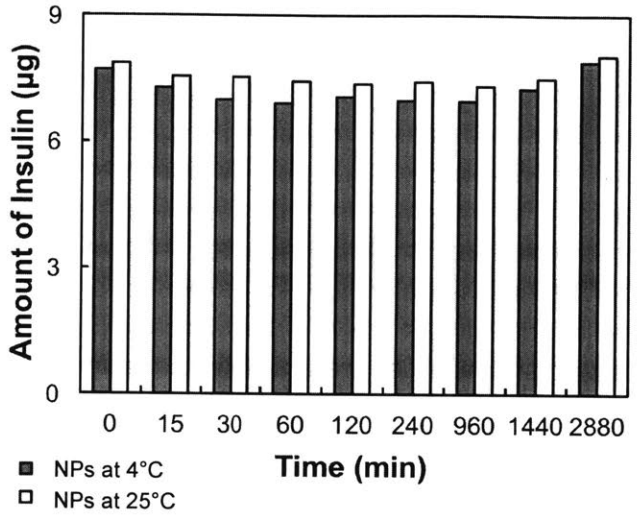

Figure A20. Changing the storage temperature of the NPs collected in between time points did not have a significant effect on the amount of insulin detected form that sample.

Dialysis experiment using Empty-NPs

Storing NPs at different temperatures between collection time points did not impact the amount of insulin detected. However, we continued to detect lesser insulin released at longer time points. Another possible source of interference could be the polymer of the NPs, which can undergo changes over time due to hydrolysis of the polymer and interfere with the accuracy of the readings at longer time points. To investigate that we performed an experiment to study the background noise generate by Emp-NPs. We studied this by preparing NPs and dividing a batch of Emp-NPs equally into aliquots and placing them in 100 kDa, Float-A-lyzer dialysis devices and incubating them at 37°C in 20 mM Phosphate buffer (pH 7.4, 150 mM NaCl). The dialysis devices were prepared according to the manufacturer's guidelines. As in the previous cases, the NPs were stirred by adding a magnetic stirrer in the dialysis chamber. 1.25 mL of the 1 mg/mL NP solution was added to each device, which were placed in a large beaker with pH 7.4 buffer at 37°C. Typically, 9-10 dialysis devices were placed in a beaker with 800-900 mL of pH 7.4 buffer.

At each predetermined time interval, an aliquot of the NPs was taken and absorbance values of the Emp-NPs was measured using the BCA assay. In the ideal case, this value should be a constant independent of time and should be subtracted from the absorbance values obtained from Ins-Eud-NPs to get the correct loading value. However, Figure A21 shows that the absorbance of empty NPs increased with time. We also observed a sudden increase in absorbance data of the Emp-NPs from 0 time point to 15 min time point. The increase in absorbance was equivalent to an insulin loading increase from 3.6 ug (t = 0) to 7.7 ug (t = 15 min). Experimentally the main difference between the sample collected at t = 0 and t = 15 mins was that the sample at t = 0 was not exposed to the dialysis chamber while the sample collected at t =15 min as well as the samples collected at other time points were all exposed to the dialysis chamber. This suggested that the constituents of the dialysis chamber or the combination of the NPs and the dialysis chamber are possibly interfering with the absorbance data.

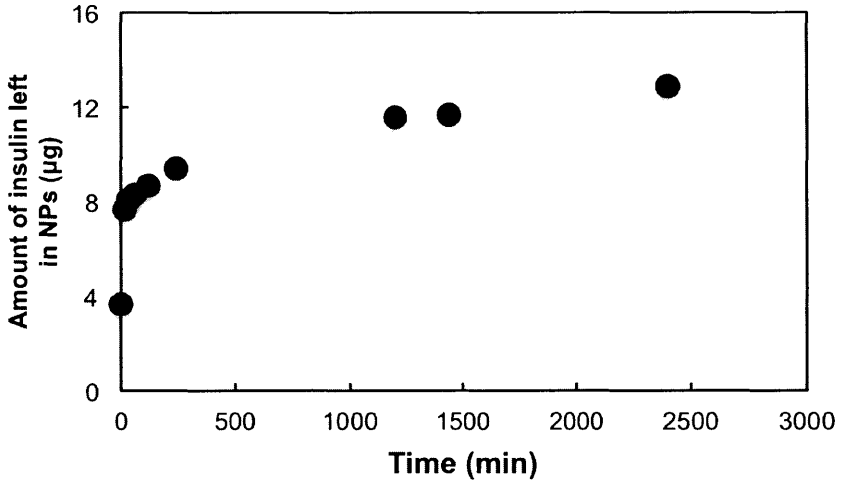

Figure A21. On performing a dialysis experiment with only Emp-NPs, the absorbance values increased with time. Here, the absorbance values are plotted for equivalent amount of insulin to emphasize the effect of the data on the insulin release data.

Absorbance data after NP incubation in dialysis devices versus in Eppendorf tubes

Studying the absorbance from Emp-NPs showed that absorbance data increased with longer incubation times in the dialysis chamber. Our hypothesis was that either the NPs are reacting with the dialysis membrane or the dialysis chambers are leaching out chemicals, which are interfering with the components of the BCA assay resulting in an increase in the absorbance data.

To test the former hypothesis, we designed an experiment where we synthesized Emp-NPs and divided them in aliquots, half of which were incubated in the Float A lyzer dialysis chamber and the other half were incubated in Eppendorf tubes. We collected the samples from both the sets at predetermined time points and measured the absorbance using the BCA assay. If the interaction between the Emp-NPs and the dialysis chamber was causing the increase in the absorbance data we would ascertain that through this experiment as the data would be different from the absorbance data collected form the samples that were incubated in the Eppendorf tubes.

Figure A22A shows that there was a minor increase in the theoretical amount of insulin with time in samples that were incubated in the Eppendorf tubes. The increase in the theoretical amount of insulin with time in the samples incubated in the dialysis chamber was more pronounced. However the difference in the data was not prominent enough to reach a conclusion.

To test our next hypothesis that potentially the dialysis chambers are leaching out chemicals that are interfering with the BCA assay and resulting in increasing theoretical value of detected insulin with increasing incubation times, we performed another experiment where instead of incubating NPs we filled the dialysis chambers with the same buffer (pH 7.4, 20 mM PBS, 150 mM NaCl) as the dialysis buffer in which the dialysis chambers were submerged. Four dialysis chambers were filled with buffer (pH 7.4, 20 mM PBS, 150 mM NaCl) and the samples were collected at predetermined time points. We used the BCA assay to estimate measure the absorbance and converted it to calculate the theoretical amount of insulin. Figure A22B shows that the value of theoretical insulin increased with increasing time points. This observation can be attributed to the presence of chemicals that can leach out of the dialysis device and interfere with the BCA assay.

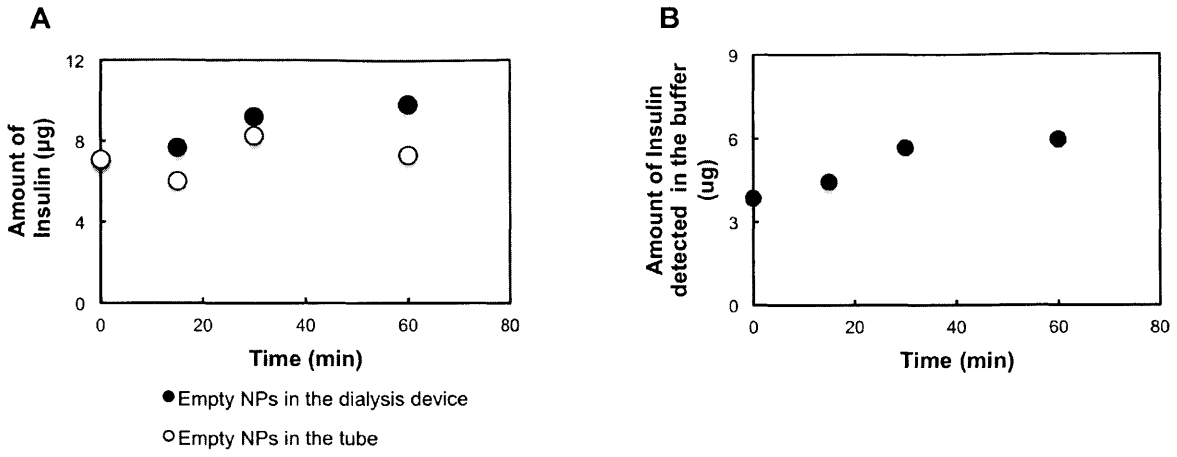

Figure A22. (A) A minor increase in the theoretical value of insulin is detected with an increase in incubation time in samples that were incubated in the Eppendorf tubes but a more prominent increase in the value of insulin was detected in NP samples that were incubated in the Float A lyzer dialysis chambers. **(B)** The value of absorbance obtained from the buffer solution increased with increasing time points. Here, we have plotted the theoretical amount of insulin calculated from the absorbance data.

Removal of interfering agents from dialysis chambers

The failure of proper removal of interfering agents from the dialysis chambers resulted in an increase in the theoretical insulin loading even from plain buffer. This possibly resulted in the anomalous *in vitro* insulin release from Ins-NPs. To ensure removal of interfering agents from the dialysis chambers we soaked the dialysis devices overnight in buffer at 37°C after preparing them according to the manufacturer's instructions. We performed the release experiment using those chambers the following day.

We studied the absorbance signal obtained from Emp-NPs using the dialysis chambers, which were soaked for 24 h. Figure A23 shows that there was no increase in the theoretical insulin loading (calculated by using the absorbance data generated from Emp-NPs) even at longer time points. This can be attributed to the longer incubation time for the chambers in the buffer that allowed unwanted interfering materials to gradually leach out of the chambers.

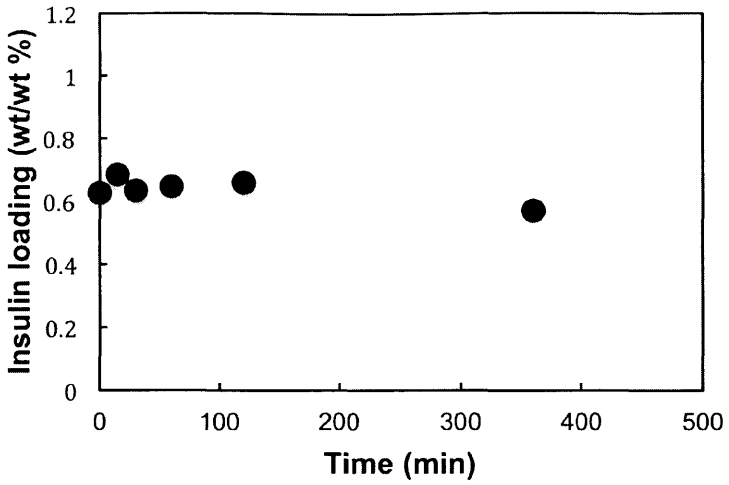

Figure A23. On incubating the dialysis chambers overnight in buffer and then using those devices to perform a dialysis experiment on Emp-NPs gives an almost constant value with increasing incubation times.

Improved experimental set up for *in vitro* insulin release study from Ins-Eud-NPs

The *in vitro* release of insulin was studied by dividing a batch of Ins-Eud-NPs equally into 100 kDa Float A Lyzer (Spectrum Labs) units and incubating them at 37°C in PBS (pH 7.4). At each predetermined time interval, an aliquot of the NPs was taken and measured for insulin loading using the BCA assay, which included heating at 60°C for 1 h as previously described. In order to increase the accuracy of the dialysis setup, a 3 mm magnetic stirrer was inserted in each Float A Lyzer unit, to allow continuous mixing of the Ins-Eud-NP solution inside the dialysis chambers. Furthermore, the beaker with the dialysis chambers was kept on an orbital shaker, to ensure mixing of the buffer solution outside the dialysis chambers. Three experiments were performed for each data point.

The dialysis devices were prepared according to the manufacturer's guidelines. The Float-A-Lyzer devices were pre-wetted, by soaking in 15% ethanol solution in a vacuum chamber for 20 minutes, in order to get rid of glycerin and to achieve maximum membrane permeability. In addition, a vacuum chamber was used to allow maximum wetting of the dialysis membrane. This was followed by thoroughly washing the membranes twice with DI water. In each wash, the solution inside the devices was aspirated out, replaced with and soaked in DI water for 30 minutes. To completely get rid of any interfering agents, after

inserting stirrers in the devices, we filled them with pH 7.4 buffer and stirred them for 24 h in a beaker containing pH 7.4 buffer. This procedure can be seen in Figure A24.

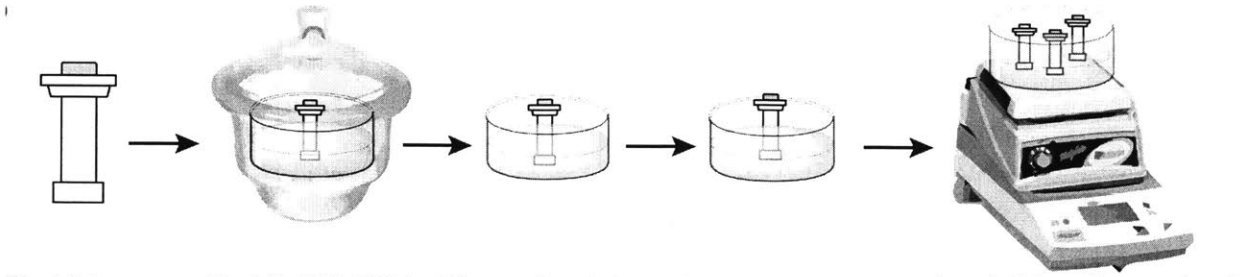

Figure A24. Design of the dialysis set up to study the *in-vitro* release of insulin.

In order to ensure the presence of a concentration gradient to allow movement of insulin, the NP samples in the devices and the surrounding buffer had to be continuously stirred with a 3 mm magnetic stirrer was inserted into each device. 1.25 mL of the 1 mg/mL NP solution was added to each device, which were placed in a large beaker with pH 7.4 buffer at 37°C. Typically, 9-10 dialysis devices were placed in a beaker with 800-900 mL of PBS buffer. In order to ensure the movement of the magnetic stirrers the base of the devices had to be close to the bottom of the beaker, which made it difficult to add an additional stirrer in the beaker to stir the dialysis buffer. Therefore, for continuous stirring of the buffer outside the dialysis devices, the beaker was put on a magnetic stirring plate, which was further placed on an orbital shaker. This set up is illustrated in Figure A24. At each predetermined time interval, an aliquot of the NPs was taken and measured for insulin loading using the BCA assay. Three experiments were performed for each data point.

pH sensitive *in vitro* release of insulin from Ins-Eud-NPs

24 hour *in vitro* release of Ins-Eud-NPs was measured according to the method mentioned above. Figure A25 shows the *in vitro* release of 20% Eudragit NPs which were synthesized in pH 5. It shows that there is a significant reduction in the rate at which insulin is released from the NPs at pH 6 as compared to pH 7.4. The half-life of insulin in pH 7.4 is between 30-60 min, while the half-life of insulin in pH 6 is 240 min. To better visualize this data and to account for the maximum measurement resolution of the experimental setup, we normalized the insulin released in pH 6 and pH 7.4 with respect to the release rate of free insulin

solution. Figure A26 shows that almost all of the insulin form the NPs gets released as soon as the NPs are exposed to pH 7.4 while there is a significantly slowed release of insulin from the NPs in pH 6.

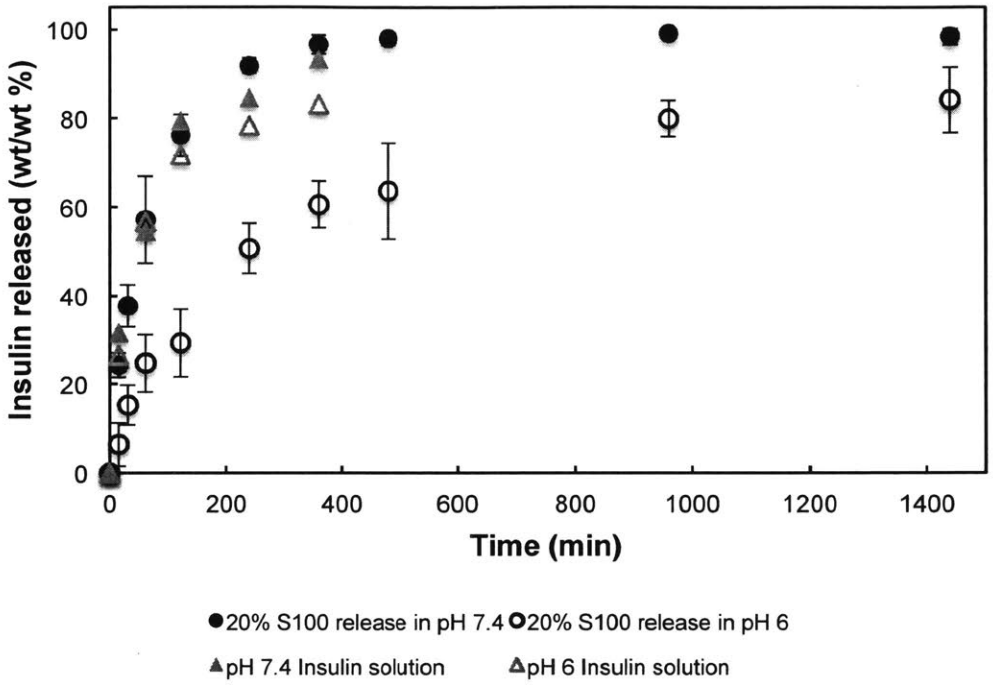

Figure A25. *In vitro* release of Ins-Eud-NPs shows that there is a significant reduction in the rate at which insulin is released from the NPs at pH 6 as compared to pH 7.4. The half-life of insulin in pH 7.4 is between 30-60 min, while the half-life of insulin in pH 6 is 240 min. The release curve of free insulin superimposes on the release curve of insulin at pH 7.4

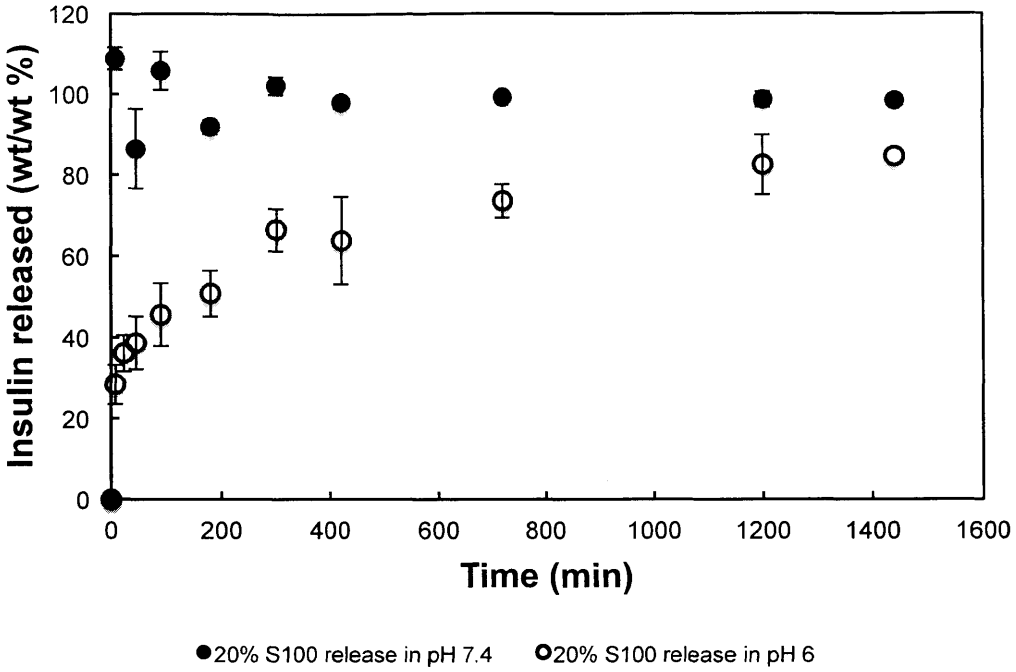

Figure A26. On normalized the insulin released in pH 6 and pH 7.4 with respect to the release rate of free insulin solution we can better visualize the difference in the release of insulin at pH 7.4 relative to pH 6.

Conclusion

The study mentioned in this section helped gain valuable insights which lead to the development of a dialysis set up that can be used to measure and characterize rapid release of insulin in the first few minutes and hours from polymeric nanoparticles. This systematic study helped understand the issues related to current *in vitro* drug release measurement protocols, such as slow diffusion, loss of drug in sampling and the attainment of equilibrium by the system. By methodically investigating each of these issues, we were able to circumvent them and provide solutions to improve the existing methods of *in vitro* drug release measurement.

References

1. Pridgen, E. M.; Alexis, F.; Kuo, T. T.; Levy-Nissenbaum, E.; Karnik, R.; Blumberg, R. S.; Langer, R.; Farokhzad, O. C., Transepithelial transport of Fc-targeted nanoparticles by the neonatal fc receptor for oral delivery. *Science translational medicine* **2013,** *5* (213), 213ra167.

2. Walsh, G., Biopharmaceutical benchmarks 2014. *Nature Biotechnology* **2014,** *32* (10), 992-1000.

3. Fosgerau, K.; Hoffmann, T., Peptide therapeutics: current status and future directions. *Drug discovery today* **2015,** *20* (1), 122-8.

4. Choonara, B. F.; Choonara, Y. E.; Kumar, P.; Bijukumar, D.; du Toit, L. C.; Pillay, V., A review of advanced oral drug delivery technologies facilitating the protection and absorption of protein and peptide molecules. *Biotechnol Adv* **2014,** *32* (7), 1269-82.

5. Uhlig, T.; Kyprianou, T.; Martinelli, F. G.; Oppici, C. A.; Heiligers, D.; Hills, D.; Calvo, X. R.; Verhaert, P., The emergence of peptides in the pharmaceutical business: From exploration to exploitation. *EuPA Open Proteomics* **2014,** *4*, 58-69.

6. Kim, E. S.; Plosker, G. L., AFREZZA®(insulin human) Inhalation powder: a review in diabetes mellitus. *Drugs* **2015,** *75* (14), 1679-1686.

7. White, S.; Bennett, D. B.; Cheu, S.; Conley, P. W.; Guzek, D. B.; Gray, S.; Howard, J.; Malcolmson, R.; Parker, J. M.; Roberts, P., EXUBERA®: pharmaceutical development of a novel product for pulmonary delivery of insulin. *Diabetes technology & therapeutics* **2005,** *7* (6), 896-906.

8. Arbit, E.; Kidron, M., Oral insulin: the rationale for this approach and current developments. *Journal of diabetes science and technology* **2009,** *3* (3), 562-567.

9. Moeller, E. H.; Jorgensen, L., Alternative routes of administration for systemic delivery of protein pharmaceuticals. *Drug Discovery Today: Technologies* **2008,** *5* (2), e89-e94.

10. Banting, F. G., Best, C.H., Collip, J.B., Campbell, W.R., Fletcher, A.A., Pancreatic extracts in the treatment of diabetes mellitus preliminary report. *Canadian Medical Association Journal* **1991,** *145* (10), 1281-1286.

11. Dey, L.; Attele, A., Type 2 diabetes. *Tradit Chinese Med* **2011,** *231* (1), 1-16.

12. Daneman, D., Type 1 diabetes. *The Lancet* **2006,** *367* (9513), 847-858.

13. Dafoulas, G. E.; Toulis, K. A.; McCorry, D.; Kumarendran, B.; Thomas, G. N.; Willis, B. H.; Gokhale, K.; Gkoutos, G.; Narendran, P.; Nirantharakumar, K., Type 1 diabetes mellitus and risk of incident epilepsy: a population-based, open-cohort study. *Diabetologia* **2017,** *60* (2), 258-261.

14. Stratton, I. M., Adler, A.I., Neil, H.A.W., Matthews, D.R., Manley, S.E., Cull, C.A., Hadden, D., Turner, R.C., Holman, R.R, Association of glycaemia with macrovascular and microvascular complications of type 2 diabetes (UKPDS 35)-prospective observational study. *BMJ* **2000,** *321*, 405-411.

15. Nichols, G. A., Erbey, J.R., Hillier, T.A., Brown, J.B., Congestive Heart Failure in Type 2 Diabetes. *Diabetes Care* **2001,** *24* (9), 1614-1619.

16. Gabbay, K. H., The sorbitol pathway and the complications of diabetes. *Seminars in Medicine of the Beth Israel Hospital* **1973,** *288* (16), 831-836.

17. Reichard, P., Nilsson, B.Y., Rosenqvist, U., The effect of Long-term intensified insulin treatment on teh development of microvascular complications of diabetes mellitus. *The New England Journal of Medicine* **1993,** *329* (5), 304-309.

18. Kim, C., Newton, K.M., Knopp, R.H., Gestational Diabetes and the Incidence of Type 2 Diabetes. *Diabetes Care* **2002,** *25* (10), 1862-1868.

19. Xiong, X. Y.; Li, Q. H.; Li, Y. P.; Guo, L.; Li, Z. L.; Gong, Y. C., Pluronic P85/poly(lactic acid) vesicles as novel carrier for oral insulin delivery. *Colloids and surfaces. B, Biointerfaces* **2013,** *111*, 282-8.

20. Card, J. W.; Magnuson, B. A., A review of the efficacy and safety of nanoparticle-based oral insulin delivery systems. *Am J Physiol Gastrointest Liver Physiol* **2011,** *301* (6), G956-67.

21. Patel, M. M., Colon targeting- an emerging frontier for oral insulin delivery. *Expert opinion in Drug Delivery* **2013,** *10* (6), 731-739.

22. Inzucchi, S. E., Bergenstal, R. M., Buse, J. B., Diamant, M., Ferrannini, E., Nauck, M., Peters, A. L., Tsapas, A., Wender, R., Matthews, D. R., Management of Hyperglycemia in Type 2 Diabetes, 2015- A Patient- Centered Approach. *Diabetes Care* **2015,** *38*, 140-149.

23. Shepherd, P. R., Kahn, B. B, Glucose transporters and insulin action - Implications for Insuin Resistance and Diabetes Mellitus. *The New England Journal of Medicine* **1999,** *341* (4), 248-257.

24. Goodyear, L. J., Kahn., B. B., Excercise, Glucose Transport, and Insulin Sensitivity. *Annual Review of Medicine* **1998,** *49*, 235-261.

25. Babu, V. R., Patel, P., Mundargi, R. C., Rangaswamy, V., Aminabhavi, T. M., Developments in polymeric devices for oral insulin delivery. *Expert opinion in Drug Delivery* **2008,** *5* (4), 403-415.

26. Carino, G. P.; Mathiowitz, E., Oral Insulin Delivery. *Advanced Drug Delivery Reviews* **1999,** *35*, 249-257.

27. Damge, C., Reis, C. P., Maincent, P., Nanoparticle strategies for the oral delivery of insulin. *Expert opinion in Drug Delivery* **2008,** *5* (1), 45-68.

28. Peppas, N. A.; Kavimandan, N. J., Nanoscale analysis of protein and peptide absorption: insulin absorption using complexation and pH-sensitive hydrogels as delivery vehicles. *Eur J Pharm Sci* **2006,** *29* (3-4), 183-97.

29. Owens, D. R., Zinman, B., Bolli, G., Alternative routes of insulin delivery. *Diabetic Medicine* **2003,** *20* (11), 886-898.

30. Owens, D. R., New horizons—alternative routes for insulin therapy. *Nature Reviews Drug Discovery* **2002,** *1* (7), 529-540.

31. Fry, A., Dip, G., Insulin Delivery Device Technology 2012- Where Are We after 90 Years? *Journal of Diabetes Science and Technology* **2012,** *6* (4), 947-953.

32. Burdick, P.; Cooper, S.; Horner, B.; Cobry, E.; McFann, K.; Chase, H. P., Use of a subcutaneous injection port to improve glycemic control in children with type 1 diabetes. *Pediatr Diabetes* **2009,** *10* (2), 116-9.

33. Praestmark, K. A.; Jensen, M. L.; Madsen, N. B.; Kildegaard, J.; Stallknecht, B. M., Pen needle design influences ease of insertion, pain, and skin trauma in subjects with type 2 diabetes. *BMJ Open Diabetes Res Care* **2016,** *4* (1), e000266.

34. Hyllested-Winge, J.; Sparre, T.; Pedersen, L. K., NovoPen Echo((R)) insulin delivery device. *Med Devices (Auckl)* **2016,** *9*, 11-8.

35. Polonsky, K. S., Given, B. B., Hirsch, L., Shapiro, E. T., Tillil, H., Beebe, C., Galloway, J. A., Frank, B. H., Karrison, T., Cauter, E.V., Quantitative Study of Insulin Secretion and Clearance in Normal and Obese Subjects. *Journal of Clinical Investigation* **1988,** *81*, 435-441.

36. Penforrnis, A., Personeni, E., Borot, S., Evolution of Deviced in Diabetes Management. *Diabetes Technology and Therapeutics* **2011,** *13*, 93-102.

37. Retnakaran, R., Hochman, J., DeVries, J. H., Hanaire-Broutin, H., Heine, R. J., Melki, V., Zinman, B., Continuous Subcutaneous Insulin Infusion Versus Multiple Daily Injections. *Diabetes Care* **2004,** *27* (11), 2590-2596.

38. Pickup, J., Mattock, M., Kerry, S., Glycaemic control with continuous subcutaneous insulin infusion compared with intensive insulin injections in patients with type 1 diabetes- meta-analysis of randomised controlled trials. *BMJ* **2002,** *324* (7339), 705.

39. Weissberg-Benchell, J., Antisdel-Lomaglio, J., Seshadri, R., Insulin Pump Therapy. *Diabetes Care* **2003,** *26* (4), 1079-1087.

40. Moser, E. G., Morris, A. A., Garg, S. K., Emerging Diabetes Therapies and Technologies. *Diabetes Research and Clinical Practice* **2012,** *97* (1), 16-26.

41. Becquemin, M. H.; Chaumuzeau, J. P., Inhaled insulin: a model for pulmonary systemic absorption? *Rev Mal Respir* **2010,** *27* (8), e54-65.

42. Wigley, F. W., Londono, J. H., Wood, S. H., Shipp, J. C., Waldman, R. H., Insulin across Respiratiry Mucosae by Aerosol Delivery *Diabetes* **1971,** *20* (8), 552-556.

43. Heinemann, L., Alternative Delivery Routes: Inhaled insulin. *Diabetes, Nutrition and Metabolism* **2002,** *15* (6), 417-422.

44. Patton, J. S., Bukar, J. G., Eldon, M. A., Clinical pharmacokinetics and pharmacodynamics of inhaled insulin. *Clinical Pharmacokinetics* **2004,** *43* (12), 781-801.

45. Alabraba, V., Farnsworth, A., Leigh, R., Dodson, P., Gough, S.C., Smyth, T., Exubera inhaled insulin in patients with type 1 and type 2 diabetes: the first 12 months. *Diabetes Technology and Therapeutics* **2009,** *11* (7), 427-430.

46. Skyler, J. S., Cefalu, W. T., Kourides, I. A., Landschulz, W. H., Balagtas, C. C., Cheng, S. L. , Efficacy of inhaled human insulin in type 1 diabetes mellitus: a randomised proof-of-concept study. *Lancet* **2001,** *357*, 331-335.

47. Gelfand, R. A., Schwartz, S. L., Horton, M, Law, C. G., Pun, E. F., Pharmacological reproducibility of inhaled human insulin in patients with type 2 diabetes mellitus. *Diabetologia* **2000,** *43*, 733.

48. Heise, T., Rave, K., Bott, s., Sha, S., Willavize, S. A., Gruber, S. , Time–action profile of an inhaled insulin preparation in comparison to insulin lispro and regular insulin. *Diabetes* **2000,** *39* (Suppl.), A10.

49. Klonoff, D. C., Afrezza Inhaled Insulin: The Fastest-Acting FDA-Approved Insulin on the Market Has Favorable Properties. *Journal of Diabetes Science and Technology* **2014,** *8* (6), 1071-1073.

50. Richardson, P. C., Boss, A. H. , Technosphere Insulin Technology *Diabetes Technology and Therapeutics* **2007,** *9* (Suppl.), S65-72.

51. Pfutzner, A., Mann, A., Steiner, S., Technosphere™insulin—a new approach for effective delivery of human insulin via the pulmonary route. *Diabetes Technology and Therapeutics* **2002,** *4*, 589-593.

52. Rave, K. M., Heise, T., Pfutzner, A., Steiner, S., Heinemann, L., Results of a dose–response study with a new pulmonary insulin formulation and inhaler. *Diabetes* **2000,** *49* (Suppl.), A7.

53. Henry, R. R., Mudaliar, S. R. D., Howland, W., Chu, N., Kim, D., An, B., Reinhardt., R. R, Inhaled Insulin Using the AERx Insulin Diabetes Management System in Healthy and Asthmatic Subjects. *Diabetes Care* **2003,** *26* (3), 764-769.

54. Kim, D.; Mudaliar, S.; Chinnapongse, S.; Chu, N.; Boies, S. M.; Davis, T.; Perera, A. D.; Fishman, R. S.; Shapiro, D. A.; Henry, R., Dose-Response Relationships of Inhaled Insulin Delivered via the Aerodose Insulin Inhaler and Subcutaneously Injected Insulin in Patients With Type 2 Diabetes. *Diabetes Care* **2003,** *26* (10), 2842-2847.

55. Heise, T.; Brugger, A.; Cook, C.; Eckers, U.; Hutchcraft, A.; Nosek, L.; Rave, K.; Troeger, J.; Valaitis, P.; White, S., PROMAXX® inhaled insulin: safe and efficacious administration with a commercially available dry powder inhaler. *Diabetes, Obesity and Metabolism* **2009,** *11* (5), 455-459.

56. Caldwell, L.; Nishihata, T.; Rytting, J. H.; Higuchi, T., Lymphatic uptake of water-soluble drugs after rectal administration. *Journal of Pharmacy and Pharmacology* **1982,** *34* (8), 520-522.

57. Matsuda, H.; Arima, H., Cyclodextrins in transdermal and rectal delivery. *Advanced Drug Delivery Reviews* **1999,** *36* (1), 81-99.

58. Yun, M.-O.; Choi, H.-G.; Jung, J.-H.; Kim, C.-K., Development of a thermo-reversible insulin liquid suppository with bioavailability enhancement. *International Journal of Pharmaceutics* **1999,** *189* (2), 137-145.

59. Aungst, B. J.; Rogers, N. J.; Shefter, E., Comparison of nasal, rectal, buccal, sublingual and intramuscular insulin efficacy and the effects of a bile salt absorption promoter. *Journal of Pharmacology and Experimental Therapeutics* **1988,** *244* (1), 23-27.

60. Khafagy, E.-S.; Morishita, M.; Onuki, Y.; Takayama, K., Current challenges in non-invasive insulin delivery systems: a comparative review. *Advanced drug delivery reviews* **2007,** *59* (15), 1521-1546.

61. Hinchcliffe, M.; Illum, L., Intranasal insulin delivery and therapy. *Advanced drug delivery reviews* **1999,** *35* (2), 199-234.

62. Pontiroli, A. E.; Alberetto, M.; Secchi, A.; Dossi, G.; Bosi, I.; Pozza, G., Insulin given intranasally induces hypoglycaemia in normal and diabetic subjects. *Br Med J (Clin Res Ed)* **1982,** *284* (6312), 303-306.

63. Kost, J., Ultrasound-assisted insulin delivery and noninvasive glucose sensing. *Diabetes technology & therapeutics* **2002,** *4* (4), 489-497.

64. Hirai, S.; Ikenaga, T.; Matsuzawa, T., Nasal absorption of insulin in dogs. *Diabetes* **1978,** *27* (3), 296-299.

65. Gizurarson, S.; Bechgaard, E., Intranasal administration of insulin to humans. *Diabetes research and clinical practice* **1991,** *12* (2), 71-84.

66. Lalej - Bennis, D.; Boillot, J.; Bardin, C.; Zirinis, P.; Coste, A.; Escudier, E.; Chast, F.; Peynegre, R.; Selam, J. L.; Slama, G., Efficacy and tolerance of intranasal insulin administered during 4 months in severely hyperglycaemic Type 2 diabetic patients with oral drug failure: a cross - over study. *Diabetic medicine* **2001,** *18* (8), 614-618.

67. Lalej - Bennis, D., Boillot, J., Bardin, C., Zirinis, P., Coste, A., Escudier, E., Chast, F., Peynegre, R., Slama, G., Selam, J. L., Six month administration of gelified intranasal insulin in 16 type 1 diabetic patients under multiple injections: efficacy vs subcutaneous injections and local tolerance. *Diabetes and Metabolism* **2001,** *27* (372-377).

68. Leary, A. C.; Stote, R. M.; Cussen, K.; O'brien, J.; Leary, W. P.; Buckley, B., Pharmacokinetics and pharmacodynamics of intranasal insulin administered to patients with type 1 diabetes: a preliminary study. *Diabetes technology & therapeutics* **2006,** *8* (1), 81-88.

69. Illum, L., Nasal drug delivery—recent developments and future prospects. *Journal of Controlled release* **2012,** *161* (2), 254-263.

70. Stote, R.; Marbury, T.; Shi, L.; Miller, M.; Strange, P., Comparison Pharmacokinetics of Two Concentrations (0.7% and 1.0%) of Nasulin™, an Ultra-Rapid-Acting Intranasal Insulin Formulation. *Journal of diabetes science and technology* **2010,** *4* (3), 603-609.

71. Frauman, A. G.; Cooper, M. E.; Parsons, B. J.; Jerums, G.; Louis, W. J., Long-term use of intranasal insulin in insulin-dependent diabetic patients. *Diabetes Care* **1987,** *10* (5), 573-578.

72. Salzman, R.; Manson, J. E.; Griffing, G. T.; Kimmerle, R.; Ruderman, N.; McCall, A.; Stoltz, E. I.; Mullin, C.; Small, D.; Armstrong, J., Intranasal aerosolized insulin: mixed-meal studies and long-term use in type I diabetes. *New England Journal of Medicine* **1985,** *312* (17), 1078-1084.

73. Hilsted, J.; Madsbad, S.; Hvidberg, A.; Rasmussen, M.; Krarup, T.; Ipsen, H.; Hansen, B.; Pedersen, M.; Djurup, R.; Oxenbøll, B., Intranasal insulin therapy: the clinical realities. *Diabetologia* **1995,** *38* (6), 680-684.

74. Nagai, T.; Machida, Y., Advances in drug delivery-mucosal adhesive dosage forms. *Pharmacy International* **1985,** *6* (8), 196-200.

75. Aungst, B. J.; Rogers, N. J., Site dependence of absorption-promoting actions of laureth-9, Na salicylate, Na2EDTA, and aprotinin on rectal, nasal, and buccal insulin delivery. *Pharmaceutical research* **1988,** *5* (5), 305-308.

76. Hoogstraate, J. A.; Wertz, P. W., Drug delivery via the buccal mucosa. *Pharmaceutical Science & Technology Today* **1998,** *1* (7), 309-316.

77. Veuillez, F.; Kalia, Y. N.; Jacques, Y.; Deshusses, J.; Buri, P., Factors and strategies for improving buccal absorption of peptides. *European journal of Pharmaceutics and Biopharmaceutics* **2001,** *51* (2), 93-109.

78. Al-Waili, N., Sublingual human insulin for hyperglycaemia in type I diabetes. *JPMA. The Journal of the Pakistan Medical Association* **1999,** *49* (7), 167-169.

79. Heinemann, L.; Jacques, Y., Oral insulin and buccal insulin: a critical reappraisal. *Journal of diabetes science and technology* **2009,** *3* (3), 568-584.

80. Kumria, R.; Goomber, G., Emerging trends in insulin delivery: Buccal route. *J Diabetol* **2011,** *2* (1), 1-9.

81. Prausnitz, M. R.; Langer, R., Transdermal drug delivery. *Nature biotechnology* **2008,** *26* (11), 1261-1268.

82. Cullander, C.; Guy, R. H., (D) Routes of delivery: Case studies:(6) Transdermal delivery of peptides and proteins. *Advanced drug delivery reviews* **1992,** *8* (2), 291-329.

83. Foldvari, M., Non-invasive administration of drugs through the skin: challenges in delivery system design. *Pharmaceutical science & technology today* **2000,** *3* (12), 417-425.

84. Kanikkannan, N., Iontophoresis-based transdermal delivery systems. *BioDrugs* **2002,** *16* (5), 339-347.

85. Andrews, S.; Lee, J. W.; Choi, S.-O.; Prausnitz, M. R., Transdermal insulin delivery using microdermabrasion. *Pharmaceutical research* **2011,** *28* (9), 2110-2118.

86. Malakar, J.; Sen, S. O.; Nayak, A. K.; Sen, K. K., Formulation, optimization and evaluation of transferosomal gel for transdermal insulin delivery. *Saudi pharmaceutical journal* **2012,** *20* (4), 355-363.

87. Freckmann, G.; Pleus, S.; Haug, C.; Bitton, G.; Nagar, R., Increasing local blood flow by warming the application site: beneficial effects on postprandial glycemic excursions. *Journal of diabetes science and technology* **2012,** *6* (4), 780-785.

88. Freckmann, G.; Pleus, S.; Westhoff, A.; Krinelke, L. G.; Buhr, A.; Jendrike, N.; Haug, C., Clinical performance of a device that applies local heat to the insulin infusion site: a crossover study. *Journal of diabetes science and technology* **2012,** *6* (2), 320-327.

89. King, M. J.; Badea, I.; Solomon, J.; Kumar, P.; Gaspar, K. J.; Foldvari, M., Transdermal delivery of insulin from a novel biphasic lipid system in diabetic rats. *Diabetes technology & therapeutics* **2002,** *4* (4), 479-488.

90. Iyer, H.; Khedkar, A.; Verma, M., Oral insulin–a review of current status. *Diabetes, obesity and metabolism* **2010,** *12* (3), 179-185.

91. Modi, P., Diabetes beyond insulin: review of new drugs for treatment of diabetes mellitus. *Current drug discovery technologies* **2007,** *4* (1), 39-47.

92. Chen, M.-C.; Sonaje, K.; Chen, K.-J.; Sung, H.-W., A review of the prospects for polymeric nanoparticle platforms in oral insulin delivery. *Biomaterials* **2011,** *32* (36), 9826-9838.

93. Morishita, M.; Peppas, N. A., Is the oral route possible for peptide and protein drug delivery? *Drug discovery today* **2006,** *11* (19), 905-910.

94. Zijlstra, E.; Heinemann, L.; Plum-Mörschel, L., Oral insulin reloaded a structured approach. *Journal of diabetes science and technology* **2014,** *8* (3), 458-465.

95. Mahadevan, V., Anatomy of the oesophagus. *Surgery (Oxford)* **2014,** *32* (11), 565-570.

96. Ellis, H., Anatomy of the stomach. *Surgery (Oxford)* **2011,** *29* (11), 541-543.

97. Buunen, M.; Rooijens, P.; Smaal, H.; Kleinrensink, G. J.; Van Der Harst, E.; Tilanus, H.; Lange, J., Vascular anatomy of the stomach related to gastric tube construction. *Diseases of the Esophagus* **2008,** *21* (3), 272-274.

98. Walker, R.; Owen, R., Intestinal barriers to bacteria and their toxins. *Annual review of medicine* **1990,** *41* (1), 393-400.

99. Watson, A. J.; Duckworth, C. A.; Guan, Y.; Montrose, M. H., Mechanisms of epithelial cell shedding in the Mammalian intestine and maintenance of barrier function. *Annals of the New York Academy of Sciences* **2009,** *1165* (1), 135-142.

100. Wright, E.; Loo, D.; Hirayama, B.; Turk, E., Sugar absorption. *Physiology of gastrointestinal tract, 4th edn. Academic, Baltimore* **2006**, 1653-1665.

101. Hellmich, M. R.; Evers, B. M., Regulation of gastrointestinal normal cell growth. *Physiology of the Gastrointestinal Tract* **2006**, 435-458.

102. Balcerzak, S. P.; Lane, W. C.; Bullard, J. W., Surface structure of intestinal epithelium. *Gastroenterology* **1970,** *58* (1), 49-55.

103. Cheng, H.; Leblond, C., Origin, differentiation and renewal of the four main epithelial cell types in the mouse small intestine I. Columnar cell. *American Journal of Anatomy* **1974,** *141* (4), 461-479.

104. Cornes, J., Number, size, and distribution of Peyer's patches in the human small intestine: Part I The development of Peyer's patches. *Gut* **1965,** *6* (3), 225.

105. Kiyono, H.; Fukuyama, S., NALT-versus Peyer's-patch-mediated mucosal immunity. *Nature Reviews Immunology* **2004,** *4* (9), 699-710.

106. Ma, T.; Anderson, J., Tight junctions and the intestinal barrier. *Physiology of the gastrointestinal tract* **2006,** *2*, 1559-1594.

107. Salama, N. N.; Eddington, N. D.; Fasano, A., Tight junction modulation and its relationship to drug delivery. *Advanced drug delivery reviews* **2006,** *58* (1), 15-28.

108. Ward, P. D.; Tippin, T. K.; Thakker, D. R., Enhancing paracellular permeability by modulating epithelial tight junctions. *Pharmaceutical science & technology today* **2000,** *3* (10), 346-358.

109. Newman, D. K., anatomy of the large intestine.

110. Sood, A.; Panchagnula, R., Peroral route: an opportunity for protein and peptide drug delivery. *Chemical Reviews* **2001,** *101* (11), 3275-3304.

111. Evans, D.; Pye, G.; Bramley, R.; Clark, A.; Dyson, T.; Hardcastle, J., Measurement of gastrointestinal pH profiles in normal ambulant human subjects. *Gut* **1988,** *29* (8), 1035-1041.

112. Ganapathy, V.; Gupta, N.; Martindale, R. In *Protein digestion and absorption*, Elsevier Inc., **2006**.

113. Bernkop-Schnürch, A., The use of inhibitory agents to overcome the enzymatic barrier to perorally administered therapeutic peptides and proteins. *Journal of controlled release* **1998,** *52* (1), 1-16.

114. Schilling, R. J.; Mitra, A. K., Degradation of insulin by trypsin and alpha-chymotrypsin. *Pharmaceutical research* **1991,** *8* (6), 721-727.

115. Brogden, R. N.; Heel, R., Human insulin. *Drugs* **1987,** *34* (3), 350-371.

116. Binder, C.; Lauritzen, T.; Faber, O.; Pramming, S., Insulin pharmacokinetics. *Diabetes Care* **1984,** *7* (2), 188-199.

117. Cone, R. A., Barrier properties of mucus. *Advanced drug delivery reviews* **2009,** *61* (2), 75-85.

118. Atuma, C.; Strugala, V.; Allen, A.; Holm, L., The adherent gastrointestinal mucus gel layer: thickness and physical state in vivo. *American Journal of Physiology-Gastrointestinal and Liver Physiology* **2001,** *280* (5), G922-G929.

119. Johansson, M. E.; Phillipson, M.; Petersson, J.; Velcich, A.; Holm, L.; Hansson, G. C., The inner of the two Muc2 mucin-dependent mucus layers in colon is devoid of bacteria. *Proceedings of the national academy of sciences* **2008,** *105* (39), 15064-15069.

120. Pelkonen, O.; Boobis, A. R.; Gundert-Remy, U., In vitro prediction of gastrointestinal absorption and bioavailability: an experts' meeting report. *European journal of clinical pharmacology* **2001,** *57* (9), 621-629.

121. Andrews, C. W.; Bennett, L.; Yu, L. X., Predicting human oral bioavailability of a compound: development of a novel quantitative structure-bioavailability relationship. *Pharmaceutical research* **2000,** *17* (6), 639-644.

122. Goldberg, M.; Gomez-Orellana, I., Challenges for the oral delivery of macromolecules. *Nature Reviews Drug Discovery* **2003,** *2* (4), 289-295.

123. Mahato, R. I.; Narang, A. S.; Thoma, L.; Miller, D. D., Emerging trends in oral delivery of peptide and protein drugs. *Critical Reviews™ in Therapeutic Drug Carrier Systems* **2003,** *20* (2&3).

124. Lane, M. E.; O'Driscoll, C. M.; Corrigan, O. I., Quantitative estimation of the effects of bile salt surfactant systems on insulin stability and permeability in the rat intestine using a mass balance model. *Journal of pharmacy and pharmacology* **2005,** *57* (2), 169-175.

125. Mesiha, M.; Plakogiannis, F.; Vejosoth, S., Enhanced oral absorption of insulin from desolvated fatty acid-sodium glycocholate emulsions. *International journal of pharmaceutics* **1994,** *111* (3), 213-216.

126. Hosny, E. A.; Al-Shora, H. I.; Elmazar, M. M., Oral delivery of insulin from enteric-coated capsules containing sodium salicylate: effect on relative hypoglycemia of diabetic beagle dogs. *International journal of pharmaceutics* **2002,** *237* (1), 71-76.

127. Fasano, A.; Uzzau, S., Modulation of intestinal tight junctions by Zonula occludens toxin permits enteral administration of insulin and other macromolecules in an animal model. *Journal of Clinical Investigation* **1997,** *99* (6), 1158.

128. Luzio, S. D.; Dunseath, G.; Lockett, A.; Broke - Smith, T.; New, R.; Owens, D. R., The glucose lowering effect of an oral insulin (Capsulin) during an isoglycaemic clamp study in persons with type 2 diabetes. *Diabetes, Obesity and Metabolism* **2010,** *12* (1), 82-87.

129. Phillips, J.; Jones, D. R.; Wright, J.; Brackenridge, A.; New, R.; Bansal, G., Early evaluation of a novel oral insulin delivery system in healthy volunteers. *Diabetes* **2004,** *53*, A113.

130. Kidron, M.; Arbit, E.; Shushlav, Y., Comparative assessment of the glucose-lowering effect of multiple oral insulin (ORMD-0801) formulation variants in pigs. *74th Scientific Sessions of the American Diabetes Association* **2014**, 13-17.

131. Eldor, R.; Arbit, E.; Corcos, A.; Kidron, M., Glucose-reducing effect of the ORMD-0801 oral insulin preparation in patients with uncontrolled type 1 diabetes: a pilot study. *PloS one* **2013,** *8* (4), e59524.

132. Eldor, R.; Kidron, M.; Miteva, Y.; Arbit, E. In *Decreased CRP levels in response to a six-week, once-daily oral insulin regimen*, 81st EAS Congress, Lyon, France, **2013**.

133. Marschütz, M. K.; Bernkop-Schnürch, A., Oral peptide drug delivery: polymer–inhibitor conjugates protecting insulin from enzymatic degradation in vitro. *Biomaterials* **2000,** *21* (14), 1499-1507.

134. Yamamoto, A.; Taniguchi, T.; Rikyuu, K.; Tsuji, T.; Fujita, T.; Murakami, M.; Muranishi, S., Effects of various protease inhibitors on the intestinal absorption and degradation of insulin in rats. *Pharmaceutical research* **1994,** *11* (10), 1496-1500.

135. AGARWAL, V.; REDDY, I. K.; KHAN, M. A., Oral delivery of proteins: Effect of chicken and duck ovomucoid on the stability of insulin in the presence of α - chymotrypsin and trypsin. *Pharmacy and Pharmacology Communications* **2000,** *6* (5), 223-227.

136. Agarwal, V.; Reddy, I. K.; Khan, M. A., Polymethyacrylate based microparticulates of insulin for oral delivery: Preparation and in vitro dissolution

stability in the presence of enzyme inhibitors. *International journal of pharmaceutics* **2001,** *225* (1), 31-39.

137. Agarwal, V.; Nazzal, S.; Reddy, I. K.; Khan, M. A., Transport studies of insulin across rat jejunum in the presence of chicken and duck ovomucoids. *Journal of Pharmacy and Pharmacology* **2001,** *53* (8), 1131-1138.

138. Marschütz, M. K.; Caliceti, P.; Bernkop-Schnürch, A., Design and in vivo evaluation of an oral delivery system for insulin. *Pharmaceutical research* **2000,** *17* (12), 1468-1474.

139. Morishita, M.; Aoki, Y.; Sakagami, M.; Nagai, T.; Takayama, K., In situ ileal absorption of insulin in rats: effects of hyaluronidase pretreatment diminishing the mucous/glycocalyx layers. *Pharmaceutical research* **2004,** *21* (2), 309-316.

140. Liu, H.; Tang, R.; Pan, W. S.; Zhang, Y.; Liu, H., Potential utility of various protease inhibitors for improving the intestinal absorption of insulin in rats. *Journal of pharmacy and pharmacology* **2003,** *55* (11), 1523-1529.

141. Takeuchi, H.; Yamamoto, H.; Kawashima, Y., Mucoadhesive nanoparticulate systems for peptide drug delivery. *Advanced drug delivery reviews* **2001,** *47* (1), 39-54.

142. Chowdary, K. P. R.; Rao, Y. S., Mucoadhesive microspheres for controlled drug delivery. *Biological and pharmaceutical Bulletin* **2004,** *27* (11), 1717-1724.

143. Hejazi, R.; Amiji, M., Chitosan-based gastrointestinal delivery systems. *Journal of controlled release* **2003,** *89* (2), 151-165.

144. Peppas, N., Devices based on intelligent biopolymers for oral protein delivery. *International Journal of Pharmaceutics* **2004,** *277* (1), 11-17.

145. Dorkoosh, F.; Stokkel, M.; Blok, D.; Borchard, G.; Rafiee-Tehrani, M.; Verhoef, J.; Junginger, H., Feasibility study on the retention of superporous hydrogel composite polymer in the intestinal tract of man using scintigraphy. *Journal of controlled release* **2004,** *99* (2), 199-206.

146. Lamprecht, A.; Saumet, J.-L.; Roux, J.; Benoit, J.-P., Lipid nanocarriers as drug delivery system for ibuprofen in pain treatment. *International journal of pharmaceutics* **2004,** *278* (2), 407-414.

147. Bernkop-Schnürch, A.; Kast, C. E.; Richter, M. F., Improvement in the mucoadhesive properties of alginate by the covalent attachment of cysteine. *Journal of Controlled Release* **2001,** *71* (3), 277-285.

148. Takeuchi, H.; Yamamoto, H.; Niwa, T.; Hino, T.; Kawashima, Y., Enteral absorption of insulin in rats from mucoadhesive chitosan-coated liposomes. *Pharmaceutical research* **1996,** *13* (6), 896-901.

149. Lowman, A.; Morishita, M.; Kajita, M.; Nagai, T.; Peppas, N., Oral delivery of insulin using pH - responsive complexation gels. *Journal of pharmaceutical sciences* **1999,** *88* (9), 933-937.

150. Foss, A. C.; Goto, T.; Morishita, M.; Peppas, N. A., Development of acrylic-based copolymers for oral insulin delivery. *European journal of pharmaceutics and biopharmaceutics* **2004,** *57* (2), 163-169.

151. Morishita, M.; Goto, T.; Peppas, N. A.; Joseph, J. I.; Torjman, M. C.; Munsick, C.; Nakamura, K.; Yamagata, T.; Takayama, K.; Lowman, A. M., Mucosal insulin delivery systems based on complexation polymer hydrogels: effect of particle size on insulin enteral absorption. *Journal of Controlled Release* **2004,** *97* (1), 115-124.

152. Morishita, M.; Goto, T.; Nakamura, K.; Lowman, A. M.; Takayama, K.; Peppas, N. A., Novel oral insulin delivery systems based on complexation polymer hydrogels: single and multiple administration studies in type 1 and 2 diabetic rats. *Journal of Controlled Release* **2006,** *110* (3), 587-594.

153. Yamagata, T.; Morishita, M.; Kavimandan, N. J.; Nakamura, K.; Fukuoka, Y.; Takayama, K.; Peppas, N. A., Characterization of insulin protection properties of complexation hydrogels in gastric and intestinal enzyme fluids. *Journal of controlled release* **2006,** *112* (3), 343-349.

154. Ponchel, G.; Montisci, M.-J.; Dembri, A.; Durrer, C.; Duchêne, D., Mucoadhesion of colloidal particulate systems in the gastro-intestinal tract. *European journal of pharmaceutics and biopharmaceutics* **1997,** *44* (1), 25-31.

155. Desai, M. P.; Labhasetwar, V.; Walter, E.; Levy, R. J.; Amidon, G. L., The mechanism of uptake of biodegradable microparticles in Caco-2 cells is size dependent. *Pharmaceutical research* **1997,** *14* (11), 1568-1573.

156. van der Lubben, I. M.; Verhoef, J. C.; Borchard, G.; Junginger, H. E., Chitosan and its derivatives in mucosal drug and vaccine delivery. *European Journal of Pharmaceutical Sciences* **2001,** *14* (3), 201-207.

157. Brayden, D. J.; Jepson, M. A.; Baird, A. W., Keynote review: intestinal Peyer's patch M cells and oral vaccine targeting. *Drug discovery today* **2005,** *10* (17), 1145-1157.

158. Tiyaboonchai, W.; Woiszwillo, J.; Sims, R. C.; Middaugh, C. R., Insulin containing polyethylenimine–dextran sulfate nanoparticles. *International Journal of Pharmaceutics* **2003,** *255* (1), 139-151.

159. Chalasani, K. B.; Russell-Jones, G. J.; Jain, A. K.; Diwan, P. V.; Jain, S. K., Effective oral delivery of insulin in animal models using vitamin B12-coated dextran nanoparticles. *Journal of Controlled Release* **2007,** *122* (2), 141-150.

160. Ma, Z.; Lim, T. M.; Lim, L.-Y., Pharmacological activity of peroral chitosan–insulin nanoparticles in diabetic rats. *International journal of pharmaceutics* **2005,** *293* (1), 271-280.

161. Avadi, M. R.; Sadeghi, A. M. M.; Mohammadpour, N.; Abedin, S.; Atyabi, F.; Dinarvand, R.; Rafiee-Tehrani, M., Preparation and characterization of insulin nanoparticles using chitosan and Arabic gum with ionic gelation method. *Nanomedicine: Nanotechnology, Biology and Medicine* **2010,** *6* (1), 58-63.

162. Ma, Z.; Yeoh, H. H.; Lim, L. Y., Formulation pH modulates the interaction of insulin with chitosan nanoparticles. *Journal of pharmaceutical sciences* **2002,** *91* (6), 1396-1404.

163. Xiong, X. Y.; Li, Y. P.; Li, Z. L.; Zhou, C. L.; Tam, K. C.; Liu, Z. Y.; Xie, G. X., Vesicles from Pluronic/poly (lactic acid) block copolymers as new carriers for oral insulin delivery. *Journal of controlled release* **2007,** *120* (1), 11-17.

164. Han, Y.; Tian, H.; He, P.; Chen, X.; Jing, X., Insulin nanoparticle preparation and encapsulation into poly (lactic-co-glycolic acid) microspheres by using an anhydrous system. *International journal of pharmaceutics* **2009,** *378* (1), 159-166.

165. Li, J. K.; Wang, N.; Wu, X. S., A novel biodegradable system based on gelatin nanoparticles and poly (lactic - co - glycolic acid) microspheres for protein and peptide drug delivery. *Journal of pharmaceutical sciences* **1997,** *86* (8), 891-895.

166. Katayama, K.; Kato, Y.; Onishi, H.; Nagai, T.; Machida, Y., Double liposomes: hypoglycemic effects of liposomal insulin on normal rats. *Drug development and industrial pharmacy* **2003,** *29* (7), 725-731.

167. Degim, Z.; Ünal, N.; Eşsiz, D.; Abbasoglu, U., The effect of various liposome formulations on insulin penetration across Caco-2 cell monolayer. *Life sciences* **2004,** *75* (23), 2819-2827.

168. Reis, C. P.; Neufeld, R. J.; Ribeiro, A. J.; Veiga, F., Nanoencapsulation I. Methods for preparation of drug-loaded polymeric nanoparticles. *Nanomedicine: Nanotechnology, Biology and Medicine* **2006,** *2* (1), 8-21.

169. Ye, S.; Wang, C.; Liu, X.; Tong, Z.; Ren, B.; Zeng, F., New loading process and release properties of insulin from polysaccharide microcapsules fabricated through layer-by-layer assembly. *Journal of controlled release* **2006,** *112* (1), 79-87.

170. Watnasirichaikul, S.; Davies, N. M.; Rades, T.; Tucker, I. G., Preparation of biodegradable insulin nanocapsules from biocompatible microemulsions. *Pharmaceutical research* **2000,** *17* (6), 684-689.

171. Mukhopadhyay, P.; Mishra, R.; Rana, D.; Kundu, P. P., Strategies for effective oral insulin delivery with modified chitosan nanoparticles: A review. *Progress in polymer science* **2012,** *37* (11), 1457-1475.

172. Agnihotri, S. A.; Mallikarjuna, N. N.; Aminabhavi, T. M., Recent advances on chitosan-based micro-and nanoparticles in drug delivery. *Journal of controlled release* **2004,** *100* (1), 5-28.

173. Jain, D.; Panda, A. K.; Majumdar, D. K., Eudragit S100 entrapped insulin microspheres for oral delivery. *Aaps Pharmscitech* **2005,** *6* (1), E100-E107.

174. Milstein, S. J.; Leipold, H.; Sarubbi, D.; Leone-Bay, A.; Mlynek, G. M.; Robinson, J. R.; Kasimova, M.; Freire, E., Partially unfolded proteins efficiently penetrate cell membranes—implications for oral drug delivery. *Journal of controlled release* **1998,** *53* (1), 259-267.

175. Li, J.; Wang, Y.; Han, L.; Sun, X.; Yu, H.; Yu, Y., Time–Action Profile of an Oral Enteric Insulin Formulation in Healthy Chinese Volunteers. *Clinical therapeutics* **2012,** *34* (12), 2333-2338.

176. Fan, J.; Kureshy, N.; Vitols, K. S.; Huennekens, F. M., Novel substrate analogs delineate an endocytotic mechanism for uptake of folate via the high-affinity, glycosylphosphatidylinositol-linked transport protein in L1210 mouse leukemia cells. *Oncology Research Featuring Preclinical and Clinical Cancer Therapeutics* **1995,** *7* (10-11), 511-516.

177. Mislick, K. A.; Baldeschwieler, J. D.; Kayyem, J. F.; Meade, T. J., Transfection of folate-polylysine DNA complexes: evidence for lysosomal delivery. *Bioconjugate chemistry* **1995,** *6* (5), 512-515.

178. Anderson, R. G.; Kamen, B. A.; Rothberg, K. G.; Lacey, S. W., Potocytosis: sequestration and transport of small molecules by caveolae. *Science* **1992,** *255* (5043), 410-412.

179. Swaan, P. W., Recent advances in intestinal macromolecular drug delivery via receptor-mediated transport pathways. *Pharmaceutical research* **1998,** *15* (6), 826-834.

180. Russell-Jones, G.; Westwood, S.; Farnworth, P.; Findlay, J.; Burger, H., Synthesis of LHRH antagonists suitable for oral administration via the vitamin B12 uptake system. *Bioconjugate chemistry* **1995,** *6* (1), 34-42.

181. Russell-Jones, G.; Westwood, S.; Habberfield, A., Vitamin B12 mediated oral delivery systems for granulocyte-colony stimulating factor and erythropoietin. *Bioconjugate chemistry* **1995,** *6* (4), 459-465.

182. Delaunay, J.; Iolascon, A., The congenital dyserythropoietic anaemias. *Best Practice & Research Clinical Haematology* **1999,** *12* (4), 691-705.

183. Ramasamy, M.; Alpers, D. H.; Tiruppathi, C.; Seetharam, B., Cobalamin release from intrinsic factor and transfer to transcobalamin II within the rat enterocyte. *American Journal of Physiology-Gastrointestinal and Liver Physiology* **1989,** *257* (5), G791-G797.

184. Beyer, U.; Roth, T.; Schumacher, P.; Maier, G.; Unold, A.; Frahm, A. W.; Fiebig, H. H.; Unger, C.; Kratz, F., Synthesis and in vitro efficacy of transferrin conjugates of the anticancer drug chlorambucil. *Journal of medicinal chemistry* **1998,** *41* (15), 2701-2708.

185. Singh, M., Transferrin as a targeting ligand for liposomes and anticancer drugs. *Current pharmaceutical design* **1999,** *5* (6), 443-452.

186. Broadwell, R. D.; Baker-Cairns, B. J.; Friden, P. M.; Oliver, C.; Villegas, J. C., Transcytosis of protein through the mammalian cerebral epithelium and endothelium: III. Receptor-mediated transcytosis through the blood–brain barrier of blood-borne transferrin and antibody against the transferrin receptor. *Experimental neurology* **1996,** *142* (1), 47-65.

187. Qian, Z. M.; Li, H.; Sun, H.; Ho, K., Targeted drug delivery via the transferrin receptor-mediated endocytosis pathway. *Pharmacological reviews* **2002,** *54* (4), 561-587.

188. Xia, C. Q.; Wang, J.; Shen, W.-C., Hypoglycemic effect of insulin-transferrin conjugate in streptozotocin-induced diabetic rats. *Journal of Pharmacology and Experimental Therapeutics* **2000,** *295* (2), 594-600.

189. Jones, A. T.; Gumbleton, M.; Duncan, R., Understanding endocytic pathways and intracellular trafficking: a prerequisite for effective design of advanced drug delivery systems. *Advanced drug delivery reviews* **2003,** *55* (11), 1353-1357.

190. Banerjee, D.; Flanagan, P. R.; Cluett, J.; Valberg, L. S., Transferrin receptors in the human gastrointestinal tract: relationship to body iron stores. *Gastroenterology* **1986,** *91* (4), 861-869.

191. Azari, P. R.; Feeney, R. E., Resistance of metal complexes of conalbumin and transferrin to proteolysis and to thermal denaturation. *Journal of Biological Chemistry* **1957**, 293-302.

192. Shah, D.; Shen, W. c., Transcellular delivery of an insulin - transferrin conjugate in enterocyte - like Caco - 2 cells. *Journal of pharmaceutical sciences* **1996,** *85* (12), 1306-1311.

193. Pridgen, E. M.; Alexis, F.; Farokhzad, O. C., Polymeric nanoparticle drug delivery technologies for oral delivery applications. *Expert Opin Drug Deliv* **2015,** *12* (9), 1459-73.

194. Dickinson, B. L.; Badizadegan, K.; Wu, Z.; Ahouse, J. C.; Zhu, X.; Simister, N. E.; Blumberg, R. S.; Lencer, W. I., Bidirectional FcRn-dependent IgG transport in a polarized human intestinal epithelial cell line. *The Journal of clinical investigation* **1999,** *104* (7), 903-911.

195. Chaudhury, C.; Mehnaz, S.; Robinson, J. M.; Hayton, W. L.; Pearl, D. K.; Roopenian, D. C.; Anderson, C. L., The major histocompatibility complex–related Fc receptor for IgG (FcRn) binds albumin and prolongs its lifespan. *Journal of Experimental Medicine* **2003,** *197* (3), 315-322.

196. Shah, U.; Dickinson, B. L.; Blumberg, R. S.; Simister, N. E.; Lencer, W. I.; Walker, A. W., Distribution of the IgG Fc receptor, FcRn, in the human fetal intestine. *Pediatric research* **2003,** *53* (2), 295-301.

197. Ward, E. S.; Zhou, J.; Ghetie, V.; Ober, R. J., Evidence to support the cellular mechanism involved in serum IgG homeostasis in humans. *International immunology* **2003,** *15* (2), 187-195.

198. Mayer, B.; Kis, Z.; Frenyó, L. V.; Hammarström, L.; Kacskovics, I., The neonatal Fc receptor (FcRn) is expressed in the bovine lung. *Veterinary immunology and immunopathology* **2004,** *98* (1), 85-89.

199. Spiekermann, G. M.; Finn, P. W.; Ward, E. S.; Dumont, J.; Dickinson, B. L.; Blumberg, R. S.; Lencer, W. I., Receptor-mediated Immunoglobulin G Transport Across Mucosal Barriers in Adult Life: Functional Expression of FcRn in the Mammalian Lung.

200. Schlachetzki, F.; Zhu, C.; Pardridge, W. M., Expression of the neonatal Fc receptor (FcRn) at the blood–brain barrier. *Journal of neurochemistry* **2002,** *81* (1), 203-206.

201. Kacskovics, I.; Kis, Z.; Mayer, B.; West, A. P.; Tiangco, N. E.; Tilahun, M.; Cervenak, L.; Bjorkman, P. J.; Goldsby, R. A.; Szenci, O., FcRn mediates elongated serum half-life of human IgG in cattle. *International immunology* **2006,** *18* (4), 525-536.

202. Haymann, J.-P.; Levraud, J.-P.; Bouet, S.; Kappes, V.; Hagege, J.; Nguyen, G.; Xu, Y.; Rondeau, E.; Sraer, J.-D., Characterization and localization of the neonatal Fc receptor in adult human kidney. *Journal of the American Society of Nephrology* **2000,** *11* (4), 632-639.

203. Ghetie, V.; Hubbard, J. G.; Kim, J. K.; Tsen, M. F.; Lee, Y.; Ward, E. S., Abnormally short serum half - lives of IgG in β2 - microglobulin - deficient mice. *European journal of immunology* **1996,** *26* (3), 690-696.

204. Yoshida, M.; Masuda, A.; Kuo, T. T.; Kobayashi, K.; Claypool, S. M.; Takagawa, T.; Kutsumi, H.; Azuma, T.; Lencer, W. I.; Blumberg, R. S. In *IgG transport across mucosal barriers by neonatal Fc receptor for IgG and mucosal immunity*, Springer seminars in immunopathology, Springer: **2006**; pp 397-403.

205. Roopenian, D. C.; Akilesh, S., FcRn: the neonatal Fc receptor comes of age. *Nature reviews immunology* **2007,** *7* (9), 715-725.

206. Raghavan, M.; Gastinel, L. N.; Bjorkman, P. J., The class I major histocompatibility complex related Fc receptor shows pH-dependent stability differences correlating with immunoglobulin binding and release. *Biochemistry* **1993,** *32* (33), 8654-8660.

207. Huber, A. H.; Kelley, R. F.; Gastinel, L. N.; Bjorkman, P. J., Crystallization and stoichiometry of binding of a complex between a rat intestinal Fc receptor and Fc. *Journal of molecular biology* **1993,** *230* (3), 1077-1083.

208. Raghavan, M.; Chen, M. Y.; Gastinel, L. N.; Bjorkman, P. J., Investigation of the interaction between the class I MHC-related Fc receptor and its immunoglobulin G ligand. *Immunity* **1994,** *1* (4), 303-315.

209. Bitonti, A. J.; Dumont, J. A., Pulmonary administration of therapeutic proteins using an immunoglobulin transport pathway. *Advanced drug delivery reviews* **2006,** *58* (9), 1106-1118.

210. Low, S.; Nunes, S.; Bitonti, A.; Dumont, J., Oral and pulmonary delivery of FSH–Fc fusion proteins via neonatal Fc receptor-mediated transcytosis. *Human reproduction* **2005,** *20* (7), 1805-1813.

211. Zhou, L.; Wang, H.-Y.; Tong, S.; Okamoto, C. T.; Shen, W.-C.; Zaro, J. L., Single chain Fc-dimer-human growth hormone fusion protein for improved drug delivery. *Biomaterials* **2017,** *117*, 24-31.

212. Mittal, G.; Sahana, D. K.; Bhardwaj, V.; Ravi Kumar, M. N., Estradiol loaded PLGA nanoparticles for oral administration: effect of polymer molecular weight and copolymer composition on release behavior in vitro and in vivo. *Journal of controlled release : official journal of the Controlled Release Society* **2007,** *119* (1), 77-85.

213. Hirsch, I., Type 1 Diabetes Mellitus and the use of Flexible Insulin Regimes. *American Family Physician* **1999,** *60* (8), 2343-52, 2355-6.

214. Sanyog Jain; Vishal V Rathi; Amit K Jain; Das, M.; Godugu, C., Folate-decorated PLGA nanoparticles as a rationally designed vehicle for the oral delivery of insulin. *Nanomedicine* **2012,** *7* (9), 1311-1337.

215. Manoharan, C.; Singh, J., Insulin loaded PLGA microspheres: effect of zinc salts on encapsulation, release, and stability. *Journal of pharmaceutical sciences* **2009,** *98* (2), 529-42.

216. Malathi, S.; Nandhakumar, P.; Pandiyan, V.; Webster, T. J.; Balasubramanian, S., Novel PLGA-based nanoparticles for the oral delivery of insulin. *Int J Nanomedicine* **2015,** *10*, 2207-18.

217. Vauthier, C.; Bouchemal, K., Methods for the preparation and manufacture of polymeric nanoparticles. *Pharmaceutical research* **2009,** *26* (5), 1025-1058.

218. Nazila Kamaly, Z. X., Pedro M. Valencia, Aleksander F. Radovic-Moreno, and Omid C. Farokhzad, Targeted polymeric therapeutic nanoparticles: design, development and clinical translation *Chemical Society reviews* **2012,** *41*, 2971–3010.

219. Cheng, J.; Teply, B. A.; Sherifi, I.; Sung, J.; Luther, G.; Gu, F. X.; Levy-Nissenbaum, E.; Radovic-Moreno, A. F.; Langer, R.; Farokhzad, O. C., Formulation of functionalized PLGA-PEG nanoparticles for in vivo targeted drug delivery. *Biomaterials* **2007,** *28* (5), 869-76.

220. Grabnar PA, K. J., The manufacturing techniques of drug-loaded polymeric nanoparticles from preformed polymers. *Journal of microencapsulation* **2011,** *28* (4), 323-335.

221. Mora-Huertas CE, F. H., Elaissari A., Polymer-based nanocapsules for drug delivery. *International Journal of Pharmaceutics* **2010,** *29* (385(1-2)), 113-42.

222. Avgoustakis, K., Pegylated Poly(Lactide) and Poly(Lactide-Co-Glycolide) Nanoparticles: Preparation, Properties and Possible Applications in Drug Delivery. *Current Drug Delivery* **2004,** *1* (4), 321-333.

223. Danhier, F.; Ansorena, E.; Silva, J. M.; Coco, R.; Le Breton, A.; Preat, V., PLGA-based nanoparticles: an overview of biomedical applications. *Journal of controlled release : official journal of the Controlled Release Society* **2012,** *161* (2), 505-22.

224. Makadia, H. K.; Siegel, S. J., Poly Lactic-co-Glycolic Acid (PLGA) as Biodegradable Controlled Drug Delivery Carrier. *Polymers* **2011,** *3* (3), 1377-1397.

225. Pandey, S. K.; Haldar, C.; Patel, D. K.; Maiti, P., Biodegradable Polymers for Potential Delivery Systems for Therapeutics. *Advances in Polymer Science* **2013,** *254*, 169-202.

226. M.L. Hans, A. M. L., Biodegradable nanoparticles for drug delivery and targeting. *Current Opinion in Solid State and Materials Science* **2002,** *6*, 319-327.

227. L. Martin-Banderas, M. D.-L., I. Muñoz-Rubio, J. Alvarez-Fuentes,; Holgado, M. F.-A. a. M. A., Functional PLGA NPs for Oral Drug Delivery- Recent Strategies and Developments. *Mini-Reviews in Medicinal Chemistry* **2013,** *13*.

228. Nilsson, P.; Nylander, T.; Havelund, S., Adsorption of Insulin on Solid Surfaces in Relation to the Surface Properties of the Monomeric and Oligomeric Forms. *Journal of Colloid and Interface Science* **1990,** *144*.

229. Arnebrant, T.; Nylander, T., Adsorption of Insulin on Metal Surfaces in Relation to Association Behavior. *Journal of Colloid and Interface Science* **1988,** *122*.

230. Marcker, K., The Binding of the "Structural" Zinc Ions in Crystalline Insulin. *Acta Chemica Scandinavica* **1960,** *14*, 2071-2074.

231. Svend Havelund, A. P., Ulla Ribel,; Ib Jonassen, A. V., Jan Markussen, and; Kurtzhals, P., The Mechanism of Protraction of Insulin Detemir, a Long-acting, Acylated Analog of Human Insulin. *Pharmaceutical Research* **2004,** *21* (8).

232. Frokjaer, S.; Otzen, D. E., Protein drug stability: a formulation challenge. *Nature reviews. Drug discovery* **2005,** *4* (4), 298-306.

233. Baumann, A., Early Development of Therapeutic Biologics - Pharmacokinetics. *Current Drug Metabolism* **2006,** *7*, 15-21.

234. Singh, J. A.; Christensen, R.; Wells, G. A.; Suarez-Almazor, M. E.; Buchbinder, R.; Lopez-Olivo, M. A.; Tanjong Ghogomu, E.; Tugwell, P., Biologics for rheumatoid arthritis: an overview of Cochrane reviews. *The Cochrane database of systematic reviews* **2009,** (4), CD007848.

235. Quesada, J. R.; Talpaz, M.; Rios, A.; Kurzrock, R.; Gutterman, J. U., Clinical Toxicity of Interferons in Cancer Patients- A Review. *Journal of Clinical Oncology* **1986,** *4*, 234-243.

236. Rossini, A. A.; Mordes, J. P.; Like, A. A., Immunology of Insulin-Dependent Diabetes Mellitus. *Annual Review of Immunology* **1985,** *3*, 289-320.

237. Sonia, T. A.; Sharma, C. P., An overview of natural polymers for oral insulin delivery. *Drug discovery today* **2012,** *17* (13-14), 784-92.

238. Mitragotri, S.; Burke, P. A.; Langer, R., Overcoming the challenges in administering biopharmaceuticals: formulation and delivery strategies. *Nature reviews. Drug discovery* **2014,** *13* (9), 655-72.

239. Ibraheem, D.; Elaissari, A.; Fessi, H., Administration strategies for proteins and peptides. *Int J Pharm* **2014,** *477* (1-2), 578-89.

240. Brigger, I.; Dubernet, C.; Couvreur, p., Nanoparticles in cancer therapy and diagnosis. *Advanced Drug Delivery Reviews* **2002,** *54*, 631-651.

241. Bertrand, N.; Wu, J.; Xu, X.; Kamaly, N.; Farokhzad, O. C., Cancer nanotechnology: the impact of passive and active targeting in the era of modern cancer biology. *Adv Drug Deliv Rev* **2014,** *66*, 2-25.

242. M., K. N.; Carraro, E.; Cotica, L. F.; Mainardes, R. M., Potential of polymeric nanoparticles in AIDS treatment and prevention. *Expert opinion on Drug Delivery* **2011,** *8* (1), 95-112.

243. Santos-Magalhaes, N. S.; Mosqueira, V. C., Nanotechnology applied to the treatment of malaria. *Adv Drug Deliv Rev* **2010,** *62* (4-5), 560-75.

244. Kattan, J.; Droz, J.-P.; Couvreur, P.; Marino, J.-P.; Boutan-Laroze, A.; Rougier, P.; Brault, P.; Vranckx, H.; Grognet, j.-M.; Morge, X.; Sancho-Garnier, Phase I clinical trial and pharmacokinetic evaluation of doxorubicin carried by polyisohexylcyanoacrylate nanoparticles. *Investigational New Drugs* **1992,** *10*, 191-199.

245. Lee, K. S.; Chung, H. C.; Im, S. A.; Park, Y. H.; Kim, C. S.; Kim, S. B.; Rha, S. Y.; Lee, M. Y.; Ro, J., Multicenter phase II trial of Genexol-PM, a Cremophor-free, polymeric micelle formulation of paclitaxel, in patients with metastatic breast cancer. *Breast cancer research and treatment* **2008,** *108* (2), 241-50.

246. Hrkach, J.; Von Hoff, D.; Mukkaram Ali, M.; Andrianova, E.; Auer, J.; Campbell, T.; De Witt, D.; Figa, M.; Figueiredo, M.; Horhota, A.; Low, S.; McDonnell, K.; Peeke, E.; Retnarajan, B.; Sabnis, A.; Schnipper, E.; Song, J. J.; Song, Y. H.; Summa, J.; Tompsett, D.; Troiano, G.; Van Geen Hoven, T.; Wright, J.; LoRusso, P.; Kantoff, P. W.; Bander, N. H.; Sweeney, C.; Farokhzad, O. C.; Langer, R.; Zale, S., Preclinical development and clinical translation of a PSMA-targeted docetaxel nanoparticle with a differentiated pharmacological profile. *Science translational medicine* **2012,** *4* (128), 128ra39.

247. Jinjun Shi, Z. X., Nazila Kamaly, and Omid C. Farokhzad, Self-Assembled Targeted Nanoparticles: Evolution of Technologies and Bench to Bedside Translation. *Accounts of Chemical Research* **2011,** *44* (10), 1123-1134.

248. Kumari, A.; Yadav, S. K.; Yadav, S. C., Biodegradable polymeric nanoparticles based drug delivery systems. *Colloids and surfaces. B, Biointerfaces* **2010,** *75* (1), 1-18.

249. Chen, M. C.; Sonaje, K.; Chen, K. J.; Sung, H. W., A review of the prospects for polymeric nanoparticle platforms in oral insulin delivery. *Biomaterials* **2011,** *32* (36), 9826-38.

250. Martin-Banderas, L., Durán-Lobato, M., Muñoz-Rubio, I., Alvarez-Fuentes, J., Fernández-Arevalo, M., Holgado, M. A. , Functional PLGA NPs for Oral Drug Delivery: Recent Strategies and Developments *Mini-Reviews in Medicinal Chemistry* **2013,** *13*.

251. Elsabahy, M.; Wooley, K. L., Design of polymeric nanoparticles for biomedical delivery applications. *Chemical Society reviews* **2012,** *41* (7), 2545-61.

252. Fuhrmann, G.; Grotzky, A.; Lukic, R.; Matoori, S.; Luciani, P.; Yu, H.; Zhang, B.; Walde, P.; Schluter, A. D.; Gauthier, M. A.; Leroux, J. C., Sustained gastrointestinal activity of dendronized polymer-enzyme conjugates. *Nature chemistry* **2013,** *5* (7), 582-9.

253. Raghuvanshi, R. S.; Katare, Y. K.; Lalwani, K.; Ali, M. M.; Singh, O.; Panda, A. K., Improved immune response from biodegradable polymer particles entrapping tetanus toxoid by use of different immunization protocol and adjuvants. *International Journal of Pharmaceutics* **2002,** *245* (1-2), 109-121.

254. Podaralla, S. K.; Ramakrishna, S.; Saini, R. T.; Diwan, P. V., Influence of microemulsion method and peptide loading on formation of poly(lactide-co-glycolide) insulin nanoparticles. *Pharmazie* **2006,** *7*, 613-617.

255. Park, J.; Wrzesinski, S. H.; Stern, E.; Look, M.; Criscione, J.; Ragheb, R.; Jay, S. M.; Demento, S. L.; Agawu, A.; Licona Limon, P.; Ferrandino, A. F.; Gonzalez, D.; Habermann, A.; Flavell, R. A.; Fahmy, T. M., Combination delivery of TGF-beta inhibitor and IL-2 by nanoscale liposomal polymeric gels enhances tumour immunotherapy. *Nature materials* **2012,** *11* (10), 895-905.

256. des Rieux, A.; Fievez, V.; Garinot, M.; Schneider, Y. J.; Preat, V., Nanoparticles as potential oral delivery systems of proteins and vaccines: a mechanistic approach. *Journal of controlled release : official journal of the Controlled Release Society* **2006,** *116* (1), 1-27.

257. Sah, E.; Sah, H., Recent Trends in Preparation of Poly(lactide-co-glycolide) Nanoparticles by Mixing Polymeric Organic Solution with Antisolvent. *Journal of Nanomaterials* **2015,** *2015*, 1-22.

258. CF, B., Dimethyl sulfoxide (DMSO): a review. *Cornall Veterinarian* **1986,** *1* (76), 61-90.

259. Naha, P. C.; Kanchan, V.; Manna, P. K.; Panda, A. K., Improved bioavailability of orally delivered insulin using Eudragit-L30D coated PLGA microparticles. *Journal of microencapsulation* **2008,** *25* (4), 248-256.

260. Tomar, L.; Tyagi, C.; Kumar, M.; Kumar, P.; Singh, H.; Choonara, Y. E.; Pillay, V., In vivo evaluation of a conjugated poly(lactide-ethylene glycol) nanoparticle depot formulation for prolonged insulin delivery in the diabetic rabbit model. *Int J Nanomedicine* **2013,** *8*, 505-20.

261. Cozar-Bernal, M. J.; Holgado, M. A.; Arias, J. L.; Munoz-Rubio, I.; Martin-Banderas, L.; Alvarez-Fuentes, J.; Fernandez-Arevalo, M., Insulin-loaded PLGA microparticles: flow focusing versus double emulsion/solvent evaporation. *Journal of microencapsulation* **2011,** *28* (5), 430-41.

262. Roach, P.; Farrar, D.; Perry, C. C., Interpretation of Protein Adsorption: Surface-Induced Conformational Changes. *Journal of American Chemical Society* **2005,** *127*, 8168-8173.

263. Pasche, S.; Voros, J.; Griesser, H. J.; Spencer, N. D.; Textor, M., Effects of Ionic Strength and Surface Charge on Protein Adsorption at PEGylates Surfaces. *Journal of Physical Chemistry B* **2005,** *109* (37), 17545-17552.

264. Brandl, F.; Bertrand, N.; Lima, E. M.; Langer, R., Nanoparticles with photoinduced precipitation for the extraction of pollutants from water and soil. *Nature communications* **2015,** *6*, 7765.

265. Monopoli, M. P.; Aberg, C.; Salvati, A.; Dawson, K. A., Biomolecular coronas provide the biological identity of nanosized materials. *Nature nanotechnology* **2012,** *7* (12), 779-86.

266. Dunn, M. F., Zinc-ligand interactions modulate assembly and stability of the insulin hexamer -- a review. *Biometals : an international journal on the role of metal ions in biology, biochemistry, and medicine* **2005,** *18* (4), 295-303.

267. Mammen, M.; Choi, S.-K.; Whitesides, G. M., Polyvalent Interactions in Biological Systems: Implications for Design and
Use of Multivalent Ligands and Inhibitors. *Angewandte Chemie* **1998,** *37* (20), 2754-2794.

268. Arai, T.; Norde, W., The behavior of some model proteins at solid-liquid interfaces 1. Adsorption from single protein solutions. *Colloids and Surfaces* **1990,** *51*, 1-15.

269. Marcker, Association of Zn-free Insulin. *Acta Chemica Scandinavica* **1960,** *14*, 194-196.

270. Hallas-Moller, K.; Petersen, K.; Schlichtkrull, J., Crystalline and Amorphous Insulin-Zinc Compounds with Prolonged Action. *Science* **1952,** *116*, 394-398.

271. Wintersteiner, O.; Abramson, H. A., The Isoelectric point of Insulin: Electrical Properties of Adsorbed and Crystalline Insulin. *J. of Biol. Chem.* **1933,** *99* (741-753).

272. Park, K., Facing the Truth about Nanotechnology in Drug Delivery. *ACS Nano* **2013,** *7* (9), 7442-7447.

273. Simmons, J. H.; McFann, K. K.; Brown, A. C.; Rewers, A.; Follansbee, D.; Temple-Trujillo, R. E.; Klingensmith, G. J., Reliability of the Diabetes Fear of Injecting and Self-Testing Questionnaire in pediatric patients with type 1 diabetes. *Diabetes Care* **2007,** *30* (4), 987-8.

274. Liu, G., Franssen, E., Fitch, M. I., Warner, E., Patient Preferences for Oral Versus Intravenous Palliative Chemotherapy. *Journal of Clinical Oncology* **1997,** *15* (1), 110-115.

275. Ward, S. E.; Kaltenthaler, E.; Cowan, J.; Marples, M.; Orr, B.; Seymour, M. T., The clinical and economic benefits of capecitabine and tegafur with uracil in metastatic colorectal cancer. *Br J Cancer* **2006,** *95* (1), 27-34.

276. Borner, M., Schoffski, P., de Wit, R., Caponigro, F., Comell, g., Silkes, A., Greim, G., Peters, G.J., van der Born, K., Wander, J., de Boer, R.F., Martin, C., Fumoleau, P., Patient preference and pharmacokinetics of oral modulated UFT versus intravenous fluorouracil and leucovorin- a randomised crossover trial in advanced colorectal cancer. *European Journal of Cancer* **2002,** *38*, 349-358.

277. Pfeiffer, P.; Mortensen, J. P.; Bjerregaard, B.; Eckhoff, L.; Schonnemann, K.; Sandberg, E.; Aabo, K.; Jakobsen, A., Patient preference for oral or intravenous chemotherapy: a randomised cross-over trial comparing capecitabine and Nordic fluorouracil/leucovorin in patients with colorectal cancer. *Eur J Cancer* **2006,** *42* (16), 2738-43.

278. Khedkar, A.; Iyer, H.; Anand, A.; Verma, M.; Krishnamurthy, S.; Savale, S.; Atignal, A., A dose range finding study of novel oral insulin (IN - 105) under fed conditions in type 2 diabetes mellitus subjects. *Diabetes, Obesity and Metabolism* **2010,** *12* (8), 659-664.

279. Hamman, J. H., Enslin, G., M., Kotze, A. F., Oral Delivery of Peptide Drugs. *Biodrugs* **2005,** *19* (3), 165-177.

280. Goldberg, M.; Gomez-Orellana, I., Challenges for the oral delivery of macromolecules. *Nature reviews. Drug discovery* **2003,** *2* (4), 289-95.

281. Qui, Y. P., K, Environment-sensitive hydrogels for drug delivery. *Advanced Drug Delivery Reviews* **2001,** *53*, 321-339.

282. Madsen, F., Peppas, N.A., Complexation graft copolymer networks-swelling properties, calcium binding and proteolytic enzyme inhibition. *Biomaterials* **1999,** *20*.

283. Torres-Lugo, M., Carcia, M., Record, R., Peppas, N.A., Physicochemical behavior and cytotoxic effects of p(methacrylic acid–g-ethylene glycol) nanospheres for oral delivery of proteins. *Journal of Controlled Release* **2002,** *80*, 197-205.

284. Kratz, F.; Beyer, U.; Roth, T.; Tarasova, N.; Collery, P.; Lechenault, F.; Cazabat, A.; Schumacher, P.; Unger, C.; Falken, U., Transferrin conjugates of doxorubicin: synthesis, characterization, cellular uptake, and in vitro efficacy. *Journal of pharmaceutical sciences* **1998,** *87* (3), 338-346.

285. Kratz, F.; Beyer, U.; Roth, T.; Tarasova, N.; Collery, P.; Lechenault, F.; Cazabat, A.; Schumacher, P.; Unger, C.; Falken, U., Transferrin conjugates of doxorubicin: synthesis, characterization, cellular uptake, and in vitro efficacy. *Journal of pharmaceutical sciences* **1998,** *87* (3), 338-46.

286. Jain, S., Rathi, V.V., Jain, A., Das, M., Godugu, C., Folate-decorated PLGA nanoparticles as a rationally designed vehicle for the oral delivery of insulin. *Nanomedicine* **2012,** *7* (9), 1311-1337.

287. He, C.; Hu, Y.; Yin, L.; Tang, C.; Yin, C., Effects of particle size and surface charge on cellular uptake and biodistribution of polymeric nanoparticles. *Biomaterials* **2010,** *31* (13), 3657-3666.

288. Sarin, H., Physiologic upper limits of pore size of different blood capillary types and another perspective on the dual pore theory of microvascular permeability. *Journal of angiogenesis research* **2010,** *2* (1), 14.

289. Khan, M. Z. I., Prebeg, Z. Kurjakovic, N., A pH-dependent colon targeted oral drug delivery system using methacrylic acid copolymers I. Manipulation of drug release using Eudragit L100-55 and Eudragit S100 combinations. *Journal of Controlled Release* **1998,** *58* (58), 215-222.

290. Gupta, V., Assmus, M.W., Beckert, T.E., Price, J.C., A novel pH- and time-based multi-unit potential colonic drug delivery system. II. Optimization of multiple response variables. *International Journal of Pharmaceutics* **2000,** *213*, 93-102.

291. Jain, D., Panda, A.K., Majumdar, D.K., Eudragit S100 entrapped insulin microspheres for oral delivery. *AAPS PharmSciTech* **2005,** *6* (1).

292. Dai, J.; Nagai, T.; Wang, X.; Zhang, T.; Meng, M.; Zhang, Q., pH-sensitive nanoparticles for improving the oral bioavailability of cyclosporine A. *Int J Pharm* **2004,** *280* (1-2), 229-40.

293. Hu, D.; Liu, L.; Chen, W.; Li, S.; Zhao, Y., A novel preparation method for 5-aminosalicylic acid loaded Eudragit S100 nanoparticles. *Int J Mol Sci* **2012,** *13* (5), 6454-68.

294. Yoo, J. W.; Giri, N.; Lee, C. H., pH-sensitive Eudragit nanoparticles for mucosal drug delivery. *Int J Pharm* **2011,** *403* (1-2), 262-7.

295. Maghsoodi, M.; Esfahani, M., Preparation of microparticles of naproxen with Eudragit RS and talc by spherical crystallization technique. *Pharm Dev Technol* **2009,** *14* (4), 442-50.

296. Leroux, J. C., Cozens, R.M., Roesel, J.L., Galli, B., Doelker, E., Gurny, R., pH-Sensitive Nanoparticles- An Effective Means to Improve the Oral Delivery of HIV-1 Protease Inhibitors in Dogs. *Pharmaceutical Research 13* (3), 485-487.

297. Lee, J. H., Park, T.G., Choi, H.K., Development of oral drug delivery system using floating microspheres. *Journal of microencapsulation* **1999,** *16* (6), 715-729.

298. Hermanson, G. T., *Bioconjugate techniques*. Academic press: **2013**.

299. Hubatsch, I.; Ragnarsson, E. G. E.; Artursson, P., Determination of drug permeability and prediction of drug absorption in Caco-2 monolayers. *Nat. Protocols* **2007,** *2* (9), 2111-2119.

300. Vila, A.; Sanchez, A.; Tobio, M.; Calvo, P.; Alonso, M., Design of biodegradable particles for protein delivery. *Journal of Controlled Release* **2002,** *78* (1), 15-24.

301. Panyam, J.; Labhasetwar, V., Biodegradable nanoparticles for drug and gene delivery to cells and tissue. *Advanced drug delivery reviews* **2003,** *55* (3), 329-347.

302. Makadia, H. K.; Siegel, S. J., Poly lactic-co-glycolic acid (PLGA) as biodegradable controlled drug delivery carrier. *Polymers* **2011,** *3* (3), 1377-1397.

303. Li, Y.-P.; Pei, Y.-Y.; Zhang, X.-Y.; Gu, Z.-H.; Zhou, Z.-H.; Yuan, W.-F.; Zhou, J.-J.; Zhu, J.-H.; Gao, X.-J., PEGylated PLGA nanoparticles as protein carriers: synthesis, preparation and biodistribution in rats. *Journal of controlled release* **2001,** *71* (2), 203-211.

304. Hickey, T.; Kreutzer, D.; Burgess, D.; Moussy, F., Dexamethasone/PLGA microspheres for continuous delivery of an anti-inflammatory drug for implantable medical devices. *Biomaterials* **2002,** *23* (7), 1649-1656.

305. Burgess, D. J.; Hickey, A. J., Microsphere technology and applications. *Encyclopedia of Pharmaceutical technology* **1994,** *10*, 1-29.

306. Bala, I.; Hariharan, S.; Kumar, M. R., PLGA nanoparticles in drug delivery: the state of the art. *Critical Reviews™ in Therapeutic Drug Carrier Systems* **2004,** *21* (5).

307. Pereira de Sousa, I.; Moser, T.; Steiner, C.; Fichtl, B.; Bernkop-Schnurch, A., Insulin loaded mucus permeating nanoparticles: Addressing the surface characteristics as feature to improve mucus permeation. *Int J Pharm* **2016,** *500* (1-2), 236-44.

308. Sheng, J.; He, H.; Han, L.; Qin, J.; Chen, S.; Ru, G.; Li, R.; Yang, P.; Wang, J.; Yang, V. C., Enhancing insulin oral absorption by using mucoadhesive nanoparticles loaded with LMWP-linked insulin conjugates. *Journal of controlled release : official journal of the Controlled Release Society* **2016,** *233*, 181-90.

309. Hosseininasab, S.; Pashaei-Asl, R.; Khandaghi, A. A.; Nasrabadi, H. T.; Nejati-Koshki, K.; Akbarzadeh, A.; Joo, S. W.; Hanifehpour, Y.; Davaran, S., Synthesis, characterization, and in vitro studies of PLGA-PEG nanoparticles for oral insulin delivery. *Chem Biol Drug Des* **2014,** *84* (3), 307-15.

310. D'Souza, S. S.; DeLuca, P. P., Development of a dialysis in vitro release method for biodegradable microspheres. *Aaps Pharmscitech* **2005,** *6* (2), E323-E328.